PATTERNS IN FOREST SOIL MICROBIAL COMMUNITY COMPOSITION ACROSS A RANGE OF REGIONAL CLIMATES IN WESTERN CANADA

by

BETH BROCKETT

BSc Hons., University of East Anglia, 2004

A THESIS SUBMITTED IN PARTIAL FULFILLMENT OF THE REQUIREMENTS FOR THE DEGREE OF

MASTER OF SCIENCE

in

The Faculty of Graduate Studies

(Forestry)

THE UNIVERSITY OF BRITISH COLUMBIA

(VANCOUVER)

February, 2008

ABSTRACT

Soil microbial communities can be characterized by community structure and function (community composition) across a spectrum of spatial scales, and variation in soil microbial composition has been associated with a number of environmental gradients. This study investigates the structure and function of soil microbial communities under mature, undisturbed forested sites across a range of regional climates in British Columbia and Alberta, and also examines the variation in community composition within sites.

Phospholipid fatty acid analysis was used to investigate the structure of soil microbial communities and total soil microbial biomass at each site. Extra-cellular enzyme assays established the functional potential of the soil microbial community at each site.

Multivariate analysis of the data showed that the soil microbial communities under different forest types did significantly separate along the regional climate gradient by both community structure and function, despite high local variation in the communities. Soil moisture content and soil organic matter concentration consistently exhibited the strongest relationship with microbial community characteristics, although the functional and structural responses to the external drivers were different. Microbial community function and structure also changed with soil depth but not with time of sampling.

Microbial community function was related to the regional annual average precipitation gradient. Most of the locations exhibited unique microbial community functional profiles in their soil layers; however the enzyme activities in the samples from the driest (Ponderosa Pine) and wettest (Mountain Hemlock) locations were notably different from each other and from those of the other locations, especially in the organic layers.

The moist maritime-influenced Coastal Western Hemlock (CWH) forest exhibited microbial community structural characteristics which were unique from those of the other forest locations. The higher abundance of bacteria relative to fungi in the CWH forest soils may be related to the significantly higher available nitrogen concentrations at this site.

TABLE OF CONTENTS

Abstract ii

Table of contents iii

List of tables vii

List of figures ix

List of abbreviations xiv

Acknowledgements xv

Dedication xvii

1. Introduction and literature review 1

1.1. Rationale 1

1.2. Literature review 2

1.2.1. The role of microorganisms in forest ecosystems 2

1.2.2. Microbial community function and structure 3

1.2.3. External drivers of microbial community function and structure 4

1.2.4. Differential responses of microbial groups to external gradients 9

1.3. Introduction to the study 10

1.4. Specific hypotheses 11

2. Methodology 13

2.1. Location of study sites along a climate gradient 13

2.2. Sampling design 18

2.3. Field measurements 19

2.4. Laboratory sample analysis 20

2.4.1. Microbial community structural analysis 21

2.4.2. Microbial community functional analysis 23

2.5. Statistical analysis 29

3. Results 33

3.1. Hypothesis one: Analysis of composite soil samples for microbial community function and structure provides the same results as analysis of individual soil samples. 33

3.2. Hypothesis two: Soil microbial community structure and function are significantly different in spring and summer. 34

3.3. Hypothesis three: It is possible to separate forest types along a regional climate gradient based on microbial community function and/or structure, despite high local microbial community variability. 47

3.3.1. Multivariate analysis of functional data for a combination of all soil profile layers 47

3.3.2. Multivariate analysis of microbial functional data for individual soil layers 48

3.3.3. Multivariate analysis of microbial structural data for a combination of all soil profile layers 52

3.3.4 Multivariate analysis of structural data for individual layers 54

3.3.5. Environmental characteristics of the PP, MH and CWH locations 57

3.4. Hypothesis four: A set of measured environmental variables can be shown to significantly correlate with microbial community function and structure across a regional climate gradient. Post-hoc hypothesis: If accepted, I hypothesize that moisture is highly correlated with microbial community function and structure. 66

3.4.1 Correlations between microbial community function and structure and measured environmental variables 66

3.4.2 Ordinations for microbial community data and measured environmental variables 70

3.5 Hypothesis five: Analysis of soil microbial structure and function will show separation of the mineral and organic layers 87

3.5.1 Microbial functional community data 87

3.5.2. Microbial structural community data 98

4. Discussion 109

4.1. Separating distinct forest types at a regional scale based on soil microbial community function and structure 109

4.2. Forest types with distinct microbial community functional profiles 109

4.3. Forest types with distinct microbial community structural profiles 111

4.4. Differences in microbial community structure and function 112

4.5. Correlations between soil microbial community function and structure and environmental site variables along the regional climate gradient 113

4.6. Correlations between components of the microbial communities 117

4.7. Changes in microbial community function and structure with soil depth 118

4.8. Changes in microbial community function and structure with season 119

4.9. Sampling design recommendations 121

5. Conclusions 123

6. Further work 124

7. References 125

Appendices 137

Appendix I. Non-metric Multidimensional Scaling (NMS) test statistics 137

Appendix II. Paired MRPP test statistics 158

Appendix III. PRS™ Probe Raw Data 163

LIST OF TABLES

Table 2.1. Study site characteristics ……15

Table 2.2. Break-down of sampling strategy ……..18

Table 2.3. Measured site variables and sampling time ……20

Table 2.4. Signature PLFAs chosen to characterize microbial community structure 23

Table 2.5. Hydrolytic enzyme assays chosen for this study ……24

Table 3.1. Test statistics from a nonparametric MANOVA on structural microbial data 33

Table 3.2. Test statistics from a nonparametric MANOVA on functional microbial data 33

Table 3.3. Statistics for measured environmental variables in the organic layers at the IDF location ……45

Table 3.4. Statistics for measured environmental variables in the organic layers at the ESSF location ……45

Table 3.5. Statistics for measured environmental variables in the organic layers at the PP location ……..45

Table 3.6. Statistics for measured environmental variables in the organic layers at the BWBS location ……46

Table 3.7. Statistics for measured environmental variables in the organic layers at the ICH location ……46

Table 3.8. Statistics for measured environmental variables in the organic layers at the MH location ……46

Table 3.9. Statistics for measured environmental variables in the organic layers at the CWH location ……..47

Table 3.10. Pair-wise MRPP analysis of enzyme activities in all soil layers combined at each location …… .48

Table 3.11. Pair-wise MRPP analysis of enzyme activities in the F layer at each location ……49

Table 3.12. Pair-wise MRPP analysis of enzyme activities in the H layer at each location…… 51

Table 3.13. Pair-wise MRPP analysis of enzyme activities in the mineral soil at each location ……52

Table 3.14. Pair-wise MRPP analysis of PLFA analysis results for each location; all soil layers combined 53

Table 3.15. Pair-wise MRPP analysis of PLFA analysis results for each location; F layer 55

Table 3.16. Pair-wise MRPP analysis of PLFA analysis results for each location; H layer…….. 56

Table 3.17. Pair-wise MRPP analysis of PLFA analysis results for each location; mineral layer…….. 57

Table 3.18. Tree species composition at the sampling sites……59

Table 3.19. Spearman's rank correlations between enzyme activities and measured environmental variables …… 67

Table 3.20. Significant correlations between PLFA signatures and measured environmental variables……68

Table 3.21. Significant correlations between PLFA signatures and enzyme activities...69

Table 3.22. Significant correlations between enzyme activities ……69

Table 3.23. Pair-wise MRPP analysis of enzyme assay results for F, H, and mineral (M) layers……87

Table 3.24. Pair-wise MRPP analysis on PLFA results for F, H, and mineral (M) soil layers ……98

LIST OF FIGURES

Figure 1.1. Visualization of the role of microbial communities in relation to biogeochemical processes in forest soils……11

Figure 2.1. Map of the biogeoclimatic zones of British Columbia showing the seven study locations……14

Figure 2.2. Sample plate outline for fluorimetric enzyme bioassay ……27

Figure 2.3. Soil buffer plate outline for fluorimetric enzyme bioassay……27

Figure 2.4. Sample plate outline for colorimetric enzyme bioassay……29

Figure 3.1. Mean phosphatase and sulfatase activities of all soil layers combined from the seven study locations……...37

Figure 3.2. Mean xylanase activity of all soil layers combined from the seven study locations……38

Figure 3.3. Mean phenoloxidase and peroxidase activities of all soil layers combined from the seven study locations …… 38

Figure 3.4. Mean arbuscular mycorrhizal and saprophytic fungi PLFA signature concentrations of all soil layers combined from the seven study locations……39

Figure 3.5. Mean total fungi PLFA signature concentration of all soil layers combined from the seven study locations …… 40

Figure 3.6. Mean temperature (˚C) of organic layers from the seven study locations….40

Figure 3.7. Mean water content (%) of organic layers from the seven study locations…41

Figure 3.8. Mean pH of organic layers from the seven study locations ……41

Figure 3.9. Mean C:N ratio of combined organic soil layers from the seven study locations …….. 42

Figure 3.10. Mean C:N ratio of mineral soil from the seven study locations ……42

Figure 3.11. Mean total C concentration (%) of organic layers combined from the seven study locations……43

Figure 3.12. Mean total C concentration (%) of mineral soil from the seven study locations……43

Figure 3.13. Mean total N concentration (%) of organic layers combined from the seven study locations ……44

Figure 3.14. Mean soil N concentration (%) of mineral soil from the seven study locations ……..44

Figure 3.15. Available nitrogen in the organic layers at the seven study locations……..60

Figure 3.16. Mean available P concentration in all soil layers combined at the seven study locations ……61

Figure 3.17. Mean available Ca, Mg, and K concentrations in all soil layers combined at the seven study locations…….. 62

Figure 3.18. Mean available S concentration in all soil layers combined at the seven study locations ……63

Figure 3.19. Mean available micronutrients (Fe, Mn, Zn, Cu, Bo) concentrations in all soil layers combined at the seven study locations ……...64

Figure 3.20. Mean available Cu concentrations in all soil layers combined at the seven study locations ……65

Figure 3.21. NMS ordination of microbial communities from all soil profile layers combined at the seven locations based on enzyme activity……..71

Figure 3.22. NMS ordination of microbial communities from organic layers at the seven locations based on enzyme activity ……73

Figure 3.23. NMS ordination of axes 2 and 3 showing microbial communities from the F layer at the seven locations based on enzyme activity……75

Figure 3.24. NMS ordination of axes 1 and 2 showing microbial communities from the H layer at the seven locations based on enzyme activity ……77

Figure 3.25. NMS ordination showing microbial communities from all layers at the seven locations based on PLFA signature microbial community groupings ……79

Figure 3.26. Mean total bacterial:total fungi PLFA signature ratios for the F layer at the seven locations ……...80

Figure 3.27. Mean total bacterial:total fungi PLFA signature ratios for the H layer, at the seven locations …….. 80

Figure 3.28. NMS ordination showing microbial communities from the F layer at the seven locations based on PLFA signature microbial community groupings ……82

Figure 3.29. NMS ordination showing microbial communities from the H layer at the seven locations based on PLFA signature microbial community groupings ……84

Figure 3.30. Mean total fungal PLFA concentration (total divided by sample biomass) in the H layer at the seven locations ……85

Figure 3.31. NMS ordination showing microbial communities from the mineral layer at the seven locations based on PLFA signatures ……86

Figure 3.32. Mean cellulase activity rates in each soil layer (spring samples) ……88

Figure 3.33. Mean cellulase activity rates in each soil layer (summer samples) …….88

Figure 3.34. Mean glucosidase activity rates in each soil layer (spring samples) ……...89

Figure 3.35. Mean glucosidase activity rates in each soil layer (summer samples) ……89

Figure 3.36. Mean xylanase activity rates in each soil layer (spring samples) ……90

Figure 3.37. Mean xylanase activity rates in each soil layer (summer samples) ……90

Figure 3.38. Mean NAG activity rates in each soil layer (spring samples) ……...91

Figure 3.39. Mean NAG activity rates in each soil layer (summer samples) ……...91

Figure 3.40. Mean urease activity rates in each soil layer (spring samples) ……...92

Figure 3.41 Mean urease activity rates in each soil layer (summer samples) ……92

Figure 3.42. Mean phosphatase activity rates in each soil layer (spring samples) …….93

Figure 3.43. Mean phosphatase activity rates in each soil layer (summer samples) ….93

Figure 3.44. Mean sulfatase activity rates in each soil layer (spring samples) ……94

Figure 3.45. Mean sulfatase activity rates in each soil layer (summer samples) ……94

Figure 3.46. Mean phenoloxidase activity rates in each soil layer (spring samples) …..95

Figure 3.47. Mean phenoloxidase activity rates in each soil layer (summer samples) ..95

Figure 3.48. Mean peroxidase activity rates in each soil layer (spring samples) ……96

Figure 3.49. Mean peroxidase activity rates in each soil layer (summer samples) ……96

Figure 3.50. NMS ordination of enzyme activities from all soil layers ……..97

Figure 3.51. Mean total microbial biomass PLFA concentration in each soil layer at the seven locations (spring samples) ……. 100

Figure 3.52. Mean total microbial biomass PLFA concentration in each soil layer at the seven locations (summer samples) ……..100

Figure 3.53. Mean total bacteria PLFA concentration in each soil layer at the seven locations (spring samples) ……. 101

Figure 3.54 Mean total bacteria PLFA concentration in the each soil layer at the seven locations (summer samples) ……101

Figure 3.55. Mean Gram-positive bacteria PLFA concentration in each soil layer at the seven locations (spring samples) ……. 102

Figure 3.56. Mean Gram-positive bacteria PLFA concentration in each soil layer at the seven locations (summer samples) ……..102

Figure 3.57. Mean Gram-negative bacteria PLFA concentration in each soil layer at the seven locations (spring samples) ……..103

Figure 3.58. Mean Gram-negative bacteria PLFA concentration in each soil layer at the seven locations (summer samples) …….. 103

Figure 3.59. Mean actinobacteria PLFA concentration in each soil layer at the seven locations (spring samples) ……. 104

Figure 3.60. Mean actinobacteria PLFA concentration in each soil layer at the seven locations (summer samples) ……..104

Figure 3.61. Mean total fungi PLFA concentration in each soil layer at the seven locations (spring samples) ……. 105

Figure 3.62. Mean total fungi PLFA concentration in each soil layer at the seven locations (summer samples) ……..105

Figure 3.63. Mean arbuscular mycorrhizal fungi PLFA concentration in each soil layer at the seven locations (spring samples) …….. 106

Figure 3.64. Mean arbuscular mycorrhizal fungi PLFA concentration in each soil layer at the seven locations (summer samples) ……... 106

Figure 3.65. Mean saprophytic fungi PLFA concentration in each soil layer at the seven locations (spring samples) ……. 107

Figure 3.66. Mean saprophytic fungi PLFA concentration in each soil layer at the seven locations (summer samples) ……. 107

Figure 3.67. NMS ordination of PLFA data for all soil layers combined ……108

LIST OF ABBREVIATIONS

BEC – Biogeoclimatic Ecosystem Classification

BWBS – Boreal White and Black Spruce

C - Carbon

CWH – Coastal Western Hemlock

DOPA - L-3, 4-dihydroxyphenylalanine

ESSF – Englemann Spruce Subalpine Fir

F – Fermentation

H - Humic

ICH – Interior Cedar Hemlock

IDF – Interior Douglas Fir

MANOVA – Multivariate Analysis Of Variance

MH – Mountain Hemlock

Min - Mineral

MRPP – Multi-Response Permutation Procedure

MUB - 4-methylumbelliferyl

N - Nitrogen

NMS – Non-metric Multi-dimensional Scaling

PLFA – PhosphoLipid Fatty Acid

PP – Ponderosa Pine

SOM – Soil Organic Matter

ACKNOWLEDGEMENTS

This has been an interesting, challenging and fun academic and personal journey and I'd like to thank the people who have helped make it so. Dr Sue Grayston for being a patient and encouraging supervisor. Dr Cindy Prescott and Dr Bill Mohn for being supportive committee members – I always enjoyed our committee meetings! Dr Gary Bradfield for kindly giving up his time to help me with my statistics. Dr Les Lavkulich for helping me unravel the mystery of the sulfur concentrations! Dr. Val LeMay for answering many statistics questions so quickly and thoroughly.

The Below Ground Ecosystems Group members and my office mates. Especially Richa Anand, Denise Brooks, Jocelyn Campbell, Shannon Daradick, Julie Deslippe, Rachelle Lalonde, Virginie Pointeau and Toktam Sajedi – many thanks for the information, advice, words of encouragement, pints of beer, cups of tea and for your help in the field and in the lab.

Our lab manager Kate Delbel for her advice, unending patience and coffee breaks. Ron Chan and Cherry for their help in the lab, special thanks to Ron for his dedication and attention to detail. Per Bengston, Candis Staley and Alice Jang for their hard work and good humour in the field. The administration staff in the Faculty of Forestry who work so hard to help grad students. The janitorial staff for a sparkling building and the daily chats.

Andre Arsenault, Mike Curran and Graeme Hope from the BC Ministry of Forests for providing me with information about my sites and showing me around the research forests. Jason Edwards and all at the University of Alberta's EMEND research station for their hospitality and help with field work in Alberta. Ionut Aron for his help with field work at UBC's Malcolm Knapp Research Forest.

Diane Cyr and all at the Canadian Commonwealth Scholarship Program. NSERC for funding this research project. The IMAJO and Van Dusen Scholarship funds.

My family and friends in the UK who have stayed in such good contact and helped me through the home-sick times. My fiancée Andrew Burwood who has supported and

encouraged me all the way through this degree and who has made this Canadian experience such an amazing one.

For Peter William Brockett and Sidney James Walker

1. INTRODUCTION AND LITERATURE REVIEW

1.1. Rationale

A combined aboveground-belowground approach to community and ecosystem ecology is enhancing our understanding of the regulation and functional significance of biodiversity and of the environmental impacts of human-induced global change phenomena (Wardle *et al.*, 2004). Established macro-ecological theory and observed biogeochemical processes are used as a basis for integrating the complex and relatively new field of soil belowground ecology with aboveground processes. Micro-organisms provide the link between these biogeochemical processes and the ecology of the soil system.

Increasing interest in the ecology of microbial communities can be attributed in part to an understanding that these organisms have direct effects on ecosystem processes (Beare *et al.,* 1995; Horner-Devine *et al.,* 2004; Fierer and Jackson, 2006) and also to the development of novel molecular-based and biochemical techniques which allow us to characterize these communities with increasing clarity and rapidity (Kirk *et al*., 2004; Neufeld and Mohn, 2006). Soil microbial communities are of particular interest as the soil environment is extremely heterogeneous and a large number of ecological niches allow a diverse community of soil micro-organisms to persist (Standing and Killham, 2007).

Cited differences between micro and macro organisms, such as rate of population growth, dispersal ability, abundance, diversity, the unique aspects of microorganisms' biology and the relatively large scales of time and space over which most microorganisms are studied, do not necessarily prevent the application of existing ecological theory to microorganisms (Prosser *et al.,* 2007). It is important to try to apply the new and growing tool-box of microbial techniques to tried-and-tested macro-ecological theory in belowground systems. The challenge facing soil microbial ecologists is to match the appropriate theoretical approach to the organism, system, scale and question of interest (Prosser *et al.,* 2007).

1.2. Literature review

1.2.1. The role of microorganisms in forest ecosystems

Micro-organisms[1] play a key role in the processes which sustain forest ecosystems, such as litter decomposition, humification, and the mineralization of Carbon (C) and Nitrogen (N). Litter decomposition involves the combined action of the decomposer community, which is composed predominantly of microorganisms, in breaking down complex organic material of plant origin (detritus) (Swift *et al.,* 1979). Some of the products from this breakdown process are utilized by the decomposer community for respiration and growth; this is termed secondary production (Swift *et al.,* 1979). The mineralization of the organic material by microorganisms converts C and nutrients from an organic (non-plant available) to an inorganic (plant-available) form. Competition between microbes and plants for limiting nutrients is often intense (Prescott, 2005a). A proportion of the nutrients and C which have been mineralized are subsequently immobilized by incorporation into microbial biomass (Swift *et al.,* 1979). Whether N, and other nutrients essential for plant growth, are immobilized or accumulate in the soil depends on the associated microorganisms' requirement for growth (Paul and Clark, 1989; Prescott, 2005a). Eventually the decomposers die and their carcasses enter the detritus compartment and are acted upon by other decomposers; this ensures the recycling of carbon and nutrients within the system (Swift *et al.,* 1979).

Although microbially-bound nutrients are temporarily unavailable, such short-term sequestration can prevent longer-term sequestration within recalcitrant materials in the soil organic matter (SOM) (Prescott *et al.* 2000b). These more recalcitrant products are called humic substances or humus. Humic substances are dark-coloured amorphous colloidal products which can be formed from a number of different parent substances (Swift *et al.*, 1979; Oxford University Press, 2004). Humification is the accumulation of these more resistant end-products via a variety of reactions taking place under natural conditions, either directly or indirectly through biological processes (Swift *et al.*, 1979).

[1] For the purpose of this thesis I will be referring to soil bacteria and fungi when I use the term 'soil microorganisms', and not to algae, viruses, and archaea which are also members of this group.

The recalcitrance of these substances means that they are not easily utilized for energy or growth products by soil microorganisms and their degradation requires a higher degree of functional specialization.

1.2.2. Microbial community function and structure

Microbial community function can be inferred from rates of ecosystem processes such as litter decomposition and N mineralization, or directly measured as microbial respiration, nutrient and carbon assimilation and enzyme activity. Litter decomposition usually proceeds through a series of well-characterized stages involving a succession of decomposer communities with different degrees of enzymatic competence; the activities of the various functional groups are temporally and spatially separated from each other, operating at different depths in the soil profile and at different times. The activity of many of these extra-cellular soil enzymes can be measured with a high degree of accuracy (Nannipieri *et al.,* 2002). Microbial biomass is the primary source of extra-cellular enzymes in soil (Tabatabai and Fu, 1992) and measuring the activity of these enzymes in relation to microbial biomass is one way of investigating the efficiency of the microbial community.

Several processes, such as carbon mineralization, are carried out by a wide variety of different microorganisms and this functional redundancy or resilience is a feature of most soil systems (Nannipieri *et al.,* 2002). The combination of functional redundancy in soil ecosystems, the huge biodiversity of the soil microbial community, and the lack of a consensus regarding a microbial species concept ensure a complex relationship between microbial community function and structure (or microbial community composition[2]). This relationship is receiving increasing amounts of interest, partly because the last decade has seen the rapid development of phylogenetic and other molecular-based techniques which give an unprecedented view of the structural diversities of such communities. Previously microbial ecologists had to rely on culture-dependent techniques in order to characterize microbial community structure. Culture-based methods still play a role in physiological and functional studies but are less useful

[2] For the purpose of this thesis microbial community composition will refer to microbial community function and structure.

for measuring ecological abundance and diversity, as it is possible to culture only a relatively small number of micro-organisms in the laboratory (Kirk *et al*., 2004). There are now a wealth of techniques which can be employed to characterize both the function and structure of microbial communities and these novel techniques have expanded the range of ecological questions that can now be addressed (Neufeld and Mohn, 2006). Those studies which integrate both functional and structural measures of microbial community characterization with measures of soil environmental processes and ecosystem functioning are termed 'polyphasic' (Torsvik and Øvreås, 2007; Thies, 2007).

1.2.3. External drivers of microbial community function and structure

"Mineralization and immobilization of inorganic nutrients by microbes, the complexing of nutrients into soil organic matter (SOM), and the relationship of these processes to factors such as litter chemistry, climate and endogenous site characteristics inter-relate to form a complex system which dictates the availability of nutrients at a particular site" (Binkley and Hart, 1989) (Figure 1.1).

Climate

Microbes have been shown to exhibit temperature and moisture respiration optima and therefore we expect climate (at a regional scale) to have an observable effect on microbial community composition or rates of processes controlled by microorganisms. Temperature directly affects the rates of physiological reactions and has many indirect effects on soil biological activity through temperature-induced changes to other aspects of the soil physiochemical environment (Killham, 1994; Voroney, 2007). The direct effect of solar radiation on soil microbial communities is mediated by diurnal and seasonal effects as well as factors such as vegetation status and composition, moisture and soil depth. In most soils with a mesophilic microbial community, there is an approximate doubling of microbial activity with each 10 ˚C rise in temperature between 0˚C and 30-35 ˚C; this is called the "Q_{10} effect" (Killham, 1994). Soil temperature often co-varies with other factors that affect microbial community composition such as lignin content, C chemistry, toughness, and initial nutrient content of the litter (Prescott, 2005a).

Soil water directly affects the growth and activity of soil microorganisms and mediates its effects through the supply of nutrients to the organisms in question, the soil aeration status, the osmotic pressure, and the pH of the soil solution (Paul and Clark, 1989;

Killham, 1994). Where water is non-limiting, biological activity may depend primarily on temperature, but as soils dry, moisture is more controlling of biological processes than is temperature (Voroney, 2007). These two environmental influences do not affect microbial activity in linear fashion but display complex, non-linear, inter-related effects that likely reflect the individual responses of the various microorganisms and their associated enzymatic systems (Voroney, 2007).

In forests of British Columbia (B.C.), moisture is the factor most highly correlated with litter decomposition rates (Prescott *et al.*, 2004) and can therefore be expected to be correlated with microbial community function and perhaps with microbial community structure. There is large variation in available moisture in B.C. forests, due to the Province's size, maritime influences and varied topography. Prescott *et al.* (2004) found a significant negative correlation between pine needle litter decomposition and potential evapo-transpiration and a positive correlation with precipitation. The wettest zones in B.C. had the greatest mass loss and driest had the least mass loss.

At high latitudes, climate is thought to play a larger role in nutrient availability and long-term ecosystem productivity than in other ecosystems (Prescott *et al.*, 2000b). High levels of mor humus accumulation in northern sites is due to climatic limitations on microbial community activity (Prescott *et al.* 2000b). The SOM provides a long-term nutrient pool for the ecosystem, but immobilizes large amount of available nutrients by complexing them within recalcitrant compounds.

Some studies have observed direct correlations between microbial community composition and regional climate gradients. Hackl *et al.* (2005) investigated the influence of regional climate on microbial community characteristics in native European forests. The authors studied zonal forests, where the vegetation communities reflect regional climate, and also azonal forests, which exhibit extreme site conditions and therefore altered vegetation communities from those predicted by the climate gradient. Using Phospholipid Fatty Acid (PLFA) analysis to characterize the microbial community structure and a number of techniques for assessing microbial biomass, they found that the microbial communities in the zonal forests were similar to each other and were strongly influenced by a gradient of mean annual temperature. Soil water availability was found to correlate with microbial community structure in the azonal forests.

Plant litter and root exudates

Climate is the main factor determining the composition of any ecosystem's vegetation climax community. The successional stage and the more detailed composition of the vegetation at a site scale are influenced by the disturbance history and site characteristics. The composition of vegetation at a site in turn influences the soil environmental conditions and so the habitat for soil microorganisms. Plants alter the soil environment by releasing root exudates and litter and by taking up available nutrients and water. The chemical composition of the exudates and litter has differential effects on the various components of the microbial community, depending on the microorganism's functional niche and associated environmental preferences.

Different tree species produce litter and root exudates of varying chemical composition and so provide a range of carbon sources for heterotrophic microorganisms (Priha *et al.*, 2001). Litter chemistry is correlated with early rates of litter decay (Prescott, 1996; Prescott, 2005a) and litter from different species often exhibit different initial decay rates (Prescott *et al.*, 2000a). This is because each chemical fraction will have an associated decomposer community and the labile or leachable fractions are quickly degraded (Prescott, 2005a). Once the litter has been humified it is a much poorer substrate for decomposing micro-organisms; it is relatively low in carbohydrates and therefore low in available C for microbial energy requirements and so will be decomposed at a much slower rate (Prescott, 2005a). However, litter decomposition rates from different tree species eventually converge (Prescott *et al.*, 2000a, Prescott *et al.*, 2003). How long it takes for this asymptote to be reached is influenced by the activities of soil macrofauna (Prescott, 2005b), climatic variables, litter quality, and especially by the availability of labile C to microbial communities (Prescott, 2005a).

The relationship between ecosystem processes and plant species composition has been investigated in a number of studies, but the findings are often contradictory and appear to be context-dependent. Welke *et al.* (2005) measured the influence of stand composition on nutrient chemistry in pure and mixed stands of Douglas-fir and paper birch in the Interior Cedar Hemlock Biogeoclimatic Ecosystem Classification (BEC) zone of B.C. They found significantly more N mineralization under pure birch stands than under Douglas-fir, with mixed-woods having an intermediate value. Concentrations of forest floor total N, exchangeable potassium and magnesium and pH were also

consistently higher. The authors related this effect to the higher nutrient concentrations of birch foliar litter. However, Thomas and Prescott (2000) found litter chemical characteristics to be poor predictors of N mineralization in a laboratory experiment using litter from three tree species. They found that N mineralization was positively correlated with forest floor total N concentration. Jerabkova *et al.* (2006) found consistently higher pH and associated higher extractable P under deciduous compared to mixed-wood and coniferous stands in the boreal forests of northern Alberta, but could not relate this directly to tree species composition.

Other studies have related tree species composition directly to that of the soil microbial community. Priha *et al.* (2001) observed a tree species effect on microbial biomass and C mineralization across adjacent pine, spruce and birch forests. This effect was modified by differences in site fertility. When soil chemical parameters were held constant Lejon *et al.* (2005) found that microbial C biomass as a percentage of total organic C was lowest under Douglas-fir compared to Norway spruce and native forest (dominated by oak and beech) and that the community profile, as characterized by genetic profiling, was unique under the different forest types. As the differences in soil pH, C:N ratio, and total organic C and N across the forest types were negligible, the authors concluded that tree species (variance in litter quality and root exudates) was the main influence on the composition of the microbial community. However, in pure stands of four tree species on northern Vancouver Island, Grayston and Prescott (2005) found that forest floor layer (fermentation vs. humus layer) had the greatest overall effect on microbial community structure, followed by site, and tree species had the least effect.

Other site variables

The biogeochemical process or mechanism of interest (and therefore the scale of investigation) drives the choice of site variables to be measured in any aboveground-belowground study (Prosser *et al.*, 2007). Patterns in soil microbial community composition have been identified at a range of scales. Grayston *et al.* (2001) observed that vegetation type and site were the main factors influencing spatial variation in soil microbial carbon and microbial respiration in temperate grassland ecosystems at a scale of metres. Stevenson *et al.* (2004) found that the ability of soil microbial communities to catabolise a range of substrates depended on land-use type, so patterns in community function could be observed at a scale of kilometres. Bengston *et al.* (2007) found spatial

patterns in microbial biomass, nutrient availability, and soil moisture content were auto-correlated at scales up to 1 km. They hypothesized that observed over-lapping spatial patterns in the forest floor and mineral layers were related directly to the hydrological processes in the soil or indirectly to soil moisture effect on nutrient availability.

In soil ecosystems there is usually high heterogeneity of resources and variation in microclimate over small distances. However, a number of studies have found correlations at a site scale between one or more site variables and microbial community composition. Trofymow (1998) found that variations in endogenous site characteristics affected soil microbial community composition in coastal temperate rain forests in B.C.; forest floor microbial biomass, basal respiration and substrate induced respiration were significantly correlated with soil C concentration and soil moisture in the forest floor. Decker *et al.* (1999) found that soil microbial community activity, measured using potential enzyme activity as a functional index, increased with increasing nutrient availability and with decreasing organic matter content in a mature oak woodland. In a study on Vancouver Island Leckie *et al.* (2004) found no statistical differences between composited samples and un-composited samples for microbial biomass estimates, PLFA biomarker concentration values, and other forest floor measurements (e.g. pH). They concluded that composite sampling within a site is likely to be suitable for characterizing microbial communities despite high site heterogeneity.

Resource availability and microclimate also vary with depth in the soil profile, and soil microbial communities can be expected to change accordingly. Soil Organic Matter (SOM) concentration, nutrient availability, soil temperature, and moisture are just some of the variables which change with depth. In an study which manipulated the temperature of different soil layers and controlled for other physiochemical factors, Blume *et al.* (2002) found the surface soil horizons had significantly higher microbial activity (measured using 3H-acetate incorporation into phospholipids) than the sub-surface horizons and that shifts in microbial community function in each layer were dependent on the incubation temperature. Jörgensen *et al.* (2002) found, at soil depths of 0-140 cm, microbial biomass C and N, concentrations of the adenylates adenosine triphosphate (ATP), adenosine diphosphate (ADP) and adenosine monophosphate (AMP), and the basal respiration rate all declined significantly with depth.

Carbon availability and the proportion of C from plant-derived sources (as opposed to SOM-derived sources) decline with soil depth (Fierer *et al.*, 2003; Kramer and Gleixner, 2008). Kramer and Gleixner (2008) found that Gram-positive bacteria preferentially utilize different SOM-derived-C and Gram-negative bacteria preferentially utilize plant-derived-C. These results agree with those of Fierer *et al.* (2003) who found that abundance of Gram-negative bacteria (measured with PLFA analysis) declined with depth along with total microbial biomass and abundances of fungi, and protozoa, whereas, Gram-positive bacteria and actinobacteria tended to increase in proportional abundance with increasing soil depth. Differential responses of microbial groups to other external gradients are explored in the next section.

1.2.4. Differential responses of microbial groups to external gradients

Different components of the microbial community respond to climate and site gradients in different ways; for example there is high variation in fungal-to-bacterial biomass ratios in forested ecosystems along resource and microclimate gradients. The influence of nutrient availability on forest floor microbial community structure was demonstrated in forests on northern Vancouver Island (Leckie *et al.* 2004): microbial community structure, characterized with PLFA analysis and Denaturing Gradient Gel Electrophoresis (DGGE), differed among forest types; fungal PLFA signatures were more abundant in nutrient-poor cedar-hemlock forests and bacterial PLFAs were proportionately more abundant in richer hemlock-amabilis fir forests. Grayston and Prescott (2005), using similar analysis techniques, also found fungal biomass to be higher on nutrient-poor sites than nutrient-rich sites on southern Vancouver Island.

Acidity has also been shown to differentially affect fungal and bacterial community composition in forest soils. Högberg *et al.* (2007) examined changes in microbial biomass and shifts in the relative proportions of different groups of soil microorganisms across a natural pH and N-supply gradient in a Fennoscandian boreal forest. The microbial community structure (characterized by PLFA analysis) changed along the natural biochemical gradients, with fungal biomass increasing with decreasing pH and increasing C:N ratio, and bacteria showing the opposite trend. They suggested that the fungal community was better able to utilize recalcitrant C sources, acclimatize to nutrient-poor conditions and tolerate/compete in lower pH conditions than bacteria.

Microbial communities can be variously described based on phylogenetic characteristics, functional traits, guild, habitat preference, growth strategy and by many other classifications. It is essential to understand how these community characteristics relate to observed macro-ecological and biogeochemical processes and at what scale these relationships manifest themselves in order to link observed aboveground processes to the belowground ecosystem (Hodkinson and Wookey, 1999; Neufeld and Mohn, 2006; Kandeler, 2007).

1.3. Introduction to the study

This study investigates the shifts in microbial community function and structure (community composition) along a regional climate gradient, and the relationship between community composition, measured site variables and regional climate (Figure 1.1). It is part of a larger study investigating the relationships among regional climate, site factors, tree species, soil organisms, and nutrient cycling processes. A variety of forest types with distinct regional climates were selected based on the provincial Biogeoclimatic Ecosystem Classification (BEC) system (*Pojar et al.,* 1986), key site factors were characterized, and forest floor and mineral soil samples were collected from each site. Phospholipid fatty acid analysis was used to investigate the structure of soil microbial communities and total soil microbial biomass, and extra-cellular enzyme assays established the functional potential of the soil microbial community at each site. The results from this study will be used to explore relationships and derive hypotheses regarding the interactions between regional climatic variables, site endogenous factors and soil microorganisms.

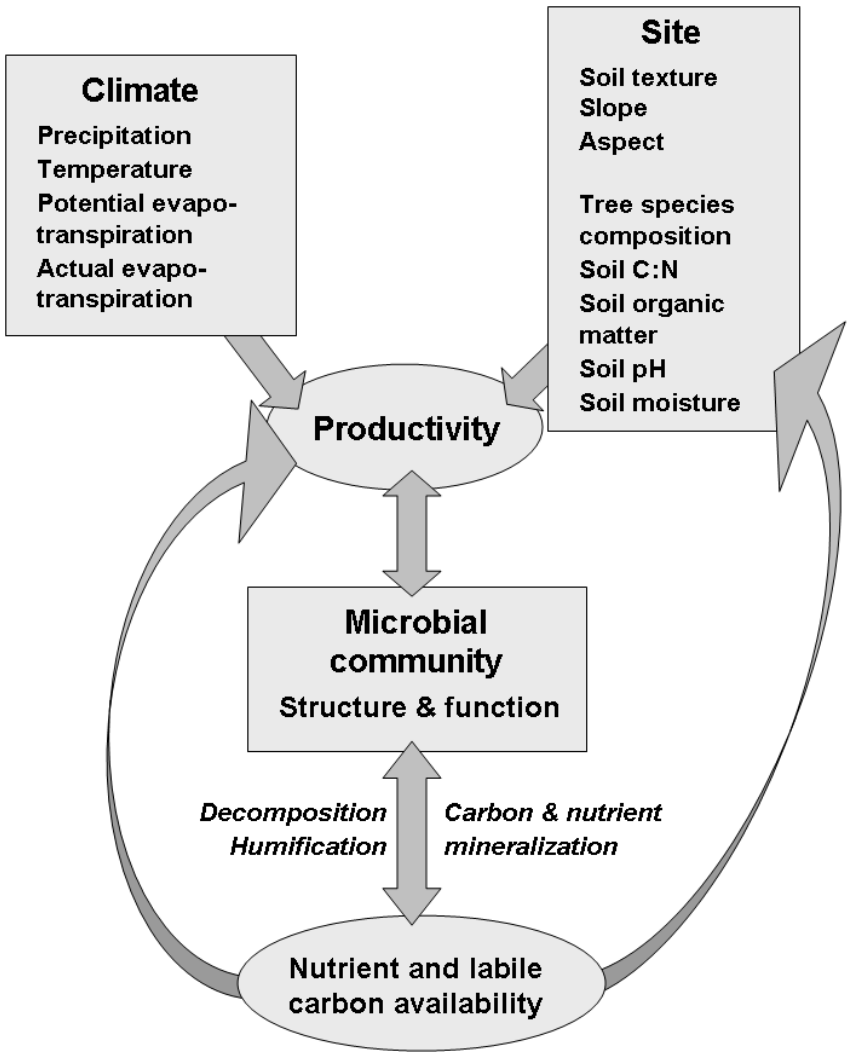

Figure 1.1. Visualization of the role of microbial communities in relation to biogeochemical processes in forest soils.

1.4. Specific hypotheses

Financial- and time-limitations often require researchers to reduce the number of samples collected and analyzed, and compositing the replicate samples is one way of achieving this. It is important that the variation in the individual samples is not obscured by this practice. **Hypothesis one:** Analysis of composite soil samples for microbial community function and structure provides the same results as analysis of individual soil samples.

This study covers the change in microbial communities and environmental factors over one field season. Changes in microbial community characteristics have been observed over annual time scales so samples were taken twice during the field season to try and capture some of this variation. **Hypothesis two:** Soil microbial community structure and function are significantly different in spring and summer.

Despite local-scale heterogeneity of site characteristics and associated high variability in microbial community composition, previous studies suggest that it is possible to detect variation in microbial community composition at a regional scale due to variation in climate. **Hypothesis three:** It is possible to separate forest types along a regional climate gradient based on microbial community function and/or structure.

Hypothesis four: A set of measured environmental variables can be shown to significantly correlate with microbial community function and structure across a regional climate gradient. Prescott *et al.* (2004a) found that the available moisture influenced litter decomposition at the same study sites. **Post-hoc hypothesis:** If Hypothesis four is not rejected; moisture is highly correlated with microbial community function and structure.

Changes in soil depth are associated with variations in resource availability and microclimate. Such variations would be expected to influence microbial community composition and therefore organic soil layers should be analyzed separately from mineral layers. **Hypothesis five:** Analysis of soil microbial structure and function will show separation of the mineral layers from the organic layers.

2. METHODOLOGY

2.1. Location of study sites along a climate gradient

Seven study locations were chosen from those sampled by Prescott *et al.* (2004) (Figure 2.1 and Table 2.1)[3]. The Biogeoclimatic Ecosystem Classification (BEC) system (Pojar *et al.*, 1986) was used to define these locations along a regional climatic gradient. The British Columbia Ministry of Forest's BEC system is widely used in B.C. as a common framework for understanding terrestrial landscape ecology in the Province. The BEC system characterizes and describes the major forest and range ecosystems in B.C. as influenced by regional climate and based on the principals of climax and succession and ecological equivalence. The broad units (zones) are divided into subzones, variants, and phases based on topographic and edaphic influences. Zonal sites are those which are representative of the regional climate. Three zonal site replicates, approximately 1 km apart[4], were chosen at each location.

The ClimateBC web-based program (Wang *et al.,* 2006) was used to establish climate variables for each of my locations in conjunction with BEC zone climate data from the Environment Canada website (http://climate.weatheroffice.ec.gc.ca), Meidinger and Pojar (1991); Hope *et al.* (2003), Kishchuk (2004), and Prescott *et al.* (2004). ClimateBC is a visual basic program which calculates seasonal and annual climate variables for specific locations based on latitude, longitude and elevation (elevation is an optional input) (Wang *et al.,* 2006). The ClimateBC program coverage includes my study locations in British Columbia and Alberta.

[3] The EMEND site was not part of this study but Jerabkova *et al.* (2006) studied litter decomposition at this site.

[4] Except in the Ponderosa Pine location, where the distances were smaller due to the size of the ecological reserve, and at the Mountain Hemlock location, because of topographical constraints.

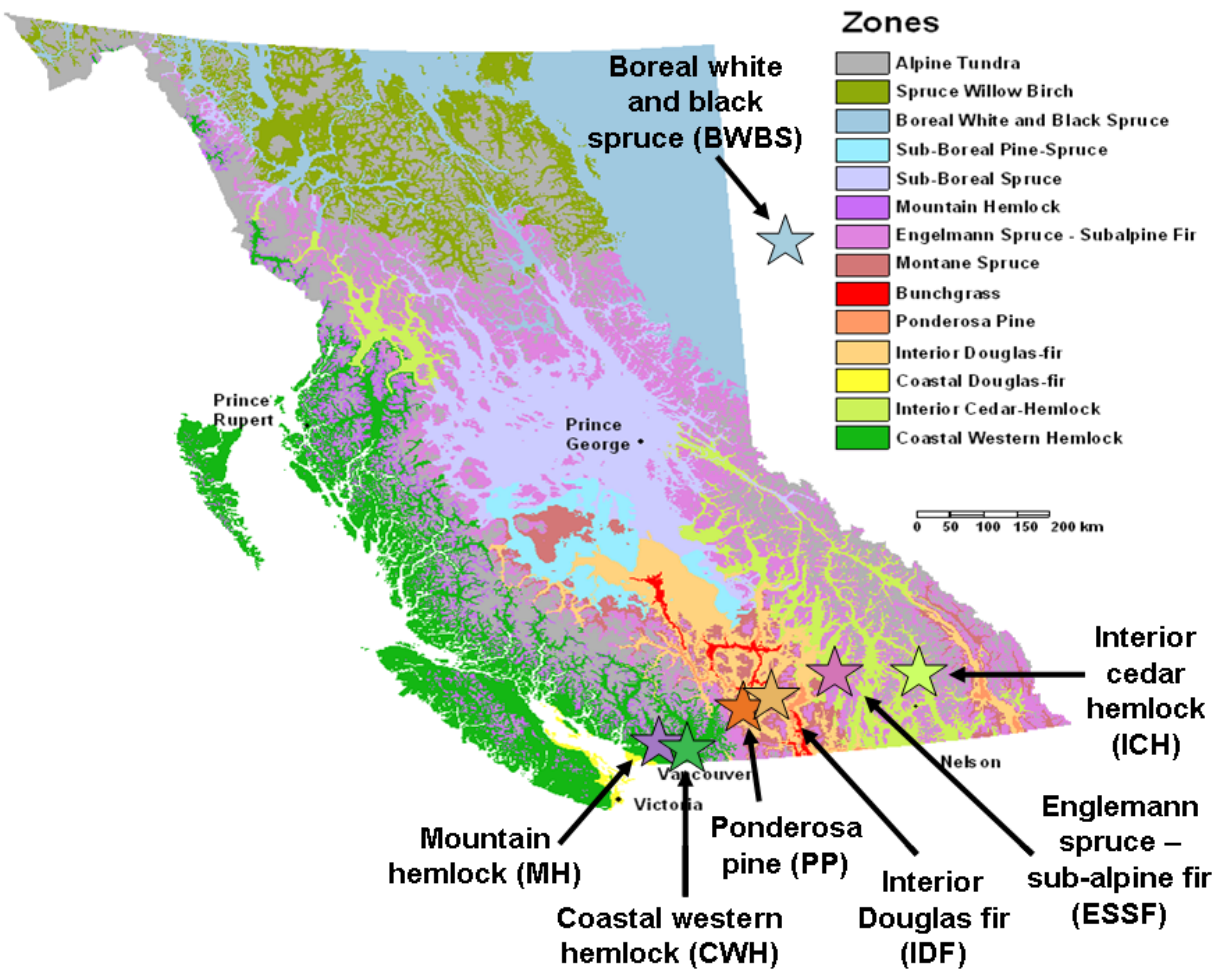

Figure 2.1. Map of the biogeoclimatic zones of British Columbia showing the seven study locations. Map based on an original from the British Columbia Ministry of Forests, 1995.

Table 2.1. Study site characteristics.

Name	BEC zone	Subzone	Elevation (m) of sample sites	Latitude (degrees) of sample sites	Longitude (degrees) of sample sites	Mean annual temperature (degrees centigrade)	Mean annual precipitation (mm)
Malcolm Knapp Research Forest	Coastal Western Hemlock (CWH)	vm1 (very wet, maritime)	240	49.22	122.34	5.2 to 10.5	2787
Sicamous Research Forest	Englemann Spruce – Sub-alpine Fir (ESSF)	wc2 (wet, cold)	1700	50.50	119.55	-2.0 to 2.0 (1.2)	400 to 2200 (930)
Mount Seven Research Forest	Interior Cedar Hemlock (ICH)	mk1 (moist, cool)	1200	51.17	116.56	2.0 to 8.7	500 to 1200
EMEND	Boreal White and Black Spruce (BWBS)	cold and dry[5]	677-880	56.44 to 56.51	118.19 to 118.27	–2.9 to 2.0	330 to 570
Cypress Park	Mountain Hemlock (MH)	mm (moist, maritime)	Approx. 1500	49.23	123.15	0 to 5	2916
Opax Mt (Mud Lake)	Interior Douglas Fir (IDF)	xh (xeric, hot)	1100	50.49	120.28	1.6 to 9.5	379
Skihist Ecological Reserve	Ponderosa Pine (PP)	xh (xeric, hot)	175	50.22	121.51	4.8 to 10	390

Information from BC Ministry of Forests website (http://www.for.gov.bc.ca/hfd/pubs/Docs/Rr/Rr24.htm); Environment Canada website (http://climate.weatheroffice.ec.gc.ca); Meidinger and Pojar (1991); Hope *et al*. (2003); Kishchuk (2004); and Prescott *et al.* (2004), and ClimateBC (Wang *et al.,* 2006).

[5] This site is in Alberta, so no BEC subzone has been assigned.

The chosen sites are mature forests which have not been exposed to any direct anthropogenic disturbance in recent history.

The **Ecosystem Management Emulating Natural Disturbance (EMEND)** site is located approximately 90 km northwest of the town of Peace River in northern Alberta. The ecosystem is equivalent to those classified in the Boreal White and Black Spruce (BWBS) BEC zone in B.C. Elevation ranges from 677 to 880 m above sea level and latitude from 56.44 to 56.51 degrees. Soils are primarily Gray Luvisols with minor occurrences of Brunisols, Gleysols, and Solonetzic soils derived from similar glaciolacustrine and glacial-till parent material is containing few coarse fragments (Kishchuk 2004). The site is cold (mean annual temperature is -0.3 ˚C, with mean January and July temperatures of –18.8 and 14.6 °C, respectively) and dry (mean annual precipitation is 433 mm) (Jerabkova *et al*., 2006). Soils are well-drained and exhibit little pedogenic variation across sites (Jerabkova *et al*., 2006). The dominant tree species at the study sites were white spruce *(Picea glauca)* and *Populus* species. The under-storey was not formally surveyed, but contained pricky rose *(Rosa acicularis),* Wood's rose *(Rosa woodsii),* saskatoon *(Amelancier alnifolia),* and various mosses and lichens.

Sicamous Research Forest is a silvicultural systems trial in the Engelmann Spruce-Subalpine Fir (ESSF) zone, in subzone wc2 (Pojar *et al.*, 1986). Elevation is approximately 1700 m above sea level and latitude is 50.50 degrees. The ESSF is relatively wet and cold compared to other BEC zones in B.C. with approximately 930-mm mean annual precipitation and a mean annual temperature of 1.2 ˚C (Prescott *et al*., 2003). The soils are derived mostly from morainal deposits laid down during the last glacial period. Soils are primarily Humo-Ferric Podzols with a discontinuous Ae layer and a Hemihumimor humus form (Hollstedt and Vyse, 1997). The soil texture varies, but is predominantly a sandy loam with 25–40 % coarse fragment content (Hollstedt and Vyse, 1997). The underlying bedrock is primarily granitic gneiss (Hollstedt and Vyse, 1997). The dominant tree species at the study sites were sub-alpine fir *(Abies lasiocarpa)* and Engelmann spruce *(Picea engelmannii)*. The under-storey was not formally surveyed, but contained rhododendron species, *Vaccinium ovalifolium,* and *Valariana* species.

Opax Mountain (**Mud Lake)** is part of the Opax Mountain Silvicultural Systems Trial in the dry Interior Douglas Fir (IDF) zone near Kamloops, BC. The site is xeric and hot (xh)

relative to other sites in the IDF zone (Pojar *et al.*, 1986). Elevation is approximately 1100 m above sea level and latitude is 50.49 degrees. Soils are loam and sandy loam textured Orthic Gray Luvisols and Orthic Eutric Brunisols, with a range in average forest floor thickness of 2.5–4.0 cm and a Hemimor humus form (Hope *et al.,* 2003). The dominant tree species at the study sites was interior Douglas-fir *(Pseudotsuga menziesii* var. *glauca).* The under-storey was not formally surveyed, but was observed to be sparse containing some grasses.

Malcolm Knapp Research Forest is in the Coastal Western Hemlock (CWH) vm1 (very wet maritime) subzone (Pojar *et al.*, 1986). Elevation is approximately 240 m above sea level and latitude is 49.22 degrees. Mean monthly temperatures for the coldest and warmest months are 1.4˚C and 16.8˚C. Mean annual precipitation is 2140 mm (Klinka and Krajina, 1986). The soils are Orthic and Sombric Humo-Ferric Podzols of gravelly loamy sand over a glaciofluvial blanket over glacial marine deposits (Carter and Lowe, 1986). The dominant tree species at the study sites were Douglas-fir (*Pseudotsuga menziesii* var. *menziesii*) and western redcedar (*Thuja plicata*). The under-storey was not formally surveyed, but contained many species of shrubs and forbs at one site, including devil's club *(Oplopanax horribilus)*, and salal *(Gaultheria shallon)* and mainly ferns and mosses at the other two sites.

Mount Seven is located in the Interior Cedar Hemlock (ICH) zone, in the mk1 (moist and cool) subzone (Pojar *et al.*, 1986) near the town of Golden, B.C. The dominant tree species at the study sites were interior Douglas-fir *(Pseudotsuga menziesii* var. *glauca)* and Engelmann spruce *(Picea engelmannii)*. Elevation is approximately 1200 m above sea level (its high elevation accounts for the lack of *Thuja plicata* and *Tsuga heterophylla* (Mike Curran, personal communication)). Latitude is 51.17 degrees. Surface soils are predominantly silt loam and loam textured over calcareous parent material with a high pH (Quesnel and Curran, 2000). The under-storey was not formally surveyed.

Cypress Park is in the Mountain Hemlock (MH) BEC zone. The total average yearly rainfall from 1954 to 1990 for nearby Hollyburn Ridge is 2115.4 mm. Mean annual temperature ranges from 0-5 ˚C. The highest daily maximum temperature occurs in July and August. The coldest of the daily minimum temperatures occurs in December and January (CEAA, 2006). Elevation is approximately 1500 m above sea level and latitude is 49.23 degrees. The dominant tree species at the study sites were mountain hemlock

(Tsuga mertensiana) and yellow-cedar *(Chamaecyparis nootkatensis)*. The under-storey was not formally surveyed, but contained *Vaccinium* and moss species.

Skihist Ecological Reserve is in the Ponderosa Pine (PP) xh (xeric and hot) BEC subzone (Pojar *et al.*, 1986). Elevation is approximately 175 m above sea level and latitude is 50.22 degrees. The dominant tree species was ponderosa pine *(Pinus ponderosa)* with some interior Douglas-fir *(Pseudotsuga menziesii* var. *glauca).* There was little to no under-storey present, except for *Pinus ponderosa* seedlings.

2.2. Sampling design

Five random soil sub-samples were taken from the fermentation (F) layer, the humic (H) layer and from the first 10 cm of the mineral (min) layer (horizon A) from each of three 10-m^2 site replicates in each BEC zone location (Table 2.2). Sampling was carried out twice in 2006 – once during the spring flush and once in mid-summer. The sampling times took into account the seasonal phenology of the seven forest sites; sites situated at higher elevations and latitudes were sampled later in the spring than those at lower altitudes and latitudes. Site-specific literature was used to identify approximate dates for the initial top-soil thaw at applicable sites, and the first sampling was timed for just after the thaw (if applicable). Each location was sampled again 60 days after the first sampling (within 1 or 2 days). Sub-samples of the individual layers were composited for each site. Some of the sub-samples from the spring sampling at the ICH location were kept separate and used to test the validity of compositing samples for microbial analysis (see Methodology section).

Table 2.2. Break-down of sampling strategy.

Hierarchical level	**Number of samples**
BEC zones/ locations	7
Site replicates for each location	3
Sub-samples at each site replicate	5 - composited
Soil layers at each sub-sample location	3
Sampling times	2
Total samples	126 (+ 15 not composited)

2.3. Field measurements

Slope aspect, slope angle, and soil temperature at 10-cm depth were recorded at each site (soil temperature was recorded at both sampling times). The species of any mature trees which had canopy overhanging the sampling area and their distance from the sampling points were recorded (a more detailed vegetation and soil diagnostic analysis and measurements of litter inputs to the sites will be carried out by Ali Araghir in 2008 as part of a related project).

A number of climate variables were estimated for each location using the ClimateBC web-based program (Wang *et al.,* 2006). These values were compared to values in the literature and to those from the Environment Canada website. Mean annual temperature (MAT) (°C), mean annual precipitation (MAP) (mm) and actual evapo-transpiration (AET) rates were calculated for each location. MAT and MAP are the main variables describing a regional climate gradient, and AET is thought to be a good predictor of soil moisture influence on litter decomposition processes across a range of climates (Prescott, 2005a). The other variables calculated were mean warmest month temperature (MWMT) (°C), mean coldest month temperature (MCMT) (°C), temperature difference between MWMT and MCMT (continentality) (°C), mean annual summer (May to Sept.) precipitation (mm), annual heat:moisture index (MAT+10)/(MAP/1000)), and summer heat:moisture index ((MWMT)/(MSP/1000)).

Five replicate sets of PRS^{TM} available-nutrient probes[6] were incubated in the F, H, and mineral soil layers for 2 months (60 days +/- 1 or 2 days) at each sampling site. After incubation the probes were thoroughly cleaned in distilled and de-ionized water and sent to Western Ag's laboratory for analysis. PRS^{TM} nutrient probes provide information on available concentrations of a range of nutrients (NO_3^+, NH_4^-, Ca^{2+}, Mg^{2+}, K^+, $H_2PO_4^-$, Fe^{3+}, Mn^{2+}, Cu^{2+}, Zn^{2+}, B^{3+}, SO_4^{2-}, Pb^{2+}, Al^{3+}). The plastic-cased probes contain a charged ion-exchange membrane window (10-cm^2 surface area). One set of four sample replicate cation probes are positively charged and one set of four sample replicate anion probes are negatively charged. Inorganic (available) ions in the soil adsorb to the membrane. Soil water content and microbial activity play a role in

[6] Manufactured by Western Ag. Innovations, Saskatoon, SK.

adsorption of ions to the probes (Qian and Schoenau, 2002). After incubation Western Ag dissolve the membranes from the four replicate probes and the concentration of ions is determined for each sample. The NO_3^--N and NH_4^+-N contents within the PRS™-probe eluate are analysed colourimetrically using an autoanalyzer (www.westernag.ca/innov/). All remaining nutrient ion contents in the eluate are measured using inductively-coupled plasma spectrometry (www.westernag.ca/innov/). The units are in micro-grams of adsorbed ions per 10cm^2 of the membrane window per burial period (days).

Table 2.3. Measured site variables and sampling time.

Site variable	**Spring sampling**	**Summer sampling**
Particle size (% sand, silt, clay)	x	
%C	x	x
%N	x	x
Available nutrients (PRS™ probes)	incubated for whole period	
Soil temperature	x	x
Soil moisture	x	x
Slope angle	x	
Slope aspect	x	
Dominant tree species	x	
Distance of sample from nearest tree	x	
pH	x	x

2.4. Laboratory sample analysis

All soil samples were stored on ice in the field and then at 4 ºC in the laboratory for a short time until storage preparation. The soils were sieved through a 2-mm mesh immediately on return to the laboratory. They were then composited, except for some of the ICH spring samples which were kept aside as individual samples, and divided into two portions. One portion was stored at -20 ºC in preparation for chemical analysis and enzyme assays and the other portion was freeze-dried in preparation for phospholipid fatty acid (PLFA) analysis.

Samples for each of the three site replicates were composited by layer for chemical and physical analysis in the laboratory. The validity of compositing the five samples from each site replicate was tested by statistically comparing the values for microbial

community characteristics in individual sub-samples taken from the ICH spring sample with those from composited samples.

Total soil C and N concentration was determined by dry combustion-CO_2 determination and then by analysis in a Leco CHN2000 analyzer. Soil pH was recorded with a pH meter after the soil sample was vortexed in de-ionized water for 30 seconds and allowed to settle for 1 hour (adapted from Hendershot *et al.*, 1993). Gravimetric moisture content was measured by weighing soil samples before and after oven-drying at 105 ºC for 48 hours. Particle size analysis (% sand, silt, clay) was performed using a hydrometer method (after Sheldrick and Wang, 1993).

2.4.1. Microbial community structural analysis

The biomass and structure of the forest floor microbial communities were assessed by analyzing the ester-linked PLFA composition of the F, H, and mineral layer samples. Phospholipids are essential components of cell membranes which are rapidly degraded after cell death. Profiling of phospholipid fatty acids can be used to monitor overall changes in subsets of the microbial community using signature biomarkers (Kandeler, 2007). Individual PLFA signature biomarkers relate to an identified group of microorganisms (Table 2.4). PLFA provides an accurate picture of the relative proportions of each microbial component in the sample (Allison *et al.,* 2007). The resolution of the technique is fairly low and provides no information on the actual species present, but authors note its ability to discriminate between samples which may have community differences too subtle for other techniques to identify (Grayston *et al.,* 2004; Leckie *et al.,* 2004a).

Briefly, lipids were extracted from 0.5 - 1.5 g samples of mineral soil and forest floor using the procedure described by Bligh and Dyer (1959) and Frostegård *et al.* (1991). The separated fatty acid methyl-esters were identified and quantified by chromatographic retention time and mass spectral comparison on an Agilent 6890N GC with an Agilent 5973N mass selective detector. The column was a HP5 MS:30m with a 250µm i.d., and 0.25 µm film thickness. The peaks were identified using a standard qualitative bacterial acid methyl ester mix (Supelco; Sigma Canada, Mississauga, Ontario, Canada) that ranged from C11 to C20, and by referring to the template in Knief *et al.* (2003).

Fatty acids are designated as the ratio of the total number of C atoms to the number of double bonds, followed by the position of the double bond from the methyl end of the molecule. The prefixes “a” and “i” refer to anteiso- and isobranching. A 10Me indicates a methyl group on the tenth C atom from the methyl end of the molecule. Cyclopropyl fatty acids are indicated by the prefix “cy” (Pennanen *et al.,* 1999).

The abundance of individual fatty acid methyl-esters in each sample was expressed as nmol PLFA g^{-1} dry forest floor or mineral soil and also as nmol % of total sample biomass. PLFA provides information on the ratios of various microbial community components (e.g. Gram-positive to Gram-negative bacteria) and measurements of abundance including total soil microbial biomass (Leckie *et al.*, 2004b). One of the major advantages of using PLFA to characterize soil microbial community structure is that it provides an accurate picture of the viable cells present at the time of sampling (Kandeler, 2007). To avoid recording fatty acid signature 18:2ω6 from plant cells (especially concentrated in plant roots) in the samples (fatty acid signature18:2ω6 was used in this study to record presence of fungal biomass) the soil was sieved and visible roots and other plant material were removed (Bardgett and McAlister, 1999).

Table 2.4. Signature PLFAs chosen to characterize microbial community structure.

Fatty acid	Organism	Reference
i15:0	Gram-positive bacteria	Bååth *et al.* 1992
a15:0	Gram-positive bacteria	Zelles 1999
15:0	total bacteria	Federle 1986, Frostegard *et al.* 1993
i16:1_7c	Gram-negative bacteria	Zogg *et al.* 1997
15:0_6m/10Me16:0	actinobacteria	Allison *et al.* 2007, Bååth *et al.* 1992, Coleman *et al.* 1993,
i16:0	Gram-positive bacteria	Frostegård *et al.* 1993, Zelles 1999
16:1_9c	Gram-positive bacteria	Fritze *et al.* 2000
16:1_7	Gram-positive bacteria	Frostegård *et al.* 1993, Zelles, 1999
16:1_5c	arbuscular mycorrhizal fungi	Federle 1986, Frostegard *et al.* 1993, Zogg *et al.* 1997
16:0	Common	
i17:1_8c	Gram-negative bacteria	Zogg *et al.* 1997
16:0_6m/10Me17:0	actinobacteria	Federle 1986, Frostegard *et al.* 1993
i17:0	Gram-positive bacteria	Bååth *et al.* 1992
a17:0	Gram-positive bacteria	Bååth *et al.* 1992
cy17:0	Gram-negative bacteria	Bååth *et al.* 1992
17:0	total bacteria	Zogg *et al.* 1997
17:0_7m/10Me18:0	actinobacteria	Federle 1986, Frostegard *et al.* 1993
18:2_6,9	saprophytic fungi	Federle 1986, Frostegard *et al.* 1993
18:1_9c	Gram-positive bacteria bacteria & fungi	Allison *et al.* 2007, Federle 1986, Frostegard *et al.* 1993, Zak *et al.* 1996
18:1_7	Gram-negative bacteria	Frostegard *et al.* 1993, Zelles, 1999
18:1_5c	Gram-negative bacteria	Zogg *et al.* 1997
18:0	Gram-positive bacteria	Zogg *et al.* 1997
18:1_7c7m/10Me19:1_7c	total microbial biomass	
18:0_8m/10Me19:0	actinobacteria	Zelles 1999
cy19:0	Gram-negative bacteria	Federle 1986, Frostegard *et al.* 1993
19:0	internal standard	

2.4.2. Microbial community functional analysis

Litter decomposition usually proceeds through a series of stages involving a succession of decomposer communities with different degrees of enzymatic competence. The activities of the various functional groups are temporally and spatially separated from each other, operating at different depths in the soil profile and at different times. Enzyme bioassays were used to obtain potential activity rates of specific extra-cellular enzymes in the soil samples when incubated with a synthetic substrate at a consistent pH and temperature.

Over 100 enzymes have been identified in soil and there is likely to be more than one enzyme acting within each decomposition stage, therefore a representative suite of

enzyme assays was chosen to try to cover a suite of identified degradative processes (Table 2.5).

Table 2.5. Hydrolytic enzyme assays chosen for this study.

Name(s) of enzyme	Assay substrate	Natural substrate group	Reaction details	Class of enzyme	Product(s) of interest
Acid phosphatase/ phosphomonoesterase	4-MUB-phosphate	Organic molecules containing P	Mineralization of principal sources of organic P in litter under acidic conditions – hydrolyzes organic phosphoric mono-esters and di-esters. Activity greatest under conditions which favor N mineralization – strongly correlated with rate of release of both inorganic N and P to the soil solution. Activity often closely related to fungal presence.	Repressible	Inorganic P
Cellobiohydrolase	4-MUB-beta-D-cellobiosid e	Cellulose and other carbohydra te polymers	Catalyzes hydrolysis of 1,4-b-D-glucosidic linkages in cellulose and cellotetraose. Cleaves successive disaccharide units (cellobiose) in the 2nd stage of cellulose degradation. Activity correlates well with fungal presence. Degrades structural components with little N or P. Activity measured by the MUB technique is mainly fungal in origin.	Adaptive	Low molecular mass C compounds
Beta-1,4-glucosidase	4-MUB-beta-D-glucoside	Cellulose and other carbohydra te polymers	Third and final enzyme (rate-limiting) in chain which breaks down labile cellulose (cellobiose) into glucose. Catalyzes the hydrolysis of terminal 1,4-linked b-D-glucose residues from b-D-glucosides, including short-chain cellulose oligomers. Degrades structural components containing little N or P. Highest activity early in decomposition of litter. Produced by fungi and bacteria.	Adaptive	Low molecular mass C compounds

Name(s) of enzyme	Assay substrate	Natural substrate group	Reaction details	Class of enzyme	Product(s) of interest
Beta-1,4-xylosidase	4-MUB-beta-D-xyloside	Cellulose and other carbohydrate polymers	Involved in C transformation. Degrades xylooligomers (short xylan[7] chains) into xylose. Degrades structural components with little N or P. Both fungi and bacteria produce this enzyme.	Adaptive	Low molecular mass C compounds
Beta-1,4-N-acetylglucosaminidase (NAG)	4-MUB- N-acetyl-beta-D-glucosaminide	Chitin	Second enzyme in chain of three. Catalyzes the hydrolysis of terminal 1,4-linked N-acetylbeta- D-glucosaminide residues in chitooligosaccharides[8]. Hydrolysis of principle sources of organic N in litter. Chitin found in fungal cell walls. Mainly produced by fungi.	Constitutive	Low molecular mass C- and N-rich compounds
Phenol oxidase	L-3,4-Dihydroxyphenylalnine	Lignin	Also known as polyphenol oxidase or laccase. One of a suite of enzymes degrading lignin. Oxidizes benzenediols[9] to semiquinones[10]. White rot fungi is a major producer of phenol oxidase. Requires co-enzymes.		Simpler compounds derived from recalcitrant polymers
Peroxidase	L-3,4-Dihydroxyphenylalnine	Lignin	One of a suite of enzymes degrading lignin. Catalyzes oxidation reactions via the reduction of H_2O_2. It is considered to be used by soil microorganisms as a lignolytic enzyme because it can degrade molecules which do not have a precisely repeated structure. Basidiomycetes are a major producer of peroxidase. Does not require co-enzymes.		Simpler compounds derived from recalcitrant polymers
Aryl sulfatase	4-MUB-aryl-sulfatase	Organic molecules containing S	S mineralization from organic compounds. Have a stabilized, extracellular, organomineral-bound component.	Repressible	Inorganic S

7 Xylans are b-1,4-linked polymers of xylopyranose - a plant structural polymer less tightly associated with plant cell walls than cellulose.

8 Chitin-derived oligomers

9 Benzenediols, or dihydroxybenzenes, are aromatic C compounds in which two hydroxyl groups are substituted onto a benzene ring.

10 A semiquinone is a free radical resulting from the removal of one hydrogen atom with its electron during the process of dehydrogenation of a hydroquinone to quinone.

Name(s) of enzyme	Assay substrate	Natural substrate group	Reaction details	Class of enzyme	Product(s) of interest
Urease	Urea	Urea	Degrades urea. Routinely produced by cells. Always extracellular. Hydrolyzes urea into CO_2 and NH_3.	Constitutive and repressible	N containing compounds

From Miller *et al*. (1998); Møller *et al.* (1999); Decker *et al.* (1999); Burns and Dick (2002); Saiya Cork *et al.* (2002); Andersson *et al.* (2004); Stursova (2006); Killham and Prosser (2007); Weintraub *et al.* (2007).

The microplate enzyme bioassay methods of Marx *et al.* (2001) and Sinsabaugh *et al.* (2000; 2003) were used as a basis for developing a fluorimetric enzyme assay protocol modified for our laboratory. The determination of enzyme activity using 4-methylumbelliferyl (MUB) substrates is a highly sensitive technique (Kjøller and Struwe, 2002).

For the fluorimetric enzyme bioassays, 0.1-g of soil (from the F, H, or mineral layer) was ground in a pestle and mortar, from frozen, for 1 min. Fifty mL of 50-mM sodium acetate (pH 5) was added to buffer each sample, along with approximately thirty sterile glass beads. The buffered conditions standardize the method and stabilize the fluorescent intensity of the 4-MUB, which is highly dependent on pH (Marx *et al.,* 2001). The solution was shaken on high for 1 hour in a shaker, and then another 50-ml of buffer was added.

A 10-µM concentration of 4-MUB standard solution was prepared and kept at -20˚C (for up to a fortnight) until needed. One hundred millilitres of the 4-MUB synthetic substrates (200-µM) were prepared in sterile water and kept until needed (for up to a week, except for 4-MUB-phosphate which was prepared fresh for each assay).

Ninety six-well black microplates were prepared as outlined in Figures 2.2 and 2.3, with 16 replicates (16 wells) for each soil sample. A quenched standard, an optical abiotic control, and a substrate control were included with each set of plates. One set of plates was used for each substrate.

Enzyme name and plate replicate #	
Std	200ul buffer + 50ul 4-MUB std (on each sample plate)
Sub	200ul buffer + 50ul sub (on each sample plate)
S1	200ul soil suspension + 50ul sub
S1	200ul soil suspension + 50ul sub
S2	“”
S2	“”
S3	“”
S3	“”
…	…
…	….
…	….
….	….

Figure 2.2. Sample plate outline for fluorimetric enzyme bioassay. Standard (Std), Sample (S), Substrate (Sub).

Soil buffer plate replicate #	
Std	200ul buffer + 50ul 4-MUB std (on each SB plate)
Q1	200ul soil suspension + 50ul MUB std
SB1	200ul soil suspension + 50ul buffer
Q2	“”
SB2	“”
Q3	“”
SB3	“”
….	….
….	….
….	…..
…	….
BB	250ul buffer (on each SB plate)

Figure 2.3. Soil buffer plate outline for fluorimetric enzyme bioassay. Standard (Std), Quench (Q), Soil Buffer (SB), Background Buffer (BB).

The plates were placed in the dark at 20 ˚C in an incubator for different periods of time, as outlined in below, according to calibration curves obtained before the analysis.

- Phosphatase: 2 hours
- B-glucosidase: 3 hours
- NAG: 3 hours
- Sulfatase: 3 hours
- Xylosidase: 4 hours
- Galactosidase: 5 hours
- Cellobiohydrolase: 7 hours

At the end of the incubation a 20-µl aliquot of 0.5-M sodium hydroxide was immediately added to each well to alkalinize the solutions for optimum fluorescence readings (Marx *et al.*, 2001). The plates were then read in a Cytofluor™ II plate reader using the Cytofluor software program. Excitation was set at 360/40 nm, emission at 460/40-nm, gain at 50, mixing for 5 seconds on a "Costar" plate-type setting. Potential activity was calculated as nmol of substrate converted per hour per gram of sample and also as nmol of substrate converted per hour per gram dry-weight of sample. If the calculated value was negative it was assumed to be a zero-activity reading.

For the colorimetric enzyme bioassays 0.5-g of soil (from the F, H , or mineral layer) was ground in a pestle and mortar, from frozen, for 1 minute. Fifty millilitres of 50-mM sodium acetate buffer (pH 5) was added to each sample in a 250-ml conical flask along with approximately 30 sterile glass beads. The buffer ensures standardized conditions. The solution was shaken on high for 1 hour in a shaker, and then another 50-ml of buffer was added.

A 25-mM L-3, 4-dihydroxyphenylalanine (DOPA) solution was prepared in 50-mM acetate buffer (pH 5.0) and kept at -4˚C in the dark (for up to 24 hours) until needed. Ninety six-well clear microplates were prepared as outlined in Figure 2.4 with 16 well-replicates for each soil sample. A DOPA standard, an optical abiotic control, and a substrate control were included with each set of plates. One set of plates was used for

each substrate. For peroxidase assays only 10-µl of 0.3 % H_2O_2 was added to the substrate and sample wells after 50-µl of DOPA was added.

Enzyme name and plate #	
Sub	200ul buffer + 50ul DOPA
SB1	200ul soil suspension + 50ul buffer
S1	200ul soil suspension + 50ul DOPA
S1	“”
SB2	“”
S2	“”
S2	“”
….	….
….	….
…	….
BB	250ul buffer

Figure 2.4. Sample plate outline for colorimetric enzyme bioassay. Sample (S), Substrate (Sub), Background Buffer (BB).

The plates were placed in the dark at 20˚C in an incubator for 5 hours before taking readings for the peroxidase activity and for 18 hours before taking readings for the phenoloxidase activity. The plates were read in a Spectra Max 340 plate reader using the Softmax Pro software program. Wavelength was set to 460-nm with the “automix option” on. Potential activity was calculated as nmol of substrate converted per hour per gram of sample and also as nmol of substrate converted per hour per dry weight gram of sample. If the calculated value was negative it was assumed to be a zero-activity reading. Peroxidase values include phenol oxidase activity: To obtain peroxidase activity alone the phenol oxidase activity was subtracted from the initial peroxidase activity.

2.5. Statistical analysis

Data were tested for normality using a Kruskal Wallis test (Statistica, version 6) and by visually examining the data. The microbial community datasets and site variables dataset were multivariate non-normal. Transformations were tried, but failed to normalize the data, therefore all data was left untransformed and was analyzed using nonparametric techniques.

All analyses (except those employed in investigating hypothesis two) combined the microbial community data from both sampling times (refer to the results section 3.2). Tests were considered significant at $p \leq 0.05$. Enzyme activity on a dry-weight soil basis and PLFA signature concentrations divided by sample biomass and reported as ratios were found to provide consistent and reproducible results and so were used for all multivariate analyses.

Multivariate statistical techniques have been shown in many similar studies to improve the discriminatory power of techniques such as PLFA and enzyme bioassays (for example Bååth *et al.,* 1992; Leckie *et al.,* 2004a; Ritz *et al.,* 2004) and as an alternative approach to single indexes (Kandeler *et al.,* 1996). Multivariate statistical analysis methods were used for all analyses.

A nonparametric Multiple Analysis of Variance (MANOVA) ("PerMANOVA" PC ORD, version 5, 1999) (mixed model - one fixed effect and one nested) was used to test hypothesis one. Traditional multivariate analysis of variance (MANOVA) is generally inappropriate for analysis of ecological communities. Nonparametric MANOVA has no assumptions of linearity or multivariate normality and sums of squares are calculated directly from the distances among data points, rather than the distances from the data points to the mean (Anderson, 2001). Nonparametric MANOVA does assume independence of sample units and similar dispersions among sample units (McCune and Grace, 2002).

Multi-Response Permutation Procedure (MRPP) analysis and paired MRPP analysis (PC-ORD for Windows, McCune and Mefford, version 5, 1999) were used to test hypotheses two, three and five. MRPP and paired MRPP have been used in a similar and successful way by Stark *et al.* (2006) in their analysis of forest seed banks. MRPP is similar to Canonical Variates Analysis but it does not require the same assumptions of data normality to be satisfied. MRPP tests the hypothesis of no difference between two or more groups of entities (using within-group homogeneity to test separation). Groups are identified *a priori* (either time of sampling, location, or soil layer) and there is a choice of distance measurements. The Sørensen distance measurement was chosen for all analyses, where appropriate, as it has been shown to consistently distinguish

ecologically distinct groups (McCune and Grace, 2002; Stark *et al.,* 2006). The effect-size (A[11]) varies between plus one and minus one. 'A-maximium' equals one when all items are identical within groups. 'A' equals zero when heterogeneity within groups equals expectation by chance. 'A' less than zero has more heterogeneity within groups than expected by chance. According to McCune and Grace (2002), when dealing with ecological data, an 'A' value greater than 0.3 indicates "very high" separation of groups (i.e. very high within-group homogeneity) and an 'A' value greater than 0.1 indicates "high" separation of groups. MRPP and paired MRPP share the same assumptions as a nonparametric MANOVA, along with the assumption that the distance measure chosen is appropriate to the data set to be tested and that the variables measured are weighted appropriately for the ecological question posed.

Paired Multi-Response Permutation Procedure (paired MRPP) (PC-ORD for Windows, McCune and Mefford, version 5, 1999) can be used in a similar way to a nonparametric MANOVA. The Ponderosa Pine location had no H layer, so the sampling design was unbalanced, and unlike nonparametric MANOVA, paired MRPP does not require a balanced design. Paired MRPP was used to examine whether combinations of pairs of locations (BEC zones) and soil layers were significantly different from each other based on microbial community characteristics. The *p* value was adjusted (Bonferroni's correction) depending on the number of pair combinations.

A Mann Whitney U test (a nonparametric t-test) (Statistica, version 6) was used to test for significant differences in enzyme activities, PLFA concentrations, and environmental variables between spring and summer sampling time, for individual locations.

Spearman's rank correlations (Statistica, version 6) were used to determine the significance and strength of any relationships between microbial community variables and measured environmental variables.

Ordination techniques provide a graphical representation of data, which can aid in interpretation and analysis. In this study, Non-metric Multidimensional Scaling (NMS) (Mather, 1976; Kruskal, 1964) (PC-ORD for Windows, McCune and Mefford, version 5,

[11] A = 1 - (observed delta/expected delta).

1999) was used to visualize microbial community function and structure data (the primary matrix), investigate which components of the microbial communities were mainly influencing the final ordination solution, and establish the dimensionality of the data set based on stress and stability measurements. The communities were grouped by location, sampling time and soil layer. Measured environmental variables were used as the secondary matrix.

NMS is a very robust ordination technique and is recommended for ecological data sets. It does not have assumptions of data multivariate normality nor linearity among variables (McCune and Grace, 2002). NMS uses ranked distances and offers a choice of distance measure. "NMS is the most generally effective ordination method for ecological community data and should be the method of choice" (McCune and Grace, 2002).

The microbial community functional and structural datasets were separately plotted on *n*-dimensions; the number of dimensions is chosen to minimize stress in the ordination. Distance between two points is inversely proportional to the similarity value for a given pair, such that points positioned close together are more similar than points plotted further apart. The Sørensen distance measure was used with a random starting configuration. Pearson and Kendall correlations (r and tau values) between the ordination axes and the environmental variables were calculated. The measured environmental variables were plotted on the ordination if their correlation with the ordination axes had an associated r^2 value greater than 0.3. The dimensionality of the dataset was assessed by referring to the minimum stress and instability of the final solution. Fifty real data runs and fifty randomized data runs were used, and Monte Carlo randomization test result probability values were reported. The stability criterion was 0.00001. All functional ordinations were orientated by the soil moisture (%) vector (in NMS the axes are orthogonal to each other).

3. RESULTS

The results from each hypothesis are presented separately.

3.1. Hypothesis one: Analysis of composite soil samples for microbial community function and structure provides the same results as analysis of individual soil samples.

There was no significant difference in microbial community structure (PLFA signature concentration) (Table 3.1) or function (enzyme activities) (Table 3.2) between the individual soil samples and the composite samples from the same site replicates at the ICH location (spring sampling time). The results suggest that composite soil sampling was successful in reproducing the same results for microbial community structural and functional analysis as were produced by five individual soil samples. The hypothesis is accepted; composite sampling was appropriate for the scale and methods employed in this study.

Table 3.1. Test statistics from a nonparametric MANOVA on structural microbial data.

Source	**df**	**SS**	**MS**	**F**	**p**
Sampling type	1	0.04	0.04	0.13	0.9
Layer	4	1.36	0.34	34.51	0
Residual	12	0.12	1		
Total	17	1.53			

Table 3.2. Test statistics from a nonparametric MANOVA on functional microbial data.

Source	**df**	**SS**	**MS**	**F**	**p**
Sampling type	1	0.09	0.09	0.22	0.9
Layer	4	1.58	0.39	10.29	0.001
Residual	12	0.46	0.38		
Total	17	2.12			

3.2. Hypothesis two: Soil microbial community structure and function are significantly different in spring and summer.

Microbial community function (T=-1.24, A=0.0052, p=0.11, n=116) and structure (T=-0.24, A=0, p=0.29, n=118) were not significantly different between spring and summer sampling periods. The results indicate that there was no difference in microbial community function and structure between the spring and summer samples, therefore the hypothesis is rejected. It was appropriate to combine the microbial community composition results from spring and summer samples.

However, when sampling times were compared for specific enzyme activities and individual PLFA signatures, there were some statistically significant differences in microbial community function and structure between spring and summer sampling times (all locations) when all the soil profile layers were combined. The enzymes activities for aryl sulfatase (T=-3.01, A=0.02, p=0.03, n=116) (Figure 3.1), acid phosphatase (T=-2.59, A=0.01, p=0.03, n=116) (Figure 3.1), xylanase (T=-2.44, A=0.01, p=0.03, n=116) (Figure 3.2), and phenoloxidase (T=-3.24, A=0.02, p=0.01, n=116) (Figure 3.3) were significantly higher in the summer sample compared to the spring sample, although, the effect-sizes (A values) were consistently low (≤0.02).

Phosphatase activity was significantly higher in the summer samples from the ESSF location (U=12, z=-2.31, p=0.021, n=17) (Figure 3.1). Sulfatase activity was significantly higher in the summer samples from the BWBS (U=3, z=-3.18, p=0.001, n=17) and ICH (U=3, z=-3.31, p=0.001, n=17) locations (Figure 3.1). Xylanase activity was significantly higher in the summer samples from the MH location (U=4, z=-2.91, p=0.004, n=17) (Figure 3.2). Phenoloxidase activity was significantly higher in the summer samples from the IDF (U=0, z=-3.464, p=0.001, n=17) and CWH locations (U=3, z=-3.311, p=0.001, n=17) (Figure 3.3).

Arbuscular fungi concentration (T=-7.83, A=0.051, p=0.00011, n=118) was significantly lower in the summer samples compared to the spring samples, although, the effect-sizes (A values) were consistently low (≤0.03). (Figure 3.4), saprophytic fungal concentration (T=-7.93, A=0.046, p=0.00017, n=118) (Figure 3.4), and total fungi concentration (T=-

4.592, A=0.0299, p=0.0045, n=118) (Figure 3.5) were significantly higher in the summer samples compared to the spring samples, although, the effect-sizes (A values) were consistently low (≤0.03).

Arbuscular mycorrhizal fungi concentration was significantly lower in the summer samples in the PP location (U=0, z=-2.88, p=0.004, n=12) and the BWBS location (U=0, z=3.57, p=0, n=18) (Figure 3.4). Saprophytic fungi concentration was significantly higher in the summer samples in the BWBS (U=0, z=-2.25, p=0.024, n=18), the ICH (U=11, z=-2.61, p=0.009, n=18), and the MH (U=11, z=-2.21, p=0.027, n=16) locations (Figure 3.4). Total fungi concentration was significantly higher in the summer samples in the ICH location (U=13, z=-2.43, p=0.015, n=18) and the MH (U=10, z=-2.31, p=0.021, n=16) locations (Figure 3.5).

Statistical tests on a selection of environmental variables for the ESSF, BWBS, ICH, MH and CWH locations in the organic soil layers (F and H layers) are presented in Tables 3.3 – 3.9. Soil temperature was significantly higher in the summer for all the locations (Figure 3.6). Soil water (%) was significantly lower in the summer samples compared to the spring samples in the CWH location only and significantly higher in the summer compared to the spring in the PP, BWBS, and ICH locations (Figure 3.7). Soil pH was significantly lower in the summer samples from the MH location (Figure 3.8).

In the organic soil layers the C:N ratios[12] were very similar in the spring and summer samples for all locations. The PP and MH locations had the highest ratios (Figure 3.9). In the mineral layer of the PP location the C:N ratio increased between the spring and summer sampling times (Figure 3.10). The C:N ratio of mineral soil at the BWBS, ICH, and MH locations decreased from the spring to summer samples (Figure 3.10). The MH location had the highest C:N ratio in the mineral layer from the spring samples (Figure 3.10). The PP and MH locations had the highest C:N ratios in the mineral layer from the summer samples (Figure 3.10).

In the organic soil layers of the ESSF location the concentration of total soil C decreased (by about 10%) between the spring and the summer samples (Figure 3.11). The

[12] C:N ratios, total soil C concentration, and total soil N concentration were not tested for significant differences between locations as there were no site replicates for these analyses.

concentration of total soil C decreased (by about 5%) in the ICH location between the spring and summer samples (Figure 3.11). The highest concentration of total soil C in the spring samples were from the ESSF, BWBS, ICH, and MH locations (Figure 3.11). The highest concentration of total soil C in the summer samples was from the MH location and the lowest concentration was from the CWH location (Figure 3.11). In the mineral layer the concentration of total soil C in the PP location increased between the spring and summer sampling times (Figure 3.12). The concentration of total soil C in the BWBS, MH, and CWH locations decreased between the spring and summer sampling times (Figure 3.12).

In the organic soil layers of the IDF and PP locations the concentration of total soil N increased between the spring and summer sampling times (Figure 3.13). The concentration of total soil N decreased between the spring and summer sampling times in the ESSF and ICH locations (Figure 3.13). In both the spring and summer samples the IDF and PP locations had lower concentrations of total soil N than the other locations. In the mineral soil layer of the ESSF and PP location the concentration of total soil N increased between spring and summer sampling times (Figure 3.14). The concentration of total soil N decreased in the MH and CWH locations between the spring and summer sampling times (Figure 3.14). The MH and CWH locations had the highest spring concentration of total soil N and the PP location had the lowest (Figure 3.14). The IDF, PP, and ICH locations had the lowest summer concentration of total soil N (Figure 3.14).

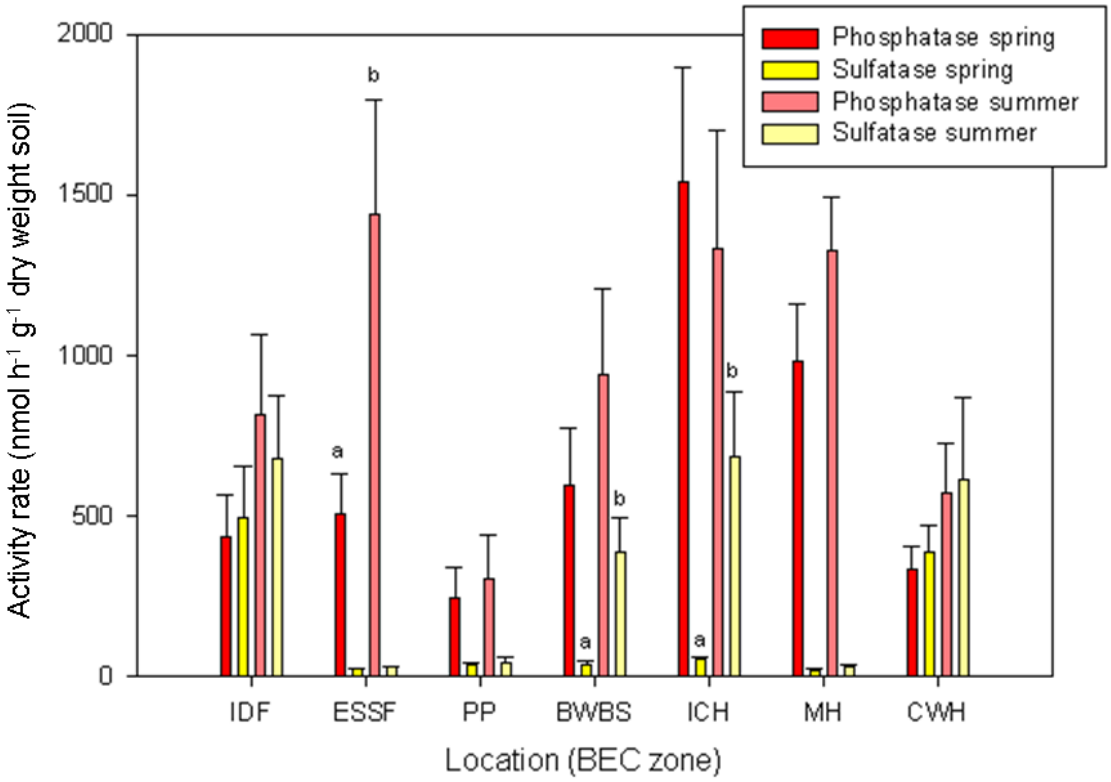

Figure 3.1. Mean phosphatase and sulfatase activities (nmol of substrate converted per hour per gram of sample) of all soil layers combined from the seven study locations. Spring and summer sampling times are shown. Different letters indicate a significant difference between spring and summer samples. Each value is the mean of 9 samples; error bars represent the standard error of the mean.

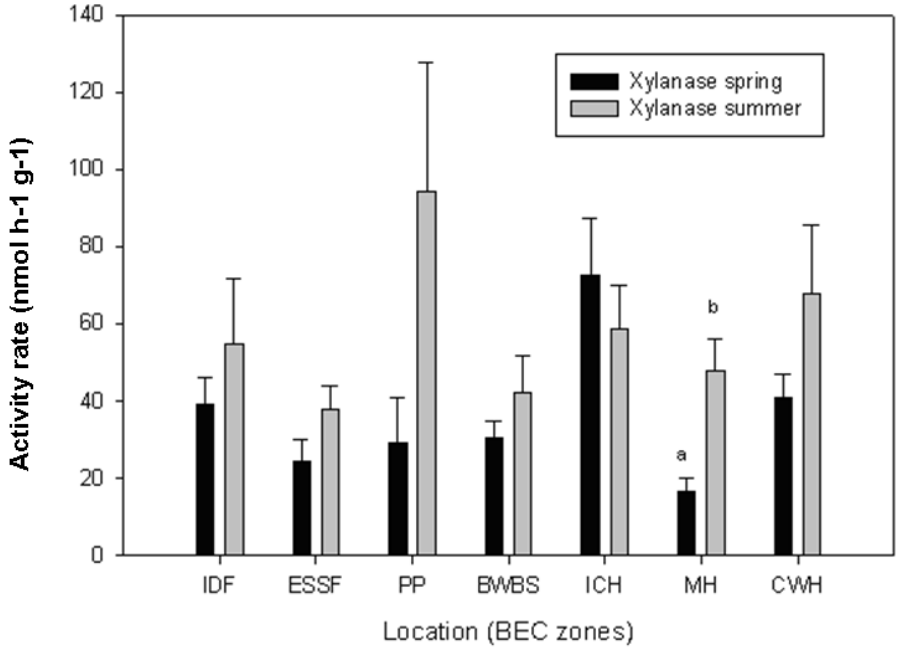

Figure 3.2. Mean xylanase activity (nmol of substrate converted per hour per gram of sample) of all soil layers combined from the seven study locations. Spring and summer sampling times are shown. Different letters indicate a significant difference between spring and summer samples. Each value is the mean of 9 samples; error bars represent the standard error of the mean.

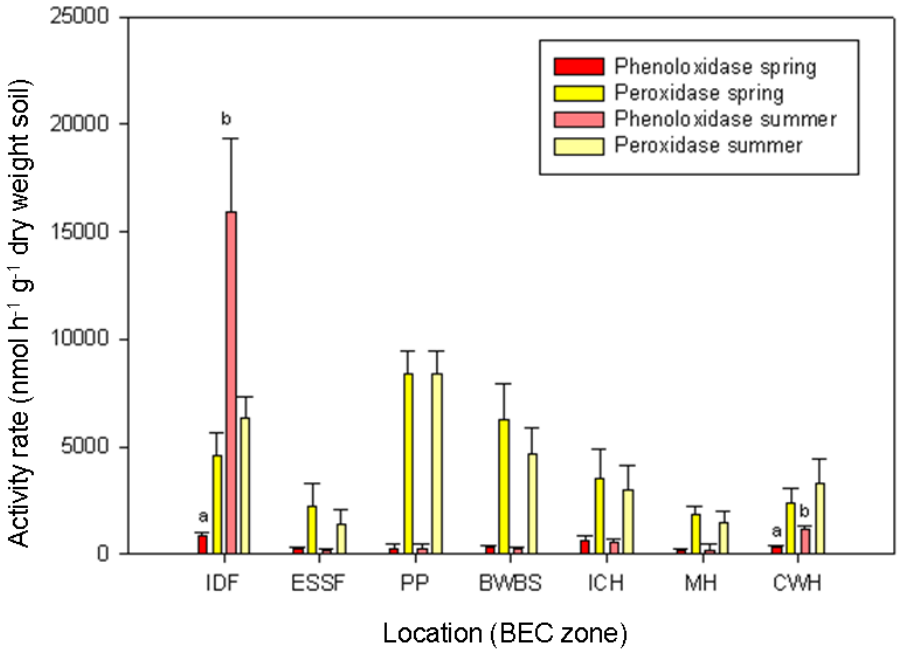

Figure 3.3. Mean phenoloxidase and peroxidase activities (nmol of substrate converted per hour per gram of sample) of all soil layers combined from the seven study locations. Spring and summer sampling times are shown. Different letters indicate a significant difference between spring and summer samples. Each value is the mean of 9 samples; error bars represent the standard error of the mean.

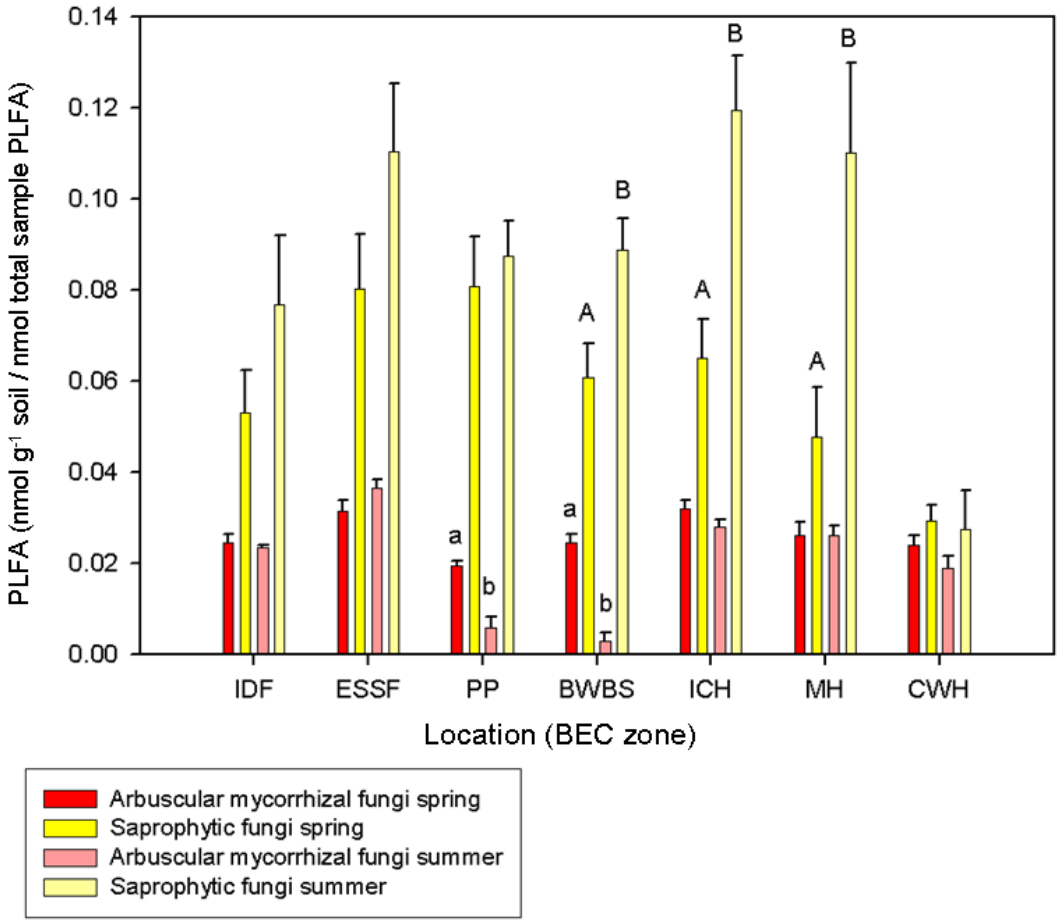

Figure 3.4. Mean arbuscular mycorrhizal and saprophytic fungi PLFA signature concentrations, relativized by total PLFA signature of all soil layers combined from the seven study locations. Spring and summer sampling times are shown; different letters indicate a significant difference between spring and summer samples. Each value is the mean of 9 samples; error bars represent +/- standard error of the mean.

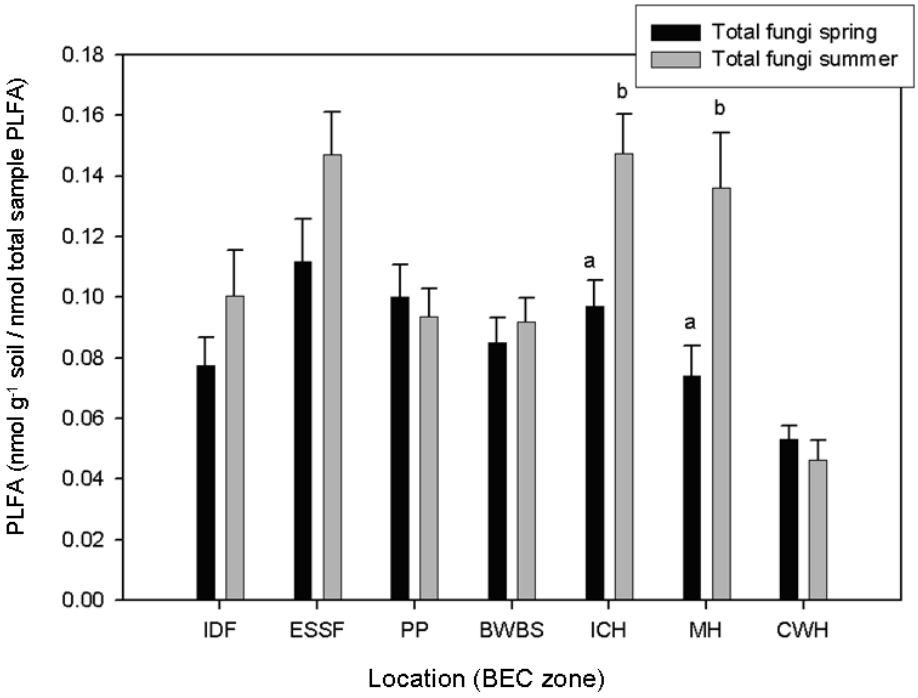

Figure 3.5. Mean total fungi PLFA signature concentration, relativized by total PLFA signature of all soil layers combined from the seven study locations. Spring and summer sampling times are shown. Different letters indicate a significant difference in the means between spring and summer samples. Each value is the mean of 9 samples; error bars represent +/- standard error of the mean.

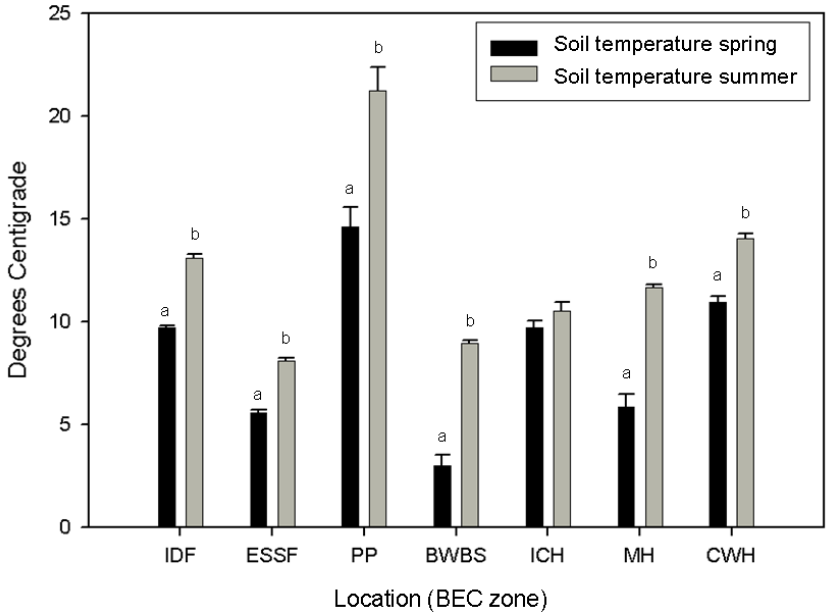

Figure 3.6. Mean temperature (˚C) of organic layers from the seven study locations, with standard error bars. All pairs of locations were significantly different from each other, except for IDF vs. ICH, IDF vs. MH, IDF vs. CWH, ESSF vs. BWBS, ESSF vs. MH, BWBS vs. MH, and ICH vs. MH, when p=0.05/7=0.007 (n=78). Different letters indicate significant differences between spring and summer samples. See Appendix 8.2 for test statistics.

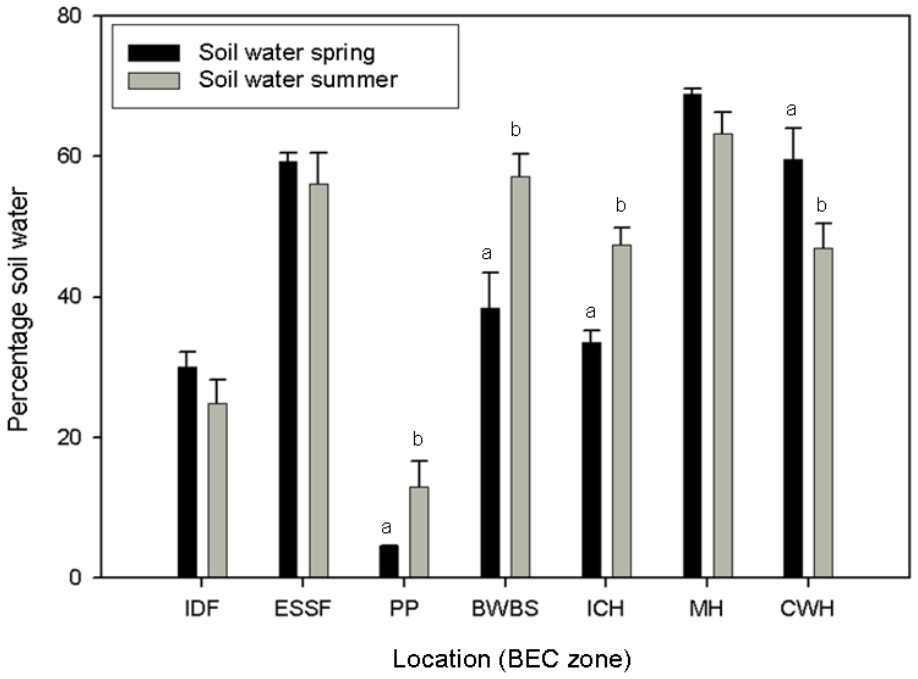

Figure 3.7. Mean water content (%) of organic layers from the seven study locations, with standard error bars. All pairs of locations were significantly different from each other, except for ESSF vs. BWBS, ESSF vs. CWH, BWBS vs. ICH, BWBS vs. CWH, and ICH vs. CWH, when p=0.05/7=0.007 (n=78). Different letters indicate significant differences between spring and summer samples. See Appendix 8.2 for test statistics.

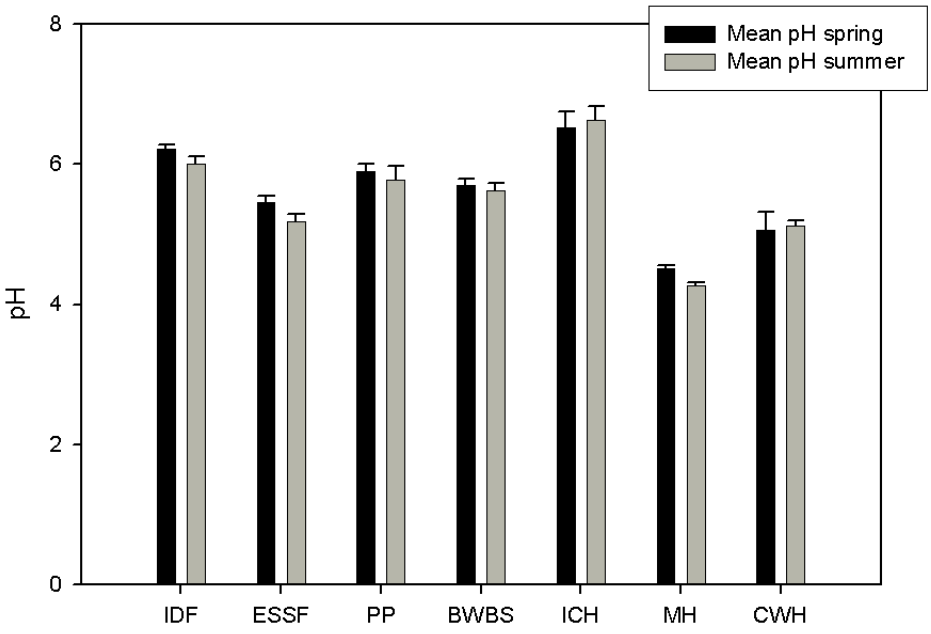

Figure 3.8. Mean pH of organic layers from the seven study locations, with standard error bars. All locations were significantly different from each other, except for IDF vs. PP, IDF vs. ICH, ESSF vs. CWH, and PP vs. BWBS, when p=0.05/7=0.007 (n=78). See Appendix 8.2 for test statistics.

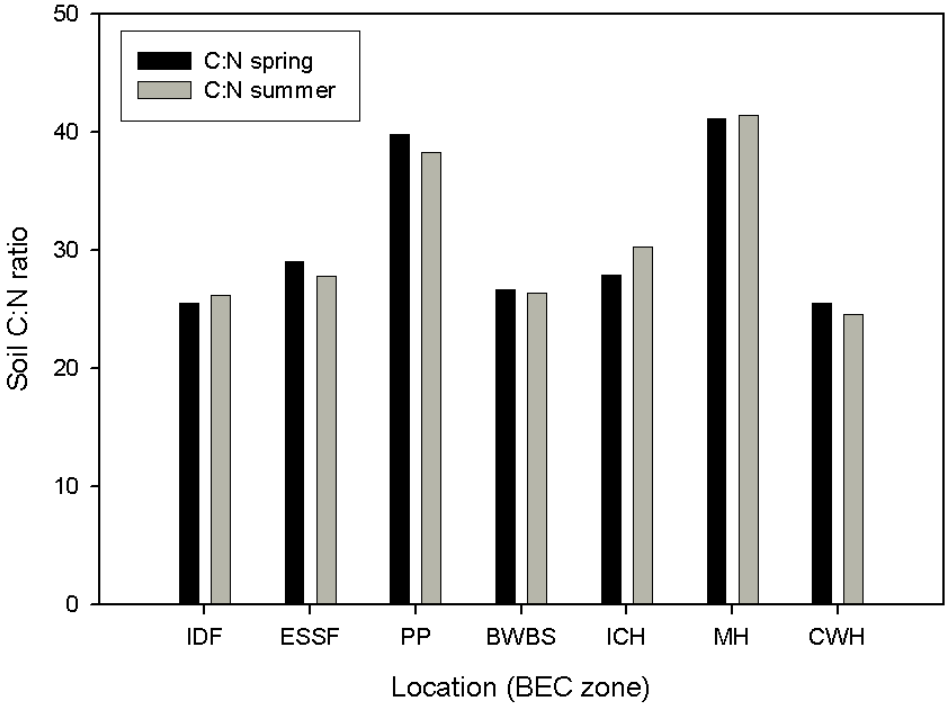

Figure 3.9. Mean C:N ratio of combined organic soil layers from the seven study locations.

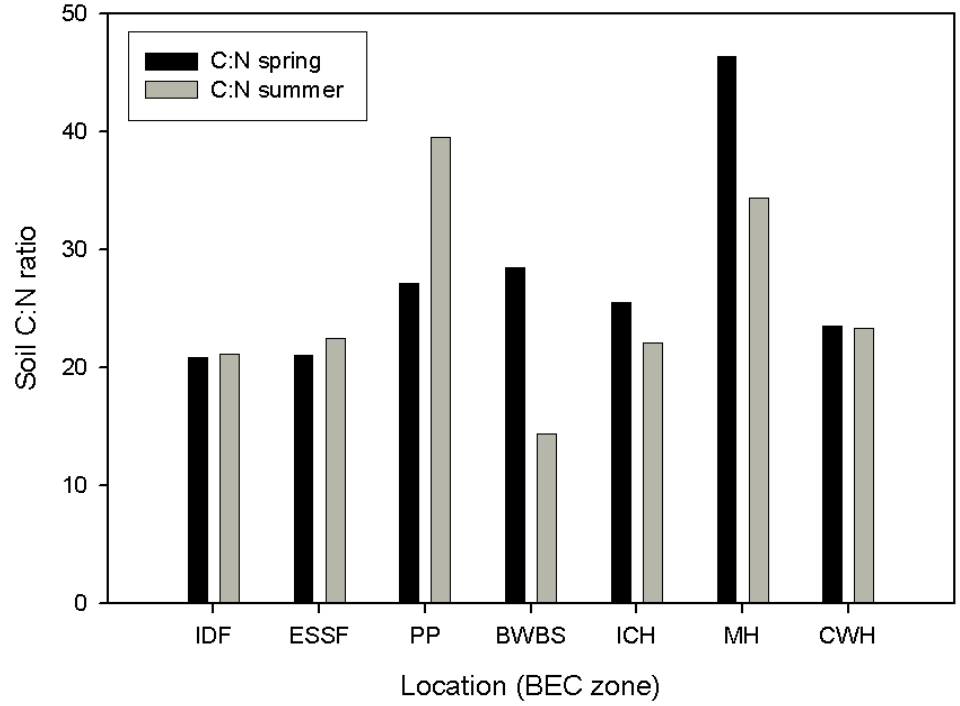

Figure 3.10. Mean C:N ratio of mineral soil from the seven study locations.

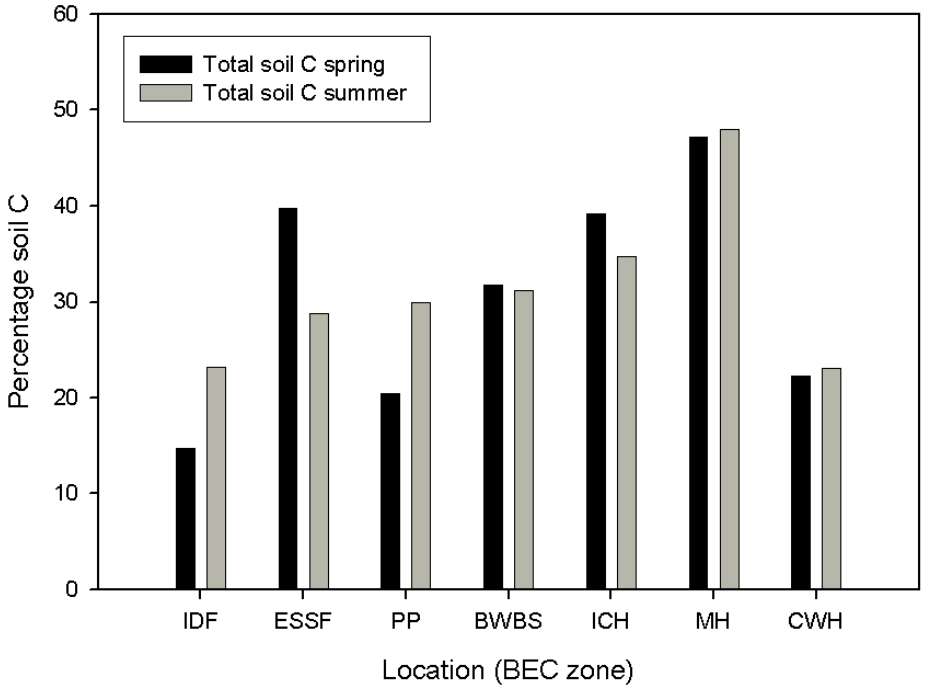

Figure 3.11. Mean total C concentration (%) of organic layers combined from the seven study locations.

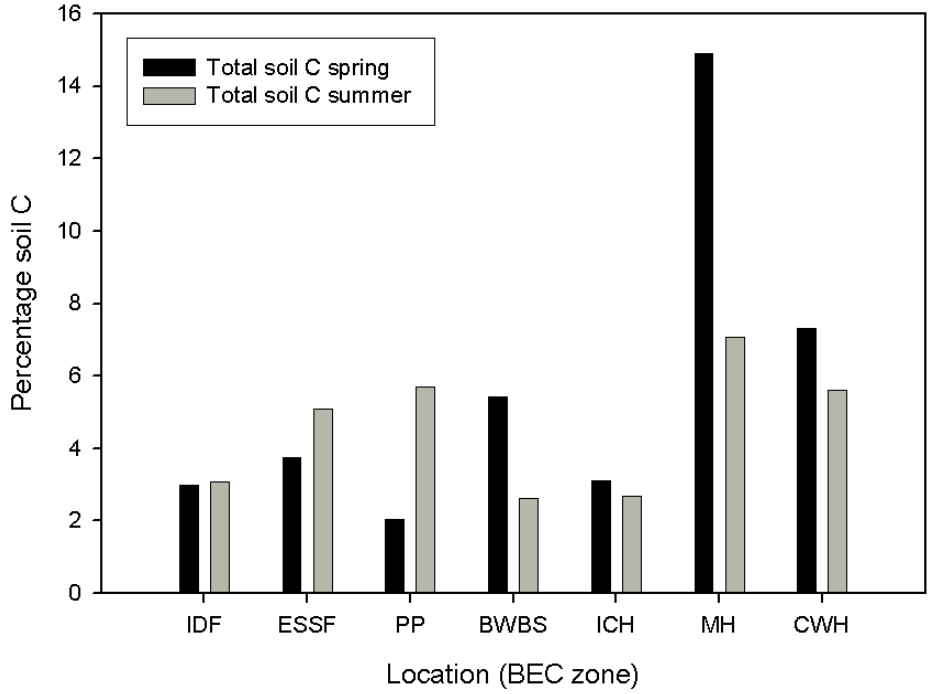

Figure 3.12. Mean total C concentration (%) of mineral soil from the seven study locations.

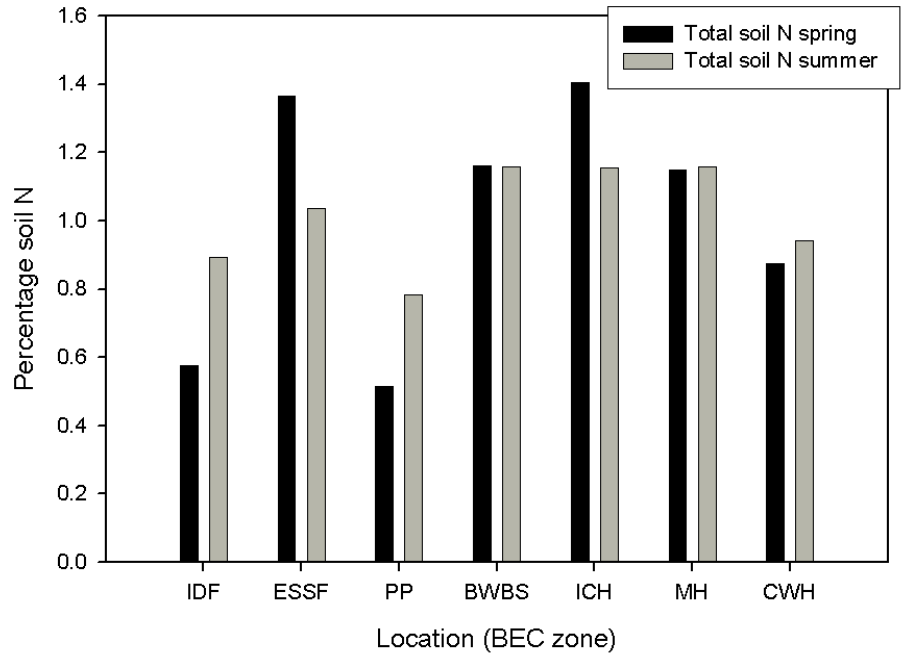

Figure 3.13. Mean total N concentration (%) of organic layers combined from the seven study locations.

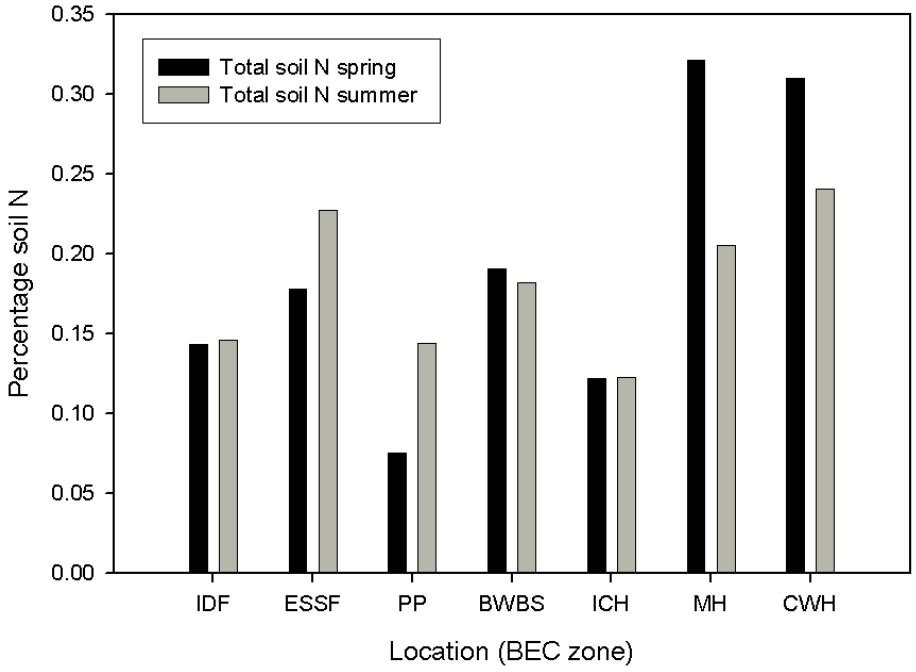

Figure 3.14. Mean soil N concentration (%) of mineral soil from the seven study locations.

Table 3.3. Statistics for measured environmental variables in the organic layers at the IDF location. p values ≤ 0.05 are in bold.

Environmental variable	**Spring mean**	**Summer mean**	**U**	**Z**	**p**	**n**
Soil temperature	9.7˚C	13.1˚C	0	-2.88	**0.004**	12
Soil water	30%	24.82%	12	0.96	0.337	12
pH	6.2	6	8	1.27	0.201	11
C:N	25.5	26.2				
Total C concentration	14.7%	23.2%				
Total N concentration	0.6%	0.9%				

Table 3.4. Statistics for measured environmental variables in the organic layers at the ESSF location. p values ≤ 0.05 are in bold.

Environmental variable	**Spring mean**	**Summer mean**	**U**	**Z**	**p**	**n**
Soil temperature	5.57˚C	8.1˚C	0	-2.88	**0.004**	12
Soil water	59.23%	56.08%	12	0.96	0.34	12
pH	5.46	5.18	6	1.64	0.1	11
C:N	29.1	27.8				
Total C concentration	39.7%	28.8%				
Total N concentration	1.4%	1%				

Table 3.5. Statistics for measured environmental variables in the organic layers at the PP location. p values ≤ 0.05 are in bold.

Environmental variable	**Spring mean**	**Summer mean**	**U**	**Z**	**p**	**n**
Soil temperature	14.63˚C	21.23˚C	0	-1.96	**0.05**	6
Soil water	4.51%	13.0%	0	-1.96	**0.05**	6
pH	5.9	5.77	3	0.65	0.513	6
C:N	39.8	38.3				
Total C concentration	20.4%	30%				
Total N concentration	0.5%	0.8%				

Table 3.6. Statistics for measured environmental variables in the organic layers at the BWBS location. p values ≤ 0.05 are in bold.

Environmental variable	Spring mean	Summer mean	U	Z	p	n
Soil temperature	3˚C	9˚C	0	-2.88	**0.004**	12
Soil water	38.44%	57.16%	3	-2.4	**0.016**	12
pH	5.69	5.62	17	0.16	0.873	12
C:N	26.7	26.8				
Total C concentration	31.8%	31.2%				
Total N concentration	1.2%	1.2%				

Table 3.7. Statistics for measured environmental variables in the organic layers at the ICH location. p values ≤ 0.05 are in bold.

Environmental variable	Spring mean	Summer mean	U	Z	p	n
Soil temperature	9.7˚C	10.53˚C	8	-1.6	0.109	12
Soil water	33.49%	47.39%	2	-2.56	**0.01**	12
pH	6.52	6.63	17	-0.16	0.87	12
C:N	27.9	30.2				
Total C concentration	39.2%	34.8%				
Total N concentration	1.4%	1.2%				

Table 3.8. Statistics for measured environmental variables in the organic layers at the MH location. p values ≤ 0.05 are in bold.

Environmental variable	Spring mean	Summer mean	U	Z	p	n
Soil temperature	6.1˚C	11.67˚C	0	-2.88	**0.004**	12
Soil water	69.14%	63.17%	6	1.92	0.055	12
pH	4.54	4.27	3	-2.4	**0.016**	12
C:N	41.9	41.4				
Total C concentration	47.2%	47.9%				
Total N concentration	1.1%	1.2%				

Table 3.9. Statistics for measured environmental variables in the organic layers at the CWH location. p values ≤ 0.05 are in bold.

Environmental variable	Spring mean	Summer mean	U	Z	p	n
Soil temperature	10.93˚C	14.07˚C	0	-2.88	**0.0039**	12
Soil water	59.6%	47%	5	2.08	**0.0374**	12
pH	5.06	5.12	16	-0.24	0.8102	12
C:N	25.5	24.5				
Total C concentration	22.3%	23%				
Total N concentration	0.9%	0.9%				

3.3. Hypothesis three: It is possible to separate forest types along a regional climate gradient based on microbial community function and/or structure, despite high local microbial community variability.

The soil layers were first analyzed together and then separately. Different layers have different chemical and physical characteristics (section 3.5) and therefore can be expected to have different microbial community characteristics. The microbial community profile of all the soil layers combined may resemble one of the layers or a mixture of all layers, depending how the much the community profile is influenced by the chemical and physical characteristics of each layer.

3.3.1. Multivariate analysis of functional data for a combination of all soil profile layers

MRPP analysis showed high significant overall separation of the seven locations when all the soil profile layers were combined (p=0, A=0.18, n=116). The microbial community, as characterized by the functional profile, was significantly different at each of the seven locations studied; therefore the hypothesis is accepted.

Pair-wise MRPP analysis (Table 3.10) indicated that the enzyme activities in soil samples from the Ponderosa Pine (PP) location were significantly different from all other locations, except for the Boreal White and Black Spruce (BWBS) location. Microbial community function (enzyme activities) was most different between the PP and Mountain Hemlock (MH) locations. Enzyme activities in soil samples from the MH sites were also significantly different from all other locations, except for at the Engelmann Spruce Sub-

alpine Fir (ESSF) location. Enzyme activities in the ESSF and the Interior Douglas Fir (IDF) locations were also significantly different from each other.

Table 3.10. Pair-wise MRPP analysis of enzyme activities in all soil layers combined) at each location (raw values, dry-weight basis).

A	IDF	ESSF	PP	BWBS	ICH	MH	CWH
IDF	1	**0.14**	**0.12**	0.07*	0.08*	**0.22**	**0.08**
ESSF		1	**0.24**	0.07	0.07*	0.03	0.07*
PP			1	0.1	**0.18**	**0.36**	**0.19**
BWBS				1	0.53	**0.12**	0.04
ICH					1	**0.15**	**0.08**
MH						1	**0.11**
CWH							1
p	IDF	ESSF	PP	BWBS	ICH	MH	CWH
IDF	1	**0**	**0.0002**	0.0028*	0.0031*	**0**	**0.0004**
ESSF		1	**0**	0.0049	0.0035*	0.0573	0.0042*
PP			1	0.0031	**0.0003**	**0**	**0**
BWBS				1	0.0189	**0.0002**	0.016
ICH					1	**0**	**0.001**
MH						1	**0.0001**
CWH							1

A>0.1 - high for ecological data - high within-group homogeneity (9 significant pair-wise comparisons)

A>0.3 very high for ecological data - very high within-group homogeneity (1 significant pair-wise comparison)

Pair-wise comparisons p sig ≤ 0.0024 (alpha 0.05/21). Significant values are shown in bold.

*significant to 0.1/21 = 0.0048 (Bonferroni's correction)

3.3.2. Multivariate analysis of microbial functional data for individual soil layers

F layer

The MRPP analysis indicated that enzyme activities in the F-layer samples significantly differed between locations (p=0, A=0.38, n=42).

Pair-wise MRPP analysis (Table 3.11) showed that the enzyme activities in F-layer samples from the PP location were significantly different from those at all other locations. The enzyme activities in the F layer at the MH location were significantly different than

those of the F layer at the IDF, PP, and the Interior Cedar Hemlock (ICH) locations, with a corresponding effect-size (A) greater than 0.3. The enzyme activities in the F layer at the MH location were significantly different from those at the Coastal Western Hemlock (CWH) and BWBS locations (A > 0.1). There were no significant differences between the enzyme activities of the F layer at the MH and ESSF locations. The enzyme activities in the F layer at the ESSF location were significantly different from those at the IDF and ICH locations (A > 0.1) and the F-layer enzyme activities at the ICH location were also significantly different from those at the BWBS and CWH locations (A > 0.1).

Table 3.11. Pair-wise MRPP analysis of enzyme activities in the F layer at each location (raw values, dry-weight basis).

A	IDF	ESSF	PP	BWBS	ICH	MH	CWH
IDF	1	**0.24**	**0.39**	0.2	0.16	**0.33**	0.13
ESSF		1	**0.5**	0.14*	**0.19**	0.09	0.11*
PP			1	**0.5**	**0.5**	**0.62**	**0.43**
BWBS				1	**0.19**	**0.17**	0.14*
ICH					1	**0.33**	**0.18**
MH						1	**0.19**
CWH							1
p	IDF	ESSF	PP	BWBS	ICH	MH	CWH
IDF	1	**0.0018**	**0.0005**	0.0074	0.0176	**0.0008**	0.013
ESSF		1	**0.0005**	0.0037*	**0.0014**	0.0299	0.003*
PP			1	**0.0005**	**0.0005**	**0.0005**	**0.0005**
BWBS				1	**0.0023**	**0.0023**	0.0025*
ICH					1	**0.0005**	**0.002**
MH						1	**0.0006**
CWH							1

A>0.1 - high for ecological data - high within-group homogeneity (6 significant pair-wise comparisons)

A>0.3 very high for ecological data - very high within-group homogeneity (8 significant pair-wise comparisons)

Pair-wise comparisons p sig ≤ 0.0024 (alpha 0.05/21). Significant values are shown in bold.

*significant to 0.1/21 = 0.0048 (Bonferroni's correction)

H layer

Enzyme activities in samples from the H layer[13] were significantly different between locations (p=0, A=0.37, n=34).

Pair-wise MRPP analysis showed a similar pattern of significant differences in enzyme activities between locations in the H layer compared to the patterns of significant differences in all soil layers combined and in the F layer (Table 3.12). Enzyme activities were significantly different in the H layer at the IDF location compared to those at the ESSF location, and were significantly different at the ICH location compared to the MH location (A > 0.1). There were significant differences in the H-layer enzyme activities of the ESSF and BWBS locations, the BWBS and ICH locations, and the ICH and MH locations (A > 0.3). There were also significant differences in the H-layer enzyme activities of the ESSF and ICH locations, the BWBS and MH locations, and the CWH and ESSF, ICH, and MH locations (A > 0.1).

[13] The PP location had no H layer so the PP location was not included in this analysis.

Table 3.12. Pair-wise MRPP analysis of enzyme activities in the H layer at each location (raw values, dry weight basis).

A	IDF	ESSF	PP	BWBS	ICH	MH	CWH
IDF	1	**0.4**	na	0.11	**0.34**	**0.4**	0.17
ESSF		1	na	**0.35**	**0.27**	0.16	**0.29**
PP			1	na	na	na	na
BWBS				1	**0.3**	**0.29**	0.08
ICH					1	**0.3**	**0.27**
MH						1	**0.18**
CWH							1
p	IDF	ESSF	PP	BWBS	ICH	MH	CWH
IDF	1	**0.0009**	na	0.036	**0.0006**	**0.0007**	0.0079
ESSF		1	na	**0.0009**	**0.0018**	0.0241	**0.0012**
PP			1	na	na	na	na
BWBS				1	**0.0006**	**0.001**	0.0668
ICH					1	**0.0005**	**0.0005**
MH						1	**0.0014**
CWH							1

A>0.1 - high for ecological data - high within-group homogeneity (5 significant pair-wise comparisons)

A>0.3 very high for ecological data - very high within-group homogeneity (6 significant pair-wise comparisons)

Pair-wise comparisons p sig ≤ 0.0024 (alpha 0.05/21). Significant values are shown in bold.

*significant to 0.1/21 = 0.0048 (Bonferroni's correction)

Mineral layer

Enzyme activities in samples from the mineral layer significantly differed between locations (p=0, A=0.37, n=40).

Pair-wise MRPP analysis (Table 3.13) showed that enzyme activities were significantly different in the mineral layer at the MH location compared to the PP, BWBS, and ICH locations (A > 0.3). The mineral-layer enzyme activities at the BWBS location were significantly different from those at the PP and ESSF locations (A > 0.1). The mineral-layer enzyme activities at the ESSF location were also significantly different from those at the ICH location (A > 0.1). The mineral-layer enzyme activities at the IDF and CWH locations were not significantly different from those at any other locations.

Table 3.13. Pair-wise MRPP analysis of enzyme activities in the mineral soil at each location (raw values, dry weight basis).

A	IDF	ESSF	PP	BWBS	ICH	MH	CWH
IDF	1	0.17*	0.23*	0.08	0.05	0.37*	0.09
ESSF		1	0.11	**0.29**	**0.17**	0.13	0
PP			1	**0.31**	0.24*	**0.52**	0.14
BWBS				1	0.11*	**0.57**	0.25*
ICH					1	**0.5**	0.12
MH						1	0.15
CWH							1
p	IDF	ESSF	PP	BWBS	ICH	MH	CWH
IDF	1	0.0027*	0.0029*	0.0173	0.0953	0.0032*	0.0481
ESSF		1	0.0205	**0.0005**	**0.0016**	0.052	0.3923
PP			1	**0.0011**	0.0045*	**0.0011**	0.0067
BWBS				1	0.044*	**0.0015**	0.0047*
ICH					1	**0.0014**	0.0293
MH						1	0.0247
CWH							1

A>0.1 - high for ecological data - high within-group homogeneity (2 significant pair-wise comparisons)

A>0.3 very high for ecological data - very high within-group homogeneity (4 significant pair-wise comparisons)

Pair-wise comparisons p sig ≤ 0.0024 (alpha 0.05/21). Significant values are shown in bold.

*significant to 0.1/21 = 0.0048 (Bonferroni's correction)

3.3.3. Multivariate analysis of microbial structural data for a combination of all soil profile layers

MRPP analysis showed significant differences in concentrations of PLFA signature molecules (microbial community structure) between locations when all soil layers were combined (p=0, A=0.18, n=118). The microbial community, as characterized by the structural profile, was significantly different at each of the seven locations studied; therefore the hypothesis is accepted.

The pattern of significant differences between locations based on the microbial community structural data was different from that based on the microbial community functional data (Table 3.14). Pair-wise MRPP analysis showed that microbial community structure at the CWH location was significantly different from the community structure at

all other locations, and particularly when compared to that at the ESSF location (A > 0.3). The microbial community structure at the ESSF location was also significantly different from those at the BWBS and ICH locations (A > 0.1). The microbial community structure at the BWBS location was also significantly different from that at the ICH location (A > 0.1). In contrast to the functional analysis, microbial community structure at the PP location was not significantly different from those of any other location.

Table 3.14. Pair-wise MRPP analysis of PLFA analysis results for each location; all soil layers combined.

A	IDF	ESSF	PP	BWBS	ICH	MH	CWH
IDF	1	**0.149431**	0.0614322	0.0994711	0.060534	-0.00989	**0.18074**
ESSF		1	**0.077176**	**0.102085**	0.027366	**0.119306**	**0.296418**
PP			1	0.013132	**0.058802**	0.031776	**0.159371**
BWBS				1	**0.097748**	0.0826475	**0.177333**
ICH					1	0.049072	**0.258367**
MH						1	**0.132195**
CWH							1
p	IDF	ESSF	PP	BWBS	ICH	MH	CWH
IDF	1	**0.000496**	0.0028843	0.0025627	0.012268	0.746136	**5.5E-06**
ESSF		1	**0.001341**	**0.000791**	0.07406	**0.000101**	**1.03E-06**
PP			1	0.206598	**0.002355**	0.0279	**8.61E-06**
BWBS				1	**0.001375**	0.0033545	**3.46E-05**
ICH					1	0.006897	**5.5E-07**
MH						1	**5.77E-05**
CWH							1

A>0.1 - high for ecological data - high within-group homogeneity (9 significant pair-wise comparisons)

A>0.3 very high for ecological data - very high within-group homogeneity (1 significant pair-wise comparison)

Pair-wise comparisons p sig ≤ 0.0024 (alpha 0.05/21). Significant values are shown in bold.

*significant to 0.1/21 = 0.0048 (Bonferroni's correction)

3.3.4 Multivariate analysis of structural data for individual layers

F layer

MRPP analysis showed that microbial community structure in the F layer was significantly different between locations (p=0 A=0.25, n=42).

Pair-wise MRPP analysis (Table 3.15) showed that the microbial community structure in the F layer at the CWH location was significantly different from those at the IDF, PP and ICH locations (A > 0.3) and the microbial community structure in the F layer at the CWH location was also significantly different from those at the BWBS and MH locations (A > 0.1). The microbial community structure in the F layer at the PP location was also significantly different from that at the ESSF location (A > 0.3) and the microbial community structure in the F layer at the ESSF location was also significantly different from those at the IDF and MH locations (A > 0.1).

Table 3.15. Pair-wise MRPP analysis of PLFA analysis results for each location; F layer.

A	IDF	ESSF	PP	BWBS	ICH	MH	CWH
IDF	1	**0.15205**	0.20094	0.070296	0.008678	0.059611	**0.371196**
ESSF		1	**0.383167**	0.127171	0.058682	**0.206832**	**0.520792**
PP			1	0.100038	0.171268	0.031216	**0.315034**
BWBS				1	0.040757	0.054102	**0.251797**
ICH					1	0.042938	**0.337033**
MH						1	**0.154642**
CWH							1
p	IDF	ESSF	PP	BWBS	ICH	MH	CWH
IDF	1	**0.001933**	0.006809	0.103215	0.314008	0.066257	**0.000769**
ESSF		1	**0.001066**	0.02187	0.153871	**0.000439**	**0.000551**
PP			1	0.05911	0.014711	0.160759	**0.000542**
BWBS				1	0.228411	0.121993	**0.000536**
ICH					1	0.110194	**0.000886**
MH						1	**0.007595**
CWH							1

A>0.1 - high for ecological data - high within-group homogeneity (4 significant pair-wise comparisons)

A>0.3 very high for ecological data - very high within-group homogeneity (5 significant pair-wise comparisons)

Pair-wise comparisons p sig ≤ 0.0024 (alpha 0.05/21). Significant values are shown in bold.

*significant to 0.1/21 = 0.0048 (Bonferroni's correction)

H layer

The microbial community structure in the H layer significantly differed among locations (p=0 A=0.37, n=35).

Pair-wise MRPP analysis (Table 3.16) indicated that microbial community structure in the H layer at the CWH location was significantly different from those at the IDF, ESSF, MH and ICH locations (A > 0.3). The microbial community structure in the H layer at the CWH location was also significantly different from that at the BWBS location (A > 0.1). The microbial community structure in the H layer at the IDF location was significantly different from that at the ESSF location (A > 0.3).

Table 3.16. Pair-wise MRPP analysis of PLFA analysis results for each location; H layer.

A	IDF	ESSF	PP	BWBS	ICH	MH	CWH
IDF	1	**0.502637**	na	0.109849	0.322777	0.138211	**0.475937**
ESSF		1	na	0.109523	0.086029	0.154784	**0.565103**
PP			1	na	na	na	na
BWBS				1	0.097897	0.05574	**0.257624**
ICH					1	0.063661	**0.50545**
MH						1	**0.439739**
CWH							1
p	IDF	ESSF	PP	BWBS	ICH	MH	CWH
IDF	1	**0.001151**	na	0.074433	0.005306	0.017307	**0.001368**
ESSF		1	na	0.022516	0.088949	0.012471	**0.000551**
PP			1	na	na	na	na
BWBS				1	0.042794	0.154077	**0.000608**
ICH					1	0.111549	**0.000582**
MH						1	**0.000682**
CWH							1

A>0.1 - high for ecological data - high within-group homogeneity (1 significant pair-wise comparison)

A>0.3 very high for ecological data - very high within-group homogeneity (5 significant pair-wise comparisons)

Pair-wise comparisons p sig ≤ 0.0024 (alpha 0.05/21). Significant values are shown in bold.

*significant to 0.1/21 = 0.0048 (Bonferroni's correction)

Mineral layer

The microbial community structure in the mineral layer significantly differed among locations (p=0.0028, A=0.14, n=41).

Pair-wise MRPP analysis on the microbial community structural data in the mineral soil (Table 3.17) showed a very different pattern of significant differences when compared to the patterns shown in all soil layers combined, the F layer, and the H layer. Microbial community structure in the mineral layer significantly differed between the PP and IDF locations only (A > 0.1).

Table 3.17. Pair-wise MRPP analysis of PLFA analysis results for each location; mineral layer.

A	IDF	ESSF	PP	BWBS	ICH	MH	CWH
IDF	1	0.142292	**0.192142**	0.197018	0.153982	-0.02666	0.130751
ESSF		1	0.040426	0.073528	-0.01981	0.070877	0.092498
PP			1	-0.01991	0.047561	0.141095	0.069629
BWBS				1	0.102433	0.147683	0.094461
ICH					1	0.0524	0.09448
MH						1	0.057826
CWH							1
p	IDF	ESSF	PP	BWBS	ICH	MH	CWH
IDF	1	0.058463	**0.001474**	0.030265	0.006328	0.622873	0.018012
ESSF		1	0.17875	0.136371	0.531042	0.156838	0.085714
PP			1	0.484779	0.12907	0.009062	0.117056
BWBS				1	0.073305	0.061647	0.102696
ICH					1	0.148478	0.06392
MH						1	0.115199
CWH							1

A>0.1 - high for ecological data - high within-group homogeneity (1 significant pair-wise comparison)

A>0.3 very high for ecological data - very high within-group homogeneity (0 significant pair-wise comparisons)

Pair-wise comparisons p sig ≤ 0.0024 (alpha 0.05/21). Significant values are shown in bold.

*significant to 0.1/21 = 0.0048 (Bonferroni's correction)

3.3.5. Environmental characteristics of the PP, MH and CWH locations

When the environmental variables at the different locations were analyzed, the PP, MH and CWH locations were found to have some unique environmental characteristics:

The soil temperature (˚C) was highest in the organic layers from the PP location for both sampling times and the soil temperatures at the PP and MH locations were significantly different (Figure 3.6).

Soil water content of the organic layer was highest at the MH location and lowest at the PP location The water content of the organic layers at the PP and MH locations were significantly different (Figure 3.7).

The soil pH in the organic layers from the CWH location was significantly lower than in all other locations, except for the MH and ESSF locations (Figure 3.8).

The C:N ratio in the organic layers from the PP and MH locations was higher than all in other locations (Figure 3.9). The mineral layer of the PP and MH locations had the highest C:N ratios in the summer and the MH location had the highest ratio in the spring (Figure 3.10).

The C concentration was highest in the MH location in both the organic and mineral soil layers (from spring and summer samples), and the C concentration in the CWH location was the lowest (summer samples) (Figures 3.11 and 3.12).

The PP location had one of the lowest concentrations of total soil N of all the locations, in the organic layers from both the spring and summer samples (Figure 3.13). In the mineral layer the highest concentrations of N in the spring samples were in the MH and CWH locations and the lowest concentrations were in the PP location samples. The lowest summer mineral soil N concentration was in the IDF and PP locations (Figure 3.14).

There were significantly higher available N concentrations in the CWH location than in the other six locations (Figure 3.15).

The tree species composition at the PP site was 90.5% ponderosa pine *(Pinus ponderosa)* and 9.5% Douglas fir *(Pseudotsuga menziesii)* (Table 3.18). The tree species composition at the MH location was 83.3% western hemlock *(Tsuga heterophylla)* and 16.7% yellow cedar *(Chamaecyparis nootkatensis)* (Table 3.18). The tree species composition at the CWH site was 64.6% *P. menziesii*, 22.9% western redcedar *(Thuja plicata)*, and 12.5% big leaf maple *(Acer macrophyllum)* (Table 3.18).

Table 3.18. Tree species composition at the sampling sites.

	Pseudotsuga menziesii %	*Picea engelmannii* %	*Picea glauca* %	*Picea mariana* %	*Abies lasiocarpa* %	*Thuja plicata* %	*Populus species* %	*Pinus ponderosa* %	*Tsuga heterophylla* %	*Acer macrophyllum* %	*Chamaecyparis nootkatensis* %
IDF	100	0	0	0	0	0	0	0	0	0	0
ESSF	0	12	0	0	88	0	0	0	0	0	0
PP	9.5	0	0	0	0	0	0	90.5	0	0	0
BWBS	0	0	76.1	8.7	0	0	15.2	0	0	0	0
ICH	59.6	40.4	0	0	0	0	0	0	0	0	0
MH	0	0	0	0	0	0	0	0	83.3	0	16.7
CWH	64.6	0	0	0	0	22.9	0	0	0	12.5	0

Additional information from Volney, 2007.

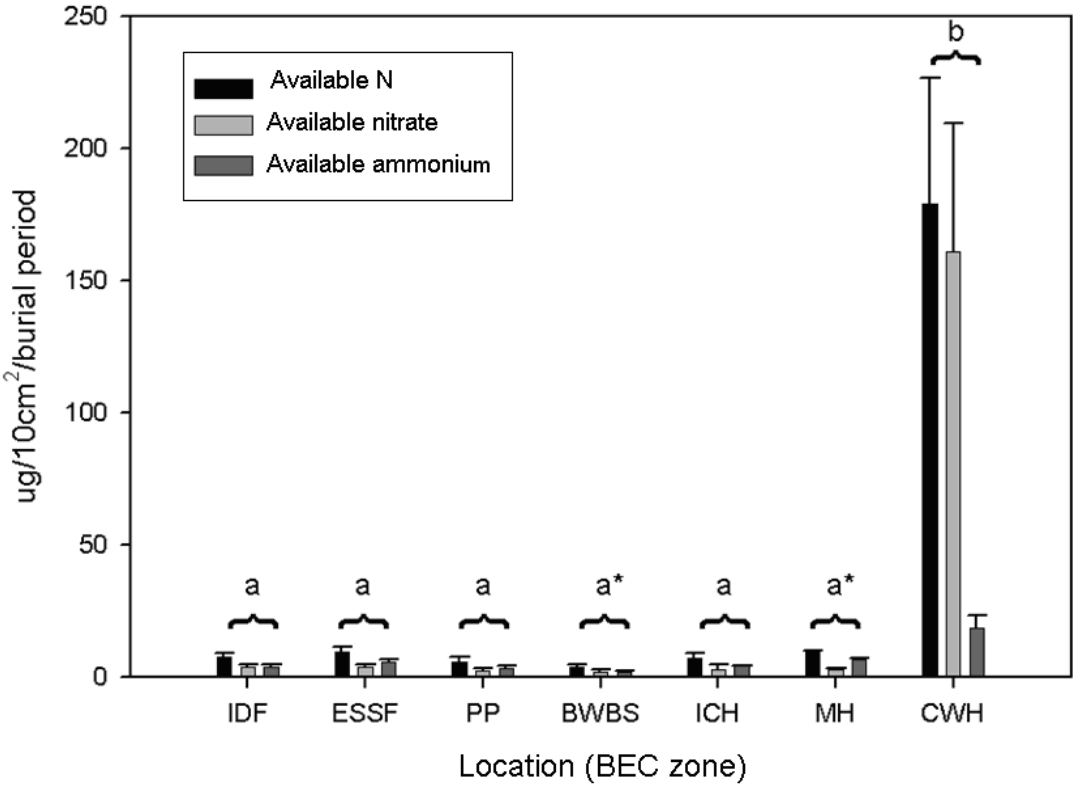

Figure 3.15. Available nitrogen (µg per $10cm^2$ ion exchange membrane per burial period in days) in the organic layers at the seven study locations. Each value is the mean of 4 probes (with standard error bars. Different letters indicate significant differences. Asterisks indicate significant differences between the BWBS and MH locations (n=39). See Appendix 8.2 for test statistics.

The seven study locations exhibited unique available nutrient concentration profiles and there were a number of significant differences in the concentrations of available nutrients when different locations were compared (see Figures 3.15 to 3.20) (see Appendix 8.3 for the complete PRS™ probe data set). As well as differences in available N (mentioned above), available P concentrations were highest at the IDF and BWBS locations and lowest at the ICH, MH, and CWH locations (Figure 3.16). Available Ca concentration was highest at the CWH and ICH and lowest at the IDF, ESSF, and PP (Figure 3.17). Available Mg concentration was highest at the IDF and lowest at the ESSF locations (Figure 3.17). Available K concentration was highest at the IDF and lowest at the CWH locations (Figure 3.17). Available S concentration was far higher at the BWBS location than at the other locations (Figure 3.18). Available Fe concentration was highest at the CWH and BWBS locations and lowest at the IDF and MH locations (Figure 3.19).

Available Mn concentration was highest at the MH and ESSF locations and lowest at the IDF and ICH locations (Figure 3.19). Available Zn concentration was highest at the MH location and lowest at the ICH location (Figure 3.19). Available Bo concentration was highest at the ICH location and lowest at the ESSF location (Figure 3.19). Available Cu concentration was highest at the SK and lowest at the BWBS and ICH locations (Figure 3.20).

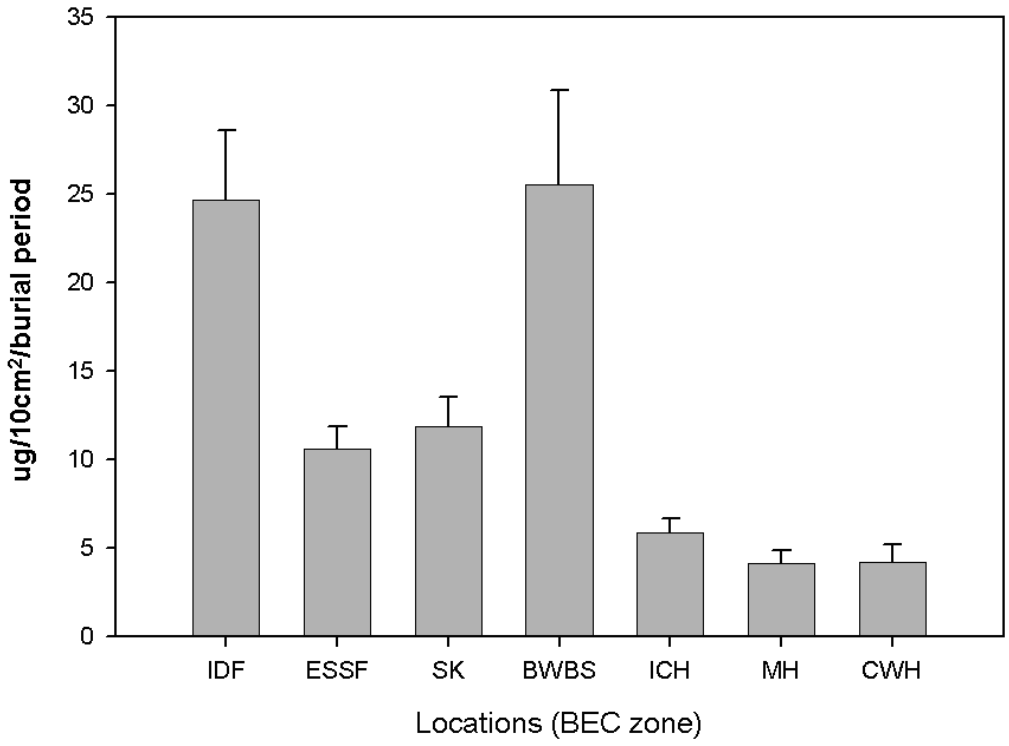

Figure 3.16. Mean available P concentration (µg per 10cm^2 ion exchange membrane per burial period in days) in all soil layers combined at the seven study locations, with standard error bars. There were significant differences between the IDF vs. ESSF, IDF vs. SK, IDF vs. ICH, IDF vs. MH, IDF vs. CWH, ESSF vs. BWBS, ESSF vs. MH, ESSF vs. CWH, SK vs. ICH, SK vs. MH, SK vs. CWH, BWBS vs. ICH, BWBS vs. MH, and BWBS vs. CWH locations (n=63). See Appendix 8.2 for test statistics.

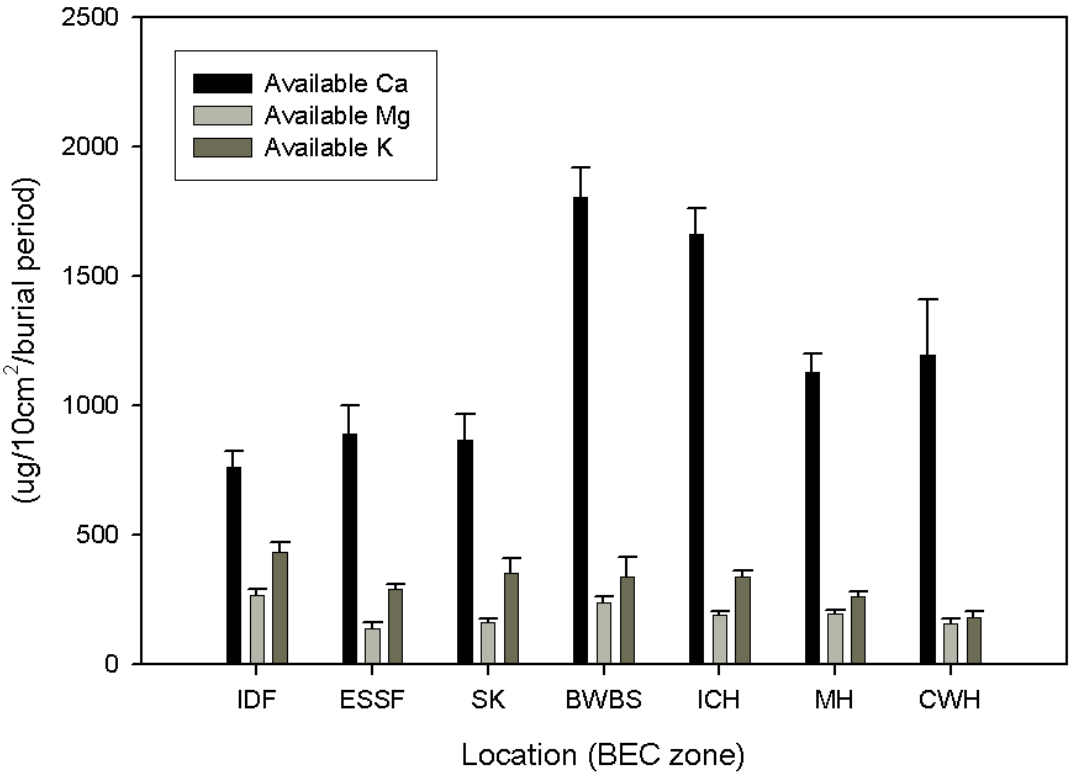

Figure 3.17. Mean available Ca, Mg, and K concentrations (µg per $10cm^2$ ion exchange membrane per burial period in days) in all soil layers combined at the seven study locations, with standard error bars. There were significant differences between the IDF vs. BWBS, IDF vs. ICH, IDF vs. MH, IDF vs. CWH, ESSF vs. BWBS, ESSF vs. ICH, SK vs. BWBS, SK vs. ICH, BWBS vs. MH, BWBS vs. CWH, and ICH vs. MH locations when p=0.05/7=0.007 (n=63). See Appendix 8.2 for test statistics.

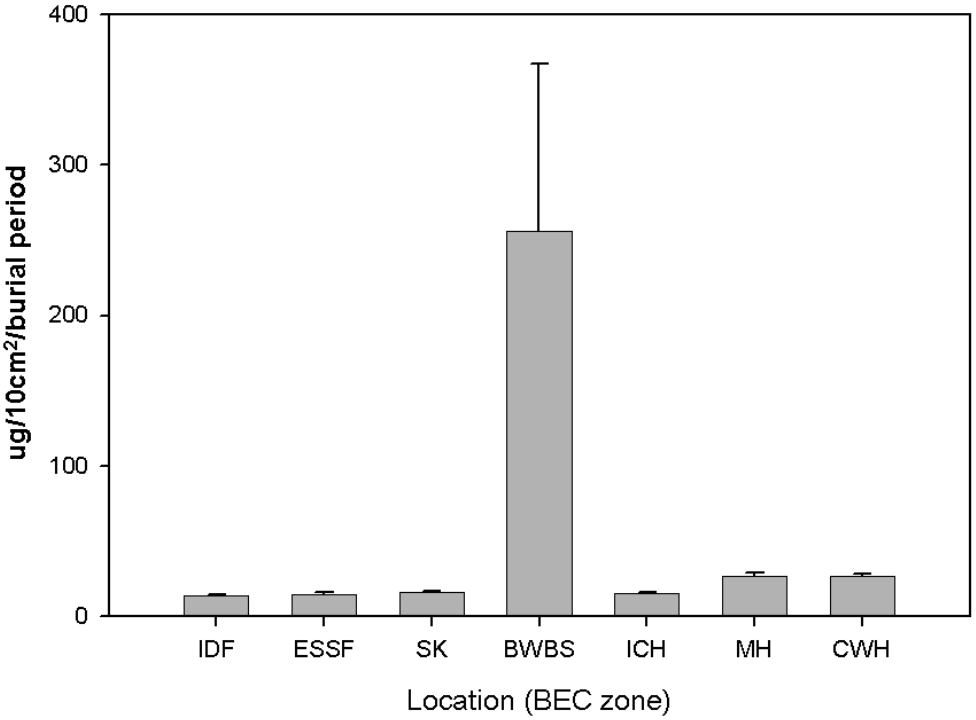

Figure 3.18. Mean available S concentration (µg per 10cm^2 ion exchange membrane per burial period in days) in all soil layers combined at the seven study locations, with standard error bars. There were significant differences between the IDF vs. BWBS, IDF vs. MH, IDF vs. CWH, ESSF vs. BWBS, ESSF vs. MH, ESSF vs. CWH, SK vs. BWBS, SK vs. MH, SK vs. CWH, BWBS vs. ICH, BWBS vs. ICH, BWBS vs. MH, BWBS vs. CWH locations when p=0.05/7=0.007 (n=63). See Appendix 8.2 for test statistics.

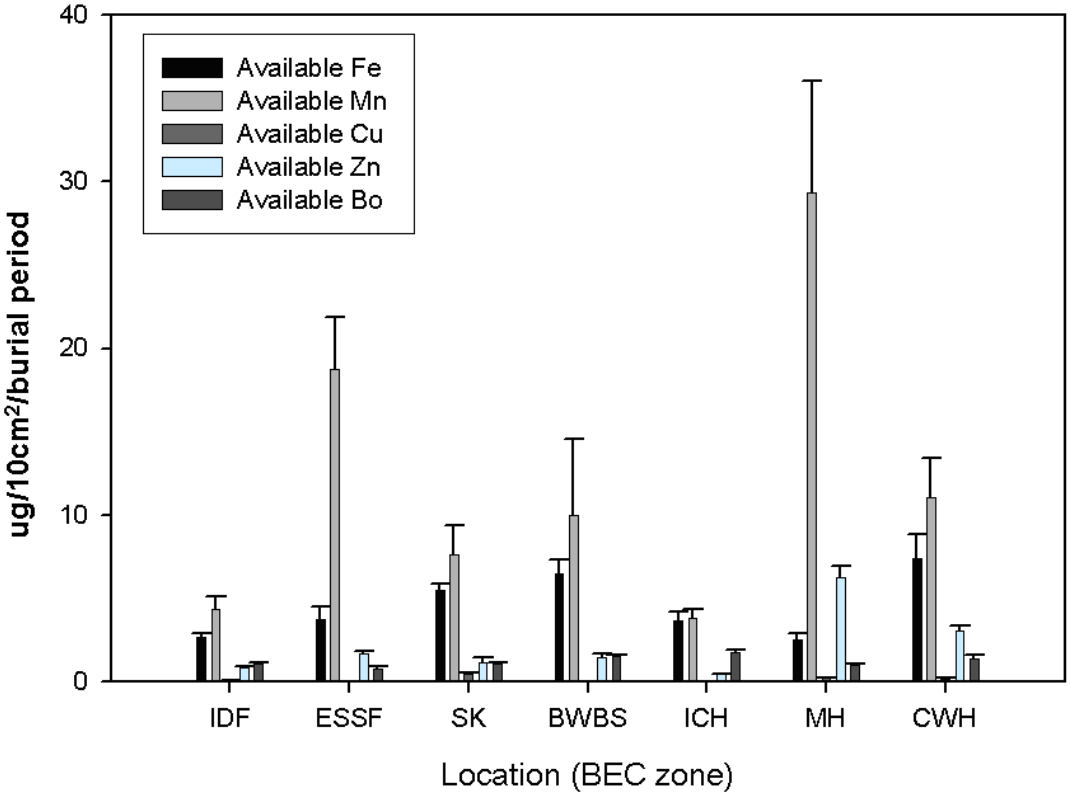

Figure 3.19. Mean available micronutrients (Fe, Mn, Zn, Cu, Bo) concentrations (µg per $10cm^2$ ion exchange membrane per burial period in days) in all soil layers combined at the seven study locations, with standard error bars. There were significant differences between the IDF vs. ESSF, IDF vs. SK, IDF vs. BWBS, IDF vs. MH, IDF vs. CWH, ESSF vs. SK, ESSF vs. BWBS, ESSF vs. ICH, SK vs. MH, BWBS vs. ICH, BWBS vs. MH, ICH vs. MH, ICH vs. CWH, and MH vs. CWH locations when p=0.05/7=0.007 (n=63). See Appendix 8.2 for test statistics.

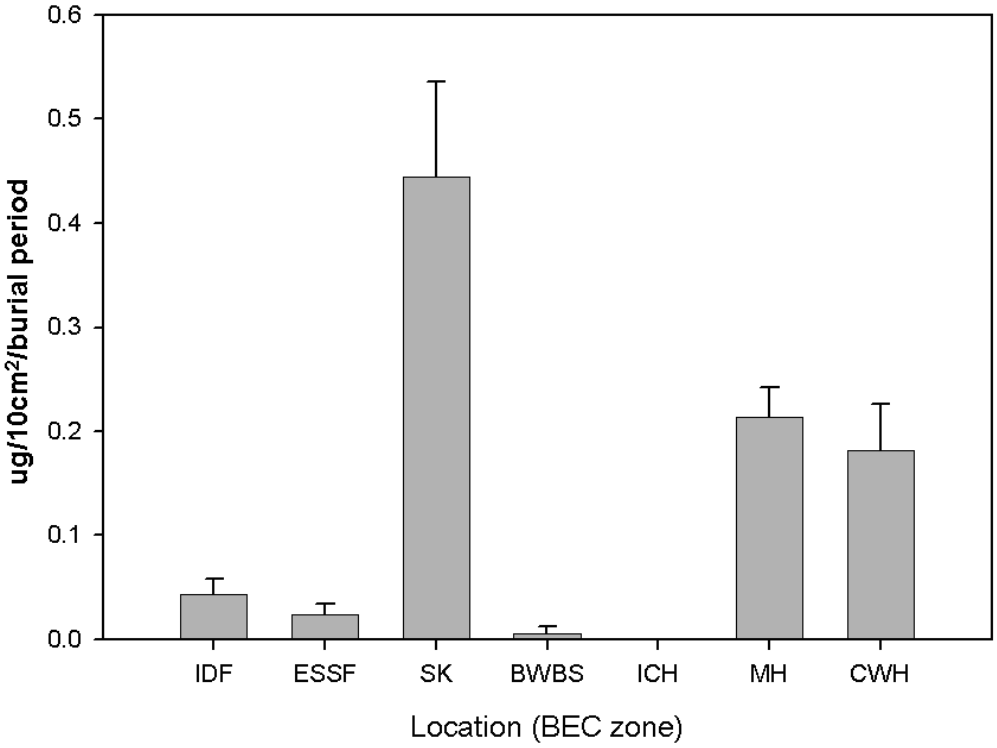

Figure 3.20. Mean available Cu concentrations (µg per 10cm^2 ion exchange membrane per burial period in days) in all soil layers combined at the seven study locations, with standard error bars (n=63). See Appendix 8.2 for test statistics.

3.4. Hypothesis four: A set of measured environmental variables can be shown to significantly correlate with microbial community function and structure across a regional climate gradient. Post-hoc hypothesis: If accepted, I hypothesize that moisture is highly correlated with microbial community function and structure.

Mean annual precipitation and mean annual temperature at each location was approximated from information from a literature search, from climate station data and from the ClimateBC software program (Table 2.1). Where a range of values was presented, the median of the range was used to create a regional annual precipitation gradient and annual temperature gradient based on the ranked values for each location[14]:

The moisture gradient, from driest to wettest was: PP < BWBS < IDF < ICH < ESSF < CWH < MH

The temperature gradient, from coldest to warmest was: BWBS < ESSF < MH < ICH = IDF < CWH = PP

Other gradients were constructed using the ClimateBC software (Wang *et al.,* 2006) (Section 2.3), but there were no clear relationships between these gradients and the soil microbial community structure and function, so these gradients are not presented. Measured environmental variables included in the analyses can be found in Table 2.3.

3.4.1 Correlations between microbial community function and structure and measured environmental variables

Spearman's rank correlations between microbial community structure (PLFA) and function (enzyme assays) and measured environmental variables (for both sampling times) are presented in Tables 3.19 to 3.22. Significant correlation values (r^2) greater than 0.4 are presented in bold.

[14] The gradients presented are site-specific and are not indicative of all BEC zone sites.

Significant correlations between enzyme activities and measured environmental variables

Soil moisture (%) was significantly negatively correlated with the activities of enzymes which degrade lignocellulase, along with the chitin-degrading enzyme beta-1,4-N-acetylglucosaminidase (NAG), and the labile C-degrading enzyme beta-1,4-glucosidase (glucosidase) (Table 3.19).

All forms of available N were significantly negatively correlated with NAG activity; total available N and available NH_4^+ were significantly negatively correlated with peroxidase activity; and available NH_4^+ was significantly negatively correlated with glucosidase activity (Table 3.19).

Other measured environmental variables which significantly correlated with enzyme activity were: Percentage sand negatively with NAG activity; total C concentration negatively with peroxidase and phenol oxidase activity, and positively with acid phosphatase (phosphatase) activity; total N concentration negatively with peroxidase, phenol oxidase, and phosphatase activity; C:N ratio negatively with phenol oxidase and aryl sulfatase (sulfatase) activity; pH positively with glucosidase, NAG, cellobiohydrolase (cellulase), and beta-1,4-xylosidase (xylanase) activity (Table 3.19).

The hypothesis and post-hoc hypothesis are accepted.

Table 3.19. Spearman's rank correlations between enzyme activities and measured environmental variables (n=105). Significant correlations (> 0.4) are in bold.

	Phenol-oxidase	Peroxidase	Urease	Beta-1,4-glucosidase	Cellobiohy-drolase	Beta-1,4-xylosidase	Beta-1,4-N-acetylglucosamini-dase	Aryl-sulfatase	Acid-phosphatase
% soil water	**-0.5**	**-0.72**	-0.24	**-0.49**	-0.34	-0.35	**-0.51**	-0.35	0.13
Total N	-0.23	**-0.44**	-0.31	-0.39	-0.27	0.2	**-0.49**	-0.08	-0.07
NO_3-N	-0.18	-0.36	-0.28	-0.26	-0.23	-0.13	**-0.4**	-0.01	-0.15
NH_4-N	-0.24	**-0.46**	-0.23	**-0.45**	-0.31	0.25	**-0.52**	-0.17	0.02
% sand	-0.1	-0.16	-0.11	-0.33	-0.29	-0.12	**-0.47**	-0.09	-0.27
% C	**-0.57**	**-0.7**	-0.08	-0.06	0.08	-0.06	-0.02	-0.3	**0.5**
% N	-0.54	**-0.73**	-0.06	0.07	0.15	0	0.09	-0.24	**-0.51**
C:N	**-0.5**	-0.25	0.03	-0.08	-0.03	-0.1	-0.01	**-0.44**	0.33
pH	0.33	0.2	0.3	**0.73**	**0.59**	**0.41**	**0.65**	0.32	0.17

Significant correlations between PLFA signatures and measured environmental variables

Soil moisture was significantly positively correlated with total microbial biomass, and with all bacterial PLFA signatures except those indicative of Gram-negative bacteria (Table 3.20). Total soil C and N concentration were significantly positively correlated with total fungi and saprophytic fungi (Table 3.20). The hypothesis and post-hoc hypothesis are accepted.

Table 3.20. Significant correlations between PLFA signatures and measured environmental variables (n=119). Significant correlations (> 0.4) are in bold.

	Total microbial biomass	Gram-positive bacteria	Gram-negative bacteria	Actinobacteria	Total bacteria	Saprophytic fungi	Arbuscular mycorrhizal fungi	Total fungi
Aspect (degrees)	0.2	0.2	0.22	0.17	0.2	0.19	0.34	0.25
Slope (degrees)	0.06	0.04	0.05	-0.02	0.05	0.1	0.013	0.12
Soil temperature (˚C)	-0.04	0.05	0.01	0.07	0.02	0.11	0.05	0.1
% sand	0.09	0.09	0.09	0.13	0.01	-0.05	0.07	0.02
% silt	-0.06	-0.06	-0.07	-0.15	-0.07	0.1	-0.02	0.06
% clay	-0.11	-0.13	-0.1	-0.12	-0.11	-0.04	-0.15	-0.08
% soil water	**0.42**	**0.42**	0.36	**0.48**	**0.42**	0.27	0.38	0.32
%C	0.39	0.38	0.31	0.36	0.38	**0.4**	0.33	**0.42**
%N	0.37	0.36	0.28	0.31	0.35	**0.41**	0.33	**0.42**
C:N	0.18	0.14	0.15	0.12	0.17	0.25	0.1	0.23
pH	-0.2	-0.19	-0.22	-0.29	-0.21	-0.04	-0.15	-0.08

Significant correlations between PLFA signatures and enzyme activities

Phosphatase activity was significantly positively correlated with all PLFA signatures except those of actinobacteria, arbuscular mycorrhizal fungi, and saprophytic fungi (Table 3.21). Xylanase activity was significantly positively correlated with all PLFA signatures (Table 3.21). Cellulase activity was significantly positively correlated with all PLFA signatures, except those indicative of actinobacteria (Table 3.21). Glucosidase activity was significantly positively correlated with total microbial biomass and total bacteria (Table 3.21). The lignocellulase-degrading enzyme, peroxidase, was significantly negatively correlated with all PLFA signatures, except total microbial biomass (Table 3.21).

Table 3.21. Significant correlations between PLFA signatures and enzyme activities (n=105). Significant correlations (> 0.4) are in bold.

	Total microbial biomass	Gram-positive bacteria	Gram-negative bacteria	Actinobacteria	Total Bacteria	Saprophytic fungi	Arbuscular mycorrhizal fungi	Total fungi
Phenol oxidase	0.01	-0.08	-0.06	-0.09	0.01	-0.25	-0.07	-0.2
Peroxidase	-0.34	**-0.47**	**-0.43**	**-0.47**	**-0.4**	**-0.47**	**-0.53**	**-0.5**
Urease	-0.13	0.05	0.06	0.07	-0.07	0.14	0.19	0.16
Beta-1,4-glucosidase	**0.48**	0.31	0.25	0.2	**0.43**	0.26	0.21	0.29
Cellobiohydrolase	**0.51**	**0.46**	**0.4**	0.36	**0.5**	**0.45**	**0.4**	**0.48**
Beta-1,4-xylosidase	**0.5**	**0.53**	**0.52**	**0.52**	**0.54**	**0.49**	**0.45**	**0.52**
Beta-1,4-N-acetylglucosaminidase	**0.45**	0.28	0.23	0.15	**0.4**	0.29	0.19	0.31
Aryl-sulfatase	0.19	0.17	0.18	0.2	0.2	0.1	0.11	0.12
Acid-phosphatase	**0.65**	**0.44**	**0.4**	0.35	**0.6**	0.35	0.33	**0.41**

Significant correlations between enzyme activities

Phosphatase activity was significantly positively correlated with the activities of the labile C-degrading enzymes glucosidase, cellulose, xylanase, the chitin-degrading enzyme NAGase, and was significantly negatively correlated with peroxidase activity (Table 3.22). Sulfatase activity was significantly positively correlated with xylanase activity (Table 3.22). NAGase activity was significantly positively correlated with the activities of labile C-degrading enzymes (glucosidase, cellulase and xylanase) (Table 3.22). The activities of labile C-degrading enzymes were all significantly positively correlated with each other (Table 3.22), and cellulase and xylanase activities were also significantly and negatively correlated with peroxidase activity (Table 3.22).

Table 3.22. Significant correlations between enzyme activities (n=105). Significant correlations (> 0.4) are in bold.

	Phenol oxidase	Peroxi dase	Urease	Beta-1,4-glucosidase	Cellobioh-ydrolase	Beta-1,4-xylosidase	Beta-1,4-N-acetylglucos-aminidase	Aryl-sulfatase	Acid-phosphat-ase
Phenol oxidase	1	0.24	-0.23	0.09	0.01	-0.09	-0.01	0.35	-0.01
Peroxidase		1	-0.2	-0.27	**-0.41**	**-0.45**	-0.29	-0.1	**-0.61**
Urease			1	-0.07	0.12	0.1	0	-0.16	-0.15
Beta-1,4-glucosidase				1	**0.86**	**0.6**	**0.87**	0.39	**0.63**
Cellobiohydrol-ase					1	**0.75**	**0.84**	0.39	**0.65**
Beta-1,4-xylosidase						1	**0.59**	**0.46**	**0.57**
Beta-1,4-N-acetylglucosaminidase							1	0.33	**0.74**
Aryl-sulfatase								1	0.2
Acid-phosphatase									1

3.4.2 Ordinations for microbial community data and measured environmental variables

Microbial functional data

NMS ordination of microbial functional data from all soil profile layers combined

NMS discriminated microbial communities from the different locations based on their enzyme activities (Figure 3.21) (see Appendix 8.1 for test statistics). When the plot is orientated using the soil moisture (%) vector, axes 1 and 2 accounted for 63% and 26% respectively of the variation in the distance matrix. Communities from all three soil layers at the PP location clustered together closely, as did the mineral soil communities from the ICH and ESSF locations (identified in Figure 3.21). Microbial communities from the other locations clustered together more loosely (except the CWH location which did not cluster) (Figure 3.21). Soil moisture, soil N concentration, and soil C concentration were strongly correlated ($r^2 \geq 0.4$) with axis 1 (r^2 = 68%, 55%, and 53% respectively). There were no strong correlations between the measured environmental variables and axis 2 ($r^2 \geq 0.4$).

When orientated by the soil moisture vector, the first NMS axis separated locations along an average precipitation gradient. Microbial communities from the drier locations (PP and IDF and BWBS to some degree) place on the left side of the ordination (although the spring F-layer samples from the IDF location were placed further to the right), along with the mineral layers of ESSF and ICH. Microbial communities from the wetter locations ESSF (organic soil layers) and ICH (organic soil layers) (and MH to some degree) place on the right side of the ordination.

The data points representing phenol oxidase and peroxidase activities were plotted at a distance from the other enzyme activities. Variation in peroxidase activity was mainly responsible for the separation of the data points along axis 1 (80% of the variance in the data explained). Variation in phosphatase and NAG activities were mainly responsible for the separation of the data points along axis 2 (45% and 41% of the variance in the data explained respectively).

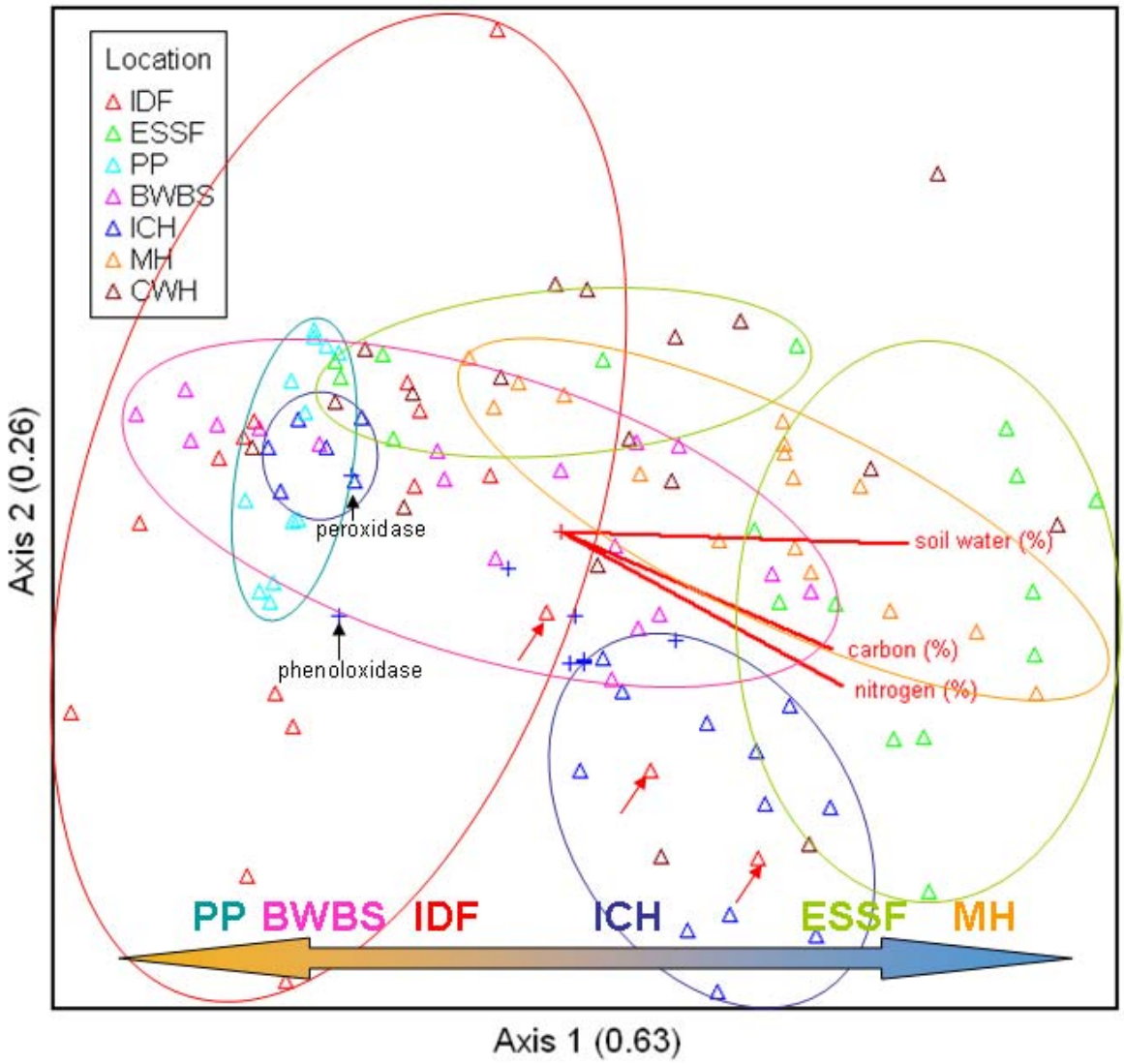

Figure 3.21. NMS ordination of microbial communities from all soil profile layers combined at the seven locations based on enzyme activity (n=116). The axes are orientated by the soil moisture vector. Red arrows indicate IDF F-layer spring samples. Large arrow indicates mean annual precipitation gradient from left to right, driest to wettest, for reference (the CWH location is not shown as the data points do not cluster).

NMS ordination of microbial functional data from the organic layers

When considering soil microbial communities only from the organic (F and H) soil layers at the seven locations, NMS again clearly discriminated microbial communities from the different locations based on their enzyme activities (Figure 3.22) (see Appendix 8.1 for test statistics). When the plot is orientated using the soil moisture vector, axes 1, 2 and 3 accounted for 22%, 52% and 17% respectively of the variation in the distance matrix.

Microbial communities from the F layer at the PP location clustered together closely. Microbial communities from the other locations clustered together more loosely. Soil water content was strongly correlated with axis 2 (r^2 = 61%). Soil N and C concentrations were correlated with axis 1 (both r^2 = 40%). There were no strong correlations between the measured environmental variables and axis 3 ($r^2 \geq 0.4$).

When orientated by the soil water content vector, the first NMS axis seemed to separate locations along an annual average precipitation gradient. This pattern is more obvious than in the ordination of all soil layers combined (Figure 3.21). Microbial communities from the drier locations (PP and IDF) placed on the left side of the ordination (although the spring F-layer samples from the IDF location were placed further to the right). Microbial communities from the wetter locations (ESSF and MH) placed on the right side of the ordination. Microbial communities from the locations which are ranked in the middle of the average annual precipitation gradient (BWBS, CWH and ICH) placed in the middle of the ordination plot.

The data points representing phenol oxidase and peroxidase activity were plotted at a distance from the other enzyme activities. Variation in phosphatase activity was mainly responsible for separation of the data points along axis 1 (53% of the variance in the data explained). Variation in peroxidase activity was mainly responsible for separation of the data points along axis 2 (50% of the variance in the data explained). There were no strong correlations between the enzyme activities and axis 3.

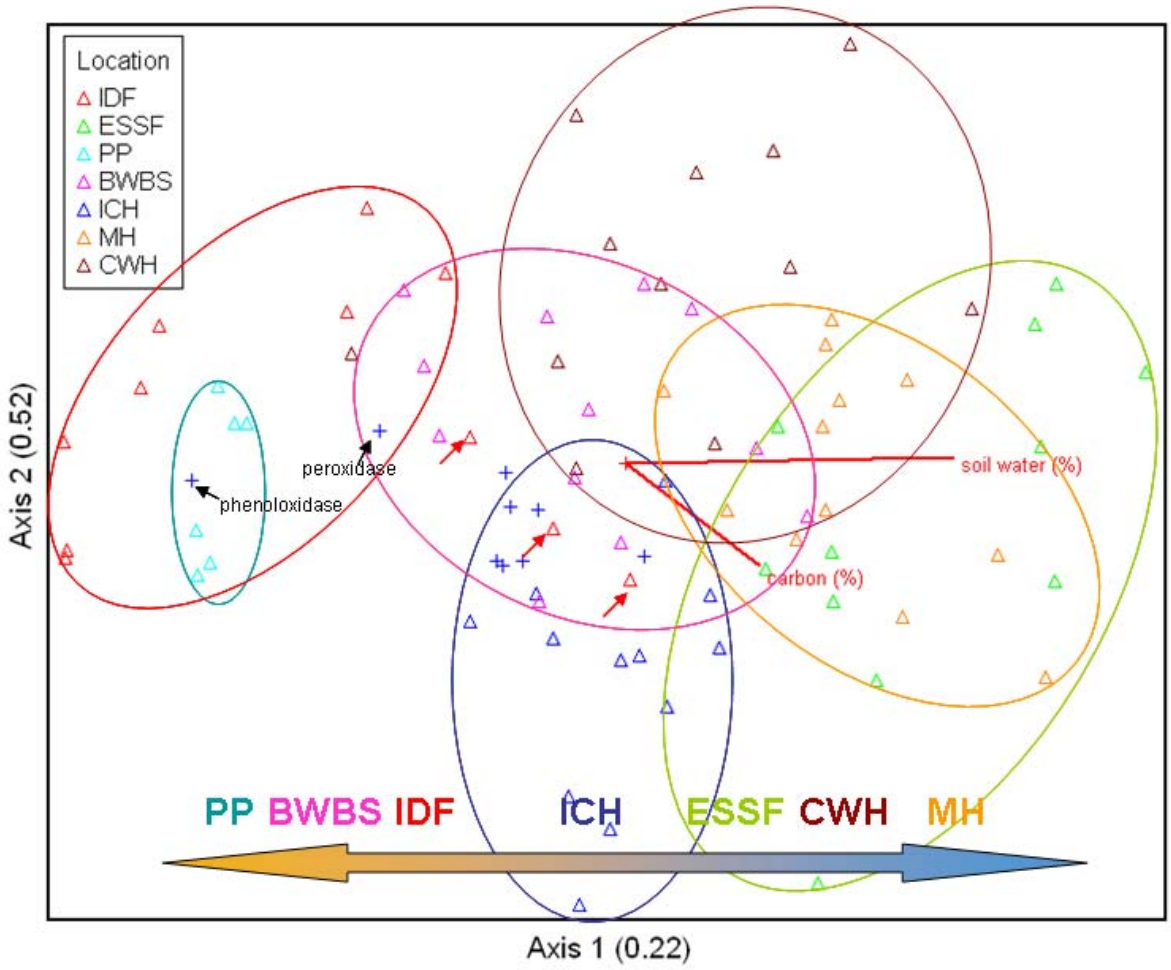

Figure 3.22. NMS ordination of microbial communities from organic layers at the seven locations based on enzyme activity (n=76). The axes are orientated by the soil moisture vector. Red arrows indicate IDF F-layer spring samples. Large arrow indicates mean annual precipitation gradient from left to right, driest to wettest.

NMS ordination of microbial functional data from the F layer

Ordinations for the organic layers (F and H) are also presented individually, as different results are observed for each layer.

When considering soil microbial communities only from the F layer at the seven locations, NMS again discriminated microbial communities from the different locations based on their enzyme activities (Figure 3.23) (see Appendix 8.1 for test statistics). When the plot was orientated using the soil moisture vector, axes 1, 2 and 3 accounted for 56%, 8% and 25% respectively of the variation in the distance matrix.

Microbial communities from the F layer at the PP location clustered together closely, as did microbial communities from the IDF location. Microbial communities from the summer and spring sampling times at the IDF location clustered separately. Microbial communities from the other locations clustered together more loosely, especially from the CWH location (Figure 3.8 and Figure 3.9). Soil moisture content was strongly correlated with axis 1 (r^2 = 58%). There were no strong correlations between the measured environmental variables and axes 2 and 3 ($r^2 \geq 0.4$).

When orientated by the soil water content vector, the first NMS axis seemed to separate locations along an annual average precipitation gradient. The first NMS axis separated the enzyme activities of the PP location and the summer samples of the IDF location to the left of the other locations and the MH and ESSF location clusters placed slightly to the right of the other location clusters.

The data points representing phenoloxidase and peroxidase activities were plotted at a distance from the other enzyme activities. Variation in peroxidase activity was mainly responsible the separation of data points along axis 1 (69% of the variance in the data explained). Phosphatase activity was mainly responsible the separation of data points along axis 2 (68% of the variance in the data explained). Phenoloxidase and sulfatase activity mainly responsible the separation of data points along axis 3 (55% and 50% of the variance in the data explained respectively).

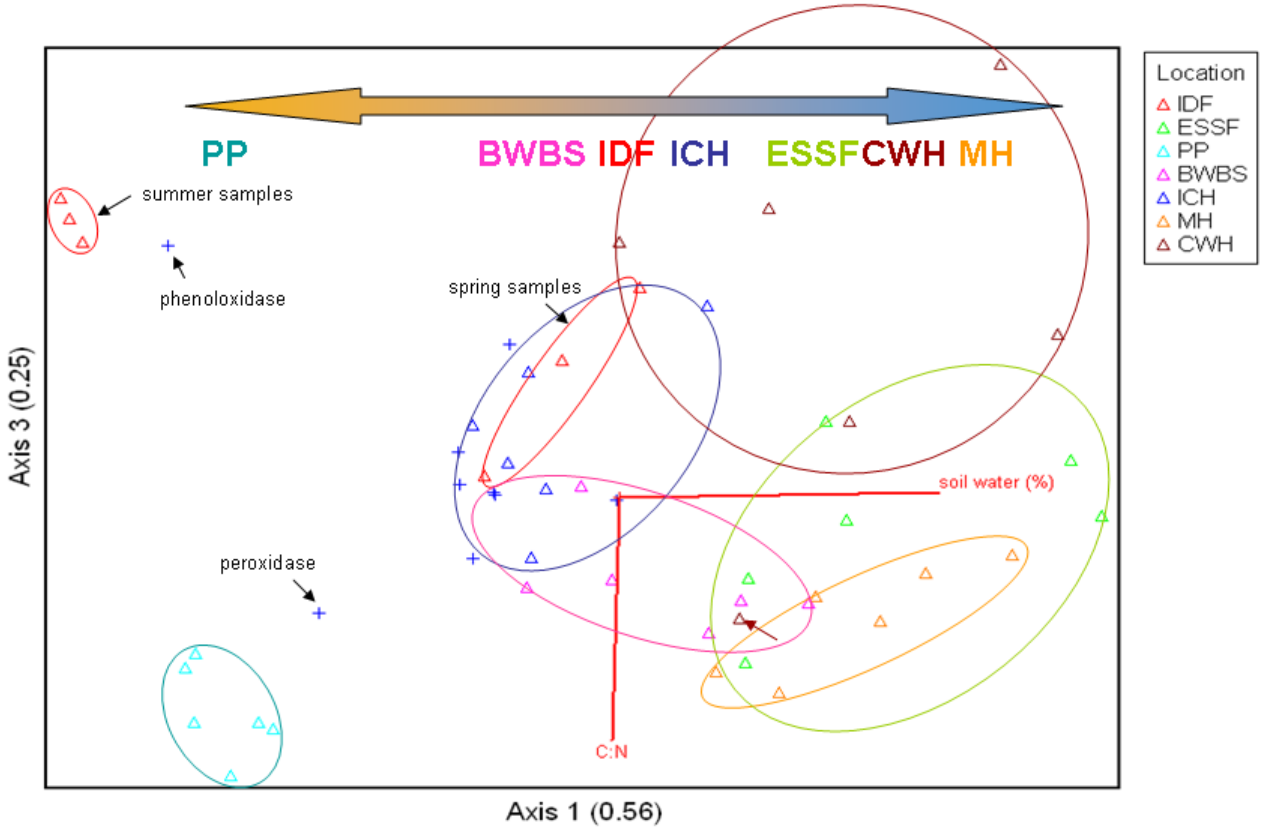

Figure 3.23. NMS ordination of axes 2 and 3 showing microbial communities from the F layer at the seven locations based on enzyme activity (n=42). The axes are orientated by the soil moisture vector. The brown arrow indicates CWH spring sample from site 3. Large arrow indicates mean annual precipitation gradient from left to right, driest to wettest.

NMS ordination of microbial functional data from the H layer

When considering soil microbial communities only from the H layer at the six locations[15], NMS again discriminated microbial communities from the different locations based on their enzyme activities (Figure 3.24) (see Appendix 8.1 for test statistics). When the plot was orientated using the soil water content vector, axes 1 and 2 accounted for 56% and 35% respectively of the variation in the distance matrix. Nitrogen concentration was correlated with axis 1 (r^2 = 44%). Soil water content was correlated with axis 2 (r^2 = 58%).

As with the previous microbial community function ordinations, when orientated by the soil water content vector, the first NMS axis seemed to separate locations along an annual average precipitation gradient. Microbial communities from the drier (IDF) location were clustered on the left side of the ordination. Microbial communities from the wetter locations (ESSF and MH) place on the right side of the ordination. Microbial communities from the locations which are ranked in the middle of the average annual precipitation gradient (BWBS, CWH and ICH) place in the middle of the ordination plot. The lack of an H layer for the PP location makes this gradient less obvious.

The data points representing phenoloxidase and peroxidase activities were plotted at a distance from the other enzyme activities. Peroxidase activity was mainly responsible the separation of data points along axis 1 (68% of the variance in the data explained) and axis 2 (46% of the variance in the data explained). Glucosidase activity was mainly responsible the separation of data points along axis 2 (44% of the variance in the data explained).

[15] The PP location had no H layer.

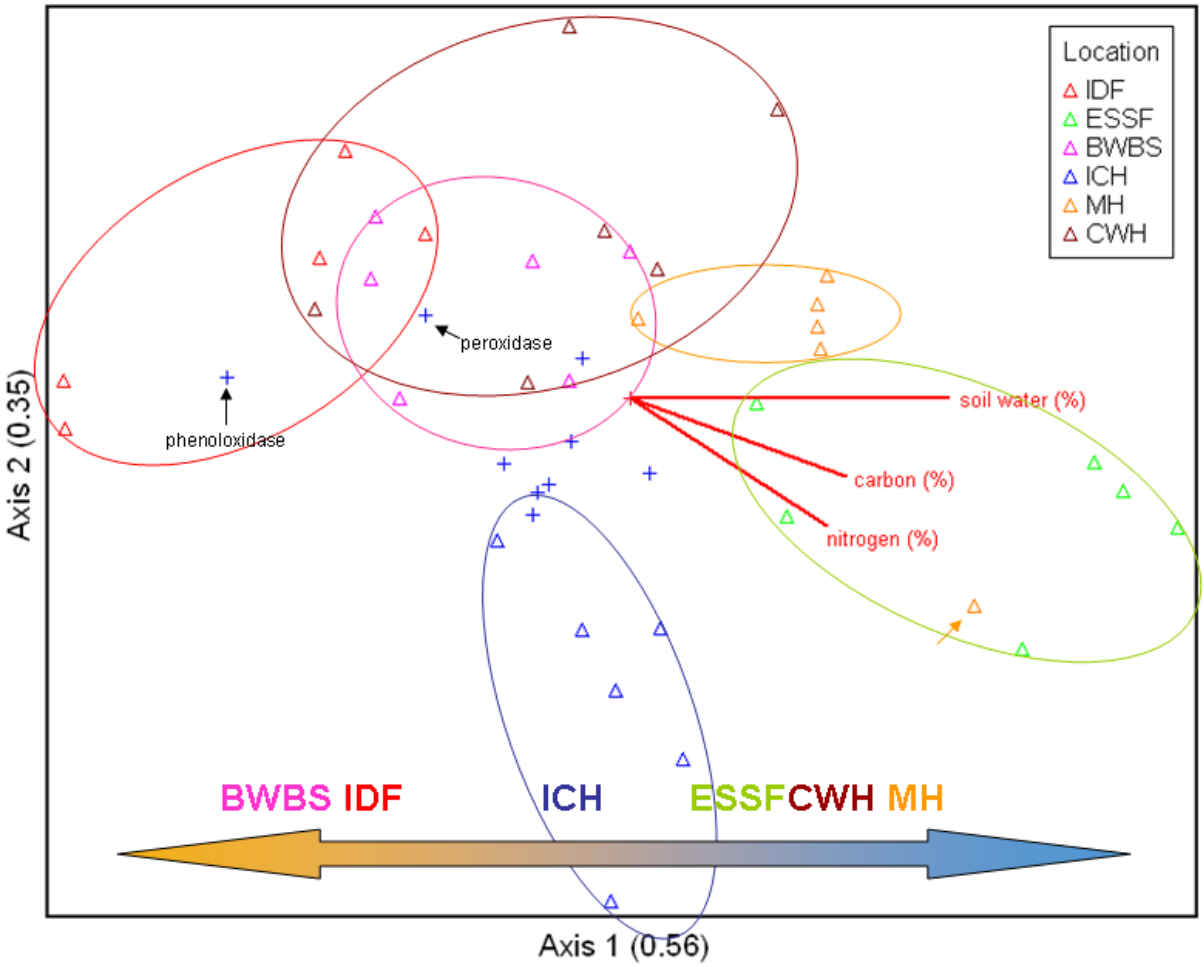

Figure 3.24. NMS ordination of axes 1 and 2 showing microbial communities from the H layer at the seven locations based on enzyme activity (n=34). PP does not have an H layer and is therefore not represented in this ordination. The axes are orientated by the soil water content vector. The brown arrow indicates CWH spring sample from site 2. Large arrow indicates mean annual precipitation gradient from left to right, driest to wettest..

NMS ordination of microbial functional data from the mineral layer

When considering soil microbial communities only from the mineral soil at the seven locations, NMS did not discriminate microbial communities from the different locations based on their enzyme activities. There was only one dimension to the ordination plot (see Appendix 8.1 for test statistics). Peroxidase activity was mainly responsible the separation of data points along the one axis (69% of the variance in the data explained), but there were no environmental variables which correlated with the single axis ($r^2 \geq 0.4$) (soil water had an r^2 value of 0.35).

Microbial structural data

NMS ordination of structural data from all soil profile layers combined

The NMS of the PLFA data for all soil layers combined did not discriminate the microbial communities from the different locations very well, relative to the discrimination of the enzyme activity data (Figure 3.25) (see Appendix 8.1 for test statistics). However, microbial communities from the CWH location clustered distinctly, except for one sample from the mineral soil which is indicated by an arrow. Axes 1 and 2 of the ordination plot accounted for 26% and 71%, respectively, of the variation in the distance matrix.

None of the environmental variables were strongly correlated with the ordination axes ($r^2 \geq 0.4$). The total bacterial:saprophytic fungal, total bacterial:total fungal, and total bacterial:arbuscular fungal PLFA ratios were plotted at a distance from the other PLFA signature ratios, near to the CWH community cluster. Figures 3.26 and 3.27 show that the total bacterial:total fungal ratios for the organic layers at the CWH location were the highest or are among the highest of all seven locations. The total bacterial:saprophytic fungal and the total bacterial:total fungal ratios were strongly correlated with axis 1 (70% and 51% of the variance in the data explained respectively). The total bacterial:arbuscular mycorrhizal fungal ratio was strongly correlated with axis 2 (56% of the variance in the data explained).

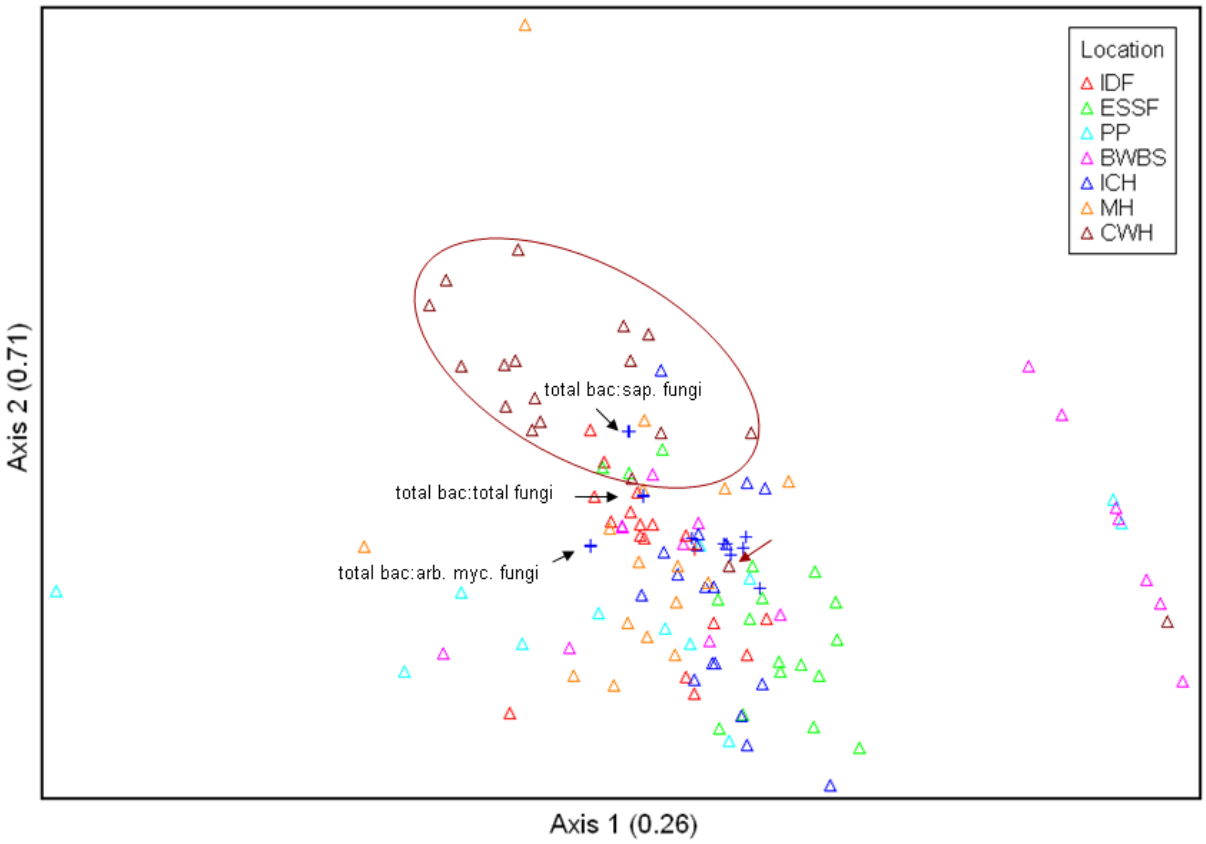

Figure 3.25. NMS ordination showing microbial communities from all layers at the seven locations based on PLFA signature microbial community groupings (n=118). The CWH location microbial community data points are circled and the spring sample from site outlier is indicated by an arrow.

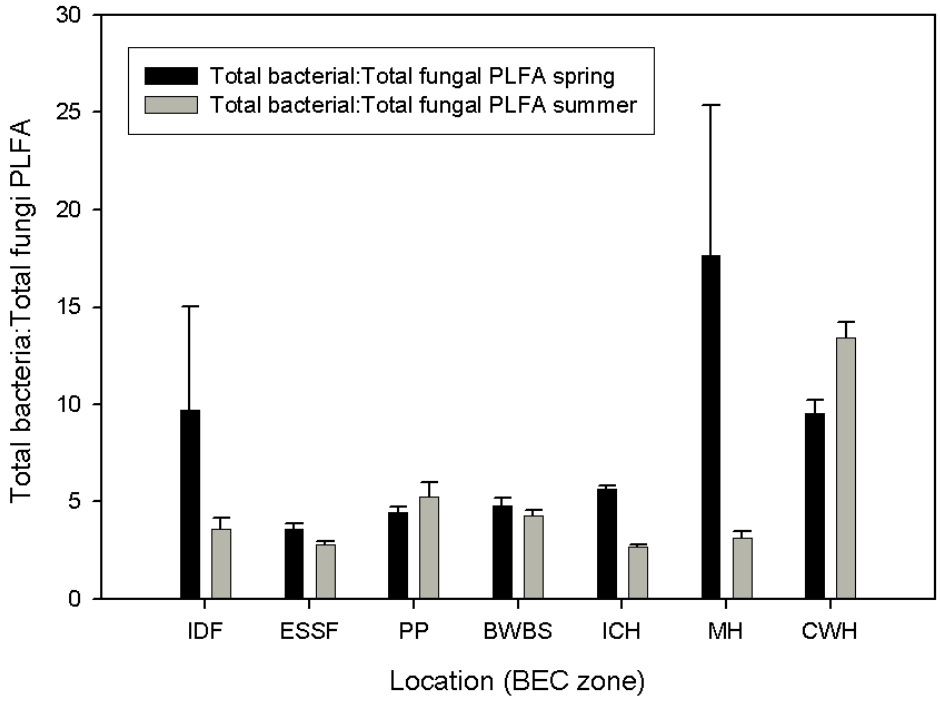

Figure 3.26. Mean total bacterial:total fungi PLFA signature ratios for the F layer at the seven locations, with standard error bars (n=42).

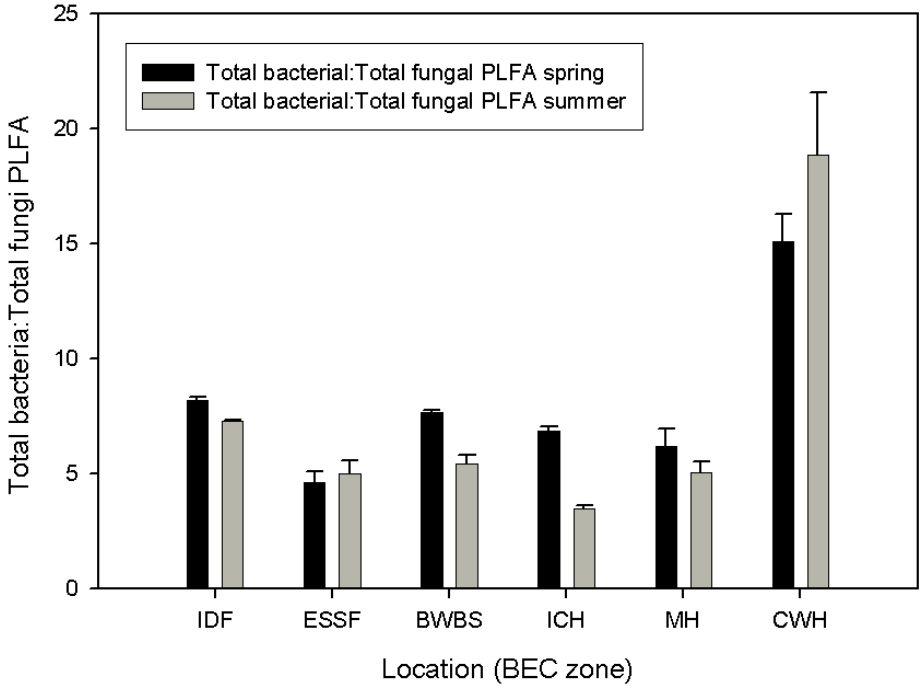

Figure 3.27. Mean total bacterial:total fungi PLFA signature ratios for the H layer, at the seven locations, with standard error bars (n=35).

NMS ordination of structural data from the F layer

As for all soil layers combined, the NMS of the PLFA data from the F layer could not discriminate the microbial communities from the different locations very well, relative to the discrimination of the enzyme activity data (Figure 3.28) (see Appendix 8.1 for test statistics). The F-layer ordination plot is very similar to the ordination plot of all soil layers combined. Only microbial communities from the CWH location clustered distinctly. Axes 1 and 2 of the ordination plot accounted for 77% and 19% respectively of the variation in the distance matrix.

None of the environmental variables were strongly correlated with the ordination axes ($r^2 \geq 0.4$). The total bacterial:saprophytic fungal, total bacterial:arbuscular mycorrhizal fungal, and total bacterial:total fungal PLFA ratios were plotted at a distance from the other PLFA signature ratios. Figure 3.26 shows that the total bacterial:total fungal ratios for the F layers at the CWH location are among the highest of all seven locations. Variation in total bacterial:total fungal, total fungal:total microbial biomass ratios, and total bacterial:saprophytic fungal ratios were mainly responsible for separation of the data points along axis 1 (49%, 46%, and 45% of the variance in the data explained respectively). Variation in total bacterial:arbuscular mycorrhizal fungal ratios was mainly responsible for separation of data points along axis 2 (77% of the variance in the data explained).

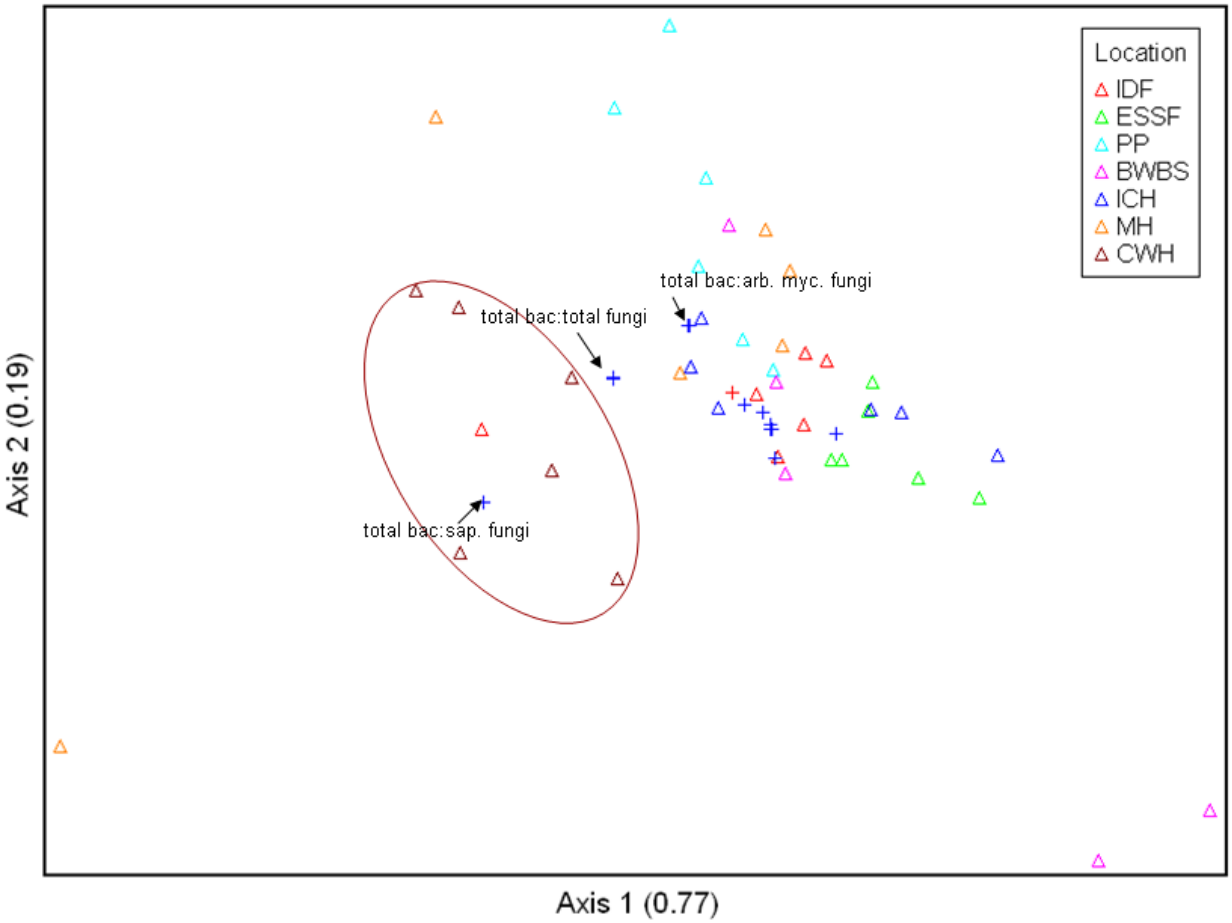

Figure 3.28. NMS ordination showing microbial communities from the F layer at the seven locations based on PLFA signature microbial community groupings (n=42). The CWH location data points are circled.

NMS ordination of structural data from the H layer

Unlike the previous NMS ordinations on microbial community structure data, the NMS of the PLFA data from the H layer discriminated the microbial communities from the different locations (Figure 3.29) (see Appendix 8.1 for test statistics). Microbial communities from the CWH location clustered on the right side of the ordination plot, away from the other locations.

The CWH locations had significantly higher available total N, NO_3-N and to a lesser extent NH_4-N than any of the other locations (Figure 3.15). The microbial communities at the CWH location had low saprophytic and total fungal biomass compared to the other locations (Figure 3.30).

When orientated by the available total N vector, axes 1 and 2 of the ordination plot accounted for 85% and 13% respectively of the variation in the distance matrix. Available total N and available nitrate were correlated with axis 2 (both r^2 = 42%). None of the environmental variables were strongly correlated with the first ordination axis ($r^2 \geq$ 0.4). Variation in the total bacterial:arbuscular mycorrhizal fungal, total fungal:total microbial biomass, total bacterial: total fungal, and total bacterial:saprophytic fungal ratios were mainly responsible for the separation of the data points along axis 1 (78%, 50%, 47%, and 43% of the variance in the data explained respectively). The total bacterial:saprophytic fungal and total bacterial:total fungal ratios were strongly correlated with axis 2 (both 73% of the variance in the data explained).

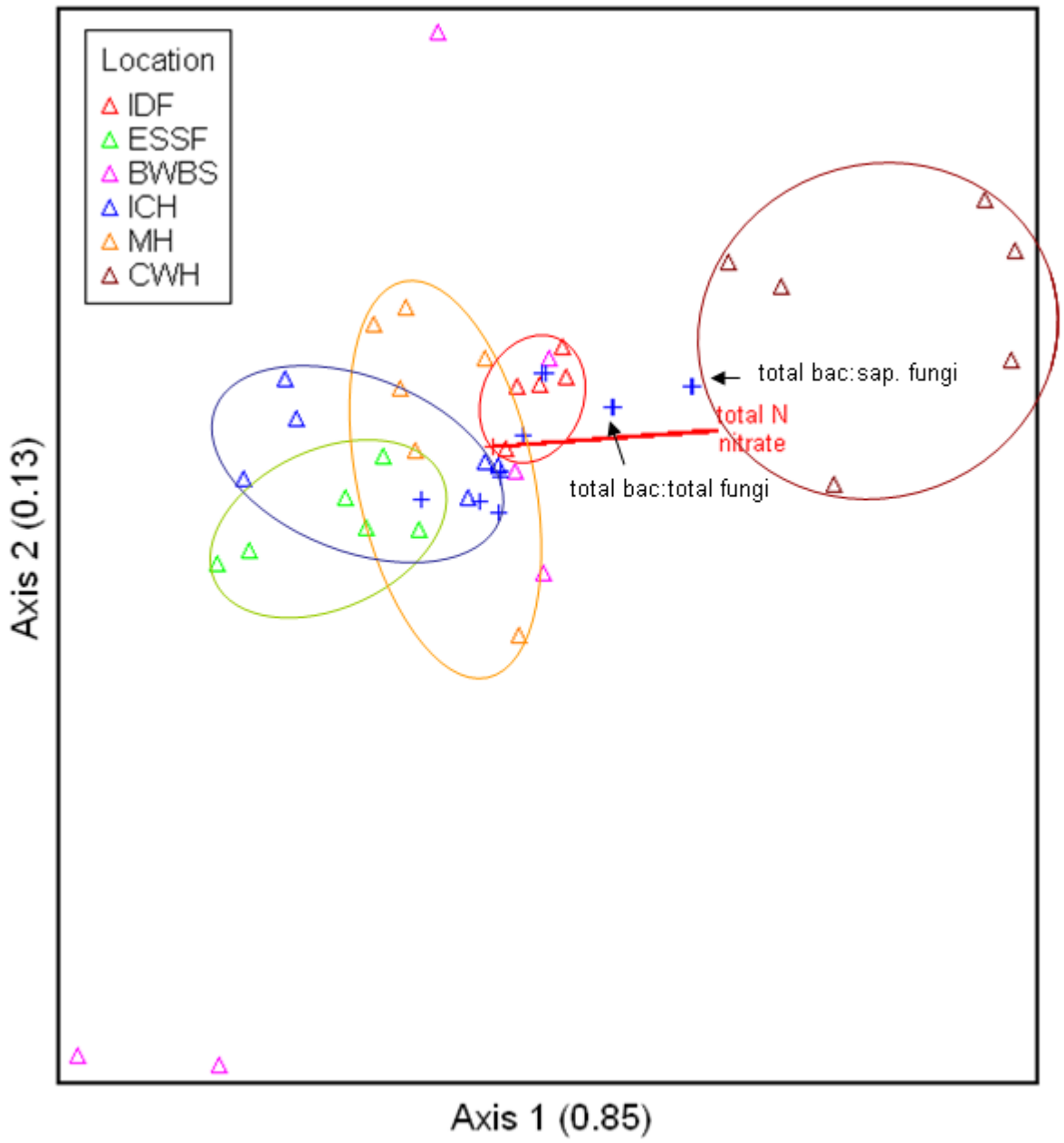

Figure 3.29. NMS ordination showing microbial communities from the H layer at the seven locations based on PLFA signature microbial community groupings (n=35).

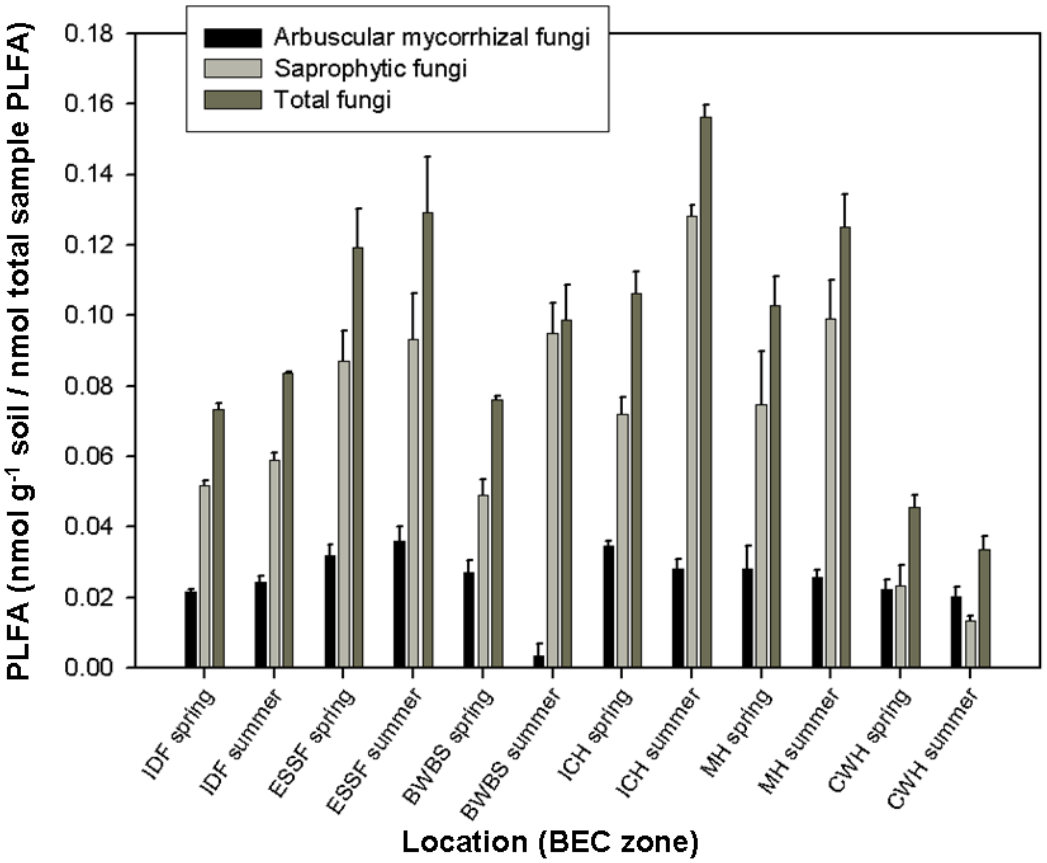

Figure 3.30. Mean total fungal PLFA concentration (total divided by sample biomass) in the H layer at the seven locations, with standard error bars (n=35).

NMS ordination of structural data from the mineral layer

As with the F layer and all soil layers combined, the NMS of the PLFA data from the mineral layer could not discriminate the microbial communities from the different locations very well relative to the discrimination of the enzyme activity data (Figure 3.31) (see Appendix 8.1 for test statistics). Axes 1 and 2 of the ordination plot accounted for 90% and 8% respectively of the variation in the distance matrix.

None of the environmental variables were strongly correlated with the ordination axes ($r^2 \geq 0.4$). The Gram-positive bacterial:Gram-negative bacterial, total bacterial:arbuscular mycorrhizal fungal, total bacterial:total fungal, and total bacterial:saprophytic fungal ratios were mainly responsible for the separation of the data points along axis 1 (57%,

46%, 46%, and 46% of the variance in the data explained respectively). The total bacterial:arbuscular mycorrhizal fungal ratio was also mainly responsible for the separation of the data points along axis 2 (45% of the variance in the data explained). The total bacterial:arbuscular mycorrhizal fungal ratio was plotted at a distance from the other PLFA signature ratios.

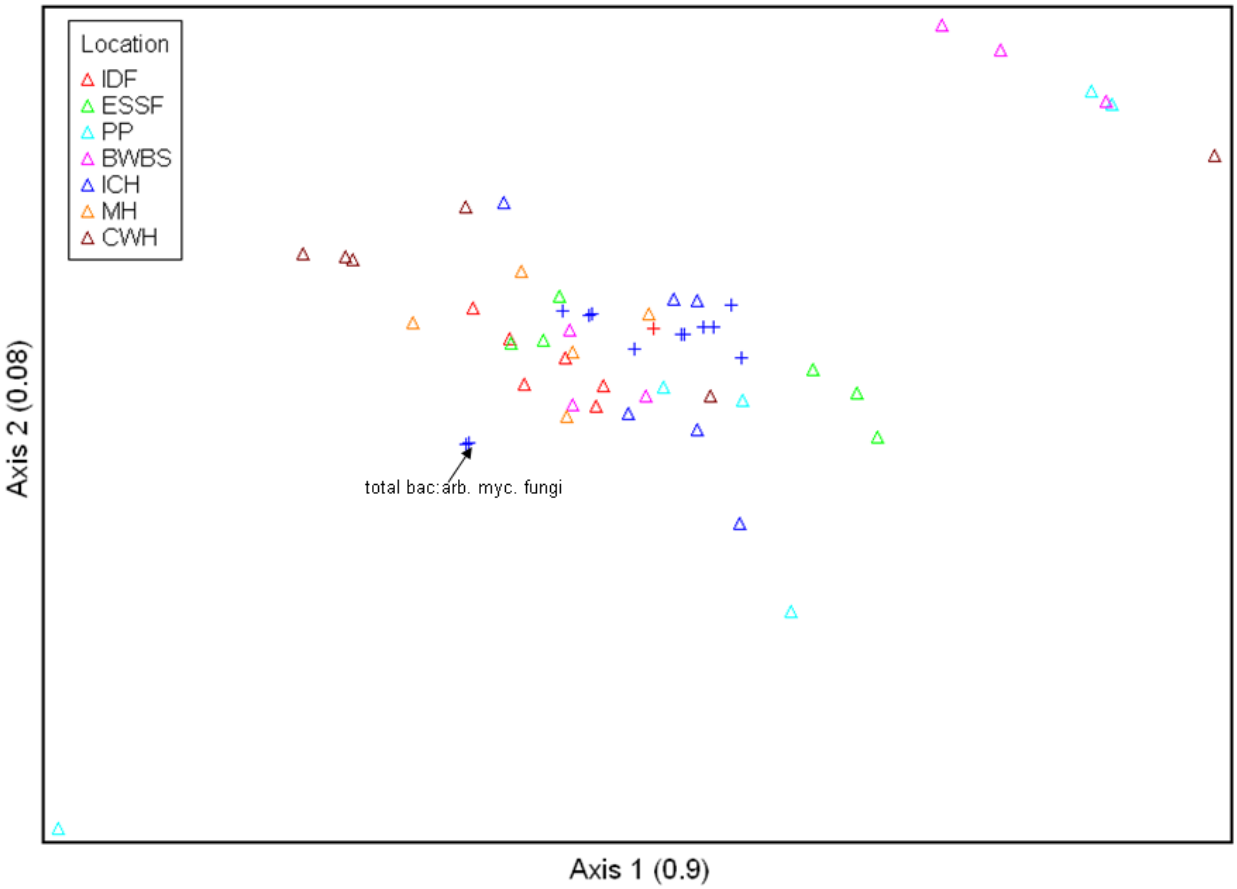

Figure 3.31. NMS ordination showing microbial communities from the mineral layer at the seven locations based on PLFA signatures (n=41).

3.5 Hypothesis five: Analysis of soil microbial structure and function will show separation of the mineral and organic layers

3.5.1 Microbial functional community data

Multivariate analysis of functional data from all soil layers combined

MRPP analysis showed high significant overall separation of the three layers (alpha 0.05) (p=0 A=0.184, n=116). The enzyme activity profile of the microbial communities from the F and H layers at all seven locations was significantly different from that of the microbial communities in the mineral soil (Table 3.23). The hypothesis is accepted.

Table 3.23. Pair-wise MRPP analysis of enzyme assay results for F, H, and mineral (M) layers.

A	F	H	M
F	1	**0.0178**	**0.2298**
H		1	**0.1751**
M			1
p	F	H	M
F	1	**0.01**	**0**
H		1	**0**
M			1
A>0.1 - high for ecological data - high within-group homogeneity			
A>0.3 very high for ecological data - very high within-group homogeneity			

Pair-wise comparisons *p* significant ≤ 0.0167 (alpha 0.05/3 - Bonferroni's correction). Significant values are shown in bold.

Patterns in individual enzyme activities down the soil profile

Labile C-mineralizing enzymes (cellulase, xylanase, and glucosidase), NAG, urease, phosphatase, and sulfatase all showed a decrease in activity down the soil profile in both spring and summer (Figures 3.32 to 3.45). However, recalcitrant C-mineralizing enzymes (phenoloxidase and peroxidase) showed an increase in activity down the soil profile, except for phenoloxidase activity in the spring sample (Figures 3.46 to 3.49).

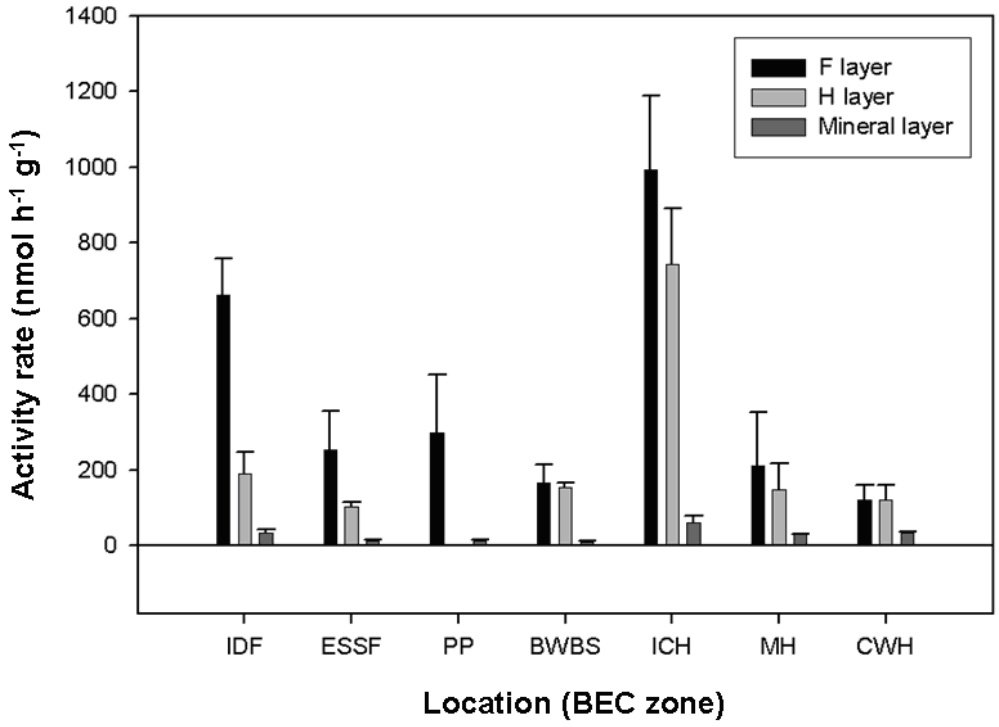

Figure 3.32. Mean cellulase activity rates (nmol of substrate converted per hour per gram of sample) in each soil layer (spring samples) with bars showing standard error.

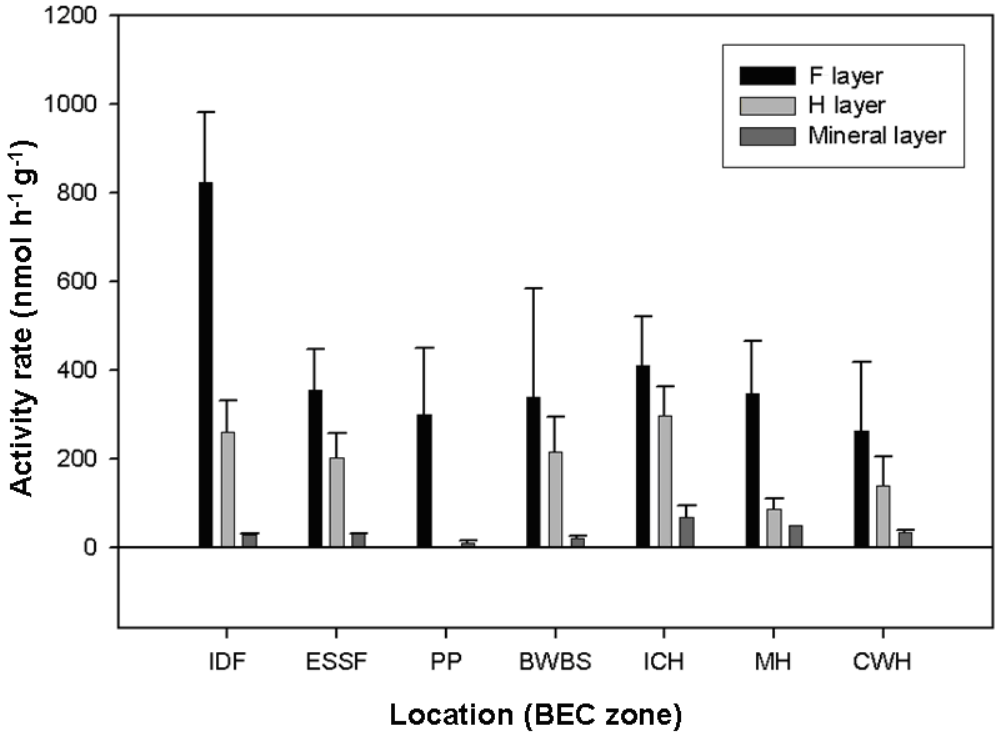

Figure 3.33. Mean cellulase activity rates (nmol of substrate converted per hour per gram of sample) in each soil layer (summer samples) with bars showing standard error.

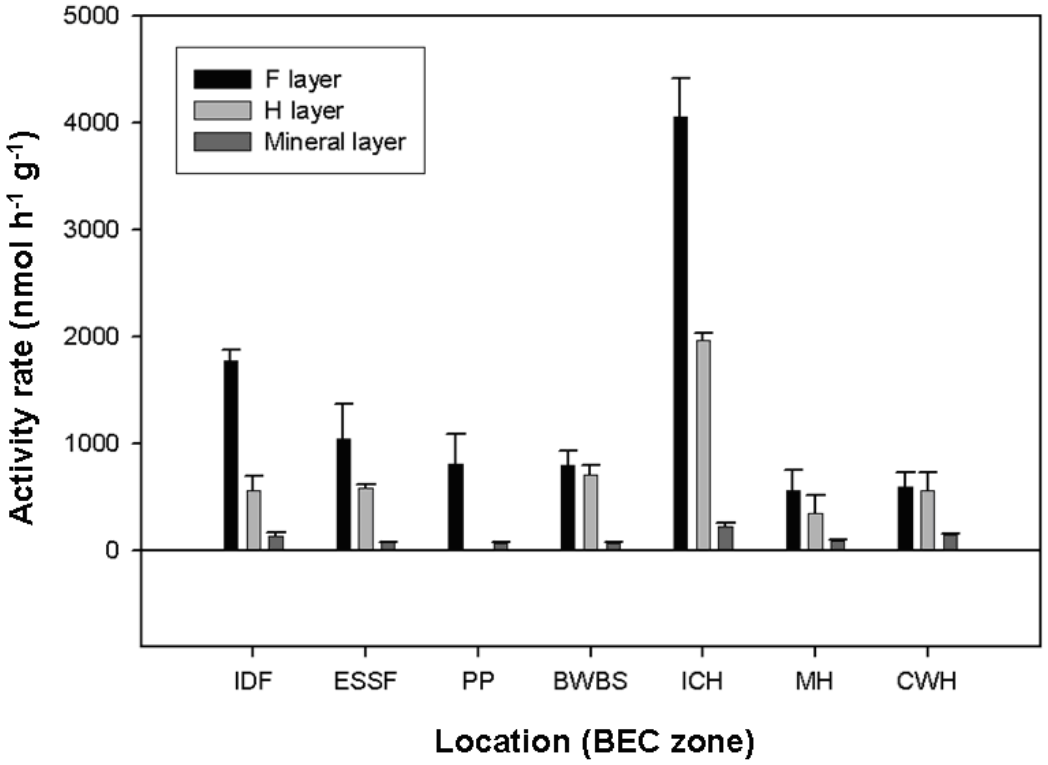

Figure 3.34. Mean glucosidase activity rates (nmol of substrate converted per hour per gram of sample) in each soil layer (spring samples) with bars showing standard error.

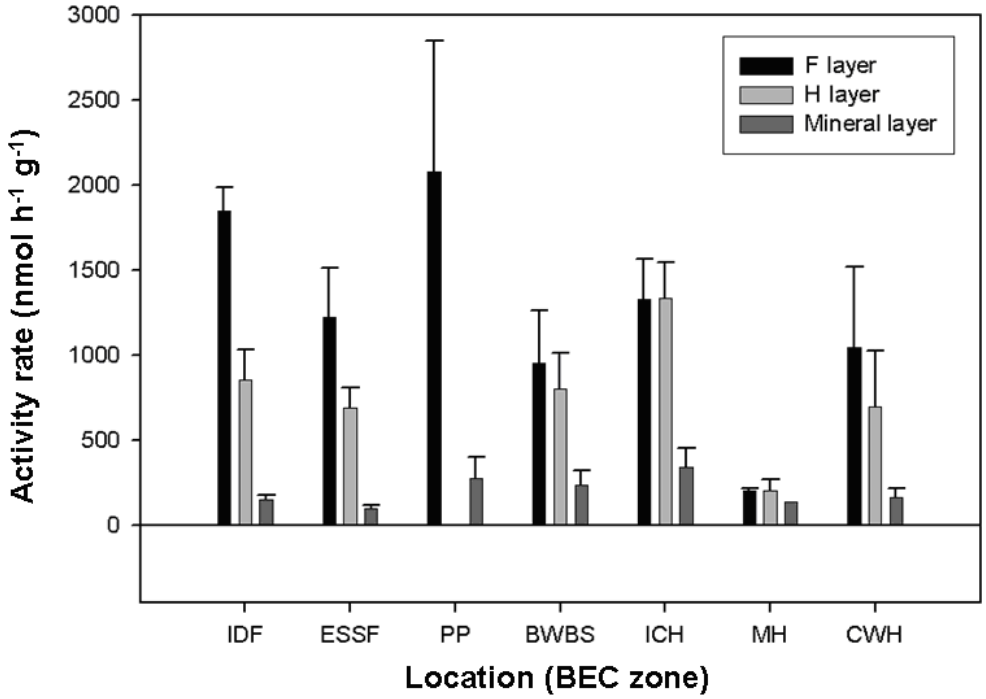

Figure 3.35. Mean glucosidase activity rates (nmol of substrate converted per hour per gram of sample) in each soil layer (summer samples) with bars showing standard error.

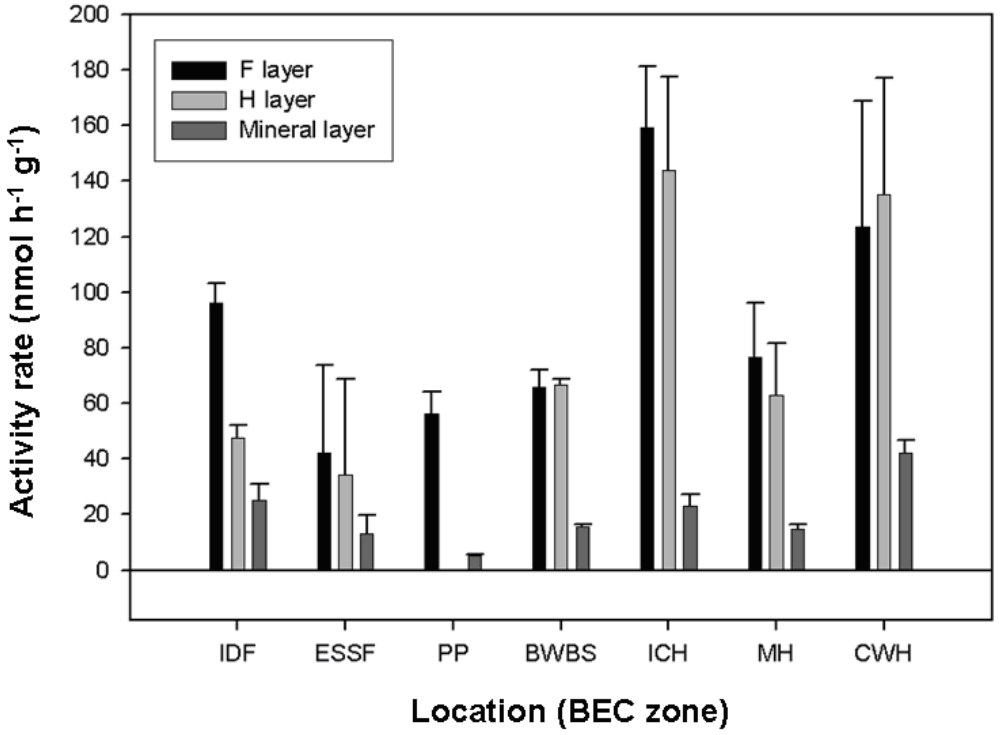

Figure 3.36. Mean xylanase activity rates (nmol of substrate converted per hour per gram of sample) in each soil layer (spring samples) with bars showing standard error.

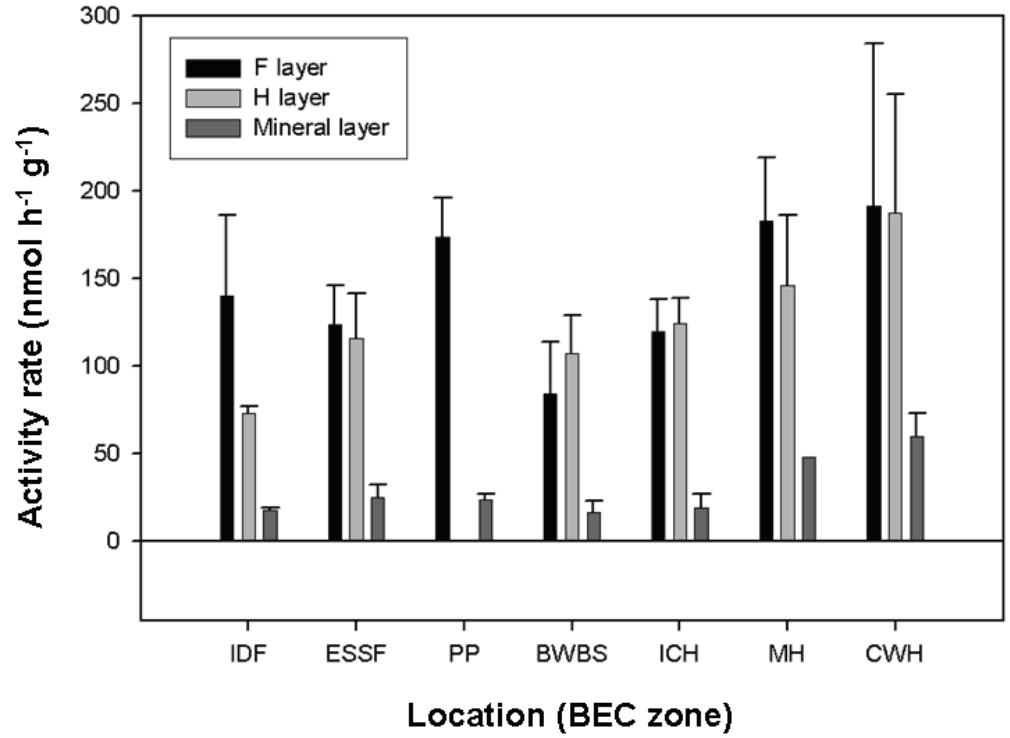

Figure 3.37. Mean xylanase activity rates (nmol of substrate converted per hour per gram of sample) in each soil layer (summer samples) with bars showing standard error.

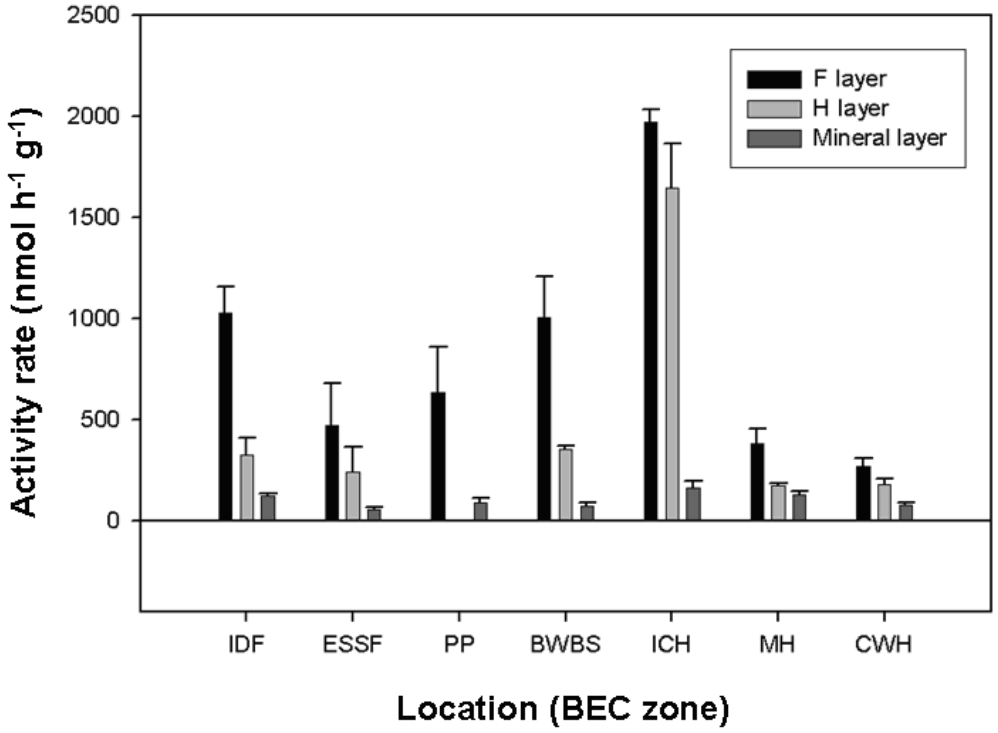

Figure 3.38. Mean NAG activity rates (nmol of substrate converted per hour per gram of sample) in each soil layer (spring samples) with bars showing standard error.

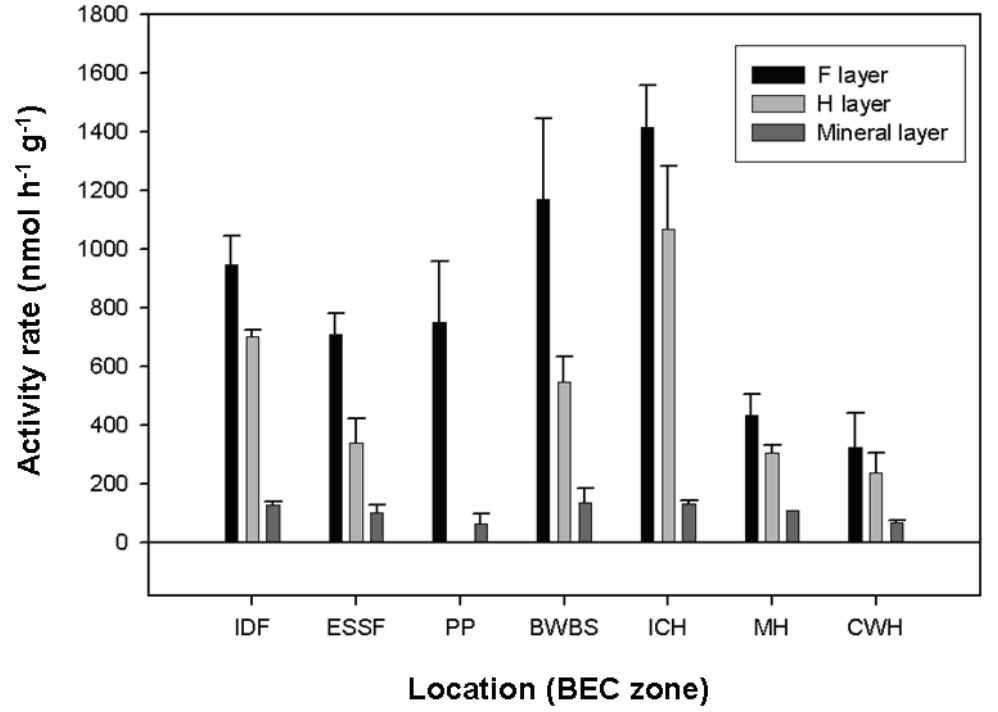

Figure 3.39. Mean NAG activity rates (nmol of substrate converted per hour per gram of sample) in each soil layer (summer samples) with bars showing standard error.

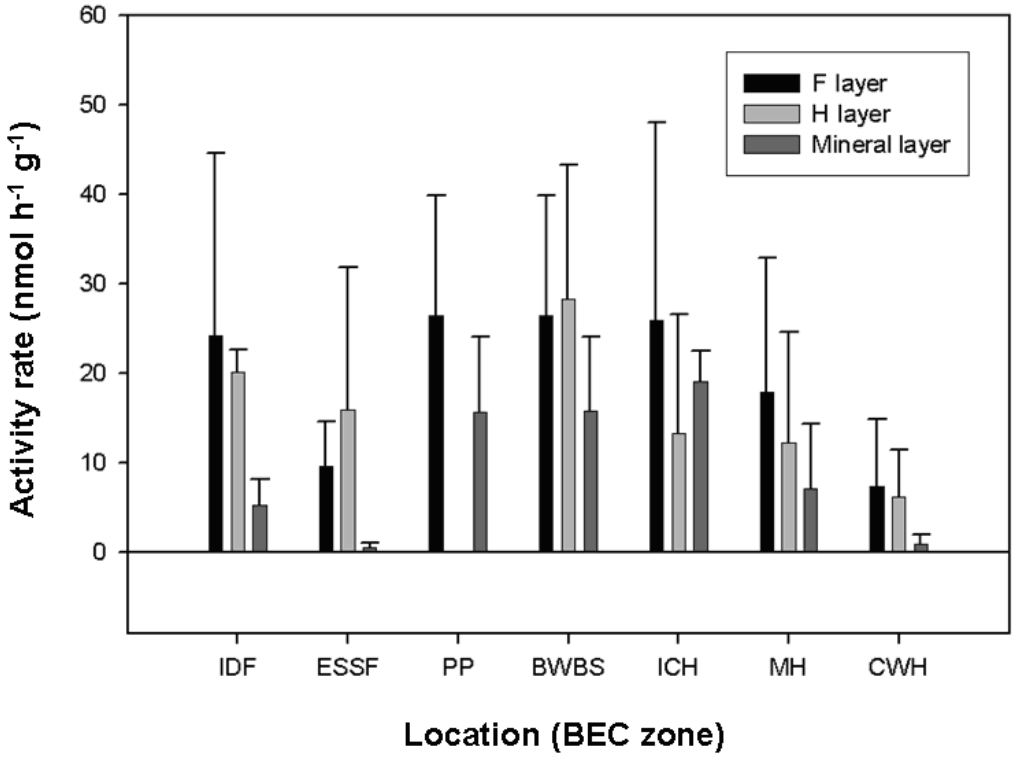

Figure 3.40. Mean urease activity rates (nmol of substrate converted per hour per gram of sample) in each soil layer (spring samples) with bars showing standard error.

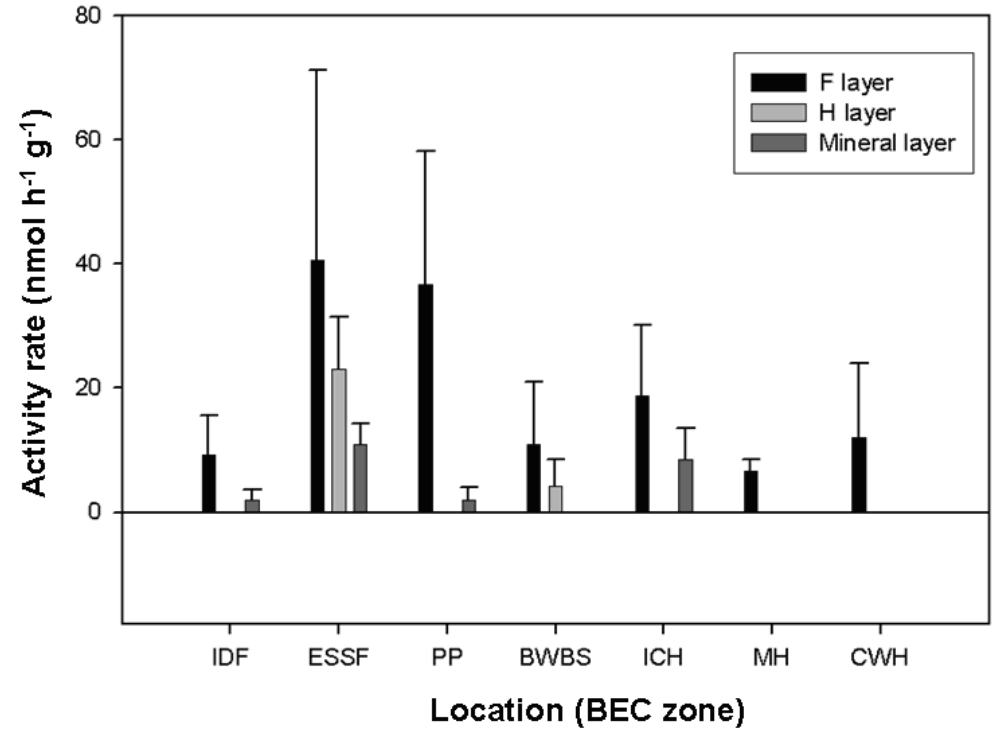

Figure 3.41 Mean urease activity rates (nmol of substrate converted per hour per gram of sample) in each soil layer (summer samples) with bars showing standard error.

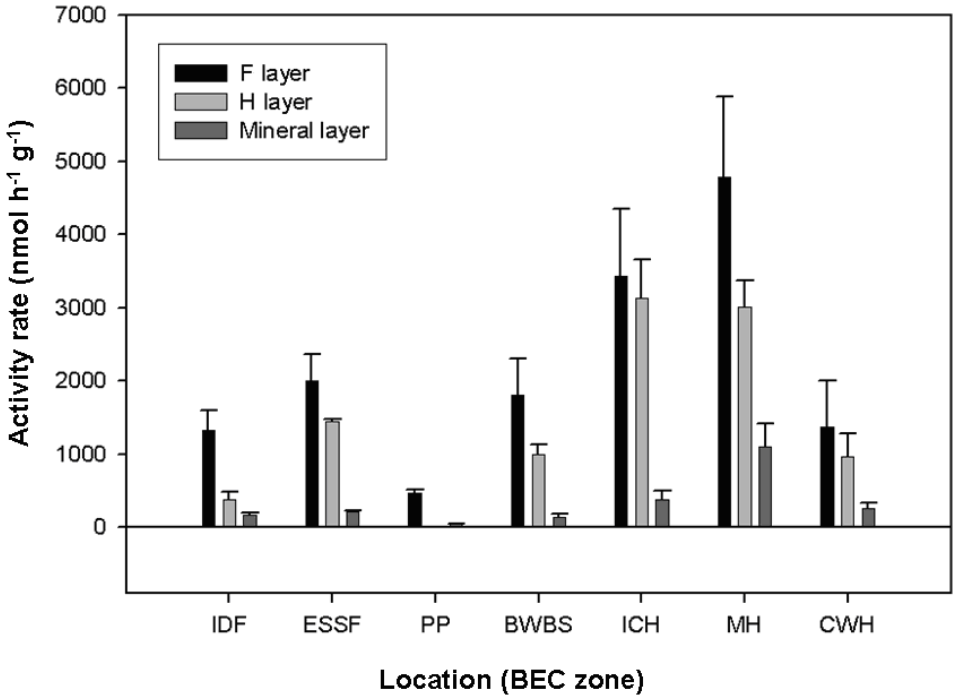

Figure 3.42. Mean phosphatase activity rates (nmol of substrate converted per hour per gram of sample) in each soil layer (spring samples) with bars showing standard error.

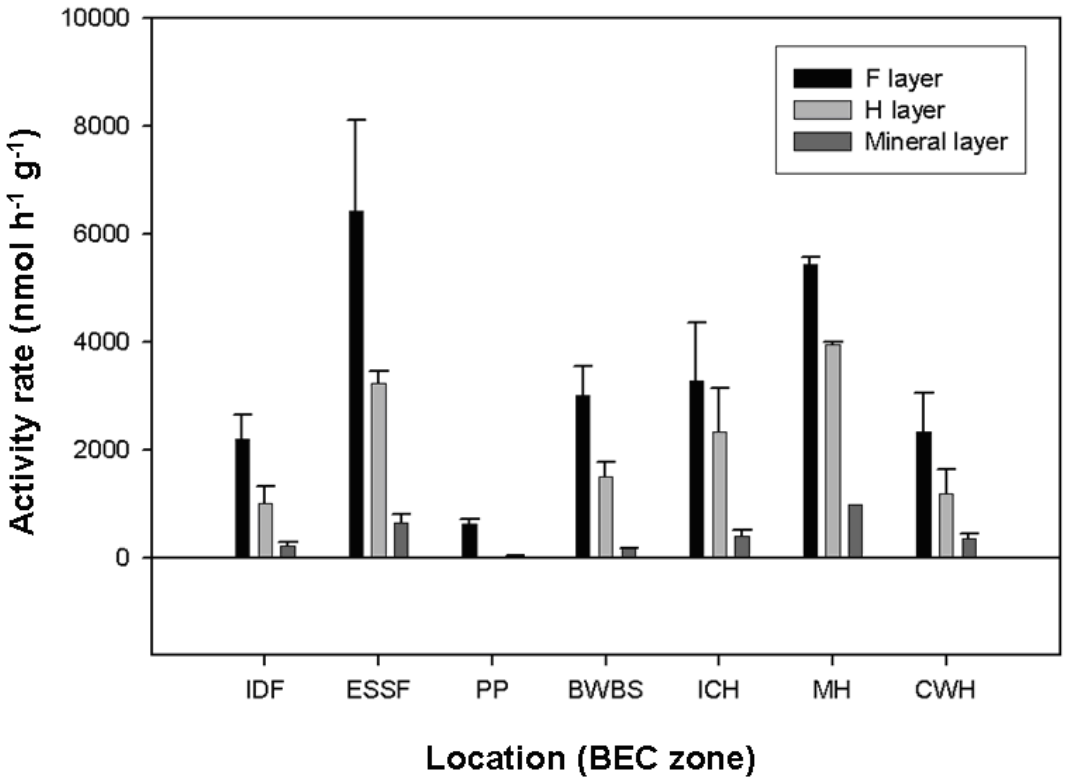

Figure 3.43. Mean phosphatase activity rates (nmol of substrate converted per hour per gram of sample) in each soil layer (summer samples) with bars showing standard error.

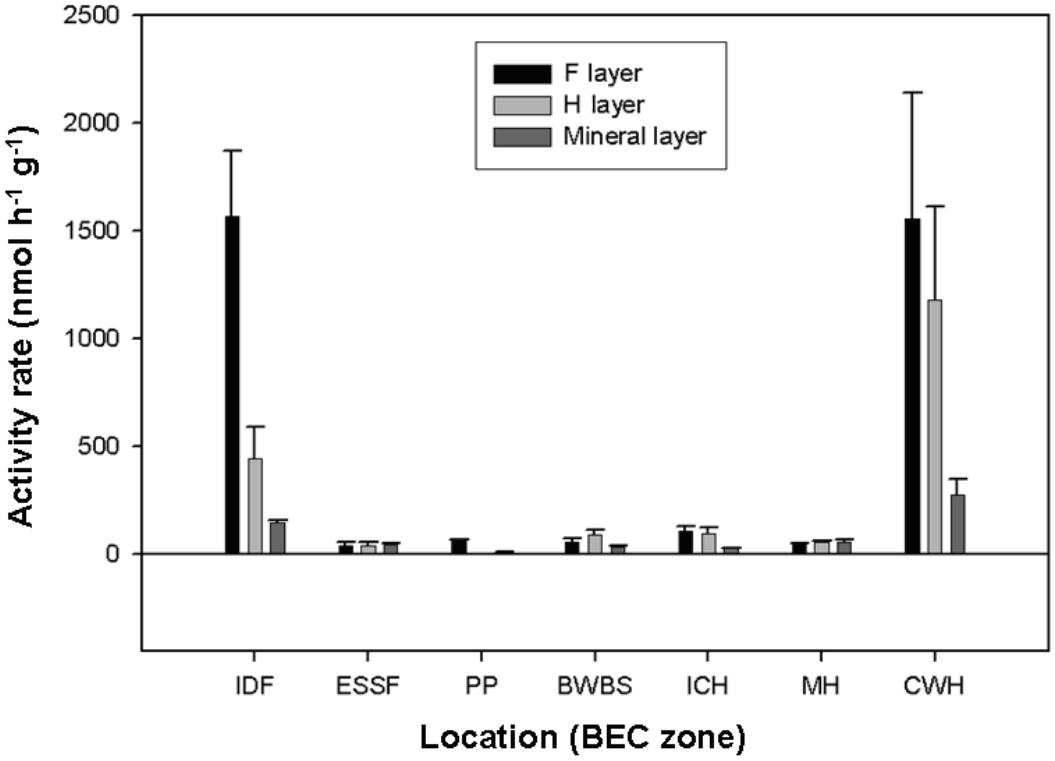

Figure 3.44. Mean sulfatase activity rates (nmol of substrate converted per hour per gram of sample) in each soil layer (spring samples) with bars showing standard error.

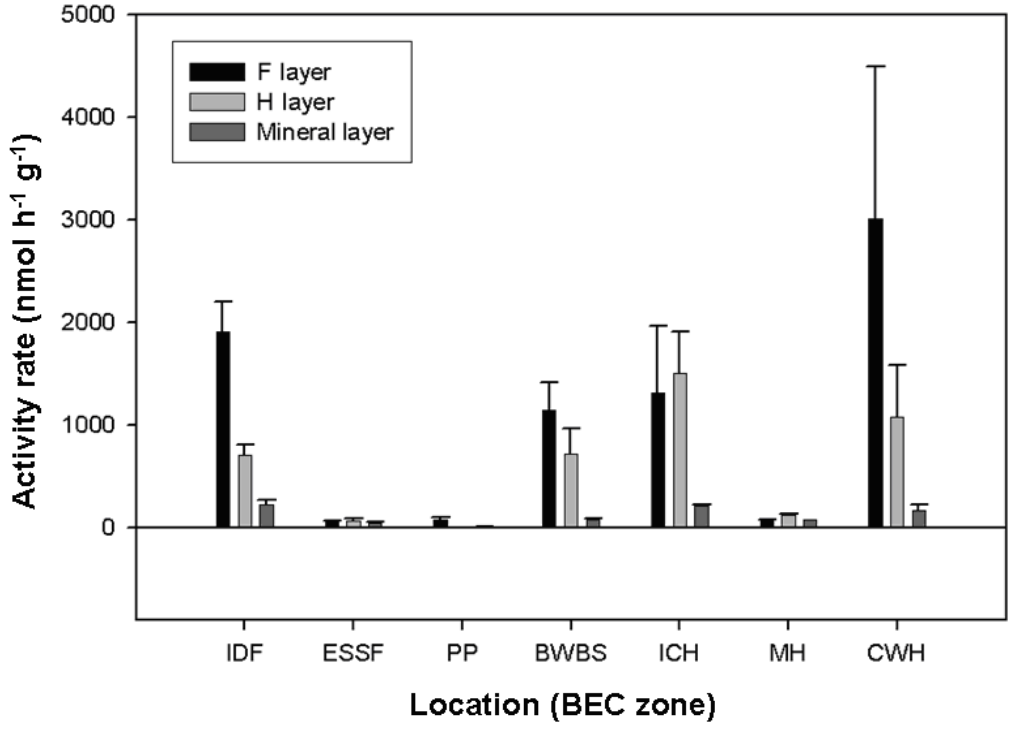

Figure 3.45. Mean sulfatase activity rates (nmol of substrate converted per hour per gram of sample) in each soil layer (summer samples) with bars showing standard error.

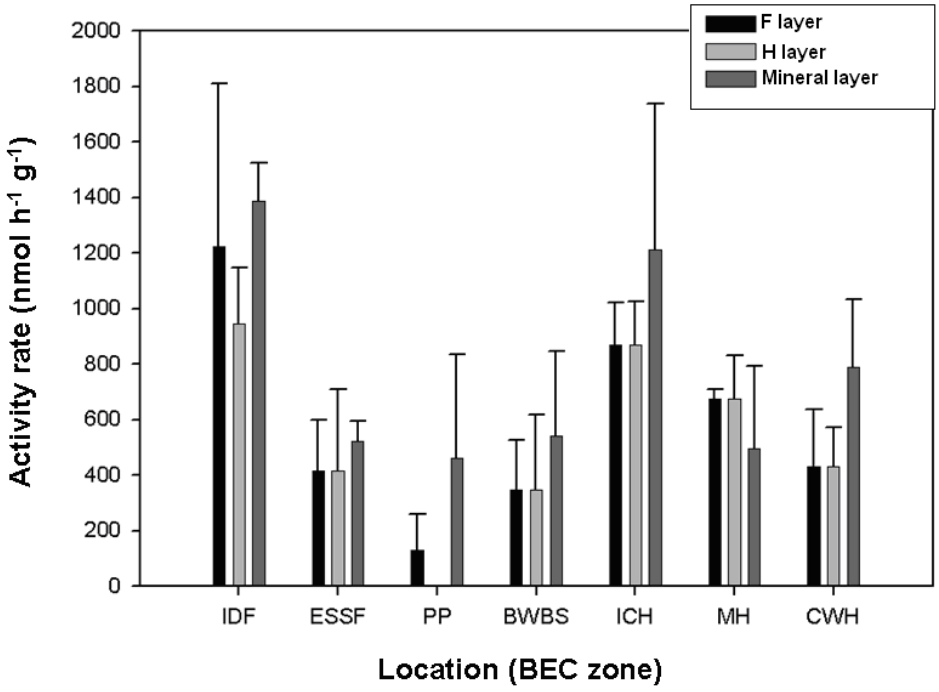

Figure 3.46. Mean phenoloxidase activity rates (nmol of substrate converted per hour per gram of sample) in each soil layer (spring samples) with bars showing standard error.

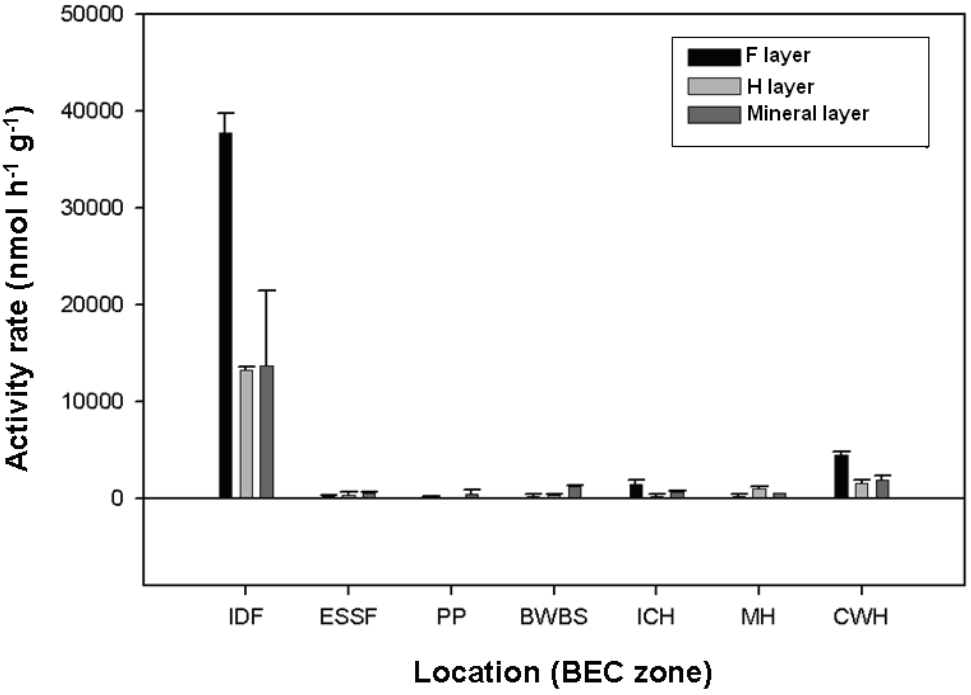

Figure 3.47. Mean phenoloxidase activity rates (nmol of substrate converted per hour per gram of sample) in each soil layer (summer samples) with bars showing standard error.

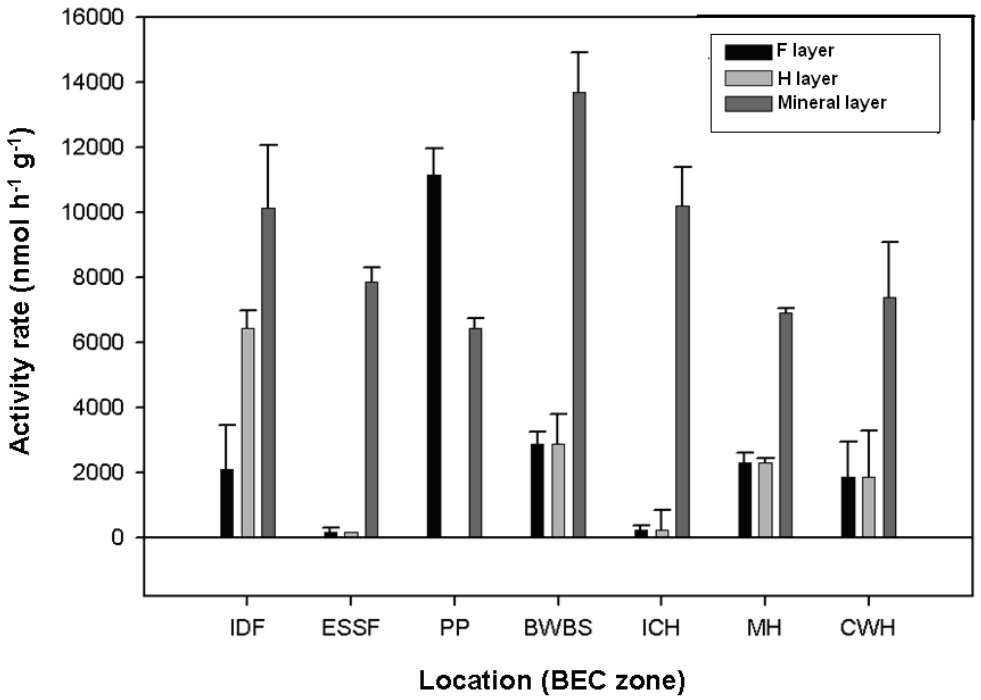

Figure 3.48. Mean peroxidase activity rates (nmol of substrate converted per hour per gram of sample) in each soil layer (spring samples) with bars showing standard error.

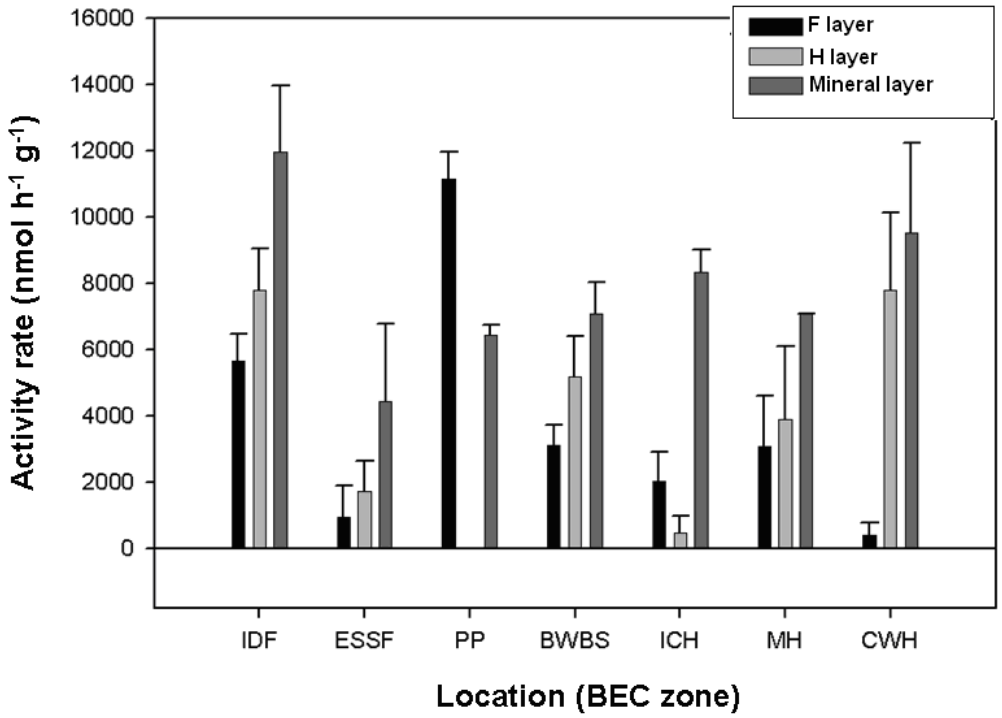

Figure 3.49. Mean peroxidase activity rates (nmol of substrate converted per hour per gram of sample) in each soil layer (summer samples) with bars showing standard error.

NMS ordination of functional data from all soil layers

NMS of the enzyme activity data enabled visualization of the discrimination of the microbial communities from the different soil layers (Figure 3.50). Microbial communities from the mineral soil clustered together, with the exception of two samples indicated by arrows (IDF summer sample site 3 and ESSF summer sample site 2).

Soil moisture content was correlated with axis 1 (r^2 = 31%). The data points representing phenol oxidase and peroxidase activities were plotted at a distance from the other enzyme activities. Variation in peroxidase activity was mainly responsible for the separation of the data points along axis 1 (80% of the variance in the data explained). Variation in phosphatase and NAG activities were mainly responsible for the separation of the data points along axis 2 (45% and 41% of the variance in the data explained respectively).

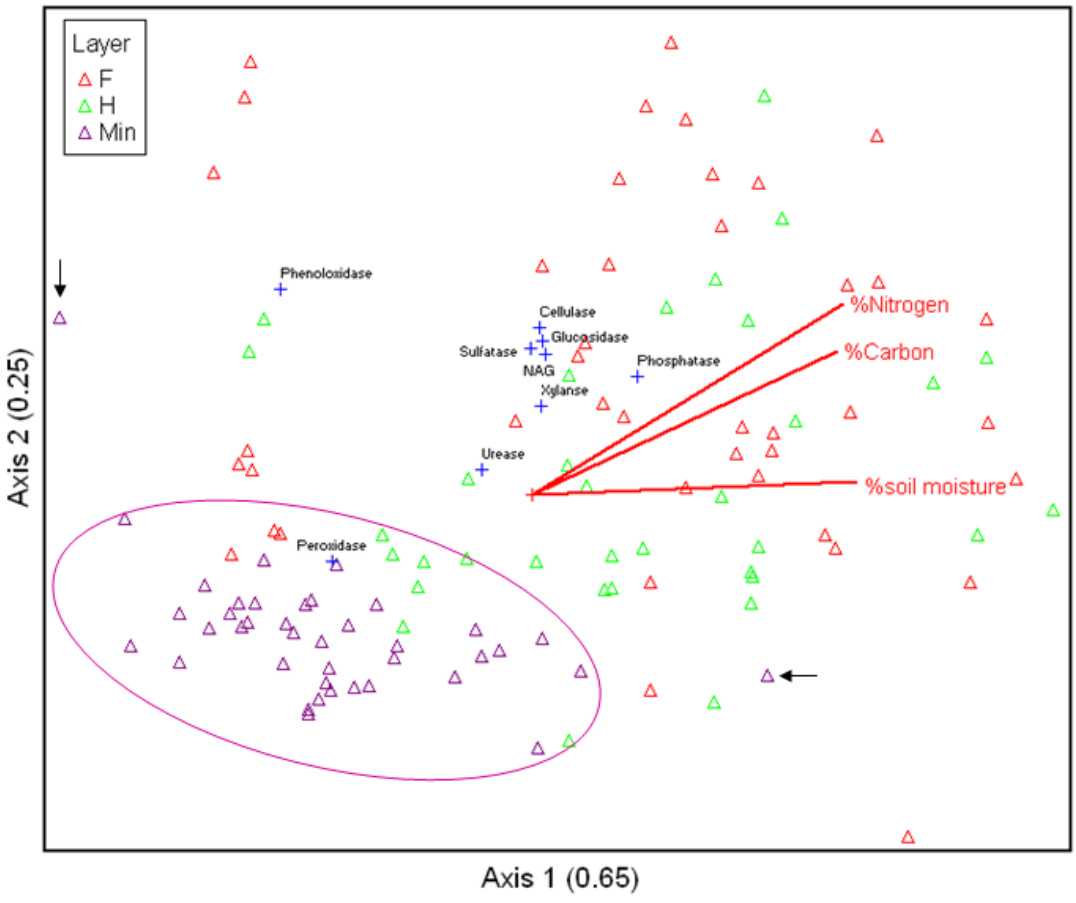

Figure 3.50. NMS ordination of enzyme activities from all soil layers (n=116). The axes are orientated by soil moisture.

3.5.2. Microbial structural community data

Multivariate analysis of structural data from all soil layers combined

MRPP analysis showed high significant separation of the three layers (alpha 0.05) (p=0 A=0.184, n=118). Microbial community structure in the F and H layers at all seven locations was significantly different from the structure of the microbial communities in the mineral soil, based on PLFA profiles (Table 3.24). The hypothesis is accepted.

Table 3.24. Pair-wise MRPP analysis on PLFA results for F, H, and mineral (M) soil layers.

A	F	H	M
F	1	**0.12**	**0.19**
H		1	**0.32**
M			1
p	F	H	M
F	1	**0**	**0**
H		1	**0**
M			1
A>0.1 - high for ecological data - high within-group homogeneity			
A>0.3 very high for ecological data - very high within-group homogeneity			
p sig ≤ 0.0167			
overall p=0 A=0.27			

Pair-wise comparisons *p* significant ≤ 0.0167 (alpha 0.05/3 – Bonferroni's correction). Significant values are shown in bold.

Patterns in microbial community structure down the soil profile

There was less overall pattern down the soil profile for the PLFA data. Total microbial biomass (all PLFA signatures combined) showed some pattern in the spring with the highest concentrations in the H layer and the lowest in the mineral layer (Figure 3.51). However, there was no discernable pattern in the summer samples (Figure 3.52).

The was no discernable pattern in total bacterial PLFA concentration in the spring samples, but in the summer samples the mineral layers had consistently low concentrations and the H layer had the highest concentrations (Figures 3.53 and 3.54). The concentrations of PLFA characteristic of Gram-positive bacteria had no discernable pattern in either the spring or summer samples (Figures 3.55 and 3.56). The concentrations of PLFA characteristic of Gram-negative bacteria was highest in the H layer in both the spring and summer samples (Figures 3.57 and 3.58). There was no discernable pattern in the concentrations of PLFA characteristic of actinobacteria down the soil profile in the spring samples, but in the summer samples the concentration in the mineral soil was consistently high (except for the CWH location sample) (Figures 3.59 and 3.60).

The concentrations of PLFA characteristic of fungi were highest in the organic layers (especially in the F layer) in the spring and summer samples (Figures 3.61 and 3.62). The concentration of PLFA characteristic of arbuscular mycorrhizal fungi had no discernable pattern down the soil profile in the spring and summer samples (Figures 3.63 and 3.64). The concentrations of PLFA characteristic of saprophytic fungi was highest in the F layer for the spring and summer samples (except for the MH location) (Figures 3.65 and 3.66).

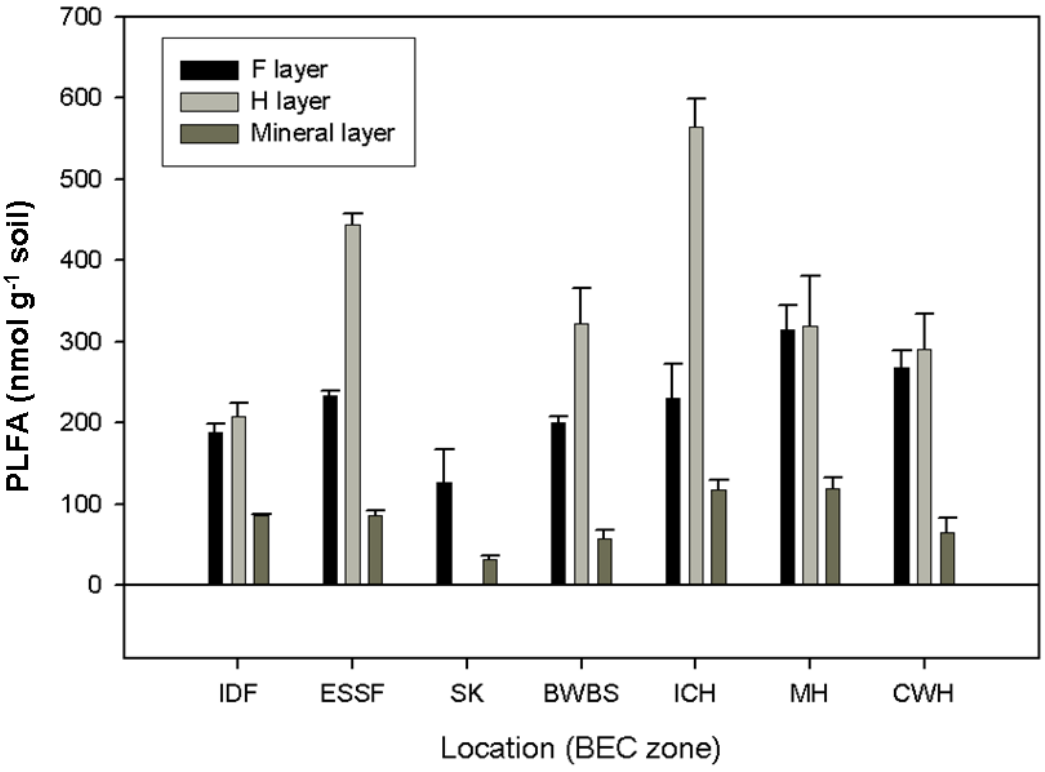

Figure 3.51. Mean total microbial biomass PLFA concentration (total divided by sample biomass) in each soil layer at the seven locations (spring samples), with standard error bars (n=60).

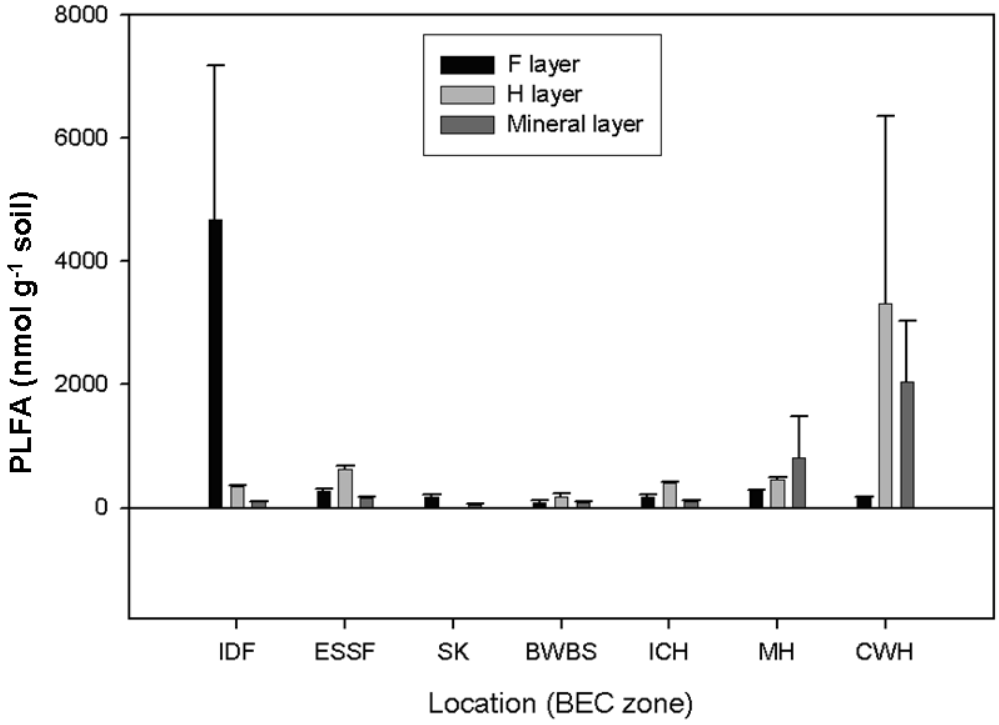

Figure 3.52. Mean total microbial biomass PLFA concentration (total divided by sample biomass) in each soil layer at the seven locations (summer samples), with standard error bars (n=58).

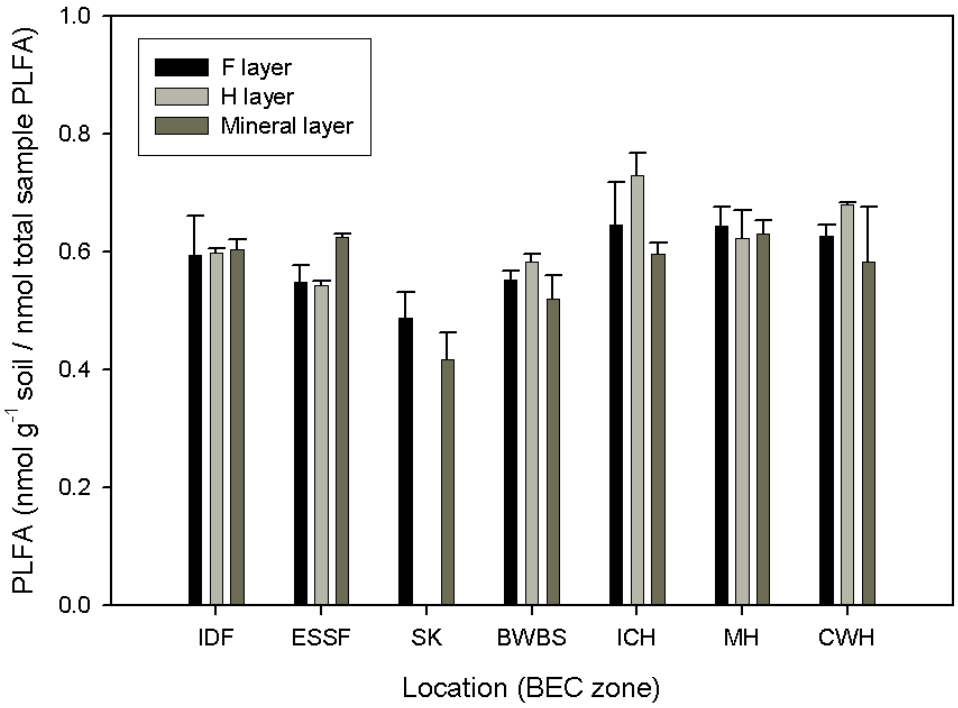

Figure 3.53. Mean total bacteria PLFA concentration (total divided by sample biomass) in each soil layer at the seven locations (spring samples), with standard error bars (n=60).

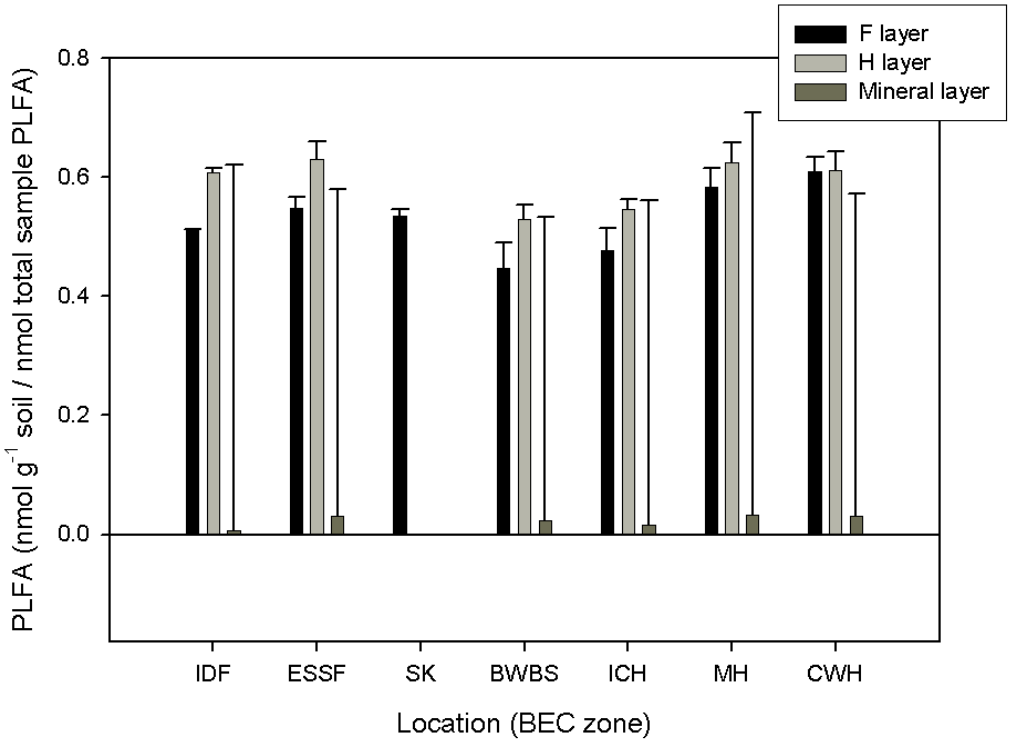

Figure 3.54 Mean total bacteria PLFA concentration (total divided by sample biomass) in the each soil layer at the seven locations (summer samples) with standard error bars (n=58).

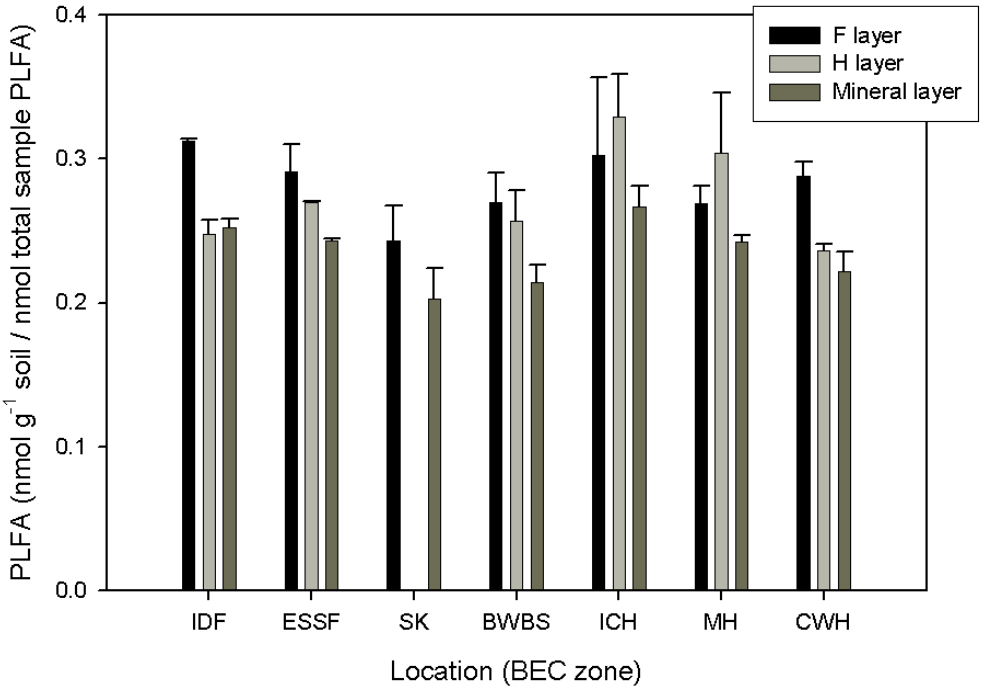

Figure 3.55. Mean Gram-positive bacteria PLFA concentration (total divided by sample biomass) in each soil layer at the seven locations (spring samples) with standard error bars (n=60).

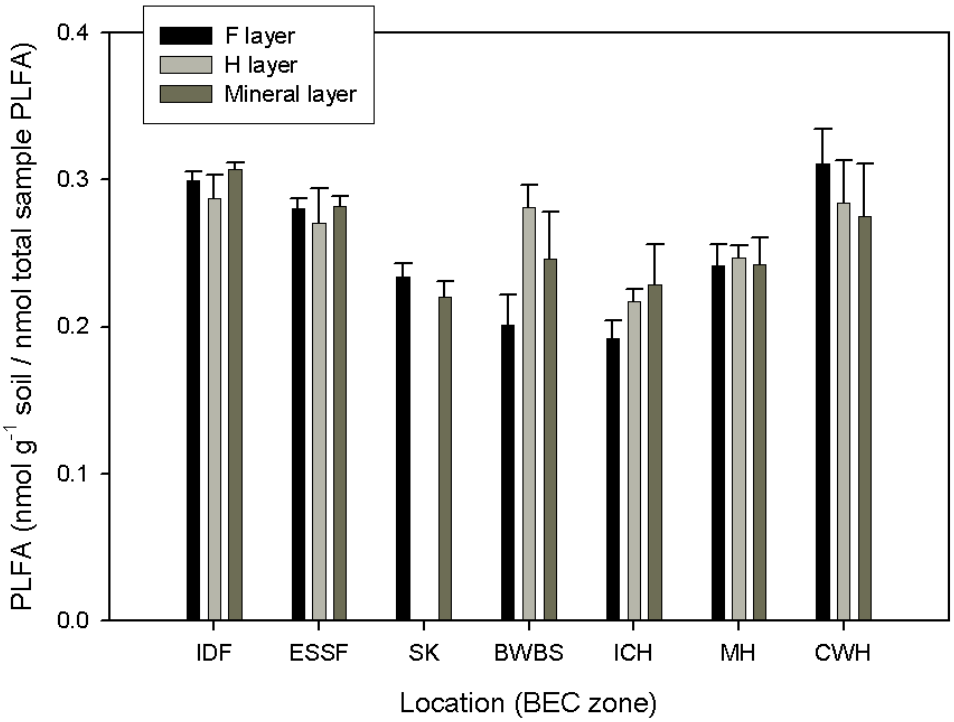

Figure 3.56. Mean Gram-positive bacteria PLFA concentration (total divided by sample biomass) in each soil layer at the seven locations (summer samples) with standard error bars (n=58).

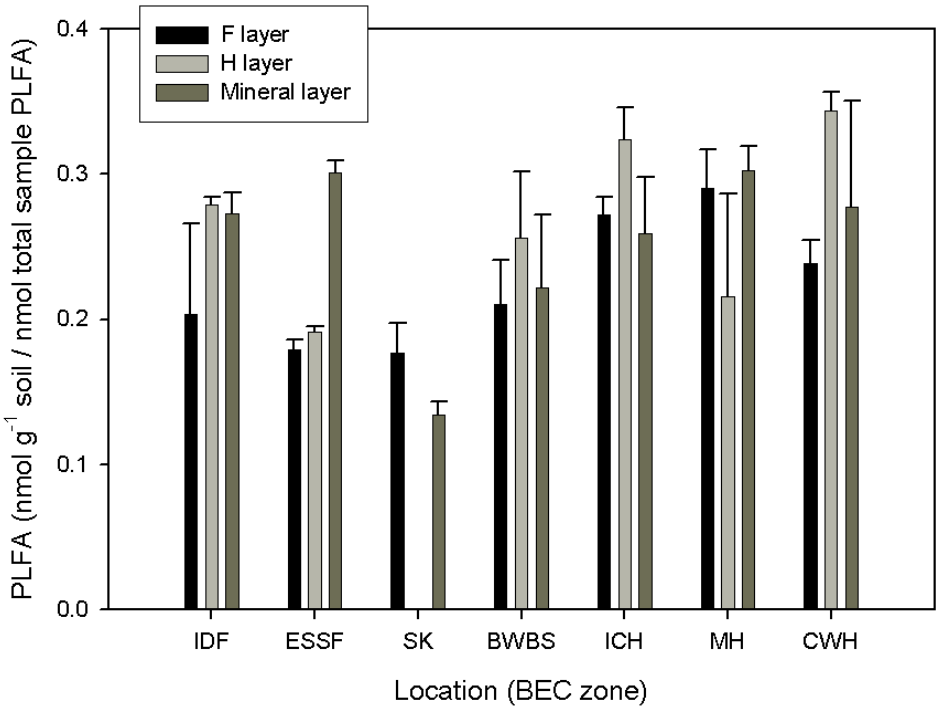

Figure 3.57. Mean Gram-negative bacteria PLFA concentration (total divided by sample biomass) in each soil layer at the seven locations (spring samples) with standard error bars (n=60).

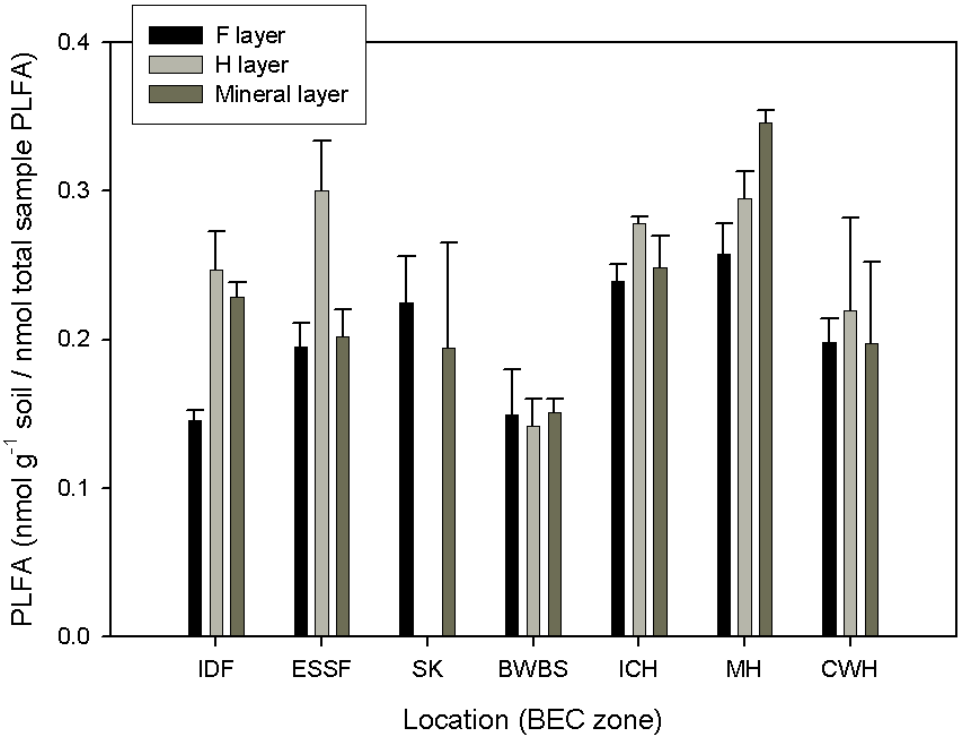

Figure 3.58. Mean Gram-negative bacteria PLFA concentration (total divided by sample biomass) in each soil layer at the seven locations (summer samples) with standard error bars (n=58).

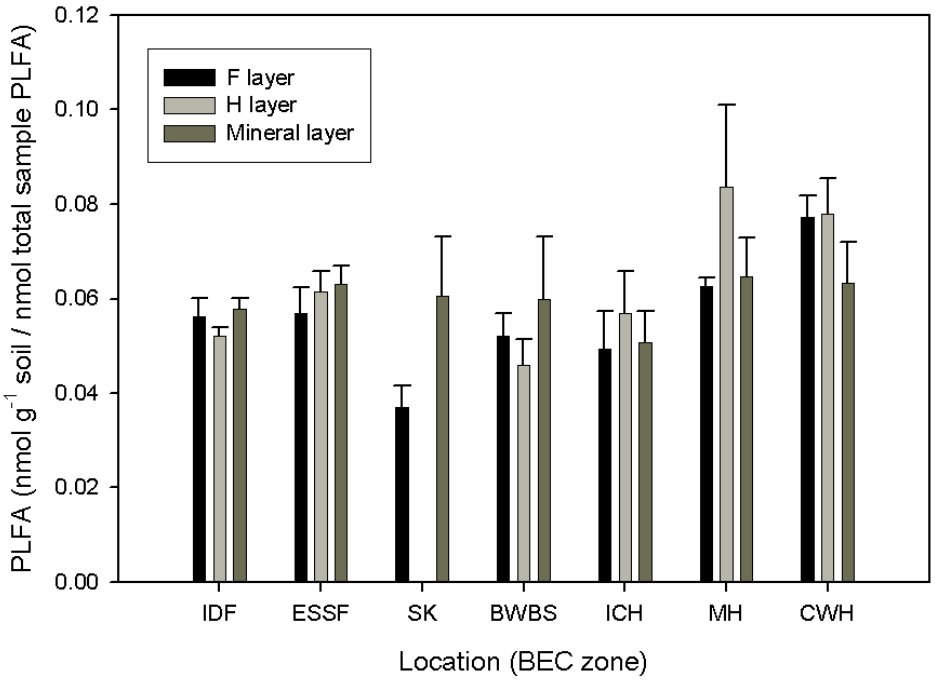

Figure 3.59. Mean actinobacteria PLFA concentration (total divided by sample biomass) in each soil layer at the seven locations (spring samples) with standard error bars (n=58).

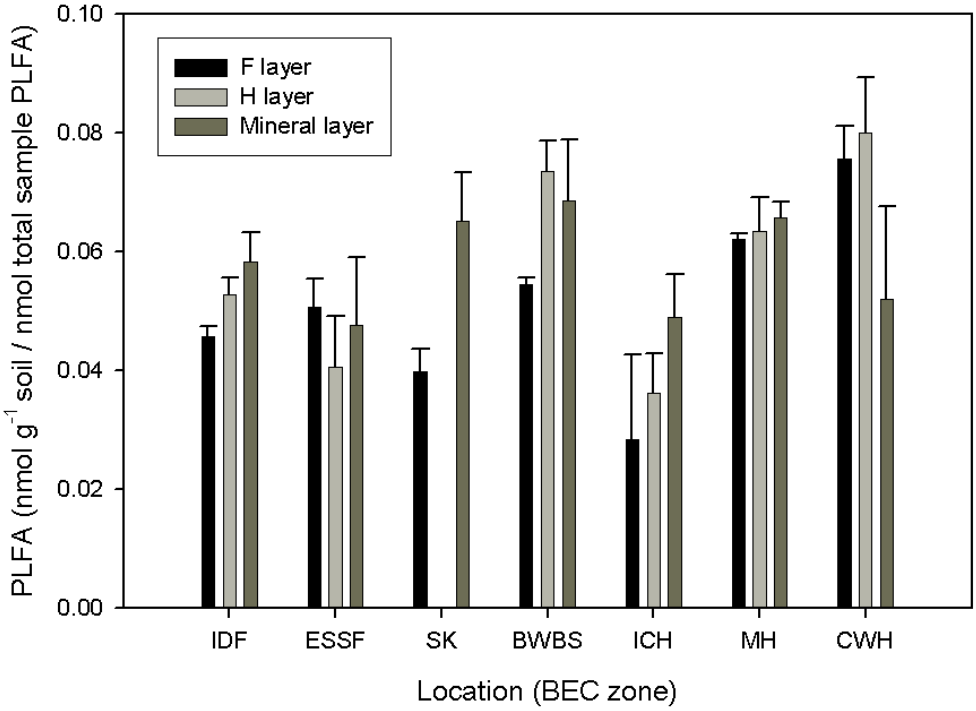

Figure 3.60. Mean actinobacteria PLFA concentration (total divided by sample biomass) in each soil layer at the seven locations (summer samples) with standard error bars (n=58).

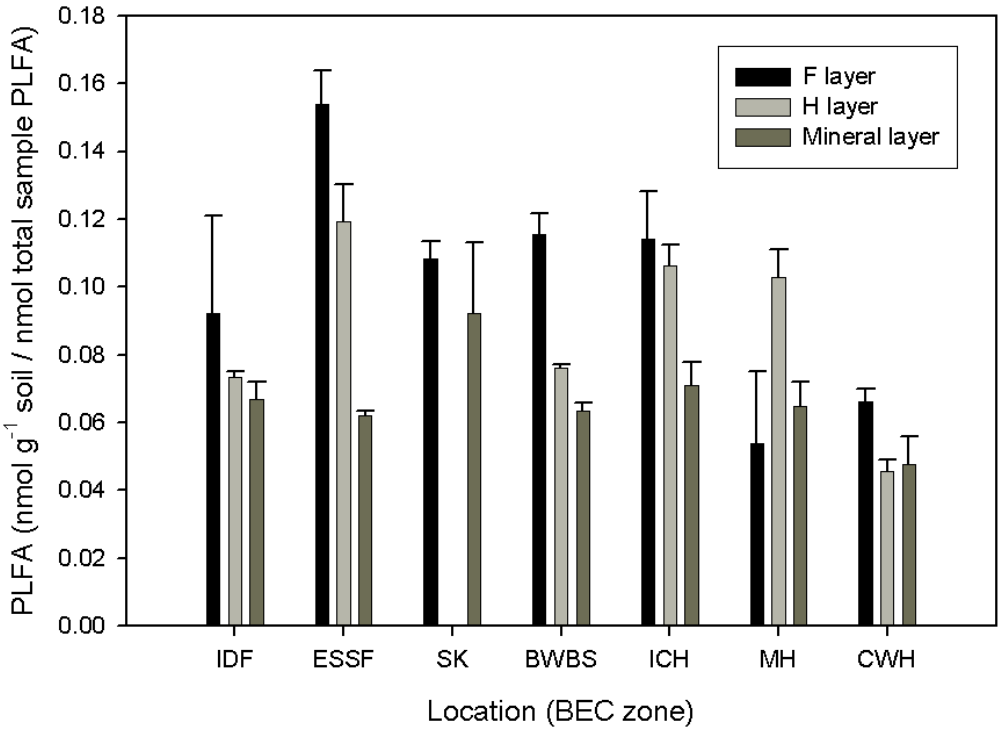

Figure 3.61. Mean total fungi PLFA concentration (total divided by sample biomass) in each soil layer at the seven locations (spring samples) with standard error bars (n=60).

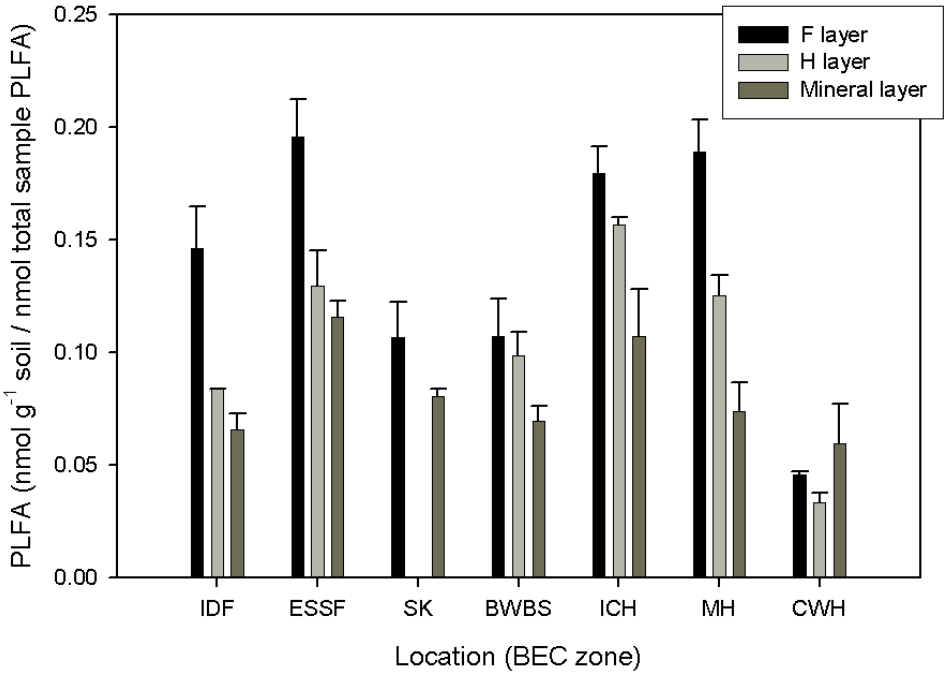

Figure 3.62. Mean total fungi PLFA concentration (total divided by sample biomass) in each soil layer at the seven locations (summer samples) with standard error bars (n=58).

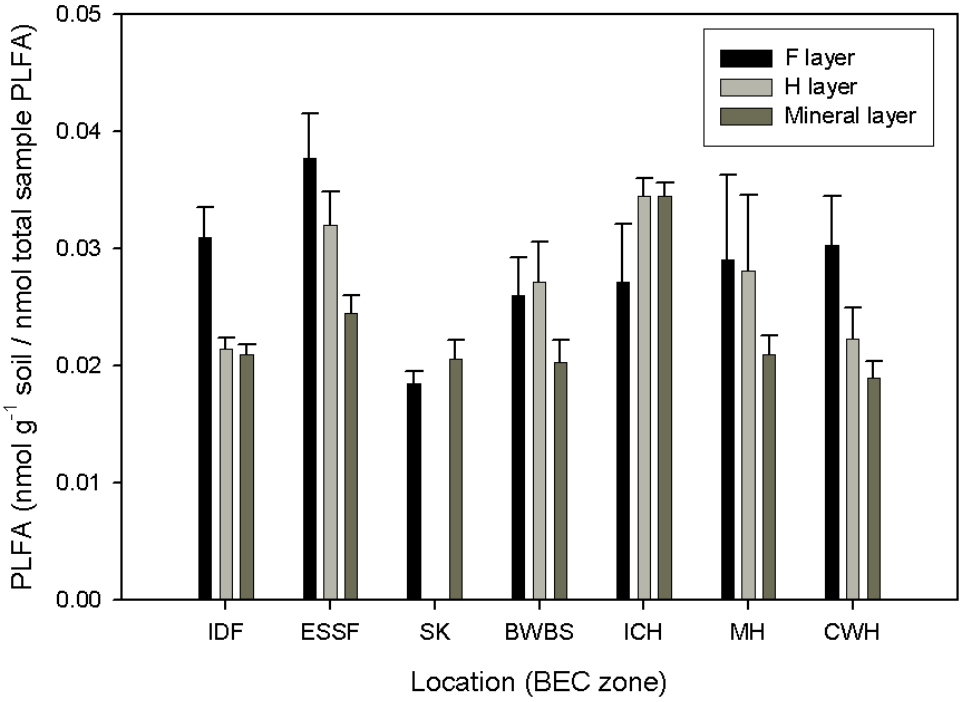

Figure 3.63. Mean arbuscular mycorrhizal fungi PLFA concentration (total divided by sample biomass) in each soil layer at the seven locations (spring samples) with standard error bars (n=60).

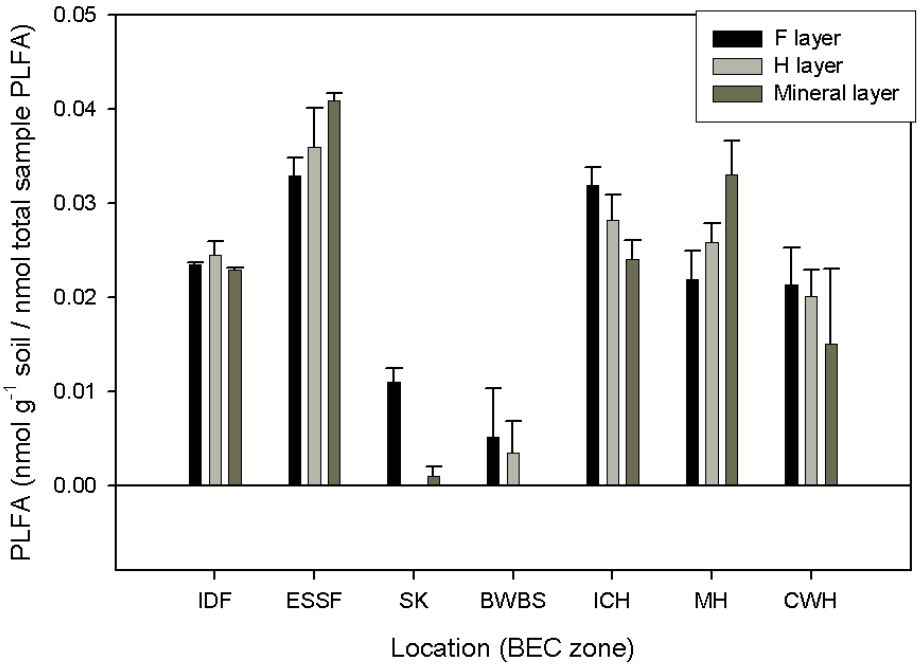

Figure 3.64. Mean arbuscular mycorrhizal fungi PLFA concentration (total divided by sample biomass) in each soil layer at the seven locations (summer samples) with standard error bars (n=58).

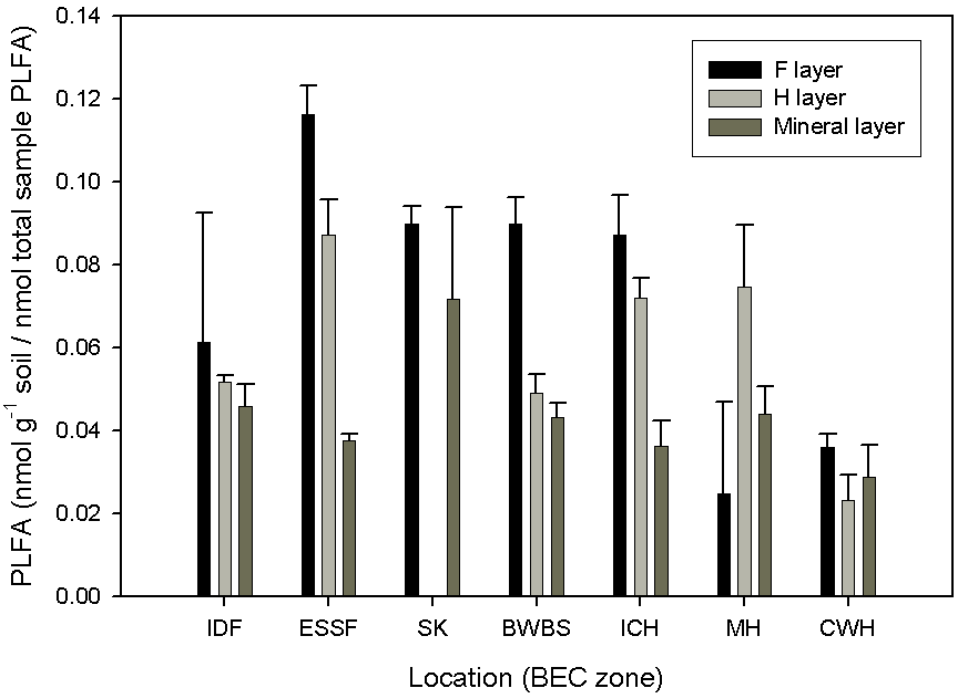

Figure 3.65. Mean saprophytic fungi PLFA concentration (total divided by sample biomass) in each soil layer at the seven locations (spring samples) with standard error bars (n=60).

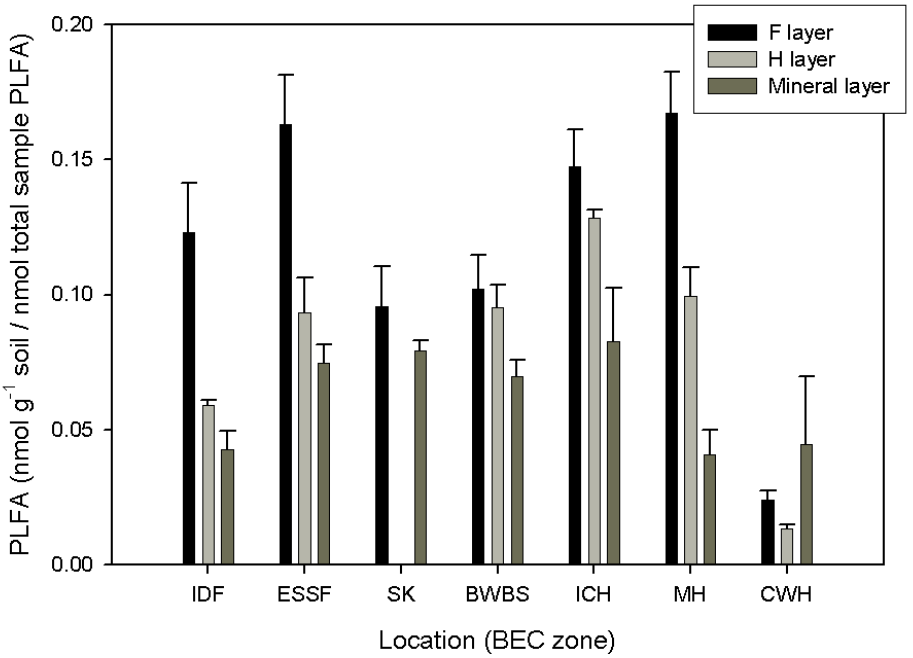

Figure 3.66. Mean saprophytic fungi PLFA concentration (total divided by sample biomass) in each soil layer at the seven locations (summer samples) with standard error bars (n=58).

NMS ordination of structural data from all soil layers

NMS of the PLFA data could not discriminate the microbial communities from the different soil layers (Figure 3.67).

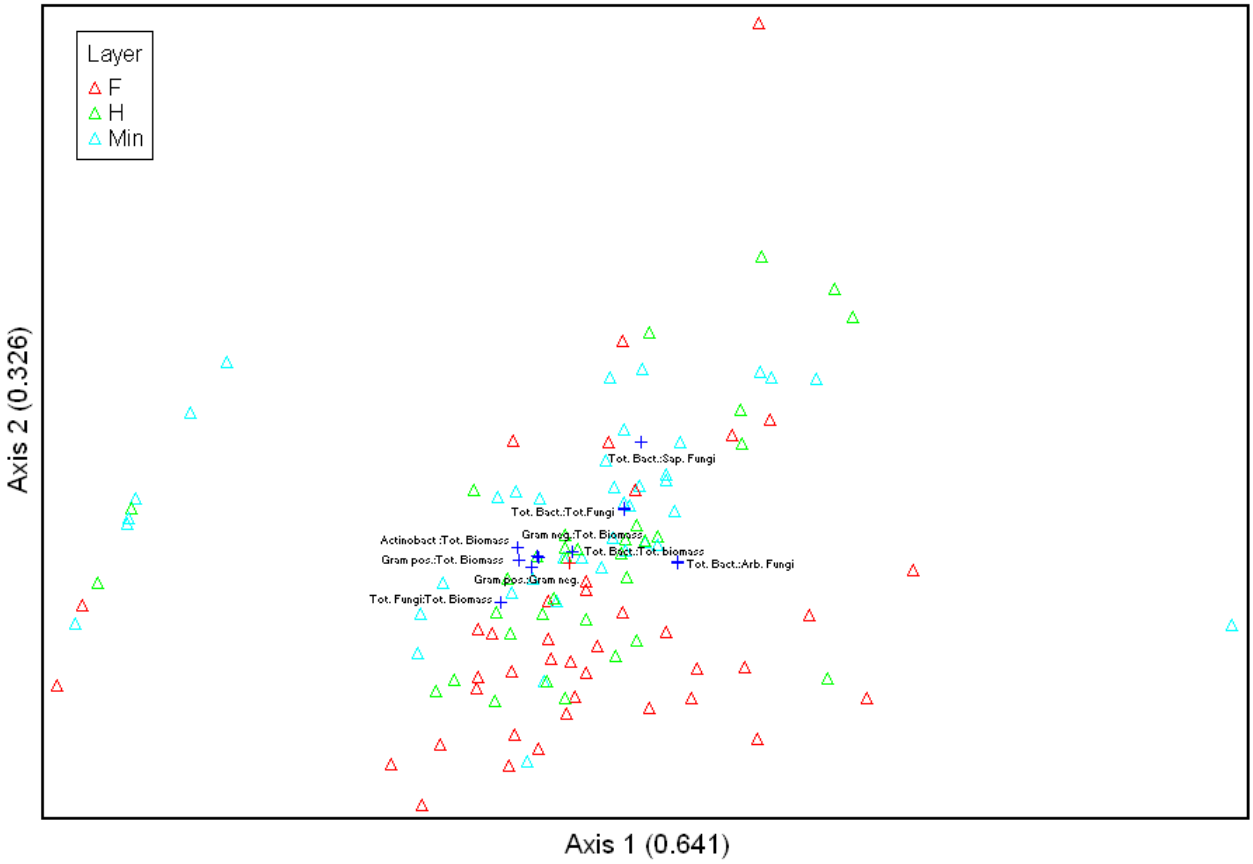

Figure 3.67. NMS ordination of PLFA data for all soil layers combined (n=118).

4. DISCUSSION

4.1. Separating distinct forest types at a regional scale based on soil microbial community function and structure

The variation in microbial community function and structure between the locations was enough to significantly separate them, despite the expectation that the microbial communities would exhibit high functional and structural diversity at the site level. Microbial communities have several nested levels of organization (Nemergut *et al.,* 2005) and characterizations of community distribution will be influenced by the choice of taxonomic or functional resolution. In soil environments, micro-site variability and a complex set of inter-dependences can often eclipse patterns explained by broader-scale environmental heterogeneity. However, this study indicates that patterns in forest soil microbial community structure and function, measured by enzyme assays and PLFA analysis, can be discerned at a regional scale.

Other studies have also identified distinct microbial community changes at a regional scale: Leckie *et al.* (2004a) found that bacterial and fungal biomass, measured using PLFA analysis and Ribosomal Intergenic Spacer Analysis (RISA), differed between two adjacent forest sites in British Columbia which exhibited different N availability and processing rates; and Decker *et al.* (1999) identified significant variations in forest soil enzyme activity at a regional scale (as well as at a water-shed and individual-tree scale) in mixed oak forests in the USA.

4.2. Forest types with distinct microbial community functional profiles

Most of the locations exhibited unique microbial community functional profiles in their soil layers; however the enzyme activities in the samples from the PP and MH locations were notably different from each other and from those of the other locations, especially in the organic layers.

The PP location was functionally distinct from the other locations due to the relatively low phosphatase activities in all layers and the relatively high peroxidase activities and relatively low phenoloxidase activities in its organic layers. As phosphatase activity has

been shown to be linked to P availability (McGill and Cole, 1981; Olander and Vitousek, 2000; Allison *et al.,* 2007) it could be that the concentration of available P in the soil at the PP location was high enough to repress production of phosphatase. The high peroxidase activities may be explained by the high soil C:N ratio in the PP location relative to the other locations. There was very little litter on the forest floor of the PP forest[16]. The litter that was present mainly consisted of pine needles (due to the lack of under-storey vegetation) which have high concentrations of phenols and other recalcitrant chemicals (Hackl *et al.,* 2005) and would be decomposed by a suite of oxidizing enzymes, probably including peroxidase. The peroxidase enzyme degrades lignocellulose and other recalcitrant compounds with high C:N ratio by catalyzing oxidation reactions via the reduction of H_2O_2 (Gianfreda and Bollag, 2002). Peroxidase is an important control of litter breakdown in the F layer (Grandy *et al.,* 2007), although the PP location also had high activity in the mineral layer. The peroxidase enzyme is produced by plants and basidiomycetes (Finlay, 2007; García-Garrado *et al.*, 2002; Gianfreda and Bollag, 2002) and the PP location had relatively high concentrations of the PLFA signatures indicative of saprophytic fungi in both the F and mineral layers.

As phenol oxidase also degrades recalcitrant material, it is counter-intuitive that phenol oxidase activity was low whilst peroxidase activity was high. A possible reason for the high peroxidase activity relative to phenol oxidase activity at the PP location is that plants have been shown to respond to stress by producing enzymes which neutralize active oxygen species (García-Garrado *et al.*, 2002) and the water-stressed soil environment of the PP location (soil water was significantly lower in both spring and summer than all of the other locations and soil temperature was higher) may have induced the production of peroxidase by the trees.

Microbial community function in the organic samples from the MH location was distinguished from those of other locations by relatively high phosphatase activities and relatively low glucosidase, NAG, and sulfatase activities (in the organic layers only). Available P in the MH samples was the lowest of all the locations. McGill and Cole (1981) suggest that phosphatase activity is responsive to P availability, as do the results

[16] The removal of litter by ants is one hypothesis for the lack of litter at these sites (C. Prescott, personal communication).

of subsequent studies (Allison *et al.*, 2007; Olander and Vitousek, 2000), and the low P availability likely explains the high phosphatase activities. The low glucosidase, NAG, and sulfatase activities in the organic layers may be related to the significantly low soil pH; Spiers *et al.* (1999) found that soil acidification was the main cause of a decrease in aryl-sulfatase activity in a contaminated soil. In the same experiment, acid phosphatase activity was not found to be affected by the increased acidity, so the low pH at the MH location would not be expected to decrease phosphatase activity.

It is also possible that the low soil temperatures (especially in spring) reduced enzyme activities by decreasing the rates of physiological reactions (Voroney, 2007) or that anaerobic soil conditions caused the low glucosidase, NAG, and sulfatase activities. The MH location had significantly higher soil water content than the other locations and McLatchey and Roddy (1998) found beta-glucosidase activity (among other enzyme activities) decreased with decreasing redox potential in experimentally-manipulated wetland soils. Unfortunately no redox measurements were taken at the study locations so it is only possible to hypothesize that the MH location would exhibit some of the lowest soil redox potentials of all the locations. However, if soil temperature and redox potential were affecting the activities of glucosidase, NAG, and sulfatase it is likely that phosphatase activity would be affected too.

The PP and MH locations have significantly different soil moisture and soil temperature values for their organic soil layers. It is notable that these locations, the driest and the wettest, are the ones which appear to have the most unique microbial community function of the seven locations. The enzyme activities of the organic layers in the IDF and ESSF locations were also significantly different from each other and the IDF zone is relatively dry compared to the ESSF zone (the ESSF zone's mean annual precipitation is approximately double that of the IDF zone (Meidinger and Pojar, 1991)).

4.3. Forest types with distinct microbial community structural profiles

The only location to exhibit a unique microbial community structure consistently in all soil layers was the CWH location. The CWH location had low saprophytic fungal biomass and a high total bacterial-to-fungal biomass ratio compared to the other locations. Douglas-fir (*Pseudotsuga menziesii*) is the dominant tree species at the CWH location (sixty percent of the trees surveyed) and *P. menziesii* stands are often associated with

high available N concentration, along with high net rates of N mineralization (Prescott and Vesterdal, 2005). The significantly high available N and low C:N ratio in the CWH location soil samples would be conducive to the proliferation of bacterial biomass over fungal biomass (Swift et al., 1979) and this finding agrees with other studies where relative soil fungal biomass has decreased with increased N availability (Myers *et al.,* 2001; Grayston and Prescott, 2005; Högberg *et al.,* 2007; Boyle *et al.,* 2008).

The presence of western redcedar *(Thuja plicata)* only at the CWH sites (21% of the trees surveyed) further explains the high total bacterial-to-fungal biomass ratio, as forest floors under *T. plicata* tend to exhibit high bacterial biomass, often due to high base-cation and pH levels (Prescott *et al.,* 2000; Leckie *et al.,* 2004a; Prescott and Vesterdal, 2005). Although the site average soil pH at the CWH location in spring and summer was not high relative to the other locations (approximately 5.0), local increases in pH under the canopy of *T. plicata* trees may have increased the bacterial biomass. The relatively high arbuscular mycorrhizal fungi biomass, compared to saprophytic and total fungal biomass, can also be explained by the presence of *T. plicata,* as *T. plicata* is unusual in its symbiosis with arbuscular mycorrhizal fungi (Smith and Read, 1997). All the other tree species in this study form ectomycorrhizal symbioses.

T. plicata is often associated with higher concentrations of nitrate relative to ammonium (Prescott and Vesterdal, 2005) and nitrate concentration was far higher than ammonium concentration in soil samples from the CWH location. Myrold and Posavatz (2007) suggest that bacteria dominate the nitrate assimilation pathway and Boyle *et al.,* (2008) found this to be true in N-limited forest soils. Bacteria are relatively more abundant in the nitrate-rich environment of the CWH location but this location does not appear to be N-limited.

4.4. Differences in microbial community structure and function

Despite successfully discriminating regionally-distinct locations based on both soil microbial community function and structure, the results of this study indicate that the functional and structural characteristics of the microbial community do not respond to changes in regional climate in the same way. The locations identified as having unique microbial community functional characteristics are not the same as the ones exhibiting unique structural characteristics, and the soil samples from each location cluster

together when based on enzyme activity data, but not when based on PLFA data (except for loose clustering in the H layer).

It is difficult to define the relationship between microbial community structural and functional diversity (Kirk *et al.,* 2004; Standing and Killham, 2007). Microbial communities exhibit a fecundity of function or ecological functional redundancy, which Folke *et al.* (2004) and Neufeld and Mohn (2006) suggest confers a degree of ecological resilience. Functional redundancy may explain the differential response of the functional and the structural aspects of the microbial community composition to a regional climate gradient in this study.

Other studies have also noted a discord between different components of microbial community function and structure along various spatial and resource gradients. At a regional scale in Mediterranean oak forests, enzyme activities and respiration rates were unrelated to spatial shifts in microbial biomass (Waldrop and Firestone 2006). Potential function of Danish forest soil microbial communities, measured by enzyme bioassays and Community Level Physiological Profiles (CLPP), was negatively correlated with estimations of bacterial abundance (Winding and Hendriksen 2007). Williams and Rice (2007) could not fully explain the change in C processing along a water-stress gradient by referring to the shifts in microbial community structure, as measured by PLFA analysis. They suggested that a change in microbial C substrate-utilization efficiency may have occurred with a change in the ratio of fungal and actinobacterial biomass relative to bacterial biomass, but that more studies are needed to elucidate the link between microbial community-level structure and community function and processes.

4.5. Correlations between soil microbial community function and structure and environmental site variables along the regional climate gradient

The regional mean annual precipitation gradient appears to influence the function of the soil microbial communities at the study locations. This observation is supported by significant negative correlations of soil moisture with enzymes which degrade lignocellulase, chitin and cellulase. Soil moisture was also consistently highly correlated with the variation in microbial community function in the ordination plots. Prescott *et al.* (2004) found that average annual precipitation, potential evapo-transpiration and actual

evapo-transpiration were the climate variables most highly correlated with litter decomposition in these forests and their results are partly explained, at the microbial community scale, by these findings.

It was not possible to directly link the regional mean annual precipitation gradient with the structure of the microbial communities based on the multivariate ordinations; however, soil moisture was significantly positively correlated with total microbial biomass and with total bacterial biomass (apart from Gram-negative bacterial biomass).

Soil moisture has been reported to significantly influence microbial community function and structure (and indirect measurements of these factors) in other studies. In a study of soil microbial community structure in zonal and azonal forest sites along a regional climate gradient, Hackl *et al.* (2004) discovered that PLFA patterns were compositionally distinct among forests with different hydrological regimes and microbial activity was limited by soil water content in the drier sites. Frey *et al.* (1999) found that soil moisture had a positive effect on fungal biomass but no effect on bacterial biomass in agricultural systems. They suggest that this effect was indirect and that the relationship was a product of the effect of water potential on factors such as pH, aeration, nutrient availability and microbivory. In a laboratory incubation study which investigated the effects of climate on litter decomposition and nutrient cycling, Van Meeteren *et al.* (2007) found that both soil moisture and temperature had a large effect on microbial P immobilization and a significant, but less pronounced, effect on microbial respiration, qCO_2, net P and N mineralization rates, nitrification, and C and N immobilization. Bengston *et al.* (2007) found available soil moisture to be auto-correlated with nutrient availability, microbial biomass, and microbial activity in a coniferous forest on Vancouver Island, B.C. They also found microbial activity to increase during rainfall events.

Soil moisture has also been shown to indirectly influence the effect of soil arthropod activity on N cycling (Persson, 1989) and further studies investigating the interaction between microorganisms and soil animals will enhance our understanding of the influence of the microbial community on biogeochemical processes.

Tree species were not identified as having direct influence on microbial community function or structure at any of the locations. Other studies have found correlations between vegetation and microbial community function and/or structure (e.g. Grayston

and Prescott, 2005; Höberg *et al.,* 2008), but these studies were focused at smaller scales, and as Wardle *et al.* (2004) point out, the effects of plant composition on decomposer communities appear to be context and scale-dependent. The observed effects of average annual precipitation on soil microbial function and structure in this study may in fact be indirect - mediated through the effect of moisture on dominant tree species. The use of the BEC zone system to identify research sites implicitly accepts the relationship between dominant tree species composition and regional climate.

As soil C and N concentrations exhibited similar patterns in relative concentration at each location and behaved similarly in relation to the microbial community structure function, the results for C and N concentrations were used together as a proxy for total soil organic matter (SOM). SOM concentration was positively correlated with total fungal biomass and with saprophytic fungal biomass. It is therefore surprising that SOM concentration was negatively correlated with the activity of lignocellulose-degrading enzymes, which are produced by saprophytic fungi (Swift *et al.,* 1979). Similarly, it is also surprising that the C:N ratio was negatively correlated with phenol-oxidase activity. These apparent anomalies may be partly or fully explained by the increase in phenol-oxidase and peroxidase activities down the soil profile. The organic layers had a higher concentration of SOM and this is where most enzyme activity occurs. Recalcitrant material is more likely to persist in the soil and become leached down the profile where it is degraded by enzymes such as phenol oxidase and peroxidase.

Soil Organic Matter (SOM) concentration was strongly correlated with the ordination axes which explained most of the variation in microbial community function in the organic layers, and this finding is supported by the results of a study by Hackl *et al.* (2005) who found that the size of the soil microbial biomass in Eastern European forest stands was tightly coupled with the SOM concentration. The same authors found that soil moisture influenced overall microbial activity, which supports the findings of this study whereby both soil moisture and SOM were found to be important drivers of the soil microbial community.

Except for positive correlations with the activities of enzymes which degrade labile C and chitin, soil pH was not one of the main explanatory variables for the patterns in microbial community function and structure in this study. A number of studies have identified soil pH as the primary, or one of the primary, environmental variables driving soil microbial

function and/or structure, such as Fierer and Jackson (2006), Hackl *et al.* (2005), and Högberg *et al.* (2007); however, these studies have either investigated a different aspect of microbial community composition or have focused their research at a scale which is different to the one investigated in this study. For example, Fierer and Jackson (2006) observed that the diversity and richness of soil bacterial communities at a global scale could largely be explained by variations in soil pH by investigating the phylogenetic diversity of soil bacteria, and Hackl *et al.* (2005) and Högberg *et al.* (2007) observed soil pH to have an influence on microbial PLFA composition over distances of a few kilometeres. It is not correct to state that, based on the findings of this study, soil pH does not have a major effect on soil microbial communities at a regional scale, but it can be stated that this study indicates soil pH plays a minor role, when compared to soil moisture and SOM, in influencing microbial community function and structure at these locations at a regional scale. These findings could be explored further by including sites with a larger range of soil pH values into the study or by experimentally manipulating the soil pH at these sites under controlled conditions.

All forms of available N (nitrate, ammonium, and their sum) were negatively correlated with the chitin-degrading enzyme NAG. NAG hydrolyzes chitin in litter (Kjøller and Struwe, 2007). Sinsabaugh *et al.* (1993) suggest NAG activity is linked to available N in some forests; therefore it is congruent that low concentrations of soil N would induce increased NAG activity. Olander and Vitousek (2000) also found that the activity of N-mineralizing enzymes was negatively correlated with the availability of inorganic N.

Phosphatase activity was negatively correlated with total soil N and significantly positively correlated with NAG activity. These results agree with Trasar-Cepeda *et al.* (1998) who found that phosphatase activity was highest under conditions which favor N-mineralization. Phosphatase activity was also significantly positively correlated with the activities of the labile C-degrading enzymes and with soil total C concentration. This indicates that phosphatase mineralization is coupled to respiration of C by soil microorganisms. This finding challenges the conceptual model of McGill and Cole (1981) which hypothesizes that P is mineralized independently of C.

Phosphatase was not significantly negatively correlated with available P as may be expected from the results of other studies (e.g. Olander and Vitousek, 2002; Sinsabaugh *et al.,* 1993). This may be due to an underestimation of available P in the samples due

to the limited mobility of P in soils (Plante, 2007) (the PRS probes require the movement of ions in solution across the membrane in order for the ions to adsorb) or possibly because P cycling in the study systems is very tight (mycorrhizal fungi may "short circuit" the conventional decomposer pathways with direct recycling of organic nutrients to plant hosts (van Elsas *et al.,* 2007)). Criquet *et al.* (2004) also failed to observe a negative feed-back system in their study on water-extractable P concentrations and P-mineralization. They suggest that some other substrate limitation may have complicated the cycle.

4.6. Correlations between components of the microbial communities

Phosphatase activity was significantly positively correlated with all PLFA signatures except for actinobacteria, arbuscular mycorrhizal fungi, and saprophytic fungi. It is not surprising that phosphatase is correlated with so many of the PLFA signatures as P is an element essential to life and phosphatase is produced by 70-80 % of the microbial population (Plante, 2007). Phosphorus plays both a structural and functional role in virtually all organisms, is found in many cell components, and plays an important role in storing and transferring biochemically useful energy (Plante, 2007). However, it is surprising that phosphatase activity is not correlated with the arbuscular mycorrhizal biomass. Not only is phosphatase activity often correlated with fungal presence, but mycorrhizal fungi play a major role in mineralizing P for plant uptake (Smith and Read, 1997; Finlay, 2007).

Phenoloxidase and peroxidase activities were visually separate from the activities of the other enzymes on the ordination graphics and peroxidase activity was negatively correlated with the activities of phosphatase, cellulase, and xylanase. These results can be explained by the different behaviours of the two groups of enzymes; the increase in peroxidase and phenol oxidase activity and the decrease in the activities of phosphatase, cellulase, and xylanase down the soil profile.

The activities of cellulase, xylanase, glucosidase and NAG all significantly positively correlated with each other. All of these enzymes play a role in mineralizing C from simple organic compounds (Nannipieri *et al.,* 2007) and would therefore be expected to be produced under similar environmental conditions.

The positive correlations of PLFA signatures with the activities of the enzymes xylanase (with all PLFA signatures), cellulase (with all PLFA signatures, except for actinobacteria), and glucosidase (with total microbial biomass and total bacterial biomass) suggest that these enzymes are closely tied to the living biomass of soil. The lignocellulase-degrading enzyme peroxidase was significantly negatively correlated with all PLFA signatures, except for total microbial biomass. Again, this may be explained by the pattern of peroxidase activity with depth in the soil profile; higher activity in the mineral soil corresponds to low abundance of microorganisms (Paul and Clark, 1989).

4.7. Changes in microbial community function and structure with soil depth

The enzyme activities of the microbial communities in the organic layers were significantly different from those in the mineral layers. This finding was confirmed by the multivariate ordination plot, where the mineral layers were clearly discriminated from the organic layers.

Soil microorganisms typically decline in biomass and number with depth in a soil profile with a concomitant decline in SOM concentration (Paul and Clark, 1989; Fierer *et al.,* 2003). This decline in microbial biomass and number is a function of the variable availability of nutrients, energy, and the vertical diversity of pedogenic factors (Agnelli *et al.,* 2004). Kramer and Gleixner (2008), who investigated the influence of C3 and C4 plants on microbial communities in soil depth profiles, found that SOM- and plant-derived-C was utilized as a microbial energy source in different ways, depending on the type of microorganism studied; Gram-negative bacteria utilize proportionately more plant-derived C than SOM-derived-C when compared to Gram-positive bacteria. The differential use of C-resources down a soil profile by various components of the microbial community suggests that the various microbial community structural groups would respond differently to environmental heterogeneity. This would contribute to the de-coupling of microbial function and structural responses to external gradients, as observed in this study.

The activities of NAG, phosphatase, sulfatase, urease, and the labile C-mineralizing enzymes decreased with depth, whereas the activity of the enzymes which degrade more complex materials (phenoloxidase and peroxidase) increased with depth (except

for the phenoloxidase summer samples)[17]. Daradick (2007) also described this phenomenon in her work in CWH forest sites on Vancouver Island. The increased recalcitrance of the ligno-cellulytic material ensures a longer retention time in the soil compared to the more labile compounds, and it is thought that the recalcitrant material leaches into the lower layers of the soil profile, where it is acted upon by phenoloxidase and peroxidase (Daradick, 2007).

The structural composition of the microbial communities in the organic layers was also significantly different from that of the mineral layer. Leckie *et al.* (2004a) and Grayston and Prescott (2005) also found microbial communities were discriminated by forest floor layer. In both studies the forest floor tended to be a better discriminator of soil microbial community samples than either forest type or site.

4.8. Changes in microbial community function and structure with season

Microbial community structure and function did not significantly differ between the two sampling times (spring and summer) in this study. Despite expectations that seasonal changes in temperature and precipitation would significantly affect the function and structure of the microbial communities in this study, as soil microbial communities possess the metabolic and genetic capability to adapt to changing environmental conditions on very short time scales (Schmidt *et al.,* 2007), this finding is not inconsistent with other studies. Boerner *et al.* (2005) did not find any significant differences in activities of acid-phosphatase, α-glucosidase, phenoloxidase, or NAG between spring and summer samples in soils from burned and unburned *Quercus*-dominated forests in the USA. Blume et al. (2002) found that the size of the microbial biomass in both the surface and the subsurface soils of agricultural land was not significantly affected by seasonal variation.

When my results were analyzed by individual enzyme activity, some significant differences in community function between spring and summer samples were observed,

[17] The relative difference in activity between the lignocellulase-degrading enzymes and the other enzymes may be under-represented, as the activities in this study were recorded relative to soil weight and the mineral soil is expected to have a higher bulk density than the organic layers.

despite the overall lack of seasonal effect on soil microbial structure and function. Activity rates of all enzymes were typically higher in the summer and the activities of phosphatase, sulfatase, xylanase and phenoloxidase were significantly higher in some locations in the summer samples. Increased summer soil temperatures would be expected to directly and positively influence microbial physiology and respiration rates, and so enzyme production (Standing and Killham, 2007). A change in temperature would also indirectly affect nutrient and substrate diffusion (Standing and Killham, 2007), which may have had a positive effect on enzyme activity. Low soil water availability may have limited spring enzyme activity at the drier (PP and BWBS) locations but increased in summer with a significant increase in soil moisture (Frey *et al.,* 1999; Voroney, 2007). However, seasonal changes in enzyme activity are unlikely to be purely controlled by soil temperature and moisture and other possible mechanisms are discussed below.

Phosphatase activity in the samples from the ESSF location was significantly higher in summer samples than in spring samples. Phosphatase activity has been shown to be linked to P availability (Sinsabaugh *et al.*, 1993; Olander and Vitousek, 2002) and there may have been a decrease in available P in the summer after the spring 'flush' of vegetative growth and a subsequent increase in phosphatase activity. Unfortunately, nutrient availability was only measured once so it is not possible to link this hypothesis to changes in P availability. However, P availability was relatively low in the ESSF location compared to the other sites, which could indicate that P may become limiting under conditions of increased vegetative and microbial growth.

Sulfatase activity in the samples from the BWBS location was significantly higher in summer samples than in spring samples. The BWBS exhibits very high S availability as the Alcan (Grey Wooded Solod) soils exhibit some minor solonetzic features and contain sulfites in the C horizon (L. Lavkulich, personal communication; Pawluk and Bayrock, 1969). These solonetzic soils are in the advanced stages of development; they were previously highly saline, but the sodium salts have been removed down the profile during pedogenic development (L. Lavkulich, personal communication). The principal salt is sodium sulfate (with some samples containing magnesium sulfate) (L. Lavkulich, personal communication; Pawluk and Bayrock, 1969). Groundwater recharge produces gypsum (calcium sulfate) crystals and so increases available S concentrations (L. Lavkulich, personal communication; Pawluk and Bayrock, 1969). At the time of spring sampling, the soil at the BWBS location was still frozen at depths of approximately 10 to

20 cm from the surface. It is possible that the luxury uptake of S by the vegetation and the lack of groundwater recharge due to the frozen soil had depleted the S levels to an extent that sulfatase activity was induced when the soil thawed.

Xylanase activity was significantly higher in the summer samples from the MH location. Soil pH was found to be significantly lower in the summer samples from this location. The effect of soil pH on the various components of the microbial community is complex (Standing and Killham, 2007). The distribution and activity of soil microbes with variations in soil pH are not simply determined by physiological pH preference (Nannipieri *et al.,* 2002). Many organisms can tolerate pH conditions that are far from their optimum (Nannipieri *et al.,* 2002). However, fungi can be highly competitive under considerable acidity (Nannipieri *et al.,* 2002). Fungi are a major producer of xylanase (Kjøller and Struwe, 2002) and the significant decrease in pH with a concomitant increase in saprophytic and total fungal biomass in the summer sample may show increased competitiveness of xylanase-producing fungi over the other components of the microbial community.

Phenol oxidase activity at the IDF location was significantly higher in the summer samples than in the spring samples. In fact, phenoloxidase activity levels in the F-layer summer samples from the IDF were orders of magnitude higher than the activities in the rest of the samples. Phenoloxidase is one of a suite of enzymes which degrades material with a high C:N ratio (Swift *et al.,* 1979) and it is therefore unsurprising that the C:N ratio was higher in the summer samples from the IDF location compared to the spring samples. It is also interesting that the extremely high total microbial biomass (relative to the other samples) in the F-layer summer sample from the IDF location was associated with extremely high phenol oxidase activity, but was not associated with an unusually large saprophytic biomass. This discrepancy indicates that either some of the saprophytic fungal biomass may not be accounted for by the PLFA signatures chosen for this study or that this enzyme is also produced by other organisms such as actinobacteria (Falcon *et al.,* 1995).

4.9. Sampling design recommendations

The similarity among composite and individual samples is consistent with the findings of Leckie *et al.* (2004a) who used phylogenetic and PLFA analyses to characterize soil

microbial communities in CWH forests on Vancouver Island. Composite samples appear to provide a representative picture of microbial communities in these forests and therefore their use is recommended when using enzyme bioassay and PLFA analysis techniques to characterize the microbial community function and structure of forest soils.

The differences in microbial community function and structure between soil layers indicate that organic layers must be analyzed separately from mineral layers.

Whilst it is interesting to look at the effect of seasonal change on microbial community composition, there were no overall differences in the microbial community function and structure between the spring and summer samples. There were interesting shifts in some of the individual components of the microbial community between the two sampling times, but as there was no seasonal replication no recommendations can be made with regard to sampling design.

5. CONCLUSIONS

- Forest types could be discriminated at a regional scale based on the attributes of soil microbial community function and structure.

- Soil microbial community function and structure were correlated with moisture availability, and microbial community function appears to be influenced by annual average precipitation along a regional climate gradient. The observed effects of average annual precipitation on soil microbial function and structure in this study may be indirectly mediated through the effect of moisture on dominant tree species.

- Most of the locations exhibited unique microbial community functional profiles in their soil layers; however the enzyme activities in the samples from the driest (Ponderosa Pine) and wettest (Mountain Hemlock) locations were notably different from each other and from those of the other locations, especially in the organic layers.

- The moist maritime-influenced Coastal Western Hemlock (CWH) forest exhibited microbial community structural characteristics which were unique from those of the other forest locations. The higher abundance of bacteria relative to fungi in the CWH forest soils may be related to the significantly higher available nitrogen concentrations at this site.

- Soil Organic Matter (SOM) concentration also influenced soil microbial community function and structure at a regional scale.

- Patterns in microbial community function and structure differed in response to external climate and environmental variables.

- Microbial community function and structure also changed with soil depth but not with time of sampling.

6. FURTHER WORK

- Archaea have been shown to be important components of the soil microbial community (Nicol and Schelper, 2006). It would be interesting to include data on soil archaeal lipid concentrations (phospholipid ether lipid analysis) in the multivariate models and ordinations.

- The measurement of redox potentials at each site would help to examine the link between microbial community composition and soil moisture.

- Correlations of individual tree species and under-storey vegetation species composition with microbial community measurements would enhance our knowledge of site-level shifts in microbial community composition and potential drivers of these shifts and the effects on litter decomposition.

- Experimental manipulation of soil moisture, SOM and pH would allow testing of new hypotheses regarding regional and site-level drivers of microbial community composition and to examine the relationship between these variables.

- Collecting data on soil macro- and meso-fauna and the shifts in their community composition with regional and site-level variables could be useful in completing the picture of the belowground ecosystem and its influence on nutrient-cycling processes.

7. REFERENCES

Agnelli, A., Ascher, J., Corti, G., Ceccherini, M.T., Nannipieri, P., Pietramellara, G. 2004. Distribution of microbial communities in a forest soil profile investigated by microbial biomass, soil respiration and DGGE of total and extracellular DNA. Soil Biology and Biochemistry 36; 859-868.

Allison, V.J., Condron, L.M., Peltzer, D.A., Richardson, S.J., Turner, B.L., 2007. Changes in enzyme activities and soil microbial community composition along carbon and nutrient gradients at the Franz Josef chronosequence, New Zealand. Soil Biology & Biochemistry 39; 1770–1781.

Anderson, M.J., 2001. A new method for non-parametric multivariate analysis of variance. Austral Ecology 26; 32-46.

Andersson, M., Kjøller, A., Struwe, S., 2004. Microbial enzyme activities in leaf litter, humus and mineral soil layers of European forests. Soil Biology and Biochemistry 36; 1527-1537.

Bååth, E., Frostegård, Å., Fritze, H., 1992. Soil bacterial biomass, activity, phospholipid fatty acid pattern, and pH tolerance in an area polluted with alkaline dust deposition. Applied Environmental Microbiology 58 (12); 4026-4031.

Bardgett, R.D., McAlister, E., 1999. The measurement of soil fungal:bacterial biomass ratios as an indicator of ecosystem self-regulation in temperate meadow grasslands. Biology and Fertility of Soils 29; 282-290.

Beare, M.H., Coleman, D.C., Crossley Jr., D.A., Hendrix, P.F., Odum, E.P., 1995. A hierarchical approach to evaluating the significance of soil biodiversity to biogeochemical cycling. Plant and Soil 170; 5-22.

Bengston, P., Basiliko, N., Prescott, C.E., Grayston, S.J., 2007. Spatial dependency of soil nutrient availability and microbial properties in a mixed forest of *Tsuga heterophylla* and *Pseudotsuga menziesii*, in coastal British Columbia, Canada. Soil Biology and Biochemistry 39; 2429-2435.

Binkley, D., Hart, S.C., 1989. The components of nitrogen availability assessments in forest soils. Advances in Soil Science 10; 57-108.

Bligh, E.G., Dyer, W.J., 1959. A rapid method of total lipid extraction and purification. Canadian Journal of Biochemistry and Physiology 37; 911–917.

Blume, E., Bischoff, M., Reichert, J.M., Moorman, T., Konopka, A., Turco, R.F., 2002. Surface and subsurface microbial biomass, community structure and metabolic activity as a function of soil depth and season. Applied Soil Ecology 20; 171-181.

Boerner, R.E.J., Brinkman, J.A., Smith A., 2005. Seasonal variations in enzyme activity and organic carbon in soil of a burned and unburned hardwood forest. Soil Biology & Biochemistry 37; 1419–1426.

Boyle, S.A., Yarwood, R.R., Bottomley, P.J., Myrold, D.D., 2008. Bacterial and fungal contributions to soil nitrogen cycling under Douglas fir and red alder at two sites in Oregan. Soil Biology and Biochemistry 40; 443-451.

Burns, R.G., Dick, R.P., (Eds), 2002. Enzymes in the Environment: Activity, Ecology, and Applications. Marcel Dekker, New York.

Carter, R.E, Lowe, L.E., 1986. Lateral variability of forest floor properties under second-growth Douglas fir stands and the usefulness of composite sampling techniques. Canadian Journal of Forest Research 16:1128-1132.

CEAA Screening and BC Parks Level 2 Review Cypress Venue – Freestyle and Snowboard May 3, 2006

Coleman, M.L., Hedrick, D.B., Lovley, D.R., White, D.C., Pye, K., 1993. Reduction of Fe(III) in sediments by sulphate-reducing bacteria. Nature 361; 436-438.

Criquet, S., Ferr, E., Farnet, A.M., Le petit, J., 2004. Annual dynamics of phosphatase activities in an evergreen oak litter: influence of biotic and abiotic factors. Soil Biology and Biochemistry 36; 1111-1118.

Daradick, S. (2007). Soil microbial enzyme activity and nutrient availability in response to green tree retention harvesting in coastal British Columbia. MSc Thesis, Forest Sciences Dept., Faculty of Graduate Studies, University of British Columbia, Vancouver, Canada.

Davidson, E.A., Belk, E., Boone, R.D., 1998. Soil water content and temperature as independent or confounding factors controlling soil respiration in a temperate mixed forest. Global Change Biology 4; 217-227.

Decker, K.L.M., Boerner, R.E.J., Jeakins Morris, S., 1999. Scale-dependent patterns of soil enzyme activity in a forested landscape. Canadian Journal of Forest Research 29 (2); 232-241.

van Elsas, J., Tam, L., Finlay, R.D., Killham, K., Trevors, J.T., 2007. The bacteria and archaea in soil. *In* van Elsas, J., Jansson, J.K., Trevors, J.T. (Eds) Modern Soil Microbiology; pp 83-106. CRC Press, London.

Falcon, M.A., Rodriguez, A., Carnicero, A., Regalado, V., Perestelo, F., Milstein, O., Fuente, G.D.L., 1995. Isolation of microorganisms with lignin transformation potential from soil of Tenerife Island. Soil Biology and Biochemistry 27; 121-126.

Federle, T.W., 1986. Microbial distribution in soil – new techniques. *In* Perspectives in Microbial Ecology. F. Megusar and M. Gantar (Eds) pp. 493-498. Slovene Society for Microbiology, Ljubljana, Slovenia.

Fierer, N., Bradford, M.A., Jackson, R.B., 2007. Towards an ecological classification of soil bacteria. Ecology 88 (6); 1354–1364.

Fierer, N., Jackson, R.B., 2006. The diversity and biogeography of soil bacterial communities. PNAS 103 (3); 626–631.

Fierer, N., Schimel, J.P., Holden, P.A., 2003. Variations in microbial community composition through two soil depth profiles. Soil Biology & Biochemistry 35; 167–176.

Finlay, R.D., 2007. The fungi in soil. *In* van Elsas, J., Jansson, J.K., Trevors, J.T. (Eds) Modern Soil Microbiology; 107-146. CRC Press, London.

Folke, C., Carpenter, S., Walker, B., Scheffer M., Elmqvist, T., Gunderson, L., Holling, C.S. 2004. Regime shifts, resilience and biodiversity in ecosystem management. Annual Review of Ecology and Systematics 35; 557-581.

Frey, S.D., Elliott, E.T., Paustian, K., 1999. Bacterial and fungal abundance and biomass in conventional and no-tillage agroecosystems along two climatic gradients. Soil Biology and Biochemistry 31; 573-585.

Frostegård, Å., Tunlid, A., Bååth, E., 1991. Microbial biomass measured as total lipid phosphate in soils of different organic content. Journal of Microbial Methods 14; 151-163.

García-Garrido, J.M., Ocampo, J.A., García-Romera, I., 2002. Chapter 5 'Enzymes in the Arbuscular Mycorrhizal Symbiosis'. *In* Enzymes in the Environment: Activity, Ecology, and Applications. Burns, R.G., Dick, R.P., (Eds). Marcel Dekker, New York.

Gianfreda, L., Bollag, J-M., 2002. Chapter 19 'Isolated Enzymes for the Transformation and Detoxification of Organic Pollutants'. *In* Enzymes in the Environment: Activity, Ecology, and Applications. Burns, R.G., Dick, R.P., (Eds). Marcel Dekker, New York.

Grandy, A.S., Neff, J.C., Weintraub, M.N., 2007. Carbon structure and enzyme activities in alpine and forest ecosystems. Soil Biology and Biochemistry 39; 2701-2711.

Grayston, S.J., Campbell, C.D., Bardgett, R.D., Mawdsley, J.L., Clegg, C.D., Ritz, K., Griffiths, B.S., Rodwell, J.S., Edwards, S.J., Davies, W.J., Elston, D.J., Millard, P. 2004. Assessing shifts in microbial community structure across a range of grasslands of differing management intensity using CLPP, PLFA and community DNA techniques. Applied Soil Ecology 25; 63-84.

Grayston, S.J., Griffith, G.S., Mawdsley, J.L., Campbell, C.D., Bardgett, R.D., 2001. Accounting for variability in soil microbial communities of temperate upland grassland ecosystems. Soil Biology & Biochemistry 33; 533-551.

Grayston, S.J., Prescott, C.E., 2005. Microbial communities in forest floors under four tree species in coastal British Columbia. Soil Biology & Biochemistry 37;1157–1167.

Grayston, S.J., Vaugham, D. and Jones, D., 1996. Rhizosphere carbon flow in trees, in comparison with annual plants: the importance of root exudation and its impact on microbial activity and nutrient availability. Applied Soil Ecology 5; 29-56.

Green, J.L., Holmes, A.J., Westoby, M., Oliver, I., Briscoe, D., Dangerfield, M., Gillings, M., and Beattie, A., 2004. Spatial scaling of microbial eukaryote diversity. Nature, 432 (9); 747-750.

Groffman, P.M., Zak, D.R., Christensen, S., Mosier, A., Tiedje, J.M., 1993. Early spring nitrogen dynamics in a temperate forest landscape. Ecology 74 (5); 1579-1585.

Hackl, E., Zechmeister-Boltenstern, S., Bodrossy, L., Sessitsch, A., 2004. Comparison of diversities and compositions of bacterial populations inhabiting natural forest soils. Applied and Environmental Microbiology 70 (9); 5057–5065.

Hackl, E., Pfeffer, M., Dona, C., Bachmann, G., Zechmeister-Boltenstern, S., 2005. Composition of the microbial communities in the mineral soil under different types of natural forest. Soil Biology and Biochemistry 37; 661-671.

Hendershot, W.H., Lalande, H., Duquette, M., 1993. *In* Soil Sampling and Methods of Analysis (Ed. M.R. Carter). Lewis Publishers, Boca Raton, Ann Arbor, London, Tokyo.

Hodkinson, I.D., Wookey, P.A., 1999. Functional ecology of soil organisms in tundra ecosystems: towards the future. Applied Soil Ecology 11; 111-126.

Högberg, M.N., Högberg, P., Myrold, D.D., 2007. Is microbial community composition in boreal forest soils determined by pH, C-to-N ratio, the trees, or all three? Oecologia 150; 590–601.

Högberg, P., Högberg, M.N., Göttlicher, S.G., Betson, N.R., Keel, S.G., Metcalfe, D.B., Campbell, C., Schindlbacher, A., Hurry, V., Lundmark, T., Linder, S., Näsholm, T., 2008. High temporal resolution tracing of photosynthate carbon from the tree canopy to forest soil microorganisms New Phytologist 177; 220–228

Hollstedt, C., Vyse, A., 1997. Sicamous Creek Silvicultural Systems Project: Workshop Proceedings April 24–25, 1996 Kamloops, British Columbia, Canada. Research Branch, B.C. Ministry of Forests, Victoria, B.C. Work Paper 24/1997.

Hope, G.D., Prescott, C.E., Blevins, L.L., 2003. Responses of available soil nitrogen and litter decomposition to openings of different sizes in dry interior Douglas-fir forests in British Columbia. Forest Ecology and Management 186; 33–46.

Horner-Devine, M.C., Lage, M., Hughes, J.B., Bohannan, B.J.M., 2004. A taxa-area relationship for bacteria. Nature 432; 750-753.

Jerabkova, L., Prescott, C.E., Kishchuk, B.E., 2006. Nitrogen availability in soil and forest floor of contrasting types of boreal mixedwood forests. Canadian Journal of Forest Research 36; 112-122.

Jörgensen, R.G., Raubuch, M., Brandt, M., 2002. Soil microbial properties down the profile of a black earth burie by colluvium. Journal of Plant Nutrition and Soil Science 165; 274-280.

Kandeler, E., 2007. Physiological and Biochemical Methods for Studying Soil Biota and Their Function. *In* Soil Microbiology, Ecology, and Biochemistry (Ed. E.A. Paul), third edition; pp. 53-84. Elsevier Academic Press, Burlington and Oxford.

Kandeler, E., Kampichler, C., Horak, O., 1996. Influence of heavy metals on the functional diversity of soil microbial communities. Biology and Fertility of Soils 23; 299–306.

Killham, K., Prosser, J.I., 2007. *In* Soil Microbiology, Ecology, and Biochemistry (Ed. E.A. Paul), third edition; pp. 119-144. Elsevier Academic Press, Burlington and Oxford.

Killham K., Staddon, W.J., 2002. Chapter 15 'Bioindicators and Sensors of Soil Health and the Application of Geostatistics'. *In* Burns, R.G., Dick, R.P. (Eds.) Enzymes in the Environment. Marcel Dekker Inc.

Killham, K., 1994. Soil Ecology. University Press, Cambridge, UK.

Kirk, J.L., Beaudette, L.A., Hart, M., Moutoglis, P., Klironomos, J.N., Lee, H., Trevors, J.T., 2004. Review: methods of studying soil microbial diversity. Journal of Microbiological Methods 58; 169–188.

Kishchuk, B.E., 2004. Soils of the Ecosystem Management Emulating Natural Disturbance (EMEND) Experimental Area, Northwestern Alberta. Information Report NOR-X-397, Canadian Forest Service, Northern Forestry Centre.

Kjøller, A.H., Struwe, S., 2002. Chapter 10 'Fungal Communities, Succession, Enzymes and Decomposition'. *In* Enzymes in the Environment: Activity, Ecology, and Applications. Burns, R.G., Dick, R.P., (Eds). Marcel Dekker, New York.

Klinka, K., Krajina, V.J., 1986. Ecosystems of the University of British Columbia Research Forest, Haney, B.C., Univ. B.C., Faculty of Forestry, Vancouver, B.C.

Knief, C., Lipski, A., Dinfiled, P.F. 2003. Diversity and activity of methanotrophic bacteria in different upland soils. Applied and Environmental Microbiology 69 (11); 6703-6714.

Kramer, C., Glexixner, G., 2008. Soil organic matter in soil depth profiles: Distinct carbon preferences of microbial groups during carbon transfer. Soil Biology and Biochemistry 40; 425-433.

Kruskal, J.B., 1964. Nonmetric multidimensional scaling: a numerical method. Pyschometrika 29; 115-129.

Leckie, S.E, Prescott, C.E., Grayston, S.J., Neufeld, J.D. and Mohn, W.W., 2004a. Characterization of Humus Microbial Communities in Adjacent Forest Types That Differ in Nitrogen Availability. Microbial Ecology 48; 29–40.

Leckie, S.E., Prescott, C.E., Grayston, S.J., Neufeld, J.D., Mohn, W.W., 2004b. Short communication: Comparison of chloroform fumigation-extraction, phospholipid fatty acid, and DNA methods to determine microbial biomass in forest humus. Soil Biology & Biochemistry 36; 529–532.

Lejon, D.P.H., Chaussod, R., Ranger, J., Ranjard, L., 2005. Microbial Community Structure and Density Under Different Tree Species in an Acid Forest Soil (Morvan, France). Microbial Ecology 50; 614-625.

Marx, M.-C., Wood M., Jarvis, S.C., 2001. A microplate fluorimetric assay for the study of enzyme diversity in soils. Soil Biology and Biochemistry 33; 1633-1640.

Mather, P.M., 1976. Computational Methods of Multivariate Analysis in Physical Geography. J. Wiley and Sons, London. 532 pp.

McCune, B., Grace, J.B., 2002. Analysis of Ecological Communities. MJM Software Design, Oregon.

McGill, W.B., Cole, C.V., 1981. Comparative aspects of cycling of organic C, N, S and P through soil organic matter. Geoderma 26; 267-286.

McLatchey, G.P., Reddy, K.R. Regulation of organic matter decomposition and nutrient release in a wetland soil. Journal of Environmental Quality 27; 1268–1274, 1998.

Meidinger, D., Pojar, J., 1991. Ecosystems of British Columbia. B.C. Min. Forests, Victoria.

Miller, M., Palojärvi, A., Rangger, A., Reeslev, M., Kjøller, A., 1998. The use of fluorogenic substrates to measure fungal presence and activity in soil. Applied Environmental Microbiology 64 ; 613–617.

Møller, J., Miller, M., Kjøller, A., 1999. Fungal-bacterial interaction on beech leaves: Influence on decomposition and dissolved organic carbon quality. Soil Biology and Biochemistry 31:367–374.

Myers, R.T., Zak, D.R., White, D.C., Peacock, A., 2001. Landscape-level patterns of microbial community composition and substrate use in upland forest ecosystems. Soil Science Society of America Journal 65; 359–367.

Myrold, D.D., Posavatz, N.R., (2007). Potential importance of bacteria and fungi in nitrate assimilation in soil. Soil Biology and Biochemistry 39; 1737-1743.

Nannipieri, P., Kandeler, E., Ruggiero, P., 2002. Chapter 1 'Enzyme Activities and Microbiological and Biochemical Processes in Soil'. *In* Enzymes in the Environment: Activity, Ecology, and Applications. Burns, R.G., Dick, R.P., (Eds). Marcel Dekker, New York.

Nemergut, D.R., Costello, E.K., Meyer, A.F., Pescador, M.Y., Weintraub, M.N., Schmidt, S.K. 2005. Structure and function of alpine and arctic soil microbial communities. Research in Microbiology 156; 775–784.

Neufeld, J.D., Mohn, W.W. 2005. Unexpectedly high bacterial diversity in Arctic tundra relative to boreal forest soils, revealed by serial analysis of ribosomal sequence tags. Applied and Environmental Microbiology 71 (10); 5710-5718.

Neufeld J.D. and Mohn, W.W., 2006. Chapter 7 'Assessment of Microbial Phylogenetic Diversity Based on Environmental Nucleic Acids. *In* Molecular Identification, Systematics, and Population Structure of Prokaryotes. E. Stackebrandt (Ed.). Springer-Verlag Berlin Heidelberg

Nichol, G.W., Schelper, C., 2006. Ammonia-oxidising Crenarchaeota: important players in the nitrogen cycle? TRENDS in Microbiology 14 (5), 207-212.

Olander, L.P., Vitousek, P.M., 2000. Regulation of soil phosphatase and chitinase activity by N and P availability. Biogeochemistry 49; 175-190.

Oxford University Press, 2004. Dictionary of Biology, online edition, 2004. Oxford, England.

Paul, E.A. and F.E. Clark, 1989. Soil Microbiology and Biochemistry, Academic Press.

Pawluk, S., Bayrock, L.A, 1969. Some characteristics and physical properties of Alberta Tills. Research Council of Alberta, Bulletin 26.

Pennanen,T., Liski, J., Bååth, E., Kitunen, V., Uotila, J., Westman, C.J., Fritze, H., 1999. Structure of the microbial communities in coniferous forest soils in relation to site fertility and stand development stage. Microbial Ecology 38; 168–179.

Persson, T., 1989. Role of soil animals in C and N mineralization. Plant and Soil 115; 241-245.

Plante, A.F., 2007. Soil Biogeochemical Cycling of Inorganic Nutrients and Metals. *In* Soil Microbiology, Ecology, and Biochemistry (Ed. E.A. Paul), third edition; pp. 389-432. Elsevier Academic Press, Burlington and Oxford.

Pojar, J., Klinka, K., Meidinger, D.V., 1986. Biogeoclimatic Ecosystem Classification in British Columbia. Province of British Columbia, Ministry of Forests, Victoria, B.C.

Prescott, C.E., 1996. Influence of forest floor type on rates of litter decomposition in microcosms. Soil Biology and Biochemistry 28 (10/11); 1319-1325.

Prescott, C.E., 2005a. Decomposition and mineralization of nutrients from litter and humus. *In* Ecological Studies, Vol. 181, Verlag, H. BassiriRad (Ed.). Nutrient Acquisition by Plants: An Ecological Perspective. Springer- Berlin Heidelberg.

Prescott, C.E., 2005b. Do rates of litter decomposition tell us anything we really need to know? Forest Ecology and Management 220 (1-3); 66-74.

Prescott, C.E., Blevins, L.L., Staley, C., 2004. Litter decomposition in British Columbia's forests: Controlling factors and influences of forestry activities. B.C. Journal of Ecosystems and Management 5 (2); 44-57.

Prescott, C.E., Chappell, H.N., Vesterdal, L., 2000a. Nitrogen turnover in forest floors of coastal Douglas-fir at sites differing in soil nitrogen capital. Ecology 81 (7); 1878-1886.

Prescott, C.E., Hope, G.D., Blevins, L.L., 2003. Effect of gap size on litter decomposition and soil nitrate concentrations in a high-elevation spruce-fir forest. Canadian Journal of Forest Research 33; 2210-2220.

Prescott, C.E., Maynard, D.G., Laiho, R., 2000b. Humus in northern forests: friend or foe? Forest Ecology and Management 133; 23-36.

Prescott, C.E., Vesterdal, L., 2005. Effects of British Columbia tree species on forest floor chemistry. *In* Tree Species Effects on Soils: Implications for Global Change, pp17-29. Springer, Netherlands.

Prosser, J.I., Bohannan, B.J.M., Curtis, T.P., Ellis, R.J., Firestone, M.K., Freckleton, R.P., Green, J.L., Green, L.E., Killham, K., Lennon, J.J., Osborn, M., Solan, M., van der Gast, C.J., Young, J.P.W., 2007. The role of ecological theory in microbial ecology. Nature 5; 384-392.

Prosser, J.I., 2007. Microorganisms cycling soil nutrients and their diversity. *In* van Elsas, J., Jansson, J.K., Trevors, J.T. (Eds) Modern Soil Microbiology; pp 237-262. CRC Press, London.

Priha, O., Grayston, S.J., Hiukka, R., Pennanen, T., Smolander, A., 2001. Microbial community structure and characteristics of the organic matter in soils under *Pinus sylvestris*, *Picea abies* and *Betula pendula* at two forest sites. Biology and Fertility of Soils 33; 17–24.

Qian. P., Schoenau, J.J., 2002. Practical applications of ion exchange resins and agricultural and environmental soil research. Canadian Journal of Soil Science 82; 9-21.

Quesnel, H.J., Curran, M.P., 2000. Shelterwood harvesting in root-disease infected stands - post-harvest soil disturbance and compaction. Forest Ecology and Management 133; 89-113.

Ritz, K., McNicol, J.W., Nunan, N., Grayston, S., Millard, P., Atkinson, D., Gollotte, A., Habeshaw, D., Boag, B., Clegg, C.D., Griffiths, B.S., Wheatley, R.E., 2004. Spatial structure in soil chemical and microbiological properties in an upland grassland. FEMS Microbiology Ecology 49; 191–205.

Saiya-Cork, K.R., Sinsabaugh, R.L., Zak, D.L., 2002. The effects of long term nitrogen deposition on extracellular enzyme activity in and Acer saccharum forest soil. Soil Biology and Biochemistry 34; 1309-1315.

Schmidt, S.K., Costello, E.K., Nemergut, D.R., Cleveland, C.C., Reed, S.C., Weintraub, M.N., Meyer, A.F., Martin, A.M., 2007. Biogeochemical consequences of rapid microbial turnover and seasonal succession in soil. Ecology 88 (6); 1379-1385.

Sheldrick, B.H., Wang, C., 1993. *In* Soil Sampling and Methods of Analysis (Ed. M.R. Carter). Lewis Publishers, Boca Raton, Ann Arbor, London, Tokyo.

Sinsabaugh, R.L., Antibus, R.K., Linkins, A.E., McClaugherty, C.A., Rayburn, L., Repert D., Weiland, T., 1993. Wood decomposition: Nitrogen and phosphorus dynamics in relation to extracellular enzyme activity. Ecology 74 (5): 1586-1593.

Sinsabaugh, R.L., Reynolds, H., Long, T.M., 2000. Short communication: Rapid assay for amidohydrolase (urease) activity in environmental samples. Soil Biology & Biochemistry 32; 2095-2097.

Sinsabaugh, R.L., Saiya-Cork, K., Long, T., Osgood, M.P., Neher, D.A., Zakd, D.R., Norby, R.J., 2003. Soil microbial activity in a *Liquidambar* plantation unresponsive to CO_2-driven increases in primary production. Applied Soil Ecology 24 (3); 263-271.

Smith, V.R., Read, D.J., 1997. Mycorrhizal Symbiosis. Academic Press, San Diego.

Standing, D., and Killham, K., 2007. The Soil Environment. *In* van Elsas, J., Jansson, J.K., Trevors, J.T. (Eds) Modern Soil Microbiology; pp 1-22. CRC Press, London.

Stark, K.E., Arsenault, A., Bradfield, B., 2006. Soil seed banks and plant community assembly following disturbance by fire and logging in interior Douglas-fir forests of south-central British Columbia. Canadian Journal of Botany 84; 1548-1560.

Stevenson, B.A., Sparling, G.P., Schipper, L.A., Degens, B.P., Duncan, L.C., 2004. Pasture and forest soil microbial communities show distinct landscape patterns in their catabolic respiration responses at a landscape scale. Soil Biology and Biochemistry 36; 49-55.

Stursova, M., Crenshaw, C.L., Sinsabaugh, R.L., 2006. Microbial responses to long-term N deposition in a semiarid grassland. Microbial Ecology 51; 90–98.

Swift, M.J., Heal, O.W., Anderson, J.M., 1979. Decomposition in terrestrial ecosystems. Blackwell Scientific, Oxford.

Tabatabai, M.A., Fu. M., 1992. Extraction of Enzymes from Soils. *In* Soil Biochemistry, Vol. 7. Stotsky, G., Bollag, J-M. (Eds). Marcel Dekker, New York.

Thies, J.E., 2007. Molecular Methods for Studying Soil Ecology. *In* Soil Microbiology, Ecology, and Biochemistry (Ed. E.A. Paul), third edition; pp. 85-118. Elsevier Academic Press, Burlington and Oxford.

Thomas, K.D., Prescott, C.E., 2000. Nitrogen availability in forest floors of three tree species on the same site: the role of litter quality. Canadian Journal of Forest Research 30; 1698-1706.

Torsvik, V.,Øvreås, L., 2007. Microbial Phylogeny and Diversity in Soils. *In* Modern Soil Microbiology (Eds. J.D. Van Elsas, J.K. Jansson, J.T. Trevors), second edition; pp. 23-54. CRC Press, Taylor and Francis Group, Boca Raton, London, New York.

Trasar-Cepeda, C., Leiros, C., Gil-Sotres, F., Seona, S., 1998. Towards a biochemical quality index for soils: An expression relating several biological and biochemical properties. Biology and Fertility of Soils 26; 100-106.

Trofymow, J.A., 1998. Detrital Carbon Fluxes and Microbial Activity in Successional Douglas-fir Forests. *In* J.A. Trofymow and A. MacKinnon, (Eds). Proceedings of a workshop on Structure, Process, and Diversity in Successional Forests of Coastal British Columbia, February 17-19, 1998, Victoria, British Columbia. Northwest Science, Vol. 72 (special issue No. 2); pp 51-53.

Van Meeteren, M.J.M., Teitema, A., Westerveld, J.W., 2007. Regulation of microbial carbon, nitrogen, and phosphorus transformations by temperature and moisture during decomposition of *Calluna vulgaris* litter. Biology and Fertility of Soils 44; 103-112.

Volney, J. Study Leader, EMEND Mensuration and Health Dataset, EMEND Database. Accessed by Jason Edwards October 17, 2007

Voroney, R.P., 2007. The Soil Habitat. *In* Soil Microbiology, Ecology, and Biochemistry (Ed. E.A. Paul), third edition; pp. 25-52. Elsevier Academic Press, Burlington and Oxford.

Waldrop, M.P., Firestone, M.K., 2006. Seasonal Dynamics of Microbial Community Composition and Function in Oak Canopy and Open Grassland Soils. Microbial Ecology 52; 470-479.

Wang, T., Hamann, A., Spittlehouse, D., Aitken, S. N., 2006. Development of scale-free climate data for western Canada for use in resource management. International Journal of Climatology 26(3); 383-397.

Wardle, D.A., Yeates, G.W., Watson, R.N., Nicholson, K.S., 1995. The detritus food-web and diversity of soil fauna as indicators of disturbance regimes in agro-ecosystems. Oikos 73; 155–166.

Wardle, D.A., Bardgett, R.D., Klironomos, J.N., Setälä, H., van der Putten, W.H., Wall, D.H., 2004. Ecological linkages between aboveground and belowground biota. Science 304; 1629-1633.

Weintraub, M.N., Scott-Denton, L.E., Schmidt, S.K., Monson, R.K., 2007. The effects of tree rhizodeposition on soil exoenzyme activity, dissolved organic carbon, and nutrient availability in a subalpine forest ecosystem. Oecologia 154; 327–338.

Welke, S.E., Hope, G.D., 2005. Influences of stand composition and age on forest floor processes and chemistry in pure and mixed stands of Douglas-fir and paper birch in interior British Columbia. Forest Ecology and Management 219 (1); 29-42.

Williams, M.A., Rice, C.W., 2007. Seven years of enhanced water availability influences the physiological, structural, and functional attributes of a soil microbial community. Applied Soil Ecology 35; 535–545.

Winding, A., Hendikson, N.B., 2007. Comparison of CLPP and Enzyme Activity Assay for Functional Characterization of Bacterial Soil Communities. Journal of Soils and Sediments. 7 (6)l 411-417.

Zak, J.C., Willig, M.R., Moorhead, D.L., Wildman, H.G., 1994. Functional diversity of microbial communities: A quantitative approach. Soil Biology and Biochemistry 26, 1101-1108.

Zelles, L., 1999. Fatty acid patterns of phospholipids and liposaccharides in the characterisation of microbial communities in soil: a review. Biology and Fertility of Soils 29: 111-129.

Zogg, G.P., Zak, D.R., Ringelberg, D.B., MacDonald, N.W., Pregitzer, K.S., White, D.C., 1997. Compositional and functional shifts in microbial communities due to soil warming. Soil Science Society of America Journal 61: 475-481.

APPENDICES

Appendix I. Non-metric Multidimensional Scaling (NMS) test statistics

NMS composite vs. individual (means) data – enzyme activities

A 2-dimensional solution was recommended. The final stress was 4.76 ('excellent' according to 'Kruskal's Rule of Thumb' see McCune and Grace, 2002). The final instability value of 0 and the stability plot suggest that a stable solution was found. The number of iterations for the final solution was 78. The probability that a similar final stress could have been obtained by chance is 0.0196; therefore (using an alpha of 0.05) it can be accepted that the solution could not have been obtained by chance.

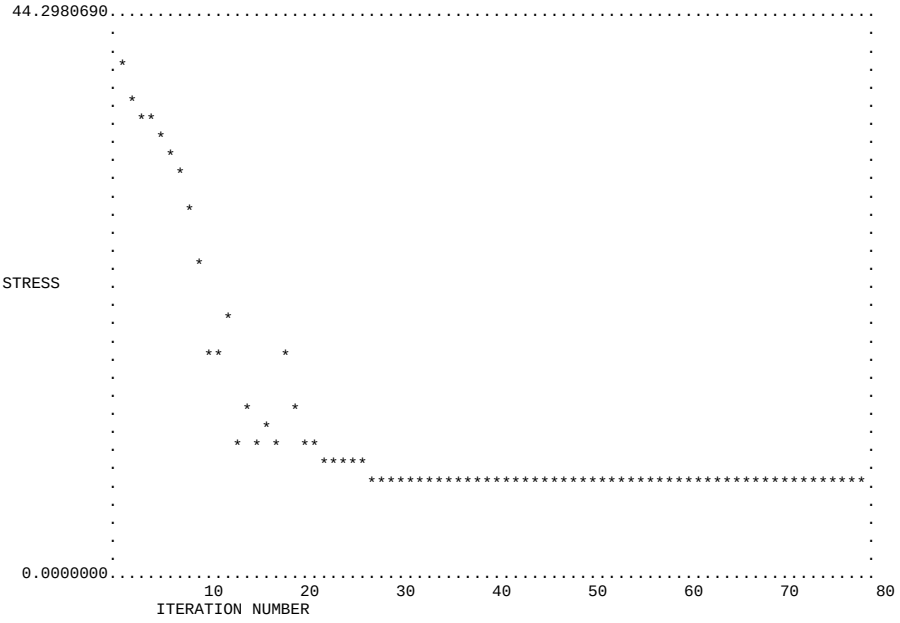

Figure 8.1. Stress plot for enzyme data.

Table 8.1. Correlations between variation in the data and ordination axes.

Axis	R Squared Increment	Cumulative
1	.874	.874
2	.105	.979

NMS ordination of functional data for a combination of all soil profile layers

A 2-dimensional solution was recommended. The final stress was 13.57409 ('fair' according to 'Kruskal's Rule of Thumb' see McCune and Grace, 2002). The final instability value of 0.00001 and the stability plot suggest that a stable solution was found. The number of iterations for the final solution was 49. The proportion of variance represented by axis 1, based on the r^2 value between distance in the ordination space and distance in the original space, is 0.629. The r^2 value for axis 2 is 0.255; therefore the cumulative proportion of variance in the dataset represented by the final 2-dimensional solution is 0.884. The probability that a similar final stress could have been obtained by chance is 0.0196; therefore (using an alpha of 0.05) it can be accepted that the solution could not have been obtained by chance.

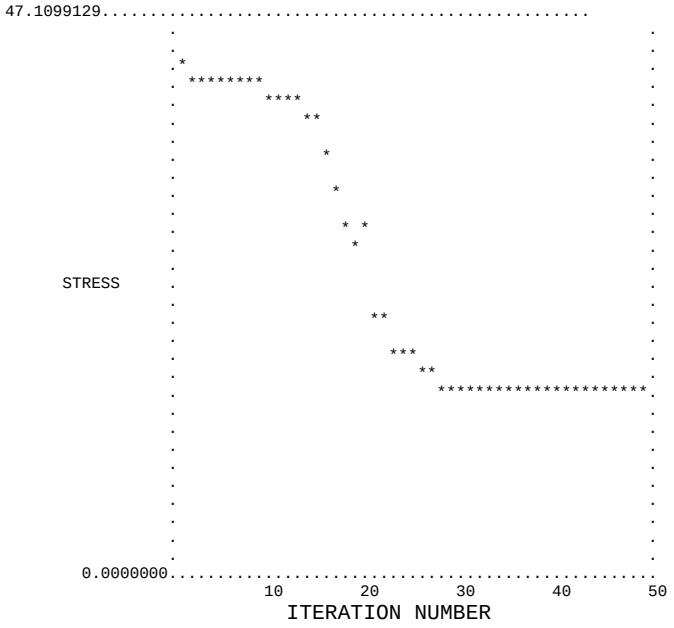

Figure 8.2. Stress plot for enzyme data.

Table 8.2. Correlations between variation in the data and ordination axes.

R Squared

Axis	Increment	Cumulative
1	.629	.629
2	.255	.884

Table 8.3. Correlations between enzyme activities and the ordination axes.

Axis:	1			2		
	r	r-sq	tau	r	r-sq	tau
Cellulas	.067	.005	.137	-.563	.317	-.566
Xylans	.069	.005	.138	-.573	.328	-.477
NAG	.082	.007	.076	-.641	.411	-.574
Phosphat	.492	.242	.413	-.670	.449	-.572
Glucosid	.027	.001	.064	-.593	.351	-.536
Sulfatas	.058	.003	-.088	-.460	.211	-.219
Phenolox	-.286	.082	-.311	-.158	.025	.025
Peroxid	-.896	.803	-.832	.346	.120	.271
Urease	-.134	.018	-.050	-.136	.018	-.069

Table 8.4. Correlations between measured environmental variables and ordination axes.

Axis:	1			2		
	r	r-sq	tau	r	r-sq	tau
TotalN	.088	.008	.294	.109	.012	-.029
NO3--N	.070	.005	.246	.110	.012	-.004
NH4+-N	.213	.046	.299	.043	.002	-.042
Ca	.036	.001	.039	-.106	.011	-.075
Mg	-.295	.087	-.185	.047	.002	.040
K	-.028	.001	-.005	-.367	.135	-.323
P	-.152	.023	-.130	-.216	.047	-.209
Fe	-.303	.092	-.280	.248	.062	.229
Mn	.312	.098	.246	.083	.007	.052
Cu	-.114	.013	-.042	.115	.013	.135
Zn	.316	.100	.204	.204	.042	.142
B	-.265	.070	-.187	.018	.000	.007
S	-.143	.021	-.003	.123	.015	.140
Pb	.247	.061	.114	.184	.034	.188
Al	.217	.047	.139	.145	.021	.099
Slopedeg	.116	.014	.098	-.108	.012	-.045
Soiltemp	-.311	.097	-.212	-.019	.000	-.010
%sand	.105	.011	.071	.256	.065	.192
%silt	-.108	.012	-.081	-.291	.085	-.194
%clay	-.034	.001	.041	-.040	.002	-.127
%water	.822	.676	.611	-.154	.024	-.131
%Carbon	.728	.530	.535	-.481	.231	-.373
%Nitrogen	.742	.551	.513	-.549	.302	-.417
C:N	.258	.066	.271	-.054	.003	-.167
pH	-.305	.093	-.210	-.245	.060	-.138

NMS ordination of functional data for the organic layers (F and H[18])

A 3-dimensional solution was recommended. The final stress was 8.99840 ('good' according to 'Kruskal's Rule of Thumb' see McCune and Grace, 2002). The final instability value of 0.00001 and the stability plot suggest a stable solution was found. The number of iterations for the final solution was 67. The proportion of variance represented by axis 1, based on the r^2 value between distance in the ordination space and distance in the original space, is 0.507. The r^2 value for axis 2 is 0.193 and for axis 3 is 0.214; therefore the cumulative proportion of variance in the dataset represented by the final 3-dimensional solution is 0.914. The probability that a similar final stress could have been obtained by chance is 0.0196; therefore (using an alpha of 0.05) it can be accepted that the solution could not have been obtained by chance.

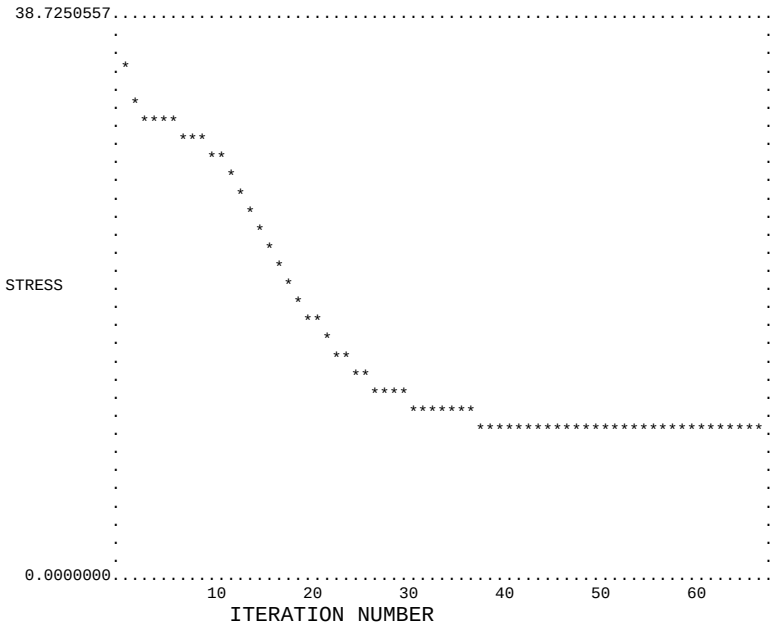

Figure 8.3. Stress plot for enzyme data.

[18] The PP location exhibits no H layer.

Table 8.5. Correlations between variation in the data and ordination axes.

Axis	R Squared Increment	Cumulative
1	.220	.220
2	.521	.741
3	.174	.915

Table 8.6. Correlations between enzyme activities and the ordination axes.

Axis:	1			2			3		
	r	r-sq	tau	r	r-sq	tau	r	r-sq	tau
Cellulas	-.203	.041	-.102	.614	.377	.526	-.315	.099	-.220
Xylans	-.071	.005	-.097	.608	.370	.475	-.109	.012	-.149
NAG	-.286	.082	-.156	.600	.360	.541	-.202	.041	-.145
Phosphat	-.729	.532	-.574	.116	.013	.061	-.148	.022	-.180
Glucosid	-.236	.056	-.077	.604	.364	.541	-.194	.038	-.263
Sulfatas	.153	.023	.211	.339	.115	.368	-.615	.379	-.275
Phenolox	.258	.067	.240	.515	.265	.276	-.410	.168	-.314
Peroxid	.552	.305	.517	.707	.499	.534	.513	.263	.432
Urease	.022	.000	.033	.325	.106	.113	.220	.048	.086

Table 8.7. Correlations between measured environmental variables and ordination axes.

Axis:	1			2			3		
	r	r-sq	tau	r	r-sq	tau	r	r-sq	tau
TotalN	.252	.064	-.006	-.153	.023	-.245	-.138	.019	-.176
NO3--N	.255	.065	.051	-.132	.017	-.195	-.111	.012	-.163
NH4+-N	.098	.010	-.058	-.292	.085	-.279	-.349	.122	-.176
Ca	-.178	.032	-.152	-.067	.004	.009	.015	.000	-.015
Mg	.335	.113	.207	.276	.076	.128	.003	.000	.017
K	.047	.002	.023	.484	.234	.330	-.043	.002	-.050
P	.232	.054	.164	.348	.121	.308	-.028	.001	.011
Fe	.407	.166	.325	.092	.008	.137	.136	.018	.243
Mn	-.227	.052	-.106	-.456	.208	-.334	.108	.012	.095
Cu	.262	.069	.239	.195	.038	-.047	.425	.180	.296
Zn	.018	.000	.090	-.459	.210	-.329	.291	.085	.235
B	.100	.010	.046	.205	.042	.185	.128	.016	.077
S	.217	.047	.203	-.009	.000	-.123	.195	.038	.265
Pb	-.070	.005	.109	-.404	.164	-.320	.224	.050	.150
Al	-.317	.101	-.231	-.460	.211	-.275	.141	.020	.026
Slopedeg	-.363	.132	-.270	.003	.000	-.028	.070	.005	-.003
Soiltemp	.264	.070	.228	.502	.252	.298	-.011	.000	-.062
%sand	.234	.055	.145	-.232	.054	-.175	-.006	.000	.042
%silt	-.259	.067	-.162	.304	.092	.232	-.094	.009	-.131
%clay	-.044	.002	-.130	-.028	.001	.008	.154	.024	.006
%water	-.338	.114	-.208	-.780	.609	-.573	-.099	.010	.001
%Carbon	-.630	.397	-.459	-.364	.132	-.270	-.010	.000	-.012
%Nitrogen	-.629	.396	-.455	-.318	.101	-.186	-.305	.093	-.233
C:N	-.234	.055	-.262	-.105	.011	-.124	.432	.187	.196
pH	.054	.003	.066	.518	.268	.399	-.212	.045	-.143

NMS ordination of microbial functional data for the F layer

A 3-dimensional solution was recommended. The final stress was 8.40868 ('good' according to 'Kruskal's Rule of Thumb' see McCune and Grace, 2002). The final instability value of 0.00001 and the stability plot suggest a stable solution was found. The number of iterations for the final solution was 74. The proportion of variance represented by axis 1, based on the r^2 value between distance in the ordination space and distance in the original space, is 0.155. The r^2 value for axis 2 is 0.303 and for axis 3 is 0.44; therefore the cumulative proportion of variance in the dataset represented by the final 3-dimensional solution is 0.898. The probability that a similar final stress could have been obtained by chance is 0.0196; therefore (using an alpha of 0.05) it can be accepted that the solution could not have been obtained by chance.

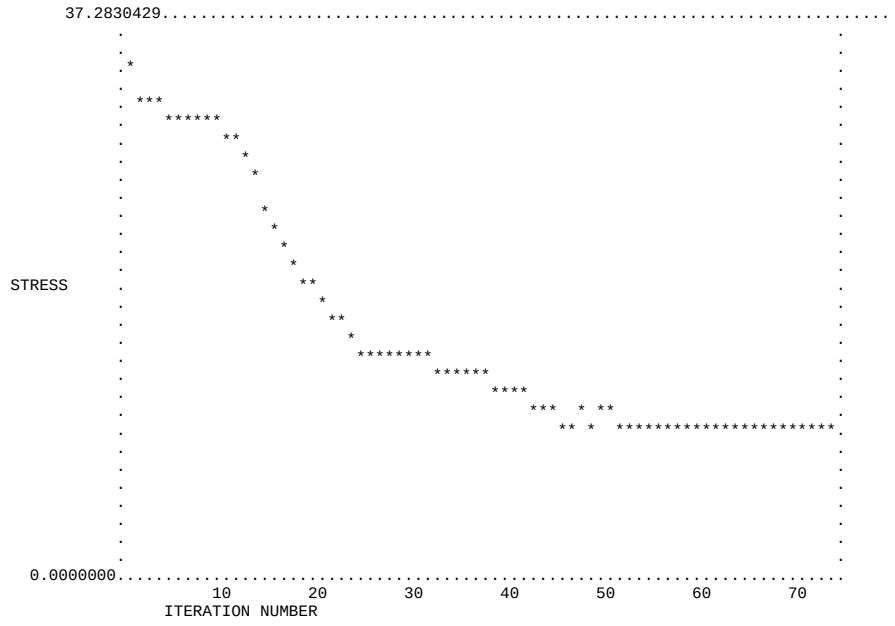

Figure 8.4. Stress plot for enzyme data.

Table 8.8. Correlations between variation in the data and ordination axes.

	R Squared	
Axis	Increment	Cumulative
1	.560	.560
2	.084	.644
3	.254	.898

Table 8.9. Correlations between enzyme activities and the ordination axes.

Axis:	1			2			3		
	r	r-sq	tau	r	r-sq	tau	r	r-sq	tau
Cellulas	-.475	.225	-.426	-.279	.078	-.151	.614	.377	.489
Xylans	-.587	.344	-.438	-.170	.029	-.161	.418	.175	.405
NAG	-.524	.275	-.477	-.303	.092	-.178	.391	.153	.366
Phosphat	-.023	.001	-.066	-.822	.676	-.719	-.009	.000	.001
Glucosid	-.510	.260	-.433	-.317	.101	-.092	.421	.177	.559
Sulfatas	-.051	.003	-.187	.001	.000	.020	.709	.503	.591
Phenolox	-.337	.114	-.076	.009	.000	-.124	.742	.551	.647
Peroxid	-.832	.692	-.736	.480	.230	.331	.067	.004	.053
Urease	-.425	.180	-.167	.073	.005	.125	.018	.000	.011

Table 8.10. Correlations between measured environmental variables and ordination axes.

Axis:	1			2			3		
	r	r-sq	tau	r	r-sq	tau	r	r-sq	tau
TotalN	.280	.078	.343	.216	.046	.024	.121	.015	.031
NO3--N	.241	.058	.282	.216	.047	.061	.111	.012	.002
NH4+-N	.471	.222	.372	.141	.020	.000	.156	.024	.059
Ca	.134	.018	-.014	-.260	.067	-.235	-.149	.022	-.040
Mg	-.160	.026	-.099	.104	.011	.066	.315	.100	.125
K	-.511	.262	-.362	.174	.030	.146	.292	.085	.205
P	-.294	.087	-.320	.263	.069	.212	.256	.066	.186
Fe	-.163	.027	-.268	.387	.150	.315	.096	.009	.125
Mn	.359	.129	.207	-.051	.003	.071	-.437	.191	-.289
Cu	-.510	.260	-.158	.467	.219	.328	-.182	.033	-.116
Zn	.324	.105	.240	.119	.014	.198	-.463	.214	-.365
B	-.273	.074	-.245	.068	.005	.024	-.020	.000	.031
S	.077	.006	.000	.227	.052	.240	-.256	.065	-.190
Pb	.274	.075	.227	-.067	.004	.114	-.377	.142	-.207
Al	.285	.081	.188	-.258	.067	-.188	-.513	.263	-.294
Slopedeg	-.299	.089	-.099	-.176	.031	-.179	-.147	.022	-.075
Soiltemp	-.550	.302	-.304	.245	.060	.194	.355	.126	.323
%sand	.187	.035	.184	.271	.073	.165	-.042	.002	-.031
%silt	-.322	.103	-.227	-.276	.076	-.168	.188	.035	.178
%clay	.129	.017	.080	-.091	.008	-.189	-.199	.040	-.083
%water	.762	.581	.477	-.206	.042	-.110	-.392	.154	-.338
%Carbon	.309	.095	.244	-.458	.209	-.311	-.457	.209	-.401
%Nitrogen	.471	.222	.180	-.511	.261	-.327	-.083	.007	-.085
C:N	-.344	.118	-.199	.101	.010	.018	-.526	.277	-.430
pH	-.414	.171	-.328	.028	.001	.040	.436	.190	.410

NMS ordination of microbial functional data for the H layer

A 2-dimensional solution was recommended. The final stress was 11.17956 ('fair' according to 'Kruskal's Rule of Thumb' see McCune and Grace, 2002). The final instability value of 0 and the stability plot suggest a stable solution was found. The number of iterations for the final solution was 131. The proportion of variance

represented by axis 1, based on the r^2 value between distance in the ordination space and distance in the original space, is 0.558. The r^2 value for axis 2 is 0.349; therefore the cumulative proportion of variance in the dataset represented by the final 2-dimensional solution is 0.907. The probability that a similar final stress could have been obtained by chance is 0.0196; therefore (using an alpha of 0.05) it can be accepted that the solution could not have been obtained by chance.

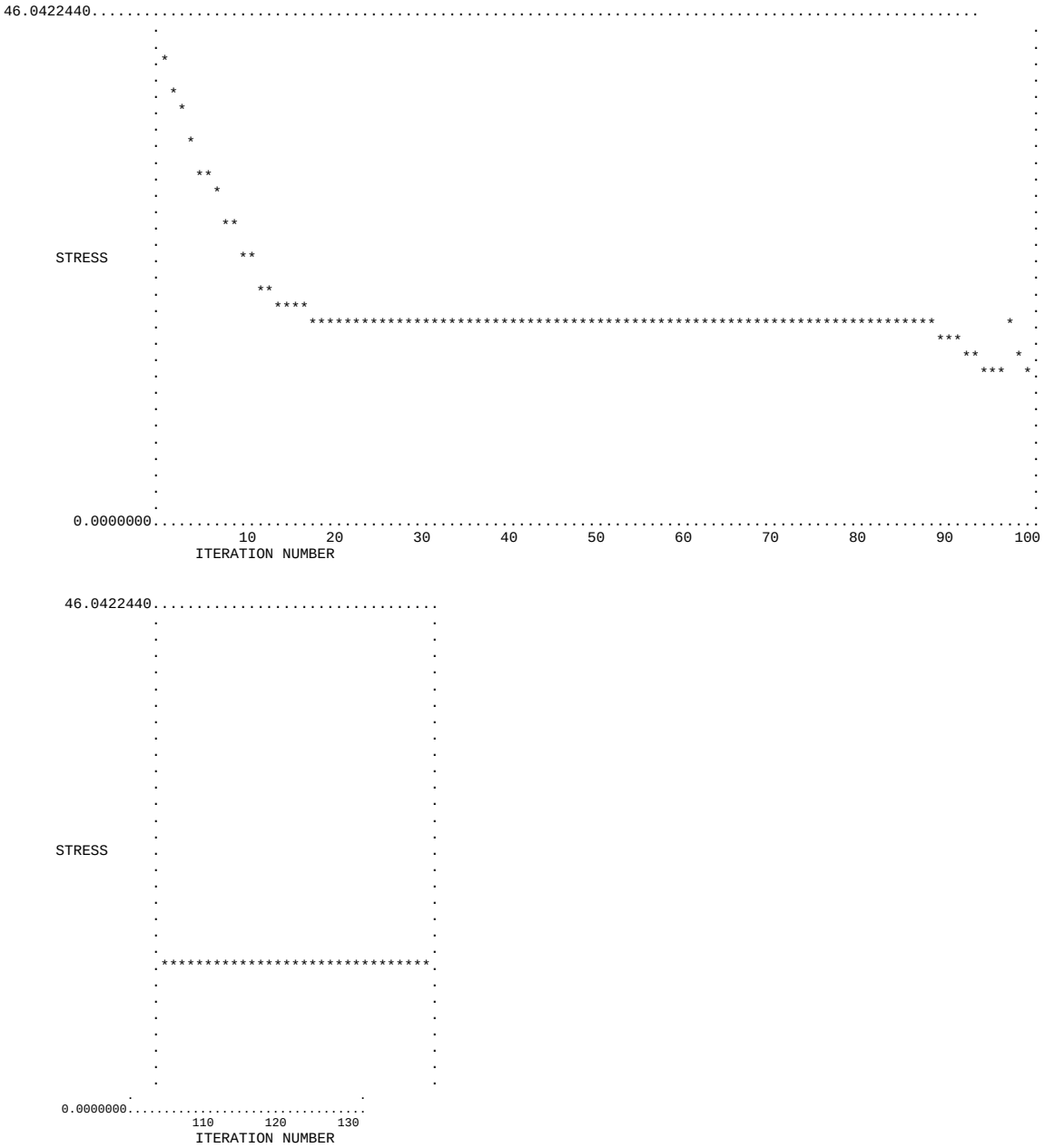

Figure 8.5. Stress plot for enzyme data.

Table 8.11. Correlations between variation in the data and ordination axes.

Axis	R Squared Increment	Cumulative
1	.558	.558
2	.349	.907

Table 8.12. Correlations between enzyme activities and the ordination axes.

Axis:	1			2		
	r	r-sq	tau	r	r-sq	tau
Cellulas	.137	.019	-.029	-.567	.322	-.590
Xylans	.043	.002	.062	-.545	.297	-.472
NAG	.196	.039	-.039	-.622	.387	-.613
Phosphat	.518	.269	.482	-.174	.030	-.086
Glucosid	.169	.029	.005	-.661	.437	-.543
Sulfatas	-.029	.001	-.234	-.539	.290	-.519
Phenolox	-.349	.122	-.455	-.567	.321	-.250
Peroxid	-.826	.683	-.712	-.675	.456	-.506
Urease	-.166	.027	-.108	-.063	.004	.018

Table 8.13. Correlations between measured environmental variables and ordination axes.

Axis:	1			2		
	r	r-sq	tau	r	r-sq	tau
TotalN	-.189	.036	.128	.079	.006	.196
NO3--N	-.190	.036	.056	.069	.005	.138
NH4+-N	-.040	.002	.169	.211	.044	.264
Ca	.171	.029	.111	-.074	.005	-.053
Mg	-.374	.140	-.278	-.429	.184	-.189
K	.093	.009	.019	-.427	.182	-.295
P	-.343	.118	-.124	-.360	.130	-.206
Fe	-.342	.117	-.220	.061	.004	.073
Mn	.225	.051	.165	.550	.302	.390
Cu	-.125	.016	-.167	.291	.085	.243
Zn	-.015	.000	-.046	.473	.224	.356
B	.021	.000	.066	-.253	.064	-.254
S	-.171	.029	-.182	.053	.003	.138
Pb	-.003	.000	-.037	.441	.195	.351
Al	.387	.150	.339	.466	.217	.216
Slopedeg	.580	.337	.378	.242	.059	.161
Soiltemp	-.175	.031	-.171	-.370	.137	-.263
%sand	-.096	.009	-.048	.398	.159	.287
%silt	.223	.050	.116	-.353	.124	-.267
%clay	-.168	.028	.007	-.205	.042	-.192
%water	.453	.206	.358	.762	.581	.543
%Carbon	.607	.369	.518	.476	.226	.258
%Nitrogen	.662	.439	.528	.399	.159	.234
C:N	.371	.137	.424	.393	.154	.261
pH	-.034	.001	-.124	-.601	.362	-.407

NMS ordination of microbial functional data for the mineral layer

A 1-dimensional solution was recommended. The final stress was 9.90937 ('good' according to 'Kruskal's Rule of Thumb' see McCune and Grace, 2002). The final instability value of 0.00001 and the stability plot (see Appendix) suggest a stable solution was found. The number of iterations for the final solution was 66. The proportion of variance represented by axis 1, based on the r^2 value between distance in the ordination space and distance in the original space, is 0.944. The probability that a similar final stress could have been obtained by chance is 0.0196; therefore (using an alpha of 0.05) it can be accepted that the solution could not have been obtained by chance.

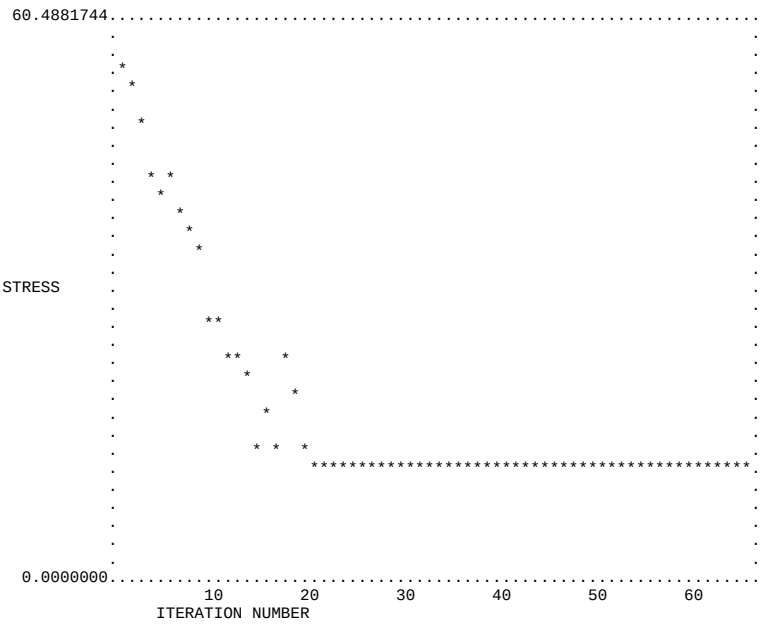

Figure 8.6. Stress plot for enzyme data.

Table 8.14. Correlations between variation in the data and ordination axes.

	R Squared	
Axis	Increment	Cumulative
1	.944	.944

Table 8.15. Correlations between enzyme activities and the ordination axes.

Axis:	1			2			3	
	r	r-sq	tau	r	r-sq	tau	r	r-sq tau
Cellulas	.080	.006	.050					
Xylans	-.085	.007	-.067					
NAG	.264	.070	.179					
Phosphat	-.286	.082	-.117					
Glucosid	.220	.048	.251					
Sulfatas	.300	.090	.115					
Phenolox	.543	.295	.335					
Peroxid	.831	.691	.916					
Urease	.106	.011	.142					

Table 8.16. Correlations between measured environmental variables and ordination axes.

Axis:	1			2			3		
	r	r-sq	tau	r	r-sq	tau	r	r-sq	tau
TotalN	-.241	.058	-.281						
NO3--N	-.242	.059	-.267						
NH4+-N	-.109	.012	-.278						
Ca	.097	.009	.093						
Mg	.321	.103	.205						
K	.171	.029	.096						
P	.513	.263	.328						
Fe	.129	.017	.153						
Mn	-.070	.005	-.182						
Cu	-.337	.113	-.296						
Zn	-.408	.167	-.349						
B	.178	.032	.221						
S	.150	.022	.035						
Pb	-.359	.129	-.215						
Al	-.323	.104	-.145						
Slopedeg	-.451	.204	-.367						
Soiltemp	.012	.000	-.049						
%sand	-.344	.118	-.296						
%silt	.183	.034	.214						
%clay	.360	.129	.286						
%water	-.594	.353	-.405						
%Carbon	-.455	.207	-.296						
%Nitrogen	-.474	.224	-.241						
C:N	-.296	.088	-.191						
pH	.382	.146	.231						

NMS ordination of structural data for a combination of all soil profile layers

A 2-dimensional solution was recommended, see Figure 3.10. The final stress was 7.84652 ('good' according to 'Kruskal's Rule of Thumb' see McCune and Grace, 2002). The final instability value of 0.00001 and the stability plot suggest a stable solution was found. The number of iterations for the final solution was 122. The proportion of variance represented by axis 1, based on the r^2 value between distance in the ordination space and distance in the original space, is 0.26. The r^2 value for axis 2 is 0.705; therefore the cumulative proportion of variance in the dataset represented by the final 2-dimensional solution is 0.966. The probability that a similar final stress could have been obtained by chance is 0.0196; therefore (using an alpha of 0.05) it can be accepted that the solution could not have been obtained by chance.

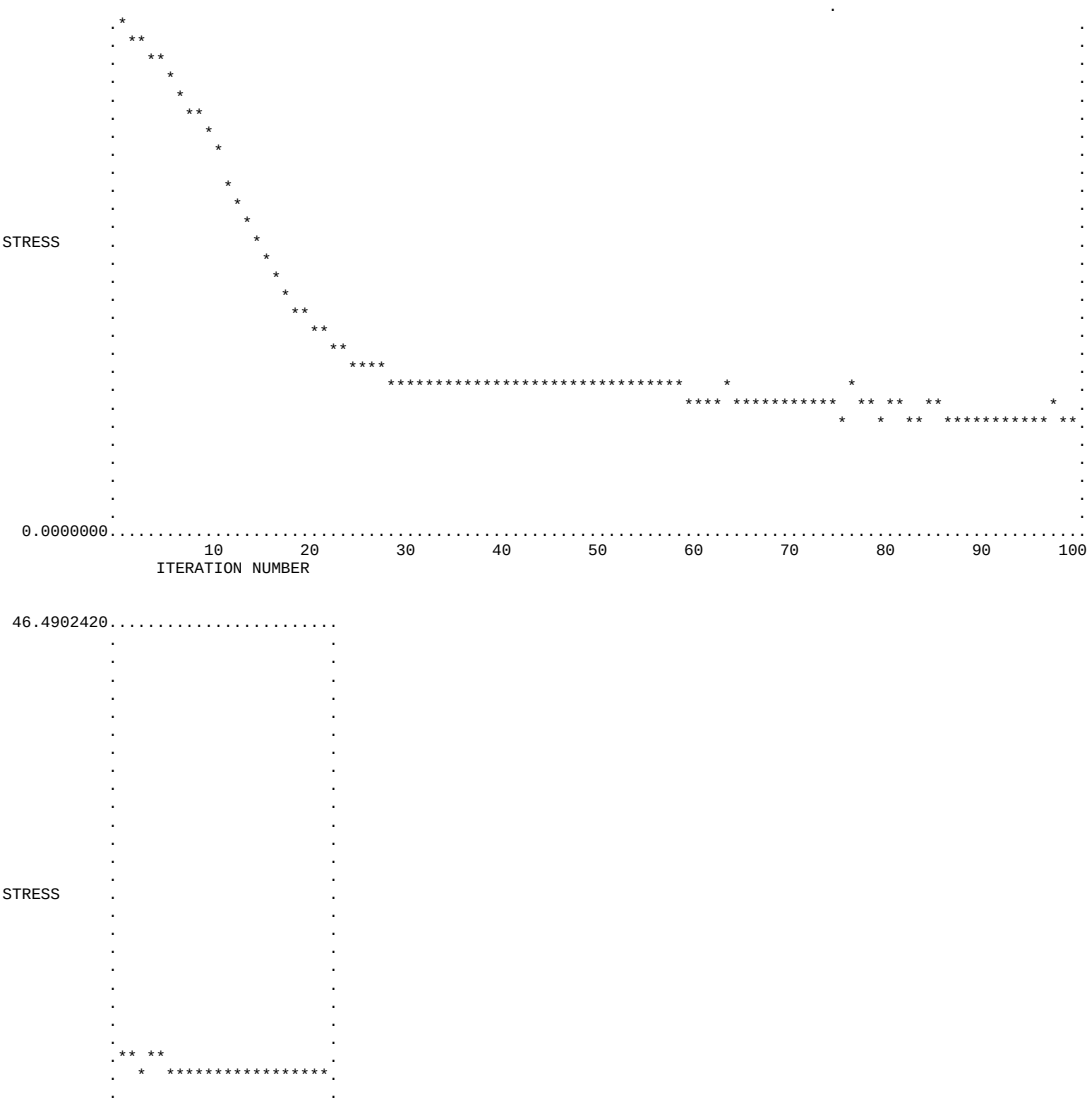

Figure 8.7. Stress plot for PLFA data.

Table 8.17. Correlations between variation in the data and ordination axes.

	R Squared	
Axis	Increment	Cumulative
1	.260	.260
2	.705	.966

Table 8.18. Correlations between PLFA concentrations and the ordination axes.

Axis:	1			2		
	r	r-sq	tau	r	r-sq	tau
Bac:SapF	-.836	.699	-.842	-.327	.107	-.324
B-ac:sap	-.831	.690	-.835	-.329	.108	-.324
Bac:ArbF	-.045	.002	-.196	-.750	.563	-.825
B-ac:arb	-.034	.001	-.181	-.745	.555	-.822
Bac:TotF	-.713	.508	-.824	-.474	.225	-.410
B-act:tf	-.702	.493	-.811	-.486	.236	-.423
Gpos:Gng	.099	.010	.138	.475	.225	.350
Bac:Tbio	-.061	.004	-.126	.232	.054	.016
B-a:tbio	-.054	.003	-.122	.221	.049	.010
TF:Tbio	.320	.103	.246	.372	.138	.239
Gps:Tbio	-.009	.000	-.100	.339	.115	.084
Gng:Tbio	-.111	.012	-.141	-.016	.000	-.093
Act:Tbio	-.101	.010	-.205	.282	.079	-.003

Table 8.19. Correlations between measured environmental variables and ordination axes.

Axis:	1			2			3	
	r	r-sq	tau	r	r-sq	tau	r	r-sq
tau								
TotalN	-.455	.207	-.079	-.221	.049	-.129		
NO3--N	-.445	.198	-.063	-.206	.042	-.110		
NH4+-N	-.324	.105	-.036	-.254	.065	-.121		
Ca	-.073	.005	-.051	.187	.035	.121		
Mg	-.062	.004	-.075	.026	.001	-.024		
K	.427	.182	.316	.074	.005	.066		
P	.258	.067	.206	.181	.033	.067		
Fe	-.343	.118	-.208	.003	.000	.004		
Mn	.042	.002	.052	-.067	.005	-.038		
Cu	-.083	.007	-.139	-.326	.106	-.320		
Zn	-.189	.036	-.144	-.206	.042	-.192		
B	-.193	.037	-.126	.029	.001	-.003		
S	-.052	.003	-.263	.196	.038	-.152		
Pb	-.269	.072	-.261	-.263	.069	-.269		
Al	-.101	.010	-.058	.072	.005	.097		
Slopedeg	.238	.057	.160	-.043	.002	.098		
Soiltemp	-.045	.002	-.052	-.172	.030	-.164		
%sand	-.265	.070	-.111	-.317	.100	-.194		
%silt	.328	.107	.164	.202	.041	.191		
%clay	.002	.000	-.017	.285	.081	.097		
%water	.056	.003	.084	.060	.004	.067		
%Carbon	.368	.135	.302	-.017	.000	.024		
%Nitrogen	.361	.130	.303	.045	.002	.097		
C:N	.196	.038	.270	-.212	.045	-.012		
pH	.241	.058	.139	.138	.019	.139		

NMS ordination of structural data for the F layer

A 2-dimensional solution was recommended, see Figure 3.11. The final stress was 8.83568 ('good' according to 'Kruskal's Rule of Thumb' see McCune and Grace, 2002). The final instability value of 0.00001 and the plot suggest a stable solution was found. The number of iterations for the final solution was 66. The proportion of variance represented by axis 1, based on the r^2 value between distance in the ordination space and distance in the original space, is 0.786. The r^2 value for axis 2 is 0.185, therefore the cumulative proportion of variance in the dataset represented by the final 2-dimensional solution is 0.953. The probability that a similar final stress could have been obtained by chance is 0.0196; therefore (using an alpha of 0.05) it can be accepted that the solution could not have been obtained by chance.

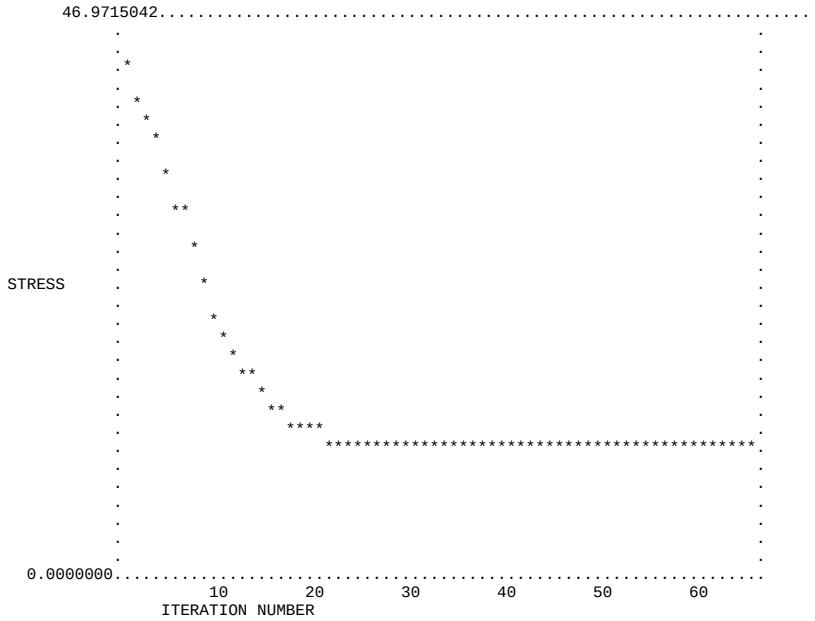

Figure 8.8. Stress plot for PLFA data.

Table 8.20. Correlations between variation in the data and ordination axes.

Axis	R Squared Increment	Cumulative
1	.768	.768
2	.185	.953

Table 8.21. Correlations between PLFA concentrations and the ordination axes.

Axis:	1			2		
	r	r-sq	tau	r	r-sq	tau
Bac:SapF	.671	.450	.509	.361	.130	.058
B-ac:sap	.668	.446	.507	.357	.128	.060
Bac:ArbF	.473	.223	.507	-.880	.774	-.777
B-ac:arb	.455	.207	.481	-.882	.778	-.802
Bac:TotF	.699	.488	.709	-.102	.010	-.040
B-act:tf	.697	.486	.716	-.112	.013	-.047
Gpos:Gng	-.200	.040	-.137	.221	.049	.184
Bac:Tbio	-.332	.110	.058	.371	.137	-.053
B-a:tbio	-.332	.110	.046	.341	.116	-.079
TF:Tbio	-.675	.456	-.560	.328	.107	.035
Gps:Tbio	-.327	.107	-.030	.372	.138	.063
Gng:Tbio	-.265	.070	.149	.217	.047	-.186
Act:Tbio	-.271	.073	.146	.508	.258	.058

Table 8.22. Correlations between measured environmental variables and ordination axes.

Axis:	1			2			3		
	r	r-sq	tau	r	r-sq	tau	r	r-sq	tau
TotalN	.403	.162	.193	.066	.004	.151			
NO3--N	.381	.145	.202	.064	.004	.118			
NH4+-N	.434	.188	.207	.053	.003	.118			
Ca	-.091	.008	-.066	.173	.030	.071			
Mg	.070	.005	.028	-.022	.001	-.038			
K	-.370	.137	-.207	.118	.014	.005			
P	-.345	.119	-.202	.207	.043	-.028			
Fe	.274	.075	.231	-.129	.017	-.169			
Mn	.094	.009	.113	-.136	.018	-.028			
Cu	.321	.103	.390	-.476	.227	-.427			
Zn	.364	.132	.264	-.115	.013	-.061			
B	-.017	.000	.047	-.043	.002	-.099			
S	.055	.003	.315	-.100	.010	-.198			
Pb	.466	.217	.437	-.133	.018	-.179			
Al	-.039	.002	-.005	-.101	.010	-.009			
Slopedeg	-.016	.000	-.029	-.299	.090	-.107			
Soiltemp	.164	.027	.182	-.412	.170	-.309			
%sand	.406	.165	.219	-.157	.025	-.026			
%silt	-.364	.133	-.268	.055	.003	.050			
%clay	-.211	.044	-.125	.207	.043	.144			
%water	.015	.000	-.079	.390	.152	.246			
%Carbon	-.189	.036	-.178	.099	.010	.023			
%Nitrogen	-.326	.106	-.347	.336	.113	.249			
C:N	.123	.015	-.063	-.362	.131	-.235			
pH	-.366	.134	-.177	.140	.020	.135			

NMS ordination of structural data for the H layer

A 2-dimensional solution was recommended, see Figure 3.12. The final stress was 4.26440 ('good' according to 'Kruskal's Rule of Thumb' see McCune and Grace, 2002). The final instability value of 0 and the plot suggest a stable solution was found. The number of iterations for the final solution was 96. The proportion of variance represented by axis 1, based on the r^2 value between distance in the ordination space and distance in the original space, is 0.853. The r^2 value for axis 2 is 0.129, therefore the cumulative proportion of variance in the dataset represented by the final 2-dimensional solution is 0.982. The probability that a similar final stress could have been obtained by chance is 0.0196; therefore (using an alpha of 0.05) it can be accepted that the solution could not have been obtained by chance.

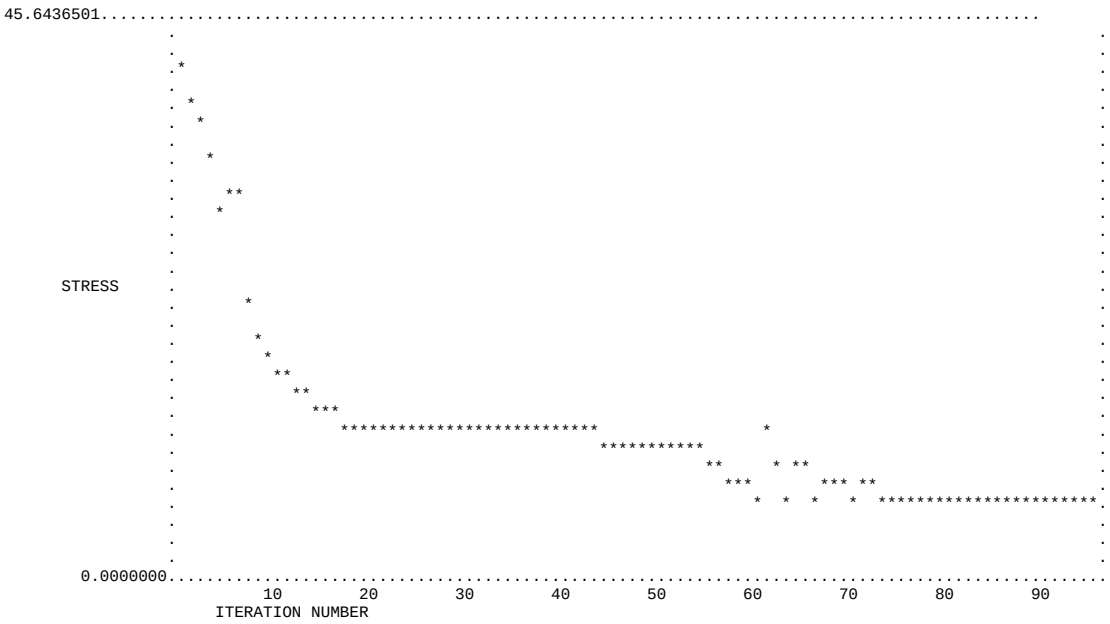

Figure 8.9. Stress plot for PLFA data.

Table 8.23. Correlations between variation in the data and ordination axes.

Axis	R Squared Increment	Cumulative
1	.853	.853
2	.129	.982

Table 8.24. Correlations between PLFA concentrations and the ordination axes.

Axis:	1			2			3	
	r	r-sq	tau	r	r-sq	tau	r	r-sq tau
Bac:SapF	.657	.432	.509	-.855	.730	-.765		
B-ac:sap	.661	.437	.503	-.848	.718	-.771		
Bac:ArbF	.883	.781	.818	-.007	.000	-.092		
B-ac:arb	.879	.773	.805	.020	.000	-.079		
Bac:TotF	.688	.474	.553	-.856	.733	-.721		
B-act:tf	.702	.493	.590	-.847	.718	-.684		
Gpos:Gng	-.360	.130	-.277	-.222	.049	-.045		
Bac:Tbio	-.180	.033	.297	-.328	.108	-.324		
B-a:tbio	-.154	.024	.314	-.306	.094	-.321		
TF:Tbio	-.706	.499	-.321	.393	.154	.388		
Gps:Tbio	-.394	.155	.160	-.259	.067	-.314		
Gng:Tbio	.231	.054	.345	-.259	.067	-.163		
Act:Tbio	-.290	.084	.240	-.394	.155	-.361		

Table 8.25. Correlations between measured environmental variables and ordination axes.

Axis:	1			2		
	r	r-sq	tau	r	r-sq	tau
TotalN	.451	.203	.164	-.649	.421	-.147
NO3--N	.435	.189	.259	-.644	.415	-.201
NH4+-N	.471	.222	.123	-.330	.109	-.017
Ca	-.167	.028	-.055	-.055	.003	-.010
Mg	-.075	.006	.109	.045	.002	-.003
K	-.378	.143	-.239	.558	.311	.167
P	-.287	.083	-.184	.181	.033	.065
Fe	.191	.037	.102	-.587	.345	-.338
Mn	.001	.000	-.034	.141	.020	.147
Cu	.444	.197	.378	-.402	.161	-.187
Zn	.219	.048	.205	-.053	.003	-.072
B	.030	.001	.027	-.246	.060	-.113
S	-.237	.056	.130	-.087	.008	-.160
Pb	.280	.078	.258	-.083	.007	-.092
Al	-.030	.001	-.177	-.137	.019	.058
Slopedeg	-.156	.024	-.224	.309	.096	.336
Soiltemp	.347	.121	.327	-.258	.067	-.141
%sand	.519	.270	.287	-.315	.099	-.058
%silt	-.402	.162	-.281	.351	.123	.175
%clay	-.359	.129	-.137	.048	.002	.086
%water	-.220	.049	-.207	.128	.016	.099
%Carbon	-.206	.042	-.251	.364	.132	.334
%Nitrogen	-.283	.080	-.310	.270	.073	.234
C:N	-.058	.003	-.254	.364	.132	.455
pH	-.070	.005	-.061	.109	.012	.013

NMS ordination of structural data for the mineral layer

A 2-dimensional solution was recommended, see Figure 3.13. The final stress was 4.54007 ('good' according to 'Kruskal's Rule of Thumb' see McCune and Grace, 2002). The final instability value of 0.00001 and the plot suggest a stable solution was found. The number of iterations for the final solution was 52. The proportion of variance represented by axis 1, based on the r^2 value between distance in the ordination space and distance in the original space, is 0.895. The r^2 value for axis 2 is 0.08, therefore the cumulative proportion of variance in the dataset represented by the final 2-dimensional solution is 0.974. The probability that a similar final stress could have been obtained by chance is 0.0196; therefore (using an alpha of 0.05) it can be accepted that the solution could not have been obtained by chance.

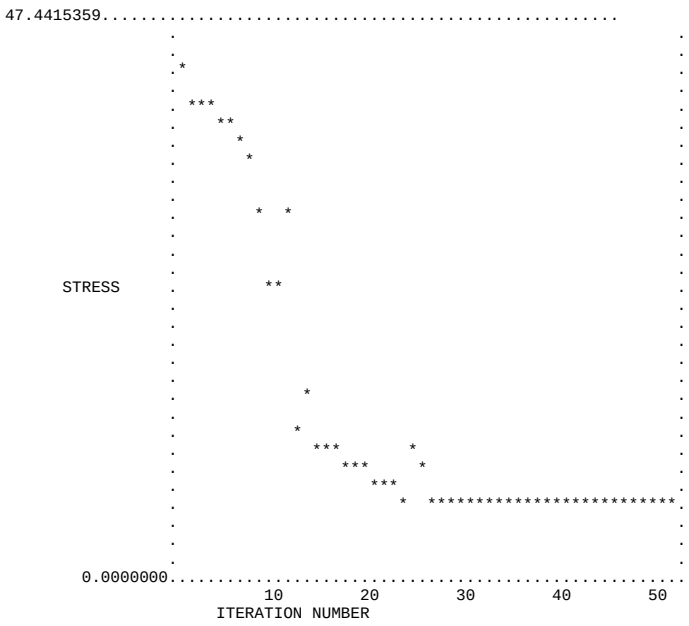

Figure 8.10. Stress plot for PLFA data.

Table 8.26. Correlations between variation in the data and ordination axes.

	R Squared	
Axis	Increment	Cumulative
1	.895	.895
2	.080	.974

Table 8.27. Correlations between PLFA concentrations and the ordination axes.

Axis:	1			2		
	r	r-sq	tau	r	r-sq	tau
Bac:SapF	.675	.455	.722	-.218	.048	-.344
B-ac:sap	.678	.460	.720	-.212	.045	-.341
Bac:ArbF	.676	.457	.729	.672	.451	.190
B-ac:arb	.672	.451	.741	.670	.448	.178
Bac:TotF	.677	.459	.729	-.255	.065	-.351
B-act:tf	.690	.477	.741	-.239	.057	-.329
Gpos:Gng	-.754	.569	-.580	-.360	.130	-.046
Bac:Tbio	-.268	.072	-.093	.076	.006	.041
B-a:tbio	-.256	.066	-.098	.092	.009	.051
TF:Tbio	-.434	.188	-.444	.233	.054	.280
Gps:Tbio	-.456	.208	-.232	-.018	.000	.034
Gng:Tbio	.180	.032	.137	.317	.100	.178
Act:Tbio	-.292	.085	-.080	-.015	.000	.010

Table 8.28. Correlations between measured environmental variables and ordination axes.

Axis:	1			2		
	r	r-sq	tau	r	r-sq	tau
TotalN	.243	.059	.204	-.105	.011	-.112
NO3--N	.220	.048	.065	-.102	.010	-.178
NH4+-N	.322	.104	.226	-.078	.006	-.073
Ca	-.168	.028	-.149	-.163	.026	-.072
Mg	-.023	.001	-.060	-.043	.002	.047
K	.214	.046	.095	.294	.087	.256
P	.018	.000	.000	-.003	.000	.087
Fe	-.212	.045	-.189	-.181	.033	-.087
Mn	.022	.000	.050	-.097	.009	-.042
Cu	.053	.003	.102	.191	.036	.058
Zn	.185	.034	.189	-.017	.000	-.107
B	.011	.000	-.035	-.061	.004	.032
S	-.225	.051	.050	-.153	.024	-.256
Pb	.217	.047	.243	.001	.000	-.013
Al	-.088	.008	-.065	-.143	.020	-.052
Slopedeg	-.056	.003	-.078	.233	.054	.159
Soiltemp	-.073	.005	-.020	.059	.003	-.076
%sand	.202	.041	.153	.048	.002	-.032
%silt	-.107	.012	-.099	.146	.021	.109
%clay	-.213	.046	-.059	-.296	.088	-.156
%water	.120	.014	.160	-.117	.014	-.079
%Carbon	.233	.054	.243	.020	.000	-.130
%Nitrogen	.182	.033	.140	-.178	.032	-.153
C:N	.186	.034	.063	.213	.046	.095
pH	-.136	.018	-.143	.182	.033	.131

Appendix II. Paired MRPP test statistics

Table 8.29. MRPP pair-wise comparisons for all available N ions and total N by location, organic layers. * indicates significant differences when p=0.05/7=0.007.

Compared			T	A	p
1	vs.	2	0.46344082	-0.02217072	0.59317082
1	vs.	3	0.01005922	-0.00072352	0.42110927
1	vs.	4	-1.53896763	0.09824691	0.07867390
1	vs.	5	-0.15252436	0.00803136	0.32386581
1	vs.	6	-2.63738834	0.09311510	0.01687117
1	vs.	7	-5.61073772	0.35667512	0.00153424*
2	vs.	3	-0.32423583	0.03445679	0.28461001
2	vs.	4	-3.49583275	0.20898026	0.00897168
2	vs.	5	-0.36484841	0.02396348	0.25199151
2	vs.	6	-0.68042049	0.03910322	0.20467693
2	vs.	7	-5.54807040	0.39163242	0.00147510*
3	vs.	4	-0.36355213	0.02990739	0.28108859
3	vs.	5	0.60258412	-0.05024699	0.67608781
3	vs.	6	-2.81342216	0.22167102	0.01257628
3	vs.	7	-3.82933318	0.36951201	0.00579687*
4	vs.	5	-1.77204150	0.08917520	0.06095658
4	vs.	6	-5.42713031	0.36313075	0.00155070*
4	vs.	7	-6.10057827	0.36494899	0.00074799*
5	vs.	6	-3.00512178	0.17442864	0.01414464
5	vs.	7	-5.53858458	0.35996605	0.00123785*
6	vs.	7	-6.03334427	0.49568968	0.00114018*

Table 8.30. MRPP pair-wise comparisons for all available N ions and total N by location, mineral layer. * indicates significant differences when p=0.05/7=0.007 (n=39).

Compared			T	A	p
1	vs.	2	-2.94509439	0.51168387	0.02180992
1	vs.	3	-2.93449404	0.77248731	0.02191185
1	vs.	4	-1.59868226	0.11994001	0.05973429
1	vs.	5	-2.30487651	0.31228083	0.02859693
1	vs.	6	-2.95830909	0.62695527	0.02174589
1	vs.	7	-2.60134669	0.43518742	0.02455896
2	vs.	3	-2.96908688	0.68379995	0.02167592
2	vs.	4	-2.54149168	0.24001426	0.02472841
2	vs.	5	-0.90583633	0.06200527	0.17575231
2	vs.	6	0.25508550	-0.03617708	0.47493838
2	vs.	7	-1.23707965	0.20499404	0.11147509
3	vs.	4	-1.50010808	0.28333060	0.07598029
3	vs.	5	-2.90508016	0.64076698	0.02207742
3	vs.	6	-2.98393165	0.79859249	0.02158744
3	vs.	7	-2.75306588	0.53609893	0.02321054
4	vs.	5	-0.90260767	0.06325372	0.17269690
4	vs.	6	-2.77871227	0.36167055	0.02296187
4	vs.	7	-2.06554359	0.25870193	0.03765161
5	vs.	6	-2.08692329	0.23210097	0.02906900
5	vs.	7	-1.92625469	0.27939711	0.04151106
6	vs.	7	-1.62305170	0.28509368	0.06280648

Table 8.31. MRPP pair-wise comparisons for all available P by location, all layers combined. * indicates significant differences when p=0.05/7=0.007 (n=63).

Compared			T	A	p
1	vs.	2	-6.04947773	0.24078419	0.00031727*
1	vs.	3	-3.46748775	0.15736363	0.00679037*
1	vs.	4	0.82931504	-0.02850579	0.81566659
1	vs.	5	-9.71750750	0.42846072	0.00003042*
1	vs.	6	-9.88865690	0.44688927	0.00002860*
1	vs.	7	-8.67169476	0.37577298	0.00004865*
2	vs.	3	-1.74975800	0.08826339	0.06156749
2	vs.	4	-4.60607517	0.18193874	0.00231698*
2	vs.	5	-3.26956412	0.16576672	0.01528942
2	vs.	6	-5.46877141	0.26791555	0.00164665*
2	vs.	7	-4.42594901	0.21690579	0.00384986*
3	vs.	4	-2.84177295	0.11641396	0.01556306
3	vs.	5	-3.57683502	0.16077003	0.00574226*
3	vs.	6	-4.72155607	0.20040205	0.00107991*
3	vs.	7	-3.74223623	0.15805806	0.00468983*
4	vs.	5	-7.07744608	0.31495177	0.00034541*
4	vs.	6	-7.15333285	0.32772499	0.00039290*
4	vs.	7	-6.31434766	0.27217495	0.00061564*
5	vs.	6	-0.63669623	0.02936439	0.19283400
5	vs.	7	-1.18220628	0.05619393	0.11346160
6	vs.	7	0.36708833	-0.01813584	0.52583018

Table 8.32. MRPP pair-wise comparisons for all available S by location, all layers combined. * indicates significant differences when p=0.05/7=0.007 (n=63).

Compared			T	A	p
1	vs.	2	0.65795854	-0.03468210	0.72116233
1	vs.	3	-1.99525649	0.11512873	0.04646336
1	vs.	4	-9.24429197	0.38252170	0.00002553*
1	vs.	5	-1.77564214	0.07799126	0.06190107
1	vs.	6	-8.97590768	0.43259950	0.00005400*
1	vs.	7	-9.24676324	0.49816041	0.00006542*
2	vs.	3	-1.65496205	0.09221348	0.06921756
2	vs.	4	-8.67053957	0.34480258	0.00003307*
2	vs.	5	-1.47326161	0.06602788	0.08559220
2	vs.	6	-6.87265718	0.32646975	0.00031371*
2	vs.	7	-7.45881557	0.39021390	0.00025286*
3	vs.	4	-5.20966348	0.19505555	0.00062848*
3	vs.	5	-2.30609406	0.14576724	0.03241722
3	vs.	6	-3.81799452	0.19732516	0.00449256*
3	vs.	7	-4.27798954	0.22731652	0.00239368*
4	vs.	5	-9.38169726	0.42040164	0.00002901*
4	vs.	6	-6.60199550	0.26324985	0.00027184*
4	vs.	7	-7.02389202	0.28650141	0.00019476*
5	vs.	6	-9.27725534	0.50549659	0.00005984*
5	vs.	7	-9.50812118	0.58906006	0.00007529*
6	vs.	7	0.54253254	-0.02639926	0.63468125

Table 8.33. MRPP pair-wise comparisons for all available K, Ca, and Mg by location, all layers combined. * indicates significant differences when p=0.05/7=0.007 (n=63).

Compared			T	A	p
1	vs.	2	-3.22081244	0.10182796	0.01236351
1	vs.	3	-2.37474733	0.12341719	0.02945430
1	vs.	4	-9.94352822	0.42194025	0.00003156*
1	vs.	5	-9.78696100	0.41973236	0.00003778*
1	vs.	6	-6.68070061	0.26122488	0.00051225*
1	vs.	7	-5.12011061	0.16775446	0.00104451*
2	vs.	3	-1.59450328	0.07944389	0.07432662
2	vs.	4	-7.87238097	0.31068342	0.00015969*
2	vs.	5	-6.56272275	0.26582617	0.00053307*
2	vs.	6	-1.57800811	0.06583896	0.07528215
2	vs.	7	-0.55417051	0.02132733	0.21654216
3	vs.	4	-4.72954421	0.21910888	0.00133137*
3	vs.	5	-4.15090694	0.20550013	0.00306630*
3	vs.	6	-2.47691558	0.13434888	0.02627244
3	vs.	7	-1.71923325	0.07675848	0.06397879
4	vs.	5	-0.36558316	0.01147584	0.25941203
4	vs.	6	-8.74125109	0.29177731	0.00004760*
4	vs.	7	-3.74213767	0.13650295	0.00852828*
5	vs.	6	-6.73821585	0.23629154	0.00035666*
5	vs.	7	-3.13856516	0.11744271	0.01565805
6	vs.	7	-1.32625661	0.04422741	0.10085158

Table 8.34. MRPP pair-wise comparisons for all available micronutrients by location, all layers combined. * indicates significant differences when p=0.05/7=0.007 (n=63).

Compared			T	A	p
1	vs.	2	-7.97004833	0.33950956	0.00016786*
1	vs.	3	-3.78804278	0.17099593	0.00477395*
1	vs.	4	-5.24863569	0.15355108	0.00132448*
1	vs.	5	-2.64863688	0.07300508	0.02256177
1	vs.	6	-9.71120443	0.41678508	0.00002993*
1	vs.	7	-7.28587279	0.27644438	0.00024236*
2	vs.	3	-3.59377341	0.15639741	0.00544085*
2	vs.	4	-4.35297290	0.15595537	0.00393477*
2	vs.	5	-8.66000050	0.35484965	0.00007460*
2	vs.	6	-2.50267790	0.07920869	0.02665037
2	vs.	7	-2.44307571	0.08289951	0.02917388
3	vs.	4	-1.66300140	0.06840443	0.06877030
3	vs.	5	-3.45719661	0.15453208	0.00752483
3	vs.	6	-5.30251830	0.21139670	0.00042977*
3	vs.	7	-2.68147968	0.11001800	0.01856582
4	vs.	5	-4.01037384	0.10453141	0.00455282*
4	vs.	6	-7.00290427	0.24929783	0.00019040*
4	vs.	7	-1.55636723	0.04467096	0.07801214
5	vs.	6	-10.40885314	0.42725361	0.00001554*
5	vs.	7	-7.59102794	0.26545796	0.00012810*
6	vs.	7	-4.59828538	0.14601319	0.00155943*

Table 8.35. MRPP pair-wise comparisons for soil water (%) by location. * indicates significant differences when p=0.05/7=0.007 (n=78).

Compared			T	A	p
1	vs.	2	-13.10993123	0.52136707	0.00000297*
1	vs.	3	-7.50713791	0.39044806	0.00014163*
1	vs.	4	-7.51784154	0.26430277	0.00026718*
1	vs.	5	-5.80039134	0.18668659	0.00102887*
1	vs.	6	-14.52340999	0.60992963	0.00000114*
1	vs.	7	-11.44180294	0.39520748	0.00000726*
2	vs.	3	-10.48457920	0.61795687	0.00001440*
2	vs.	4	-2.47476233	0.07449771	0.03059808
2	vs.	5	-7.93130254	0.31614141	0.00025792*
2	vs.	6	-5.57304992	0.17512927	0.00193778*
2	vs.	7	-1.21247288	0.03890384	0.11013066
3	vs.	4	-8.88437152	0.46660482	0.00004571*
3	vs.	5	-9.60005526	0.50892222	0.00002073*
3	vs.	6	-10.77399248	0.65829350	0.00001181*
3	vs.	7	-10.18988245	0.54901406	0.00001510*
4	vs.	5	-1.23475571	0.04180286	0.10332148
4	vs.	6	-7.22226770	0.23100420	0.00029211*
4	vs.	7	0.55563574	-0.01623310	0.64336178
5	vs.	6	-11.71737197	0.48024254	0.00000864*
5	vs.	7	-3.77079511	0.13328708	0.00929258
6	vs.	7	-5.72822333	0.21158007	0.00169192*

Table 8.36. MRPP pair-wise comparisons for soil temperature (˚C) by location. * indicates significant differences when p=0.05/7=0.007 (n=84).

Compared			T	A	p
1	vs.	2	-11.22797138	0.42819599	0.00000539*
1	vs.	3	-9.09370846	0.34898072	0.00004310*
1	vs.	4	-6.48963077	0.25980716	0.00047289*
1	vs.	5	-1.91186768	0.08264780	0.05475198
1	vs.	6	-3.24565940	0.12879577	0.01376498
1	vs.	7	-0.89074260	0.03908930	0.14022146
2	vs.	3	-14.31577613	0.58202684	0.00000090*
2	vs.	4	-2.50682671	0.09954657	0.02935852
2	vs.	5	-10.66691975	0.40420650	0.00001262*
2	vs.	6	-2.30600520	0.09933582	0.03760627
2	vs.	7	-12.87630184	0.50568675	0.00000197*
3	vs.	4	-11.09671373	0.39915252	0.00000284*
3	vs.	5	-12.57373314	0.50879309	0.00000378*
3	vs.	6	-9.89525237	0.36014460	0.00001104*
3	vs.	7	-7.31302180	0.27117089	0.00025111*
4	vs.	5	-5.43109055	0.23407482	0.00167350*
4	vs.	6	-2.34439283	0.09145270	0.03500551
4	vs.	7	-8.11929812	0.31612308	0.00008827*
5	vs.	6	-2.94201237	0.11943988	0.01848482
5	vs.	7	-6.11241964	0.24318517	0.00108431*
6	vs.	7	-4.61027104	0.18378261	0.00337784*

Table 8.37. MRPP pair-wise comparisons for soil pH by location. * indicates significant differences when p=0.05/7=0.007 (n=76).

Compared			T	A	p
1	vs.	2	-11.26042865	0.48120443	0.00001200*
1	vs.	3	-1.69913803	0.08902274	0.06726816
1	vs.	4	-7.56192076	0.29044780	0.00029172*
1	vs.	5	-3.84763747	0.14284511	0.00812745
1	vs.	6	-14.71116769	0.75822732	0.00000149*
1	vs.	7	-10.94801352	0.45269166	0.00001903*
2	vs.	3	-5.00867047	0.25655222	0.00206071*
2	vs.	4	-4.42751607	0.16036441	0.00451572*
2	vs.	5	-11.62395418	0.48373136	0.00000944*
2	vs.	6	-13.09766777	0.56409771	0.00000309*
2	vs.	7	-0.98812182	0.03560752	0.13619781
3	vs.	4	-0.32843233	0.01626585	0.26396407
3	vs.	5	-4.33747638	0.22964972	0.00491864*
3	vs.	6	-10.98623655	0.67913691	0.00001182*
3	vs.	7	-5.39889964	0.27399913	0.00179406*
4	vs.	5	-9.68421484	0.37591444	0.00004522*
4	vs.	6	-15.02978506	0.68438435	0.00000098*
4	vs.	7	-6.76164071	0.24364376	0.00056078*
5	vs.	6	-15.04093542	0.70607881	0.00000104*
5	vs.	7	-12.05483979	0.46707677	0.00000648*
6	vs.	7	-9.03394000	0.33914983	0.00007273*

Appendix III. PRS™ Probe Raw Data

PRS™-Probe Supply Rate (μg/10cm²/burial period)											
Location	**Sample**	**#Cation**	**#Anion**	**Layer**	**Total N**	**NO_3^--N**	**NH_4^+-N**	**Ca**	**Mg**	**K**	**P**
Method Detection Limits (mdl):					***2***	***2***	***2***	***2***	***4***	***4***	***0.2***
IDF	1	4	4	F	6	<mdl	6	714	239	885	37.3
IDF	2	4	4	H	<mdl	<mdl	<mdl	787	264	403	14.7
IDF	3	4	4	M	<mdl	<mdl	<mdl	848	321	418	17.4
IDF	4	4	4	F	15	5	10	513	186	614	49.8
IDF	5	4	4	H	8	4	4	860	285	870	31.4
IDF	6	4	4	M	5	3	3	631	249	795	20.3
IDF	7	4	4	F	4	<mdl	4	979	303	558	40.1
IDF	8	4	4	H	<mdl	<mdl	<mdl	877	380	471	23.4
IDF	9	4	4	M	<mdl	<mdl	<mdl	594	277	404	13.4
IDF	10	4	4	F	7	<mdl	7	803	295	646	48.0
IDF	11	4	4	H	2	<mdl	2	1045	316	439	34.0
IDF	12	4	4	M	2	<mdl	2	946	378	370	15.6
IDF	13	4	4	F	3	<mdl	3	1524	452	411	83.9
IDF	14	4	4	H	<mdl	<mdl	<mdl	1968	638	232	56.7
IDF	15	4	4	M	<mdl	<mdl	<mdl	1474	392	256	44.9
IDF	16	3	4	F	4	<mdl	4	559	164	691	42.6
IDF	17	4	4	H	4	<mdl	4	747	194	654	23.4
IDF	18	4	4	M	<mdl	<mdl	<mdl	617	184	191	9.3
IDF	19	4	4	F	9	4	5	525	140	414	32.7
IDF	20	3	4	H	12	9	3	648	165	297	15.5
IDF	21	4	4	M	4	<mdl	4	647	229	335	28.4
IDF	22	4	4	F	8	4	4	443	116	611	30.3
IDF	23	4	4	H	2	<mdl	2	573	168	354	11.3
IDF	24										
IDF	25	4	4	F	16	10	7	693	217	557	20.7
IDF	26	4	4	H	18	14	4	479	184	370	11.7
IDF	27										

PRS™-Probe Supply Rate (μg/10cm^2/burial period)											
Location	**Sample**	**#Cation**	**#Anion**	**Layer**	**Total N**	**NO_3^--N**	**NH_4^+-N**	**Ca**	**Mg**	**K**	**P**
Method Detection Limits (mdl):					***2***	***2***	***2***	***2***	***4***	***4***	***0.2***
IDF	28	4	4	F	14	8	6	568	207	330	18.9
IDF	29	4	4	H	<mdl	<mdl	<mdl	420	206	163	9.8
IDF	30										
IDF	31	2	2	F	7	2	5	750	430	332	24.2
IDF	32	4	3	H	5	5	<mdl	859	537	249	15.8
IDF	33										
IDF	34	4	4	F	7	<mdl	7	768	206	618	20.0
IDF	35										
IDF	36										
IDF	37	4	4	F	17	13	5	704	205	484	12.9
IDF	38	4	4	H	11	11	<mdl	585	190	427	14.3
IDF	39										
IDF	40	3	2	F	23	10	14	535	168	565	22.4
IDF	41	4	4	H	13	8	6	749	269	428	13.3
IDF	42										
IDF	43	4	4	F	6	4	2	827	360	368	19.6
IDF	44	4	4	H	3	3	<mdl	608	236	355	7.9
IDF	45										
ESSF	46	4	4	F	7	4	3	758	129	157	5.6
ESSF	47										
ESSF	48	4	4	M	26	<mdl	26	297	56	279	9.9
ESSF	49	4	4	F	10	3	7	286	58	125	2.7
ESSF	50										
ESSF	51	4	4	M	3	<mdl	3	124	33	144	2.4
ESSF	52	3	3	F	24	12	12	800	111	101	46.5
ESSF	53										
ESSF	54	4	4	M	65	21	44	866	136	667	36.2
ESSF	55	4	4	F	10	2	7	363	157	224	9.2
ESSF	56										
ESSF	57	4	4	M	5	<mdl	5	381	129	326	7.0
ESSF	58	4	4	F	19	6	13	557	77	271	6.6
ESSF	59										
ESSF	60	4	4	M	10	5	5	390	58	363	11.0

PRS™-Probe Supply Rate (μg/10cm^2/burial period)											
Location	**Sample**	**#Cation**	**#Anion**	**Layer**	**Total N**	**NO_3^--N**	**NH_4^+-N**	**Ca**	**Mg**	**K**	**P**
Method Detection Limits (mdl):					***2***	***2***	***2***	***2***	***4***	***4***	***0.2***
ESSF	61	4	4	F	9	5	4	655	99	391	17.0
ESSF	62	4	4	H	10	5	5	474	62	397	25.3
ESSF	63	4	4	M	9	3	6	377	49	400	5.1
ESSF	64	4	4	F	13	8	5	670	89	160	7.0
ESSF	65	4	4	H	12	6	7	919	77	233	11.8
ESSF	66	4	4	M	10	4	6	598	53	287	11.8
ESSF	67	4	4	F	29	12	17	913	92	96	13.2
ESSF	68	4	4	H	19	7	13	677	47	101	9.6
ESSF	69	4	4	M	9	3	6	377	38	145	4.1
ESSF	70	4	4	F	8	4	4	787	154	430	19.4
ESSF	71	4	4	H	8	2	6	667	115	529	7.8
ESSF	72	4	4	M	8	4	4	738	65	158	4.1
ESSF	73	4	4	F	10	5	5	1087	131	362	10.6
ESSF	74	4	4	H	9	5	4	1037	99	296	12.4
ESSF	75	4	4	M	8	4	4	917	79	256	2.8
ESSF	76	4	4	F	9	4	4	1697	271	89	4.0
ESSF	77	4	4	H	7	4	3	1239	225	284	18.9
ESSF	78	4	4	M	12	6	7	1655	312	148	2.5
ESSF	79	4	4	F	5	2	3	1565	199	453	9.1
ESSF	80	4	4	H	7	5	2	1787	229	305	10.7
ESSF	81	4	4	M	4	<mdl	4	1397	206	272	4.9
ESSF	82	4	4	F	3	<mdl	3	1045	152	209	6.6
ESSF	83	4	4	H	3	<mdl	3	1096	183	406	8.8
ESSF	84	4	5	M	6	2	4	1401	252	272	12.0
ESSF	85	4	4	F	6	<mdl	6	982	242	344	6.3
ESSF	86	4	4	H	6	3	4	1007	197	448	8.2
ESSF	87	4	4	M	6	<mdl	6	1407	292	233	1.7
ESSF	88	4	4	F	3	<mdl	3	811	120	253	7.1
ESSF	89			H							
ESSF	90	4	4	M	6	2	4	814	179	341	2.5
PP	91	4	4	F	2	<mdl	2	999	148	278	7.6
PP				H							
PP	93	4	4	M	<mdl	<mdl	<mdl	1129	182	212	10.8

PRS™-Probe Supply Rate (μg/10cm^2/burial period)											
Location	**Sample**	**#Cation**	**#Anion**	**Layer**	**Total N**	**NO_3^--N**	**NH_4^+-N**	**Ca**	**Mg**	**K**	**P**
Method Detection Limits (mdl):					***2***	***2***	***2***	***2***	***4***	***4***	***0.2***
PP	94	4	4	F	10	4	6	507	76	249	17.9
PP	95			H							
PP	96	4	4	M	3	3	<mdl	1065	188	194	7.4
PP	97	4	4	F	4	<mdl	4	881	162	314	23.5
PP	98			H							
PP	99	4	4	M	<mdl	<mdl	<mdl	1026	198	395	6.3
PP	100	4	4	F	6	3	3	715	95	283	14.5
PP	101			H							
PP	102			M							
PP	103	4	4	F	5	3	2	578	106	312	10.8
PP	104			H							
PP	105			M							
PP	106	4	4	F	7	3	4	606	129	533	8.2
PP	107			H							
PP	108			M							
PP	109	4	4	F	10	4	6	596	136	628	14.7
PP	110			H							
PP	111			M							
PP	112	4	4	F	10	5	5	688	148	497	15.4
PP	113			H							
PP	114			M							
PP	115	3	4	F	7	3	4	747	131	614	26.7
PP	116			H							
PP	117			M							
PP	118	4	4	F	10	5	5	961	273	878	18.9
PP	119			H							
PP	120			M							
PP	121	4	4	F	7	4	3	586	187	550	26.3
PP	122			H							
PP	123			M							
PP	124	4	4	F	7	3	4	504	125	473	24.9
PP	125			H							
PP	126			M							

PRS™-Probe Supply Rate (μg/10cm^2/burial period)											
Location	**Sample**	**#Cation**	**#Anion**	**Layer**	**Total N**	**NO_3^--N**	**NH_4^+-N**	**Ca**	**Mg**	**K**	**P**
Method Detection Limits (mdl):					***2***	***2***	***2***	***2***	***4***	***4***	***0.2***
PP	127	4	4	F	<mdl	<mdl	<mdl	544	91	189	4.2
PP	128			H							
PP	129			M							
PP	130	4	4	F	<mdl	<mdl	<mdl	478	89	330	5.9
PP	131			H							
PP	132			M							
PP	133	4	4	F	3	<mdl	3	556	117	409	14.4
PP	134			H							
PP	135			M							
BWBS	136	4	3	F	<mdl	<mdl	<mdl	1843	232	448	23.4
BWBS	137	4	4	H	<mdl	<mdl	<mdl	2146	246	179	7.4
BWBS	138	4	4	M	<mdl	<mdl	<mdl	2654	260	27	1.0
BWBS	139	4	4	F	3	<mdl	3	1793	191	494	31.9
BWBS	140	4	4	H	<mdl	<mdl	<mdl	2048	241	202	39.0
BWBS	141	4	4	M	<mdl	<mdl	<mdl	2310	243	84	5.0
BWBS	142	4	4	F	<mdl	<mdl	<mdl	1390	166	494	51.1
BWBS	143	4	4	H	<mdl	<mdl	<mdl	1669	194	237	5.3
BWBS	144	4	4	M	<mdl	<mdl	<mdl	2668	249	18	2.7
BWBS	145	5	4	F	3	3	<mdl	1625	181	525	29.5
BWBS	146	4	4	H	4	4	<mdl	1602	238	316	17.3
BWBS	147	4	4	M	3	3	<mdl	2324	276	47	4.1
BWBS	148	4	4	F	3	3	<mdl	1837	232	263	15.1
BWBS	149	4	4	H	2	<mdl	2	2446	279	53	6.5
BWBS	150	4	4	M	<mdl	<mdl	<mdl	2770	234	12	0.8
BWBS	151	3	4	F	4	<mdl	4	1340	145	1040	31.8
BWBS	152	4	4	H	7	<mdl	7	1419	256	459	20.8
BWBS	153	4	4	M	7	5	2	1943	383	98	4.2
BWBS	154	4	3	F	7	4	4	1901	223	308	41.4
BWBS	155	4	4	H	5	2	3	2070	372	143	10.5
BWBS	156	4	3	M	4	<mdl	4	2135	361	72	9.0
BWBS	157	3	3	F	7	2	5	2034	189	725	128.7
BWBS	158	4	4	H	3	<mdl	3	2116	294	359	95.3
BWBS	159	4	4	M	<mdl	<mdl	<mdl	1581	275	355	69.7

PRS™-Probe Supply Rate (μg/10cm^2/burial period)											
Location	**Sample**	**#Cation**	**#Anion**	**Layer**	**Total N**	**NO_3^--N**	**NH_4^+-N**	**Ca**	**Mg**	**K**	**P**
Method Detection Limits (mdl):					***2***	***2***	***2***	***2***	***4***	***4***	***0.2***
BWBS	160	4	4	F	11	5	5	1258	167	623	52.1
BWBS	161	4	4	H	<mdl	<mdl	<mdl	1474	261	336	24.9
BWBS	162	4	4	M	2	<mdl	2	1810	344	143	27.1
BWBS	163	4	4	F	2	<mdl	2	1436	248	583	42.0
BWBS	164	4	4	H	<mdl	<mdl	<mdl	1525	284	772	27.6
BWBS	165	4	4	M	5	5	<mdl	2160	343	182	22.1
BWBS	166	4	4	F	<mdl	<mdl	<mdl	1572	116	676	33.6
BWBS	167			H							
BWBS	168	4	4	M	<mdl	<mdl	<mdl	1017	172	212	7.9
BWBS	169	4	4	F	7	<mdl	7	1312	155	758	22.1
BWBS	170			H							
BWBS	171	4	4	M	3	<mdl	3	1747	355	123	9.9
BWBS	172	4	4	F	<mdl	<mdl	<mdl	1348	110	585	25.6
BWBS	173			H							
BWBS	174	4	4	M	2	<mdl	2	1986	319	164	20.6
BWBS	175	4	4	F	5	5	<mdl	886	58	606	7.8
BWBS	176			H							
BWBS	177	4	4	M	3	3	<mdl	1741	211	105	9.3
BWBS	178	4	4	F	18	18	<mdl	1452	105	640	18.9
BWBS	179			H							
BWBS	180	4	4	M	4	2	2	1628	167	301	19.7
ICH	181	4	4	F	7	<mdl	7	1040	164	485	5.5
ICH	182			H							
ICH	183	4	4	M	6	<mdl	6	666	158	317	1.6
ICH	184	4	4	F	4	<mdl	4	1925	206	309	10.5
ICH	185			H							
ICH	186	4	4	M	4	<mdl	4	1589	220	742	5.5
ICH	187	4	3	F	4	<mdl	4	1453	160	484	16.3
ICH	188			H							
ICH	189	4	2	M	2	<mdl	2	1169	184	285	3.8
ICH	190	4	4	F	20	12	8	1481	182	411	5.9
ICH	191	4	4	H	27	22	6	1719	220	290	2.4
ICH	192	4	4	M	20	17	3	932	120	140	3.7

PRS™-Probe Supply Rate (μg/10cm^2/burial period)											
Location	**Sample**	**#Cation**	**#Anion**	**Layer**	**Total N**	**NO_3^--N**	**NH_4^+-N**	**Ca**	**Mg**	**K**	**P**
Method Detection Limits (mdl):					***2***	***2***	***2***	***2***	***4***	***4***	***0.2***
ICH	193	4	4	F	3	<mdl	3	1123	127	436	6.7
ICH	194	4	4	H	3	<mdl	3	2124	205	503	9.2
ICH	195	4	4	M	3	<mdl	3	1290	159	360	4.9
ICH	196	4	4	F	4	<mdl	4	1579	185	548	6.1
ICH	197	4	4	H	5	<mdl	5	1615	306	318	2.8
ICH	198	4	4	M	5	<mdl	5	591	106	596	1.9
ICH	199	4	4	F	4	<mdl	4	2166	213	223	5.4
ICH	200	4	4	H	5	<mdl	5	1197	184	256	2.7
ICH	201	4	4	M	3	<mdl	3	2408	168	117	2.0
ICH	202	3	4	F	4	<mdl	4	3024	138	321	3.9
ICH	203			H							
ICH	204	4	2	M	<mdl	<mdl	<mdl	1907	84	170	2.4
ICH	205	4	4	F	3	<mdl	3	1596	155	645	7.9
ICH	206	4	3	H	<mdl	<mdl	<mdl	1694	141	383	4.2
ICH	207	4	5	M	3	<mdl	3	1319	181	299	1.6
ICH	208	4	4	F	7	<mdl	7	1601	145	324	12.3
ICH	209	4	4	H	2	<mdl	2	1614	153	313	5.5
ICH	210	4	4	M	12	<mdl	12	1181	189	264	5.0
ICH	211	4	4	F	3	<mdl	3	1493	130	348	12.6
ICH	212			H							
ICH	213	4	4	M	2	<mdl	2	1530	272	235	2.8
ICH	214	4	4	F	3	<mdl	3	2548	215	253	10.8
ICH	205			H							
ICH	216	4	4	M	<mdl	<mdl	<mdl	2622	330	83	6.5
ICH	217	4	4	F	4	2	2	2358	243	268	9.2
ICH	218			H							
ICH	219	4	4	M	6	4	2	1874	303	228	6.9
ICH	220	4	4	F	3	<mdl	3	1266	75	184	6.6
ICH	221			H							
ICH	222	4	3	M	3	<mdl	3	2497	205	233	4.6
ICH	223	4	4	F	7	2	5	932	96	308	8.6
ICH	224			H							
ICH	225	4	4	M	3	<mdl	3	1724	323	244	10.4

PRS™-Probe Supply Rate (μg/10cm^2/burial period)											
Location	**Sample**	**#Cation**	**#Anion**	**Layer**	**Total N**	**NO_3^--N**	**NH_4^+-N**	**Ca**	**Mg**	**K**	**P**
Method Detection Limits (mdl):					***2***	***2***	***2***	***2***	***4***	***4***	***0.2***
MH	226	4	4	F	9	<mdl	9	1360	192	52	1.2
MH	227	4	4	H	15	4	11	1147	142	339	3.7
MH	228	4	3	M	16	<mdl	16	1414	257	357	1.5
MH	229	4	4	F	8	<mdl	8	1403	152	346	4.6
MH	230	4	4	H	6	<mdl	6	311	50	531	5.4
MH	231	4	4	M	10	<mdl	10	549	112	534	2.1
MH	232	4	4	F	8	2	5	833	124	554	3.3
MH	233	4	4	H	16	9	7	458	128	310	2.5
MH	234	4	4	M	7	<mdl	7	1264	141	156	1.3
MH	235	4	4	F	16	10	6	1738	281	185	5.2
MH	236	4	4	H	11	<mdl	11	761	141	179	1.4
MH	237	4	4	M	10	2	8	1773	230	77	1.9
MH	238	4	4	F	14	<mdl	14	892	203	402	3.7
MH	239	4	4	H	8	<mdl	8	813	146	333	4.9
MH	240	4	4	M	10	2	8	1249	169	134	0.8
MH	241	4	4	F	10	3	7	749	236	364	17.8
MH	242	4	4	H	6	<mdl	6	1023	193	464	4.2
MH	243	4	4	M	13	<mdl	13	925	268	334	3.4
MH	244	4	4	F	10	3	6	1198	188	195	2.6
MH	245	4	4	H	14	8	6	892	186	154	1.7
MH	246			M							
MH	247	4	4	F	12	7	4	1773	175	100	2.8
MH	248	4	4	H	7	2	5	1598	138	174	2.2
MH	249			M							
MH	250	4	4	F	7	3	4	1109	272	182	8.0
MH	251	4	4	H	10	4	7	455	362	194	1.8
MH	252			M							
MH	253	4	4	F	8	3	5	1305	195	253	2.2
MH	254	4	4	H	5	<mdl	5	1348	194	169	1.2
MH	255			M							
MH	256	4	4	F	8	3	5	667	132	348	1.7
MH	257	4	4	H	12	6	7	978	387	395	12.9
MH	258	4	4	M	17	10	7	479	201	276	1.7

PRS™-Probe Supply Rate (μg/10cm^2/burial period)											
Location	**Sample**	**#Cation**	**#Anion**	**Layer**	**Total N**	**NO_3^--N**	**NH_4^+-N**	**Ca**	**Mg**	**K**	**P**
Method Detection Limits (mdl):					***2***	***2***	***2***	***2***	***4***	***4***	***0.2***
MH	259	3	4	F	17	4	14	553	147	334	3.1
MH	260	5	4	H	6	<mdl	6	660	185	404	10.5
MH	261	4	4	M	9	<mdl	9	468	118	223	15.3
MH	262	4	4	F	9	5	4	1574	165	136	3.7
MH	263	3	4	H	7	2	5	1985	179	279	3.4
MH	264	3	4	M	10	4	5	2347	223	217	1.5
MH	265	4	4	F	7	3	4	1744	137	102	1.6
MH	266	3	4	H	11	6	5	2178	195	66	1.4
MH	267	1	0	M	N/A	N/A	3	1705	239	75	N/A
MH	268	4	5	F	7	4	3	1020	155	144	1.6
MH	269	4	4	H	5	<mdl	5	1326	191	224	13.5
MH	270	4	4	M	8	3	6	1074	143	261	9.5
CWH	271	4	4	F	203	161	42	1186	160	384	4.3
CWH	272	3	4	H	156	120	36	382	55	383	5.2
CWH	273	4	4	M	187	126	61	937	103	308	5.1
CWH	274	4	4	F	255	249	6	702	79	136	2.3
CWH	275	4	4	H	347	341	6	1678	175	64	1.5
CWH	276	3	4	M	320	306	14	1133	159	183	5.8
CWH	277	4	4	F	230	170	60	1378	157	256	9.0
CWH	278	4	4	H	147	138	9	833	92	134	3.8
CWH	279	4	4	M	190	173	17	871	116	313	4.5
CWH	280	4	4	F	170	100	69	1035	163	332	15.1
CWH	281	4	4	H	215	182	34	852	133	152	17.6
CWH	282	4	4	M	212	169	43	604	86	291	6.6
CWH	283	4	4	F	204	183	21	1598	214	277	18.1
CWH	284	4	4	H	51	41	10	1601	215	350	7.4
CWH	285	4	4	M	184	125	59	1215	132	62	1.9
CWH	286	4	4	F	175	125	50	796	138	425	4.4
CWH	287	4	4	H	43	17	25	548	83	129	3.0
CWH	288	4	4	M	27	20	7	531	92	41	1.8
CWH	289	4	4	F	43	22	21	420	73	207	2.2
CWH	290	4	4	H	32	24	8	1587	157	61	1.2
CWH	291	3	4	M	18	9	9	349	55	101	1.1

PRS™-Probe Supply Rate (μg/10cm^2/burial period)											
Location	**Sample**	**#Cation**	**#Anion**	**Layer**	**Total N**	**NO_3^--N**	**NH_4^+-N**	**Ca**	**Mg**	**K**	**P**
Method Detection Limits (mdl):					***2***	***2***	***2***	***2***	***4***	***4***	***0.2***
CWH	292	4	4	F	43	23	20	959	208	166	5.7
CWH	293	4	4	H	18	11	6	592	225	201	1.0
CWH	294	4	4	M	24	17	7	290	58	122	0.9
CWH	295	4	4	F	28	10	18	327	81	249	2.3
CWH	296	4	4	H	19	8	11	641	152	153	1.5
CWH	297	4	4	M	10	5	5	244	31	106	0.6
CWH	298	4	4	F	24	15	9	247	75	347	2.5
CWH	299	4	4	H	15	9	6	357	103	276	1.1
CWH	300	4	4	M	10	7	3	242	52	221	1.4
CWH	301	4	4	F	332	326	6	2360	285	80	6.2
CWH	302	4	4	H	444	439	5	2586	262	53	1.4
CWH	303	4	4	M	214	211	3	1752	217	120	1.4
CWH	304	4	4	F	264	244	20	1422	179	218	11.9
CWH	305	4	4	H	248	246	3	1914	204	132	3.2
CWH	306	4	4	M	308	303	5	1817	203	148	2.3
CWH	307	4	4	F	207	201	6	1836	212	170	3.6
CWH	308	4	4	H	240	235	5	2198	210	116	1.9
CWH	309	4	4	M	321	317	4	1913	221	124	1.0
CWH	310	4	4	F	274	261	13	1955	270	143	3.5
CWH	311	4	4	H	460	456	4	2032	287	47	0.9
CWH	312	4	4	M	380	370	9	1810	286	62	1.3
CWH	313	4	4	F	261	244	17	2028	219	109	7.8
CWH	314	4	4	H	229	224	5	1980	195	112	1.3
CWH	315	4	4	M	301	297	3	1970	219	61	1.2

PRS™-Probe Supply Rate (mg/10cm^2/burial period)											
Location	**Sample**	**#Cation**	**#Anion**	**Layer**	**Fe**	**Mn**	**Cu**	**Zn**	**B**	**S**	**Pb**
Method Detection Limits (mdl):					***0.4***	***0.2***	***0.2***	***0.2***	***0.2***	***2***	***0.2***
IDF	1	4	4	F	2.8	7.1	0.4	1.2	0.9	17	<mdl
IDF	2	4	4	H	3.0	2.9	0.3	0.8	0.9	15	<mdl
IDF	3	4	4	M	2.8	1.7	0.3	0.9	1.1	18	<mdl
IDF	4	4	4	F	1.8	9.0	<mdl	0.8	0.7	17	<mdl
IDF	5	4	4	H	4.0	5.4	<mdl	1.0	0.8	16	<mdl
IDF	6	4	4	M	1.6	7.7	<mdl	1.0	0.8	13	<mdl
IDF	7	4	4	F	2.3	5.0	0.3	1.2	1.0	17	<mdl
IDF	8	4	4	H	1.6	2.4	<mdl	0.8	1.0	15	<mdl
IDF	9	4	4	M	3.0	1.0	<mdl	0.6	0.9	13	<mdl
IDF	10	4	4	F	1.3	6.8	<mdl	1.2	0.8	16	<mdl
IDF	11	4	4	H	1.4	2.6	<mdl	1.0	0.7	23	<mdl
IDF	12	4	4	M	3.0	3.1	<mdl	1.1	1.0	19	<mdl
IDF	13	4	4	F	4.7	2.8	<mdl	1.7	0.9	19	<mdl
IDF	14	4	4	H	4.7	1.9	<mdl	1.5	1.4	15	<mdl
IDF	15	4	4	M	5.9	1.5	<mdl	1.4	0.7	18	<mdl
IDF	16	3	4	F	3.1	5.3	0.3	0.9	1.1	15	0.7
IDF	17	4	4	H	2.3	4.3	0.2	1.0	1.8	12	0.3
IDF	18	4	4	M	3.1	2.1	<mdl	0.8	2.7	14	1.8
IDF	19	4	4	F	2.4	4.1	<mdl	0.6	0.8	13	0.4
IDF	20	3	4	H	1.8	1.7	<mdl	0.4	1.0	13	1.2
IDF	21	4	4	M	1.0	3.4	<mdl	0.5	0.7	13	0.7
IDF	22	4	4	F	1.1	6.7	<mdl	0.6	0.4	11	0.3
IDF	23	4	4	H	3.1	4.8	<mdl	0.5	0.8	10	0.6
IDF	24										
IDF	25	4	4	F	1.9	4.8	<mdl	0.5	0.6	11	0.9
IDF	26	4	4	H	1.0	1.1	<mdl	0.3	1.1	11	0.8
IDF	27										
IDF	28	4	4	F	1.7	4.0	<mdl	0.6	0.6	11	0.6
IDF	29	4	4	H	0.8	3.5	<mdl	0.4	1.1	10	0.7
IDF	30										

					PRS™-Probe Supply Rate (mg/10cm^2/burial period)						
Location	**Sample**	**#Cation**	**#Anion**	**Layer**	**Fe**	**Mn**	**Cu**	**Zn**	**B**	**S**	**Pb**
Method Detection Limits (mdl):					***0.4***	***0.2***	***0.2***	***0.2***	***0.2***	***2***	***0.2***
IDF	31	2	2	F	0.7	2.6	<mdl	0.5	0.5	10	0.3
IDF	32	4	3	H	5.3	2.3	<mdl	0.5	1.9	11	0.6
IDF	33										
IDF	34	4	4	F	1.1	6.1	<mdl	0.9	0.7	11	0.3
IDF	35										
IDF	36										
IDF	37	4	4	F	3.1	4.2	<mdl	0.8	0.9	10	0.4
IDF	38	4	4	H	3.5	2.9	<mdl	0.7	0.5	12	2.9
IDF	39										
IDF	40	3	2	F	4.7	17.2	<mdl	0.9	0.7	12	0.3
IDF	41	4	4	H	1.3	5.9	<mdl	0.8	1.1	10	0.5
IDF	42										
IDF	43	4	4	F	9.1	18.2	<mdl	0.6	0.7	13	0.6
IDF	44	4	4	H	2.7	2.7	<mdl	0.5	1.3	7	1.1
IDF	45										
ESSF	46	4	4	F	2.9	49.5	<mdl	3.4	0.2	10	<mdl
ESSF	47										
ESSF	48	4	4	M	9.8	11.0	0.4	1.6	0.9	15	9.9
ESSF	49	4	4	F	3.1	19.3	<mdl	1.2	0.3	10	<mdl
ESSF	50										
ESSF	51	4	4	M	13.2	2.7	<mdl	1.1	1.1	15	2.7
ESSF	52	3	3	F	1.6	41.3	<mdl	2.5	0.3	12	<mdl
ESSF	53										
ESSF	54	4	4	M	4.2	60.1	<mdl	4.2	0.3	26	1.5
ESSF	55	4	4	F	2.8	14.6	<mdl	1.4	0.3	10	<mdl
ESSF	56										
ESSF	57	4	4	M	10.7	7.1	<mdl	1.4	0.7	14	3.2
ESSF	58	4	4	F	2.2	33.6	<mdl	1.4	0.3	10	<mdl
ESSF	59										
ESSF	60	4	4	M	3.3	14.2	<mdl	1.7	<mdl	16	<mdl
ESSF	61	4	4	F	2.8	34.2	<mdl	1.8	0.2	13	<mdl
ESSF	62	4	4	H	2.6	13.7	<mdl	1.4	<mdl	24	<mdl
ESSF	63	4	4	M	3.6	9.7	<mdl	1.3	<mdl	14	0.3

					PRS™-Probe Supply Rate (mg/10cm^2/burial period)						
Location	**Sample**	**#Cation**	**#Anion**	**Layer**	**Fe**	**Mn**	**Cu**	**Zn**	**B**	**S**	**Pb**
Method Detection Limits (mdl):					***0.4***	***0.2***	***0.2***	***0.2***	***0.2***	***2***	***0.2***
ESSF	64	4	4	F	1.0	28.1	<mdl	1.6	0.6	8	<mdl
ESSF	65	4	4	H	2.0	38.2	<mdl	2.5	1.4	15	1.0
ESSF	66	4	4	M	2.7	25.2	<mdl	2.9	0.8	14	1.3
ESSF	67	4	4	F	1.1	36.6	<mdl	2.8	0.7	9	0.4
ESSF	68	4	4	H	2.4	24.7	<mdl	5.1	0.5	12	1.2
ESSF	69	4	4	M	3.0	11.1	<mdl	2.3	0.8	17	0.7
ESSF	70	4	4	F	2.2	26.5	<mdl	1.3	0.4	12	<mdl
ESSF	71	4	4	H	2.1	19.6	<mdl	1.4	0.4	10	0.3
ESSF	72	4	4	M	4.4	11.0	<mdl	1.7	0.4	11	<mdl
ESSF	73	4	4	F	1.6	40.1	<mdl	1.9	0.4	10	0.4
ESSF	74	4	4	H	1.8	27.0	<mdl	2.1	0.4	9	0.4
ESSF	75	4	4	M	1.7	12.3	<mdl	1.5	0.4	9	0.3
ESSF	76	4	4	F	3.5	10.1	<mdl	0.9	0.5	7	<mdl
ESSF	77	4	4	H	4.5	9.0	<mdl	1.0	1.2	13	1.6
ESSF	78	4	4	M	5.3	9.4	<mdl	1.2	1.2	11	<mdl
ESSF	79	4	4	F	1.4	5.0	<mdl	0.9	1.1	9	<mdl
ESSF	80	4	4	H	3.3	5.0	<mdl	0.9	1.6	12	0.2
ESSF	81	4	4	M	4.5	3.3	<mdl	1.2	1.7	17	<mdl
ESSF	82	4	4	F	2.6	8.4	<mdl	1.4	1.0	9	<mdl
ESSF	83	4	4	H	2.6	6.7	<mdl	1.5	1.0	17	0.3
ESSF	84	4	5	M	7.3	5.0	<mdl	1.2	0.9	36	<mdl
ESSF	85	4	4	F	2.8	39.4	<mdl	0.9	0.9	15	<mdl
ESSF	86	4	4	H	3.2	7.2	0.2	0.8	1.1	33	0.3
ESSF	87	4	4	M	5.7	8.9	0.3	0.9	1.7	31	0.3
ESSF	88	4	4	F	3.2	15.6	<mdl	0.8	1.4	10	<mdl
ESSF	89			H							
ESSF	90	4	4	M	11.0	12.6	<mdl	1.0	1.7	15	0.7
PP	91	4	4	F	5.6	3.3	0.4	0.8	2.0	14	<mdl
PP				H							
PP	93	4	4	M	6.1	3.7	0.3	0.8	1.2	13	<mdl
PP	94	4	4	F	7.3	5.7	0.5	1.0	0.9	20	<mdl
PP	95			H							
PP	96	4	4	M	5.5	5.1	0.3	0.6	1.2	13	<mdl

					PRS™-Probe Supply Rate (mg/10cm^2/burial period)						
Location	**Sample**	**#Cation**	**#Anion**	**Layer**	**Fe**	**Mn**	**Cu**	**Zn**	**B**	**S**	**Pb**
Method Detection Limits (mdl):					***0.4***	***0.2***	***0.2***	***0.2***	***0.2***	***2***	***0.2***
PP	97	4	4	F	2.6	11.0	0.4	1.2	1.2	24	<mdl
PP	98			H							
PP	99	4	4	M	3.1	6.3	0.3	0.8	0.6	13	<mdl
PP	100	4	4	F	4.0	4.2	0.5	1.1	0.6	19	<mdl
PP	101			H							
PP	102			M							
PP	103	4	4	F	6.8	6.9	0.3	1.1	1.0	14	<mdl
PP	104			H							
PP	105			M							
PP	106	4	4	F	6.3	9.7	0.6	1.8	0.9	16	0.2
PP	107			H							
PP	108			M							
PP	109	4	4	F	12.3	19.2	0.9	3.0	0.6	20	0.8
PP	110			H							
PP	111			M							
PP	112	4	4	F	8.3	13.2	0.4	1.5	1.1	22	0.4
PP	113			H							
PP	114			M							
PP	115	3	4	F	4.6	7.0	0.7	1.4	0.9	19	0.7
PP	116			H							
PP	117			M							
PP	118	4	4	F	5.4	30.3	0.5	3.6	0.9	19	0.5
PP	119			H							
PP	120			M							
PP	121	4	4	F	7.7	17.2	0.9	2.8	1.2	21	0.5
PP	122			H							
PP	123			M							
PP	124	4	4	F	6.1	11.8	0.8	1.8	1.2	29	0.5
PP	125			H							
PP	126			M							
PP	127	4	4	F	4.3	0.5	0.9	0.4	1.2	12	0.7
PP	128			H							
PP	129			M							

					PRS™-Probe Supply Rate (mg/10cm^2/burial period)						
Location	**Sample**	**#Cation**	**#Anion**	**Layer**	**Fe**	**Mn**	**Cu**	**Zn**	**B**	**S**	**Pb**
Method Detection Limits (mdl):					***0.4***	***0.2***	***0.2***	***0.2***	***0.2***	***2***	***0.2***
PP	130	4	4	F	4.3	5.1	0.6	0.8	1.5	11	0.5
PP	131			H							
PP	132			M							
PP	133	4	4	F	3.9	9.0	1.0	2.0	1.7	20	0.9
PP	134			H							
PP	135			M							
BWBS	136	4	3	F	5.2	3.5	0.3	1.5	1.4	109	0.3
BWBS	137	4	4	H	12.3	2.2	<mdl	0.6	0.9	1151	<mdl
BWBS	138	4	4	M	8.8	0.5	<mdl	0.5	1.1	1478	<mdl
BWBS	139	4	4	F	3.8	7.3	<mdl	1.3	1.0	244	<mdl
BWBS	140	4	4	H	7.7	5.2	<mdl	0.8	0.8	216	<mdl
BWBS	141	4	4	M	20.1	2.5	<mdl	0.5	1.2	669	<mdl
BWBS	142	4	4	F	1.5	1.0	<mdl	0.8	2.2	54	<mdl
BWBS	143	4	4	H	8.4	0.7	<mdl	0.5	2.3	175	<mdl
BWBS	144	4	4	M	9.5	<mdl	<mdl	0.3	1.6	1114	<mdl
BWBS	145	5	4	F	2.0	2.6	<mdl	1.3	2.2	29	<mdl
BWBS	146	4	4	H	4.4	3.1	<mdl	0.7	1.7	43	<mdl
BWBS	147	4	4	M	9.4	5.1	<mdl	0.5	1.2	157	<mdl
BWBS	148	4	4	F	5.1	0.5	<mdl	1.1	1.6	232	<mdl
BWBS	149	4	4	H	9.1	1.1	<mdl	0.4	1.4	1237	<mdl
BWBS	150	4	4	M	3.6	0.5	<mdl	0.3	2.5	1659	<mdl
BWBS	151	3	4	F	1.8	3.8	<mdl	1.7	0.4	60	0.3
BWBS	152	4	4	H	2.4	7.9	<mdl	1.3	1.4	53	<mdl
BWBS	153	4	4	M	7.2	4.6	<mdl	1.1	1.6	63	<mdl
BWBS	154	4	3	F	4.0	4.1	<mdl	3.2	1.1	11	<mdl
BWBS	155	4	4	H	4.6	2.1	<mdl	1.5	2.3	15	<mdl
BWBS	156	4	3	M	4.5	1.3	<mdl	1.5	2.6	30	<mdl
BWBS	157	3	3	F	9.8	6.0	<mdl	4.4	2.3	105	<mdl
BWBS	158	4	4	H	14.0	14.4	<mdl	5.5	1.4	94	<mdl
BWBS	159	4	4	M	11.8	17.5	<mdl	4.9	1.3	43	<mdl
BWBS	160	4	4	F	2.7	9.0	<mdl	2.1	0.5	19	<mdl
BWBS	161	4	4	H	3.2	27.0	<mdl	3.2	0.8	72	<mdl
BWBS	162	4	4	M	5.2	14.5	<mdl	2.6	1.5	57	0.3

					PRS™-Probe Supply Rate (mg/10cm^2/burial period)						
Location	**Sample**	**#Cation**	**#Anion**	**Layer**	**Fe**	**Mn**	**Cu**	**Zn**	**B**	**S**	**Pb**
Method Detection Limits (mdl):					***0.4***	***0.2***	***0.2***	***0.2***	***0.2***	***2***	***0.2***
BWBS	163	4	4	F	3.0	3.6	<mdl	1.3	1.7	55	<mdl
BWBS	164	4	4	H	3.1	2.6	<mdl	1.2	1.5	39	0.4
BWBS	165	4	4	M	14.6	6.4	<mdl	1.3	1.6	203	0.3
BWBS	166	4	4	F	2.6	11.3	<mdl	1.4	1.3	30	<mdl
BWBS	167			H							
BWBS	168	4	4	M	6.1	28.3	<mdl	0.9	1.9	34	0.3
BWBS	169	4	4	F	3.5	6.9	<mdl	1.0	0.8	26	<mdl
BWBS	170			H							
BWBS	171	4	4	M	6.4	68.5	<mdl	1.0	1.2	35	<mdl
BWBS	172	4	4	F	1.4	5.0	<mdl	0.9	1.8	25	<mdl
BWBS	173			H							
BWBS	174	4	4	M	15.0	73.7	<mdl	0.7	2.5	244	0.4
BWBS	175	4	4	F	2.7	2.8	<mdl	0.5	2.2	18	<mdl
BWBS	176			H							
BWBS	177	4	4	M	5.7	34.8	<mdl	0.4	2.1	28	0.3
BWBS	178	4	4	F	3.7	2.5	<mdl	1.0	1.0	25	<mdl
BWBS	179			H							
BWBS	180	4	4	M	7.4	22.8	<mdl	0.6	0.7	32	0.2
ICH	181	4	4	F	3.3	11.7	<mdl	0.7	1.0	14	<mdl
ICH	182			H							
ICH	183	4	4	M	15.7	15.0	<mdl	0.4	2.0	15	0.6
ICH	184	4	4	F	4.1	1.9	<mdl	0.4	1.4	13	<mdl
ICH	185			H							
ICH	186	4	4	M	3.1	1.5	<mdl	0.3	2.1	13	0.3
ICH	187	4	3	F	3.9	2.9	<mdl	0.6	1.8	19	<mdl
ICH	188			H							
ICH	189	4	2	M	11.1	6.9	<mdl	0.4	2.8	20	0.6
ICH	190	4	4	F	1.9	1.5	<mdl	0.4	1.9	12	<mdl
ICH	191	4	4	H	3.4	0.7	<mdl	0.4	2.1	17	<mdl
ICH	192	4	4	M	1.5	<mdl	<mdl	0.3	2.7	16	0.6
ICH	193	4	4	F	3.9	2.4	<mdl	0.5	1.9	12	<mdl
ICH	194	4	4	H	0.9	1.5	<mdl	0.3	1.8	12	<mdl
ICH	195	4	4	M	<mdl	1.2	<mdl	0.4	3.6	14	0.3

Location	Sample	#Cation	#Anion	Layer	PRS™-Probe Supply Rate (mg/10cm^2/burial period) Fe	Mn	Cu	Zn	B	S	Pb
Method Detection Limits (mdl):					***0.4***	***0.2***	***0.2***	***0.2***	***0.2***	***2***	***0.2***
ICH	196	4	4	F	1.0	3.3	<mdl	0.5	1.7	12	<mdl
ICH	197	4	4	H	1.0	10.9	<mdl	0.5	1.5	12	<mdl
ICH	198	4	4	M	3.3	3.2	<mdl	0.4	1.2	17	0.8
ICH	199	4	4	F	3.6	2.3	<mdl	0.5	1.8	15	<mdl
ICH	200	4	4	H	3.0	5.3	<mdl	0.5	1.5	15	<mdl
ICH	201	4	4	M	5.0	1.9	<mdl	0.3	1.5	14	<mdl
ICH	202	3	4	F	2.3	1.7	<mdl	0.3	1.0	12	<mdl
ICH	203			H							
ICH	204	4	2	M	4.8	1.2	<mdl	0.6	3.4	12	0.3
ICH	205	4	4	F	2.4	3.5	<mdl	0.5	1.4	15	<mdl
ICH	206	4	3	H	3.9	2.6	<mdl	0.4	1.2	15	<mdl
ICH	207	4	5	M	4.5	1.5	<mdl	0.3	1.6	14	<mdl
ICH	208	4	4	F	2.1	2.4	<mdl	0.3	2.2	15	<mdl
ICH	209	4	4	H	2.1	2.1	<mdl	0.3	1.9	15	<mdl
ICH	210	4	4	M	3.9	3.5	<mdl	0.3	0.9	20	0.4
ICH	211	4	4	F	2.5	3.4	<mdl	0.6	0.8	18	<mdl
ICH	212			H							
ICH	213	4	4	M	4.0	5.0	<mdl	0.4	1.4	17	0.4
ICH	214	4	4	F	3.6	3.0	<mdl	0.7	1.5	12	<mdl
ICH	205			H							
ICH	216	4	4	M	4.6	1.8	<mdl	0.5	2.2	25	0.6
ICH	217	4	4	F	4.4	12.2	<mdl	0.3	1.2	17	<mdl
ICH	218			H							
ICH	219	4	4	M	6.6	10.5	<mdl	0.4	1.8	19	0.4
ICH	220	4	4	F	5.2	2.4	<mdl	0.4	1.6	15	<mdl
ICH	221			H							
ICH	222	4	3	M	7.2	5.2	<mdl	0.5	1.8	12	0.9
ICH	223	4	4	F	5.1	1.9	<mdl	0.4	0.7	12	<mdl
ICH	224			H							
ICH	225	4	4	M	6.1	7.9	<mdl	0.5	1.4	20	<mdl
MH	226	4	4	F	4.0	7.6	0.2	10.2	0.6	20	1.3
MH	227	4	4	H	4.3	54.3	0.3	12.2	1.0	19	4.2
MH	228	4	3	M	3.6	29.5	0.4	12.5	0.5	59	11.6

PRS™-Probe Supply Rate (mg/10cm^2/burial period)											
Location	**Sample**	**#Cation**	**#Anion**	**Layer**	**Fe**	**Mn**	**Cu**	**Zn**	**B**	**S**	**Pb**
Method Detection Limits (mdl):					***0.4***	***0.2***	***0.2***	***0.2***	***0.2***	***2***	***0.2***
MH	229	4	4	F	3.0	69.5	0.3	5.3	0.6	20	8.4
MH	230	4	4	H	2.4	12.7	<mdl	2.1	0.7	51	4.0
MH	231	4	4	M	2.8	24.9	<mdl	3.5	0.8	23	5.5
MH	232	4	4	F	2.7	103.2	<mdl	2.8	1.0	17	1.4
MH	233	4	4	H	2.9	18.2	0.2	5.1	0.8	17	3.5
MH	234	4	4	M	2.4	11.0	<mdl	5.1	1.4	16	3.8
MH	235	4	4	F	1.6	92.0	0.3	7.4	0.4	24	4.9
MH	236	4	4	H	5.8	11.0	<mdl	4.7	0.4	18	2.1
MH	237	4	4	M	3.4	5.1	<mdl	9.3	0.6	21	0.9
MH	238	4	4	F	4.1	44.8	0.4	4.2	0.6	29	6.1
MH	239	4	4	H	5.2	17.2	<mdl	6.3	0.6	27	1.8
MH	240	4	4	M	6.2	7.0	<mdl	5.2	1.0	17	6.8
MH	241	4	4	F	4.7	39.6	0.6	6.2	0.7	64	3.4
MH	242	4	4	H	1.7	39.3	0.4	6.0	1.1	24	4.8
MH	243	4	4	M	1.6	59.3	0.3	9.6	1.8	21	2.3
MH	244	4	4	F	2.7	33.9	<mdl	5.4	0.9	46	2.3
MH	245	4	4	H	1.2	7.9	0.2	9.3	1.3	42	4.3
MH	246			M							
MH	247	4	4	F	2.5	33.8	<mdl	4.4	0.5	24	2.0
MH	248	4	4	H	3.1	12.3	<mdl	4.3	0.7	35	2.9
MH	249			M							
MH	250	4	4	F	3.2	33.5	0.5	6.9	1.6	31	10.6
MH	251	4	4	H	7.5	10.8	0.3	8.3	1.3	27	5.0
MH	252			M							
MH	253	4	4	F	1.6	58.4	0.3	5.2	2.0	13	5.9
MH	254	4	4	H	2.2	41.5	<mdl	8.0	1.4	17	4.9
MH	255			M							
MH	256	4	4	F	2.1	21.3	0.4	4.3	0.7	18	5.4
MH	257	4	4	H	2.7	23.6	0.4	16.3	0.9	40	5.9
MH	258	4	4	M	2.3	12.2	0.3	6.4	0.9	28	3.0
MH	259	3	4	F	1.6	16.7	0.2	2.2	0.6	20	1.0
MH	260	5	4	H	4.5	26.7	0.5	6.6	1.4	30	4.6
MH	261	4	4	M	2.0	13.1	0.3	3.5	1.8	36	4.6

					PRS™-Probe Supply Rate (mg/10cm^2/burial period)						
Location	**Sample**	**#Cation**	**#Anion**	**Layer**	**Fe**	**Mn**	**Cu**	**Zn**	**B**	**S**	**Pb**
Method Detection Limits (mdl):					***0.4***	***0.2***	***0.2***	***0.2***	***0.2***	***2***	***0.2***
MH	262	4	4	F	0.5	8.7	0.4	2.7	1.6	19	11.5
MH	263	3	4	H	<mdl	9.5	0.3	3.6	0.9	34	7.9
MH	264	3	4	M	<mdl	10.8	0.4	3.8	1.2	32	19.4
MH	265	4	4	F	<mdl	4.6	0.4	5.6	0.8	24	4.3
MH	266	3	4	H	2.7	4.7	0.2	5.4	0.6	50	3.4
MH	267	1	0	M	N/A	N/A	N/A	N/A	N/A	N/A	N/A
MH	268	4	5	F	0.8	15.4	<mdl	3.3	0.3	13	1.3
MH	269	4	4	H	0.8	27.0	0.2	5.8	0.2	26	2.5
MH	270	4	4	M	1.3	10.6	<mdl	4.9	0.7	24	2.1
CWH	271	4	4	F	4.7	23.5	0.3	4.0	0.4	28	0.6
CWH	272	3	4	H	4.6	2.6	0.2	1.4	0.7	28	0.3
CWH	273	4	4	M	3.0	11.5	0.2	3.9	0.6	26	0.7
CWH	274	4	4	F	25.5	10.8	0.3	2.3	0.7	45	3.3
CWH	275	4	4	H	18.5	23.2	0.3	3.9	0.8	35	3.8
CWH	276	3	4	M	14.5	20.4	0.2	3.5	0.4	35	3.6
CWH	277	4	4	F	8.3	23.0	0.3	4.2	0.7	31	1.1
CWH	278	4	4	H	5.6	6.7	<mdl	2.5	0.8	29	0.9
CWH	279	4	4	M	5.2	16.1	<mdl	3.2	0.8	25	0.5
CWH	280	4	4	F	4.3	23.5	<mdl	4.0	1.2	27	1.3
CWH	281	4	4	H	9.9	19.1	0.2	3.6	2.1	37	2.3
CWH	282	4	4	M	6.1	10.0	<mdl	1.9	2.3	30	0.6
CWH	283	4	4	F	8.1	32.4	0.3	3.6	1.1	32	2.3
CWH	284	4	4	H	7.4	17.7	0.2	3.2	1.0	23	1.3
CWH	285	4	4	M	6.3	18.4	<mdl	3.6	1.6	23	1.7
CWH	286	4	4	F	0.5	29.3	<mdl	2.3	0.7	23	0.3
CWH	287	4	4	H	1.5	5.2	<mdl	1.8	0.8	35	0.7
CWH	288	4	4	M	2.8	1.8	<mdl	3.3	0.8	21	1.6
CWH	289	4	4	F	2.3	8.8	<mdl	1.2	0.8	20	0.3
CWH	290	4	4	H	1.2	22.4	0.3	4.1	0.4	30	2.4
CWH	291	3	4	M	2.4	2.7	<mdl	1.5	0.4	16	0.5
CWH	292	4	4	F	2.6	25.9	0.2	5.0	0.8	34	3.1
CWH	293	4	4	H	2.8	10.0	0.2	11.1	1.1	34	3.0
CWH	294	4	4	M	3.3	5.3	<mdl	2.3	0.9	27	0.9

PRS™-Probe Supply Rate (mg/10cm^2/burial period)											
Location	**Sample**	**#Cation**	**#Anion**	**Layer**	**Fe**	**Mn**	**Cu**	**Zn**	**B**	**S**	**Pb**
Method Detection Limits (mdl):					***0.4***	***0.2***	***0.2***	***0.2***	***0.2***	***2***	***0.2***
CWH	295	4	4	F	1.2	12.0	<mdl	1.6	0.8	11	0.2
CWH	296	4	4	H	1.9	18.4	<mdl	4.7	1.3	17	1.3
CWH	297	4	4	M	2.1	3.2	<mdl	1.6	1.2	14	0.8
CWH	298	4	4	F	2.2	12.7	<mdl	1.4	0.8	15	<mdl
CWH	299	4	4	H	4.3	8.4	<mdl	2.8	1.3	24	1.0
CWH	300	4	4	M	2.3	5.2	<mdl	1.5	0.8	16	0.8
CWH	301	4	4	F	32.3	8.8	0.9	5.6	1.0	31	5.6
CWH	302	4	4	H	21.4	5.9	0.9	3.9	1.4	41	5.7
CWH	303	4	4	M	4.6	1.2	<mdl	1.3	1.9	31	0.4
CWH	304	4	4	F	12.9	6.0	0.3	2.7	2.0	31	1.8
CWH	305	4	4	H	7.4	2.9	0.2	2.4	2.0	23	1.4
CWH	306	4	4	M	6.5	2.3	0.2	2.2	2.3	21	1.7
CWH	307	4	4	F	9.5	2.7	0.2	2.0	3.0	22	0.4
CWH	308	4	4	H	4.4	0.7	0.3	2.4	1.7	31	1.3
CWH	309	4	4	M	9.8	2.5	0.4	3.5	2.3	25	1.9
CWH	310	4	4	F	9.0	5.4	0.2	2.5	1.5	24	1.3
CWH	311	4	4	H	15.9	9.7	0.4	3.1	2.8	27	2.7
CWH	312	4	4	M	10.2	7.7	0.4	2.4	3.2	27	2.7
CWH	313	4	4	F	4.1	2.9	<mdl	2.2	2.4	26	0.4
CWH	314	4	4	H	8.4	3.8	0.3	2.8	3.3	19	1.4
CWH	315	4	4	M	10.8	4.8	0.3	2.8	2.7	28	2.1

PRS™-Probe Supply Rate (mg/10cm^2/burial period)					
Location	**Sample #**	**#Cation**	**#Anion**	**Layer**	**Al**
Method Detection Limits (mdl):					***0.4***
IDF	1	4	4	F	9.2
IDF	2	4	4	H	10.4
IDF	3	4	4	M	10.2
IDF	4	4	4	F	8.1
IDF	5	4	4	H	7.3
IDF	6	4	4	M	7.7
IDF	7	4	4	F	9.2
IDF	8	4	4	H	9.9
IDF	9	4	4	M	8.8
IDF	10	4	4	F	7.7
IDF	11	4	4	H	8.6
IDF	12	4	4	M	9.1
IDF	13	4	4	F	9.8
IDF	14	4	4	H	12.9
IDF	15	4	4	M	9.7
IDF	16	3	4	F	20.9
IDF	17	4	4	H	23.6
IDF	18	4	4	M	29.8
IDF	19	4	4	F	21.5
IDF	20	3	4	H	17.5
IDF	21	4	4	M	18.5
IDF	22	4	4	F	16.1
IDF	23	4	4	H	19.8
IDF	24				
IDF	25	4	4	F	16.2
IDF	26	4	4	H	19.9
IDF	27				
IDF	28	4	4	F	23.0
IDF	29	4	4	H	21.5
IDF	30				
IDF	31	2	2	F	15.0
IDF	32	4	3	H	35.5
IDF	33				
IDF	34	4	4	F	25.2
IDF	35				
IDF	36				
IDF	37	4	4	F	22.4
IDF	38	4	4	H	21.1
IDF	39				
IDF	40	3	2	F	26.0
IDF	41	4	4	H	24.3
IDF	42				
IDF	43	4	4	F	32.1
IDF	44	4	4	H	25.7
IDF	45				
ESSF	46	4	4	F	40.7
ESSF	47				

PRS™-Probe Supply Rate (mg/10cm^2/burial period)					
Location	**Sample #**	**#Cation**	**#Anion**	**Layer**	**Al**
Method Detection Limits (mdl):					***0.4***
ESSF	48	4	4	M	55.9
ESSF	49	4	4	F	42.2
ESSF	50				
ESSF	51	4	4	M	43.7
ESSF	52	3	3	F	37.8
ESSF	53				
ESSF	54	4	4	M	49.1
ESSF	55	4	4	F	38.6
ESSF	56				
ESSF	57	4	4	M	67.5
ESSF	58	4	4	F	48.5
ESSF	59				
ESSF	60	4	4	M	47.1
ESSF	61	4	4	F	45.2
ESSF	62	4	4	H	44.5
ESSF	63	4	4	M	41.4
ESSF	64	4	4	F	52.2
ESSF	65	4	4	H	36.9
ESSF	66	4	4	M	43.1
ESSF	67	4	4	F	52.5
ESSF	68	4	4	H	43.8
ESSF	69	4	4	M	37.9
ESSF	70	4	4	F	48.0
ESSF	71	4	4	H	58.0
ESSF	72	4	4	M	83.0
ESSF	73	4	4	F	68.9
ESSF	74	4	4	H	51.2
ESSF	75	4	4	M	61.6
ESSF	76	4	4	F	54.3
ESSF	77	4	4	H	44.7
ESSF	78	4	4	M	82.9
ESSF	79	4	4	F	55.7
ESSF	80	4	4	H	73.1
ESSF	81	4	4	M	77.6
ESSF	82	4	4	F	53.8
ESSF	83	4	4	H	38.8
ESSF	84	4	5	M	44.7
ESSF	85	4	4	F	35.1
ESSF	86	4	4	H	76.7
ESSF	87	4	4	M	114.1
ESSF	88	4	4	F	41.0
ESSF	89			H	
ESSF	90	4	4	M	64.3
PP	91	4	4	F	37.4
PP				H	
PP	93	4	4	M	19.6
PP	94	4	4	F	14.9

PRS™-Probe Supply Rate (mg/10cm^2/burial period)					
Location	**Sample #**	**#Cation**	**#Anion**	**Layer**	**AI**
Method Detection Limits (mdl):					***0.4***
PP	95			H	
PP	96	4	4	M	19.8
PP	97	4	4	F	18.8
PP	98			H	
PP	99	4	4	M	34.8
PP	100	4	4	F	36.5
PP	101			H	
PP	102			M	
PP	103	4	4	F	36.4
PP	104			H	
PP	105			M	
PP	106	4	4	F	40.7
PP	107			H	
PP	108			M	
PP	109	4	4	F	55.2
PP	110			H	
PP	111			M	
PP	112	4	4	F	43.3
PP	113			H	
PP	114			M	
PP	115	3	4	F	30.6
PP	116			H	
PP	117			M	
PP	118	4	4	F	51.9
PP	119			H	
PP	120			M	
PP	121	4	4	F	29.1
PP	122			H	
PP	123			M	
PP	124	4	4	F	22.7
PP	125			H	
PP	126			M	
PP	127	4	4	F	27.9
PP	128			H	
PP	129			M	
PP	130	4	4	F	24.3
PP	131			H	
PP	132			M	
PP	133	4	4	F	29.8
PP	134			H	
PP	135			M	
BWBS	136	4	3	F	45.9
BWBS	137	4	4	H	40.3
BWBS	138	4	4	M	47.5
BWBS	139	4	4	F	30.8
BWBS	140	4	4	H	31.6
BWBS	141	4	4	M	43.5

PRS™-Probe Supply Rate (mg/10cm^2/burial period)					
Location	**Sample #**	**#Cation**	**#Anion**	**Layer**	**Al**
Method Detection Limits (mdl):					***0.4***
BWBS	142	4	4	F	32.1
BWBS	143	4	4	H	33.7
BWBS	144	4	4	M	42.0
BWBS	145	5	4	F	41.1
BWBS	146	4	4	H	37.7
BWBS	147	4	4	M	58.0
BWBS	148	4	4	F	28.4
BWBS	149	4	4	H	28.9
BWBS	150	4	4	M	40.7
BWBS	151	3	4	F	23.8
BWBS	152	4	4	H	39.9
BWBS	153	4	4	M	38.3
BWBS	154	4	3	F	49.1
BWBS	155	4	4	H	48.8
BWBS	156	4	3	M	46.2
BWBS	157	3	3	F	45.7
BWBS	158	4	4	H	53.3
BWBS	159	4	4	M	49.8
BWBS	160	4	4	F	24.5
BWBS	161	4	4	H	39.5
BWBS	162	4	4	M	56.5
BWBS	163	4	4	F	32.6
BWBS	164	4	4	H	37.0
BWBS	165	4	4	M	41.2
BWBS	166	4	4	F	30.5
BWBS	167			H	
BWBS	168	4	4	M	46.5
BWBS	169	4	4	F	28.2
BWBS	170			H	
BWBS	171	4	4	M	59.0
BWBS	172	4	4	F	28.3
BWBS	173			H	
BWBS	174	4	4	M	74.7
BWBS	175	4	4	F	36.5
BWBS	176			H	
BWBS	177	4	4	M	67.4
BWBS	178	4	4	F	40.5
BWBS	179			H	
BWBS	180	4	4	M	45.5
ICH	181	4	4	F	42.4
ICH	182			H	
ICH	183	4	4	M	66.7
ICH	184	4	4	F	33.9
ICH	185			H	
ICH	186	4	4	M	40.2
ICH	187	4	3	F	46.4
ICH	188			H	

PRS™-Probe Supply Rate (mg/10cm^2/burial period)					
Location	**Sample #**	**#Cation**	**#Anion**	**Layer**	**Al**
Method Detection Limits (mdl):					***0.4***
ICH	189	4	2	M	69.8
ICH	190	4	4	F	36.7
ICH	191	4	4	H	36.5
ICH	192	4	4	M	41.5
ICH	193	4	4	F	44.3
ICH	194	4	4	H	45.3
ICH	195	4	4	M	51.1
ICH	196	4	4	F	27.3
ICH	197	4	4	H	36.7
ICH	198	4	4	M	46.5
ICH	199	4	4	F	56.0
ICH	200	4	4	H	49.5
ICH	201	4	4	M	49.2
ICH	202	3	4	F	36.1
ICH	203			H	
ICH	204	4	2	M	97.1
ICH	205	4	4	F	41.4
ICH	206	4	3	H	56.3
ICH	207	4	5	M	35.8
ICH	208	4	4	F	46.3
ICH	209	4	4	H	35.4
ICH	210	4	4	M	34.7
ICH	211	4	4	F	35.2
ICH	212			H	
ICH	213	4	4	M	38.8
ICH	214	4	4	F	47.2
ICH	205			H	
ICH	216	4	4	M	45.0
ICH	217	4	4	F	41.1
ICH	218			H	
ICH	219	4	4	M	47.5
ICH	220	4	4	F	39.1
ICH	221			H	
ICH	222	4	3	M	59.0
ICH	223	4	4	F	32.2
ICH	224			H	
ICH	225	4	4	M	42.1
MH	226	4	4	F	23.7
MH	227	4	4	H	26.2
MH	228	4	3	M	50.5
MH	229	4	4	F	40.0
MH	230	4	4	H	21.9
MH	231	4	4	M	69.8
MH	232	4	4	F	47.1
MH	233	4	4	H	24.0
MH	234	4	4	M	45.5
MH	235	4	4	F	43.2

PRS™-Probe Supply Rate (mg/10cm^2/burial period)					
Location	**Sample #**	**#Cation**	**#Anion**	**Layer**	**Al**
Method Detection Limits (mdl):					***0.4***
MH	236	4	4	H	49.4
MH	237	4	4	M	38.0
MH	238	4	4	F	48.0
MH	239	4	4	H	43.8
MH	240	4	4	M	47.1
MH	241	4	4	F	48.3
MH	242	4	4	H	64.4
MH	243	4	4	M	41.5
MH	244	4	4	F	60.8
MH	245	4	4	H	54.9
MH	246			M	
MH	247	4	4	F	56.6
MH	248	4	4	H	62.3
MH	249			M	
MH	250	4	4	F	77.3
MH	251	4	4	H	57.9
MH	252			M	
MH	253	4	4	F	44.9
MH	254	4	4	H	44.2
MH	255			M	
MH	256	4	4	F	50.0
MH	257	4	4	H	41.0
MH	258	4	4	M	26.5
MH	259	3	4	F	10.4
MH	260	5	4	H	32.3
MH	261	4	4	M	34.6
MH	262	4	4	F	35.2
MH	263	3	4	H	26.7
MH	264	3	4	M	29.2
MH	265	4	4	F	18.3
MH	266	3	4	H	23.3
MH	267	1	0	M	N/A
MH	268	4	5	F	20.9
MH	269	4	4	H	30.2
MH	270	4	4	M	36.3
CWH	271	4	4	F	29.6
CWH	272	3	4	H	32.0
CWH	273	4	4	M	42.1
CWH	274	4	4	F	72.2
CWH	275	4	4	H	75.9
CWH	276	3	4	M	57.1
CWH	277	4	4	F	54.6
CWH	278	4	4	H	36.7
CWH	279	4	4	M	60.8
CWH	280	4	4	F	37.5
CWH	281	4	4	H	39.8
CWH	282	4	4	M	37.4

PRS™-Probe Supply Rate (mg/10cm^2/burial period)					
Location	**Sample #**	**#Cation**	**#Anion**	**Layer**	**Al**
Method Detection Limits (mdl):					***0.4***
CWH	283	4	4	F	23.4
CWH	284	4	4	H	26.0
CWH	285	4	4	M	50.6
CWH	286	4	4	F	12.9
CWH	287	4	4	H	15.0
CWH	288	4	4	M	27.3
CWH	289	4	4	F	11.4
CWH	290	4	4	H	25.8
CWH	291	3	4	M	17.7
CWH	292	4	4	F	51.2
CWH	293	4	4	H	64.1
CWH	294	4	4	M	36.1
CWH	295	4	4	F	32.4
CWH	296	4	4	H	31.9
CWH	297	4	4	M	37.9
CWH	298	4	4	F	26.9
CWH	299	4	4	H	47.7
CWH	300	4	4	M	59.2
CWH	301	4	4	F	50.5
CWH	302	4	4	H	92.1
CWH	303	4	4	M	46.5
CWH	304	4	4	F	42.3
CWH	305	4	4	H	62.6
CWH	306	4	4	M	55.4
CWH	307	4	4	F	42.7
CWH	308	4	4	H	46.9
CWH	309	4	4	M	69.0
CWH	310	4	4	F	57.0
CWH	311	4	4	H	83.6
CWH	312	4	4	M	88.6
CWH	313	4	4	F	48.4
CWH	314	4	4	H	64.9
CWH	315	4	4	M	64.1